1990

PALAEONTOGRAPHICA

BEITRÄGE ZUR NATURGESCHICHTE DER VORZEIT

ABTEILUNG B

PALÄOPHYTOLOGIE

HERAUSGEGEBEN VON

H.-J. SCHWEITZER

IN BONN

BAND 218

LIEFERUNG 1—3

UNTER MITARBEIT VON

CH. BECK, MICHIGAN; R. BELOW, BONN; M. BOULTER, LONDON; W. L. FRIEDRICH, AARHUS; J. GALTIER, MONTPELLIER; CH. HILL, LONDON; CH. MILLER, MISSOULA; G. PLAYFORD, ST. LUCIA; A. TRAVERSE, UNIVERSITY PARK; D. VOGELLEHNER, FREIBURG/BR.

INHALT:

STUTTGART
E. SCHWEIZERBART'SCHE VERLAGSBUCHHANDLUNG
(NÄGELE u. OBERMILLER)
1990

A DINOCYST CALIBRATION OF THE EUROPEAN BOREAL BARREMIAN

BY

IAN C. HARDING, Cambridge*)

With 31 plates, 19 figures and 7 tables in the text and on 1 foldout

PART I: INTRODUCTION, STRATIGRAPHY, SYSTEMATICS

Summary

This study describes the dinocysts extracted from Barremian age sediments from Boreal western Europe from a biostratigraphic viewpoint. The first part of the study introduces the project and details the sample localities and their stratigraphy. The systematic section which follows describes the P-type (peridinioid), Gc-type (ceratioid) and Gv-type (compressed gonyaulacoid) and Gs-type (sexiform gonyaulacoid) dinocysts.

Routine high resolution observation of dinocyst strew-mounts has been pioneered using the scanning electron microscope (SEM). This high resolution study has allowed an investigation of the application of the species concept to dinocyst systematics. The SEM micrographs obtained have enabled precise morphological constraints to be placed on individual 'species'. A total of eleven (11) new species are described and seven species are emended after observation of the type and new topotype material. Over half of these taxa have limited time ranges, which will be detailed in the second part of this paper.

Key Words: Dinocysts – palynostratigraphy – early Cretaceous – Boreal Europe.

Contents

*) Address of the author: Dr. I. HARDING, Department of Earth Sciences, University of Cambridge, Downing St., Cambridge, CB2 3EQ, England.

Present address of the author: Dr. I. HARDING, Dept. Geology, University of Southampton, Southampton, S09 5NH, England.

0375–0299/90/0218–0001 $ 53.10

© 1990 E. Schweizerbart'sche Verlagsbuchhandlung, D-7000 Stuttgart 1

Acknowledgements

I would like to thank Dr. Norman Hughes for his untiring help and support during this research project. Funding was kindly provided by the Natural Environment Research Council (Grant GT4/82/GS/122) and the Cambridge Philosophical Society. I also wish to thank the Trustees of the Tansley Fund of The New Phytologist for kindly providing financial support towards the publication of this paper. Thanks are also due to Prof. J. W. Neale (Hull) and Dr. J. Mutterlose (Hannover) for their help in the field, and to the latter colleague and Norman Hughes for access to their sample collections. I must express my gratitude to Dr. J. Richardson (BMNH) for allowing access to type specimens, and to Prof. C. Downie, Dr. R. J. Davey, Dr. P. F. Rawson, Dr. S. Conway-Morris, Dr. J. H. J. Penny and Dr. M. C. Boulter for their helpful assistance and discussion of the original manuscript. Thanks are also extended to Mrs. A. B. MacDougal, Mr. D. Newling, Mr. R. Lee for their expertise in technical assistance. Finally I would like to express my thanks to Prof. E. R. Oxburgh for allowing me to use the Departmental facilities. This paper is dedicated to my parents, Mr. and Mrs. R. A. Harding. This is Cambridge Earth Sciences Contribution No. 1341.

1. Introduction

The Barremian age of the early Cretaceous period, although apparently one of the shortest ages in the Phanerozoic (estimates have varied from 2-6Ma – Kennedy & Odin 1982; Hallam et al., 1985 and Odin 1985), has had a most confused history and has consequently been a difficult age to define. The age/stage takes its name from the village of Barrême (Basses-Alpes), in southern France, and was erected by Coquand (1862: 535), although no stratotype was designated. The error in this definition of the Barremian was in the belief that the Urgonian stage, created by d'Orbigny (1847), lay above the Barremian. It was only later recognised that the Urgonian was (in part) a lateral facies variation of the Barremian.

Table 1. Progressive changes in the ammonite zonation of the Barremian type-section at Angles, southeastern France.

AGE	BUSNARDO, 1965a		BUSNARDO (in ROGER 1980)	BUSNARDO (in RAWSON 1983)
	ZONE	SUB-ZONE		
EARLY APTIAN	Deshayesites	Puzozia matheroni	"Prodeshayesites"	(not stated)
LATE BARREMIAN	Silesites seranonis	? Leptoceras puzosianum Heteroceras astieri *Hemihoplites* feraudi ?	Colchidites securiformis Heteroceras astieri *Hemihoplites* feraudi Emericiceras barremense	Colchidites sp. Heteroceras astieri *Hemihoplites* feraudi "Emericiceras" barremense
EARLY BARREMIAN	Nicklesia pulchella	? *Pulchellia* compressissima Holcodiscus kiliani	Heinzia ouachensis *Pulchellia* compressissima Spitidiscus hugii	Moutoniceras sp. *Pulchellia* compressissima Spitidiscus hugii
LATE HAUTERIVIAN	Pseudothurmannia angulicostata	Pseudothurmannia angulicostata and Crioceras binelli	Pseudothurmannia angulicostata	Pseudothurmannia angulicostata

As envisaged by COQUAND (1862), the Barremian also encompassed the Upper Hauterivian of present day usage (BUSNARDO 1965a: 102). It was KILLIAN (1888) and his followers who confused the usage of this stage by arbitrarily excluding the *angulicostata* zone from the base of Coquand's stage. The disregard for Coquand's 'priority' was based on KILLIAN's (1888) lithological and palaeontological studies of the Montage de Lure. Thus, two conflicting definitions of the Barremian age/stage were in use for several decades before any stability was created (BUSNARDO 1965a; MOULLADE 1966).

Not until a century after the first definition of the Barremian was the stratotype designated as the Angles roadside section in the Basses-Alpes département of southern France (BUSNARDO 1965a: COQUAND 1862, having mentioned this sequence along with those at Barrême and Vergons); for the sake of stability, the *angulicostata* zone was retained in the Hauterivian stage following Killian's interpretation of the Barremian. The published ammonite zonation scheme for the Barremian stratotype (Table 1, BUSNARDO 1965), divided the Angles sequence into two ammonite zones. Two other zonations have subsequently been reported (Table 1, BUSNARDO 1980; BUSNARDO 1983) *in* ROGER (1980) and RAWSON (1983), although neither of these zonations have been formally described.

These ammonite zones can be traced over wide geographic areas, from southern France into Czechoslovakia, Bulgaria, the Crimea and Caucasus, N. Africa, Spain and the Himalayas (BUSNARDO 1965b) and (with less accuracy), into South and Central America and Japan (RAWSON 1980). Unfortunately, it is not possible to extend this zonation into areas of North America, the USSR or northern Europe.

The area over which correlation of the Angles scheme can be traced corresponds generally with the palaeoequatorial Tethyan Province. The Tethyan Province was separated from the northern Boreal Province by major land

AGE	AMMONITE ZONES (after KEMPER, 1976)		BELEMNITE ZONES (after MUTTERLOSE, 1983)
BARREMIAN	Parancyloceras bidentatum		Oxyteuthis depressa
	Parancyloceras scalare		
	Simancyloceras stolleyi		Oxyteuthis germanica
	Ancyloceras innexum		
	Simancyloceras pingue		Oxyteuthis brunsvicensis
	Paracrioceras denckmanni		
	Paracrioceras elegans		
	Paracrioceras *fissicostatum*		Aulacoteuthis spp.
	Paracrioceras rarocinctum		Praeoxyteuthis pugio
	Simbirskites (Craspedodiscus) *variabilis*	Simbirskites (Craspedodiscus) discofalcatus	Hibolites jaculoides
LATE HAUTERIVIAN	Simbirskites (Simbirskites) marginatus		
	Simbirskites (Craspedodiscus) gottschei		

Table 2. Cephalopod zonations for the European Boreal realm. Note: the *discofalcatus* zone is recognised in Germany, whereas the *marginatus* and *variabilis* zones are recognised only in England.

barriers (whose extent varied considerably with time), although connecting seaways did exist between the two provinces during much of early Cretaceous time (Rawson 1973). The Boreal Region included the Boreal Ocean (centred on the present day Arctic Ocean) and was fringed by a series of shallow epicontinental seas extending over North America, Siberia and northern Europe. As with the Tethyan Province, the Boreal Province was first distinguished on the basis of its endemic ammonite faunas. Many other organisms followed this provincial distribution in addition to the ammonites (Casey & Rawson 1973).

The low level of faunal interchange between the two provinces has meant that biostratigraphic correlation between the two areas has been extremely limited. The use of cephalopods is limited due to the nature of the two endemic faunas in these provinces. Only during rare periods of faunal migration between the two provinces can a correlation of the two biostratigraphic zonations be performed. Such migrations resulted in faunal intermixing in the mid-Hauterivian (Kemper et. al., 1981; Michael 1979; Rawson 1973; Thieuloy 1977), but due to the closing of the connecting seaways, this did not occur in the Barremian.

The evolution of an endemic cephalopod fauna in the Boreal province has resulted in separate ammonite and belemnite biostratigraphic zonation schemes being erected for this province which does not includes Tethyan forms (see Tables 1 and 2). The zonation of the Boreal Barremian is further complicated by poor preservation and absence of cephalopod fossils in many parts of some successions, and also because some of these Boreal cephalopod zones can only be recognised in Germany and some only in England. In Lincolnshire and Norfolk, Barremian sediments are known largely from boreholes (there being little outcrop exposure) and have been correlated lithostratigraphically. However, even using this method, lateral facies variations can lead to confusion unless the nature of the variation is known.

In addition to the two marine provinces in existence at this time, there were also extensive areas of non-marine deposition in the Wealden Basin. The nature of the deposition in the Wealden area makes attempts at correlation with the standard marine NW European zonations impossible using any of the recognised marine mega-fossil groups.

The problems involved in the cross-correlation of the biostratigraphic zonations of different palaeozoogeographical provinces are thus considerable and complex. Attempts have been made to correlate between different provinces on a lithological basis, using limestone/marl cyclicities (Cotillon 1984), but these are unlikely to give the fine degree of resolution possible using fossil organisms. Solutions to these problems have been thought to lie in the use of an indirect, overlapping fossil zonation system, involving the tracing of zones based on terrestrial palynomorphs from an area of non-marine deposition into a marginal marine sequence where such a zonation could then be related to a standard marine zonation. This set of marine organisms might be picked up in a region of faunal/floral interchange between two marine provinces, thus creating a tie-in between three different provinces (see Hughes 1973). This solution was proposed because of the lack of fossils common to both non-marine and marine strata. However, during the course of the research presented here it emerged that this was not as limiting a factor as first believed (depending on the group of organisms being studied).

A study of fossil dinocysts has shown that a potential solution to alleviate the problems caused by the use of cephalopod zonation systems is now feasible. These microfossils have several well known advantages over conventional mega-fossil zonal indices. Amongst these are their small size, ease of transportation by watercurrents and their abundance. Dinocysts are common in many sedimentary rocks, their small size causing them to act as sedimentary particles and so to be deposited along with the inorganic component of the sediment. Sediments with grain sizes of silt or clay contain the greatest abundance of palynomorphs and these lithologies are dominant in the Barremian of western Europe. The planktonic nature of most dinoflagellates means that their distribution is largely affected by oceanic currents and may thus have wide geographic ranges. It is thus conceivable that such organisms may display distributions that show less provincial control than do cephalopods.

This paper represents the first stage of an attempt to create a unified worldwide dinocyst calibration scheme for the Barremian. This first stage is represented by the establishment of a new standard dinocyst calibration scheme for the whole of northwestern Europe. It has been found that this scheme can also be used directly to correlate the Wealden succession of the Warlingham borehole, Surrey (Worssam & Ivimey-Cook 1976) with the standard marine successions of northwest Europe for the first time. This has been accomplished using the periodic influxes of ?brackishwater, low diversity dinocyst assemblages into the Wealden Basin (data used in this correlation – Hughes & Harding 1985; Harding 1986a). It is shown that the use of dinocysts in the correlation of Mesozoic

sediments can, when integrated with the existing cephalopod zonation schemes, greatly increase the applicability and accuracy of this type of stratigraphical correlation. However, for this to become possible an observation technique needs to be employed which lends itself to the fine resolution of detail necessary for the requisite discrimination of such small organisms. For this study a method of routine SEM scan-search observation of strew-mounted palynologic residues has been developed (HARDING 1986c). This method is no more time-consuming than the observation of light microscope slides once the observer is familiar with the technique, and the image resolution far exceeds that possible with the light microscope, so enabling better circumscription of taxa.

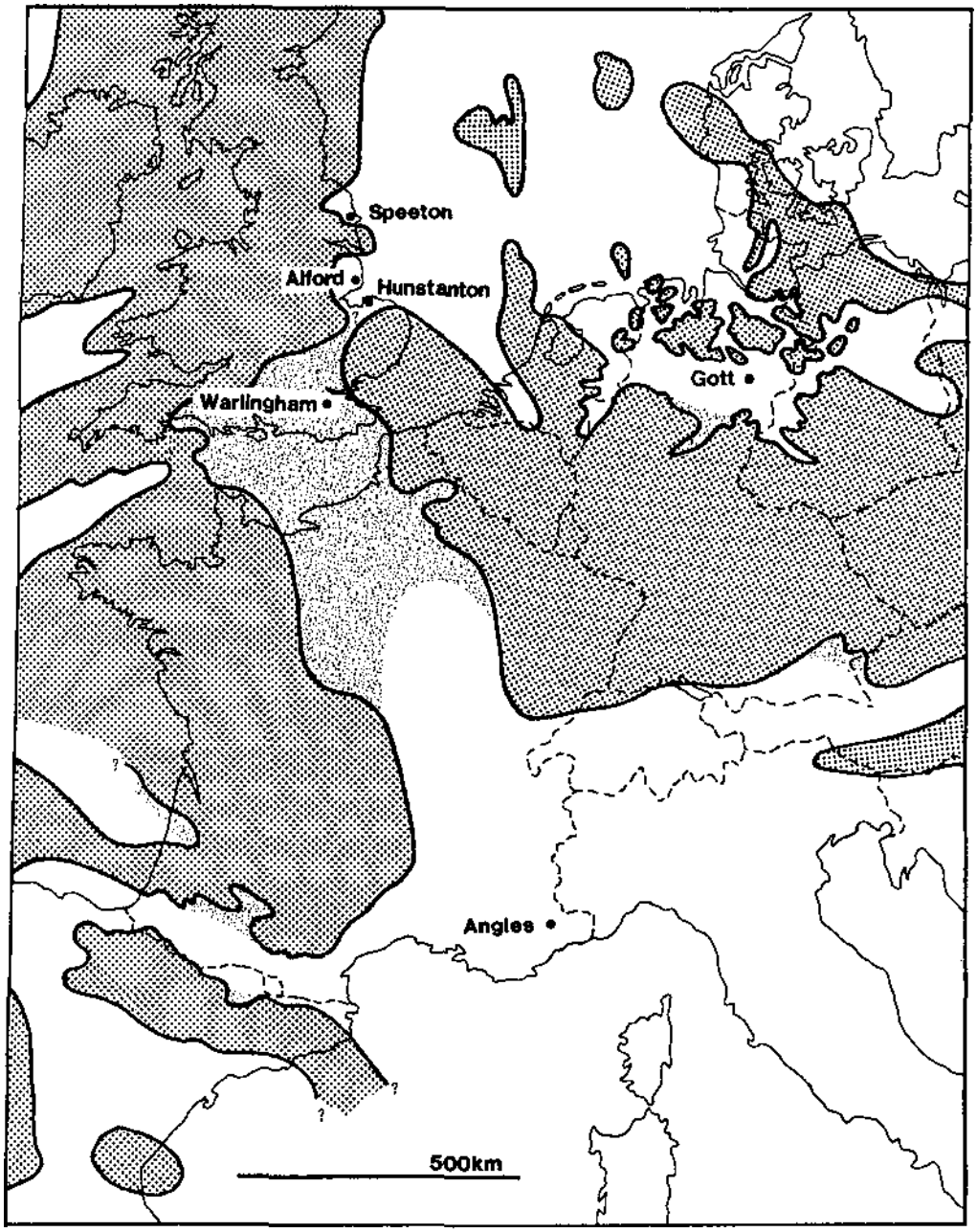

Text-fig. 1. The locations of the five main localities studied in this work, the Angles type-section is also shown. Palaeogeographic reconstruction shows land (heavy stipple) and areas of non-marine deposition (light stipple). The southeast corner of the map, due to complications imposed by plate tectonics, has been excluded from this reconstruction (compiled from SCHOTT 1969; FERRY & SCHAAF 1981 and KELLY & RAWSON 1983).

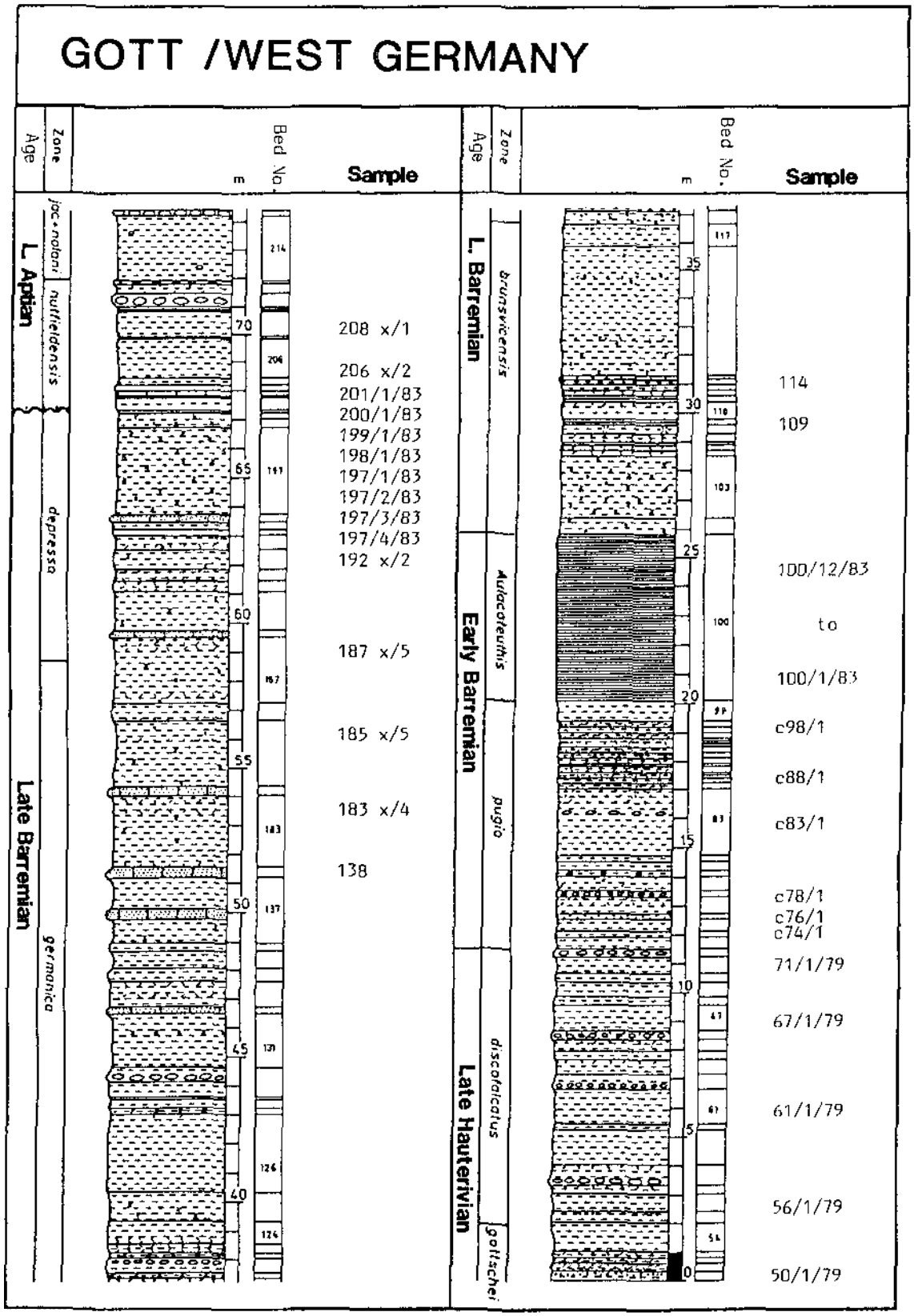

Text-fig. 2. Lithologic log of the Gott succession, showing cephalopod zonations, bed numbers and the sampled horizons (after MUTTERLOSE 1984).

2. Sample provenance

Samples from five main localities have been studied (Text-fig. 1).

2.1. The Gott claypit, Sarstedt, West Germany

Location: 1 km E. of the Hannover-Hildesheim road (B6); 1 km NE of Sarstedt. Map reference TK 25, Nr. 3725; re: 35 60 400, h: 57 90 650.

The Gott claypit at Sarstedt contains excellent exposures of Upper Hauterivian to Upper Aptian clays. The clays dip at 25° to the NW, tilted by the rising of the Sarstedt-Lehrter salt dome to the SE (MUTTERLOSE 1984: fig. 16). Detailed lithologic descriptions of the Gott sequence can be found in ALIMIRZAIE (1972), MUTTERLOSE (1983, 1984) *and* TARKIAN *(1968).*

The samples studied came from a collection made by the author and samples kindly made available by Dr. J. MUTTERLOSE from the collection of the Institut für Geologie and Paläontologie, Hannover. Some forty samples were studied between Beds 50 and 208 (see Text-fig. 2).

The lower beds, of late Hauterivian age, comprise about 12 m of rhythmic light and dark grey clays, frequently showing bioturbation. The lower 5.6 m of the Barremian clays are also of this nature.

The following 5.7 m of sediment is a very distinctive horizon called the Hauptblätterton (sensu MUTTERLOSE 1983). This almost black clay, of high organic carbon content, consists of very finely laminated pale and dark layers. The pale layers are calcareous microlenses composed of coccoliths (MUTTERLOSE & HARDING 1987a and b). The Hauptblätterton is greatly enriched in carbonates and pyrite.

*The Upper Barremian beds comprise 40 m of sediments, the lower part (≅ 15 m) resembling the pre-*Hauptblätterton Lower Barremian sequence, containing two thin black clay (Blätterton) horizons. The upper part is lithologically monotonous, the clays becoming darker and occasionally very pyritic with several marly sandstone intercalations.

The Barremian sequence is unconformably overlain by Upper Aptian clays (≅ 7 m) containing two tuff horizons (GAIDA et al., 1978; ZIMMERLE 1979).

The cephalopods at Gott have been studied by KOENEN (1902), MUTTERLOSE (1983) and those from the Aptian by GAIDA et al. (1978) The sequence exposed in this claypit is thus accurately tied into the German ammonite zonations and also the belimnite zonation of MUTTERLOSE (1983).

Hauterivian and Barremian dinocysts from northern Germany have been studied by ALBERTI *(1961),* GOCHT (1957, 1959) and MICHAEL (1964). BELOW (1982a) described the dinocysts from the Upper Barremian and Upper Aptian sediments of the Gott claypit.

2.2 The Speeton coastal section Yorkshire

Location: A 1.2 km coastal section of low cliffs at the southern end of Filey Bay. This section lies in the parish of Speeton on the borders of North Yorkshire and Humberside.

The exposures at Speeton vary from year to year as the soft clays are prone to slumping. The sediments dip at about 15°, the structure being complicated by many low angle faults. This is the type locality for the Speeton Clay Formation which is only otherwise known from boreholes and rare exposures along the foot of the Chalk scarp in the Vale of Pickering (JUDD 1870: 326–329; LAMPLUGH 1896: 184–191). Boreholes in the area (at Speeton Beck, West Heslerton and Fordon) have elucidated the structure of the rocks below the Chalk. The Speeton Clay is the most complete exposed succession of marine Lower Cretaceous rocks in western Europe.

The samples studied came from collections made in September 1972 for Dr. N. F. HUGHES and collections by the author in March 1983 under the guidance of Prof. J. W. NEALE. This latter collection was made during conditions of unusually good exposure at the site. About forty samples have been analysed in total (Text-fig. 3).

PHILLIPS (1829: 75) first used the term Speeton Clay to describe the blue clays between the Chalk and the Corallian in Filey Bay. The first subdivisions were by LECKENBY (1859), JUDD (1868, 1870) and by LAMPLUGH (1889, 1896, 1924). The latter subdivision, based on belemnite faunas, divided the Speeton Clay into five parts labelled A to E in descending sequence. Refinements of the succession were lithological, LAMPLUGH (1889) recognising the

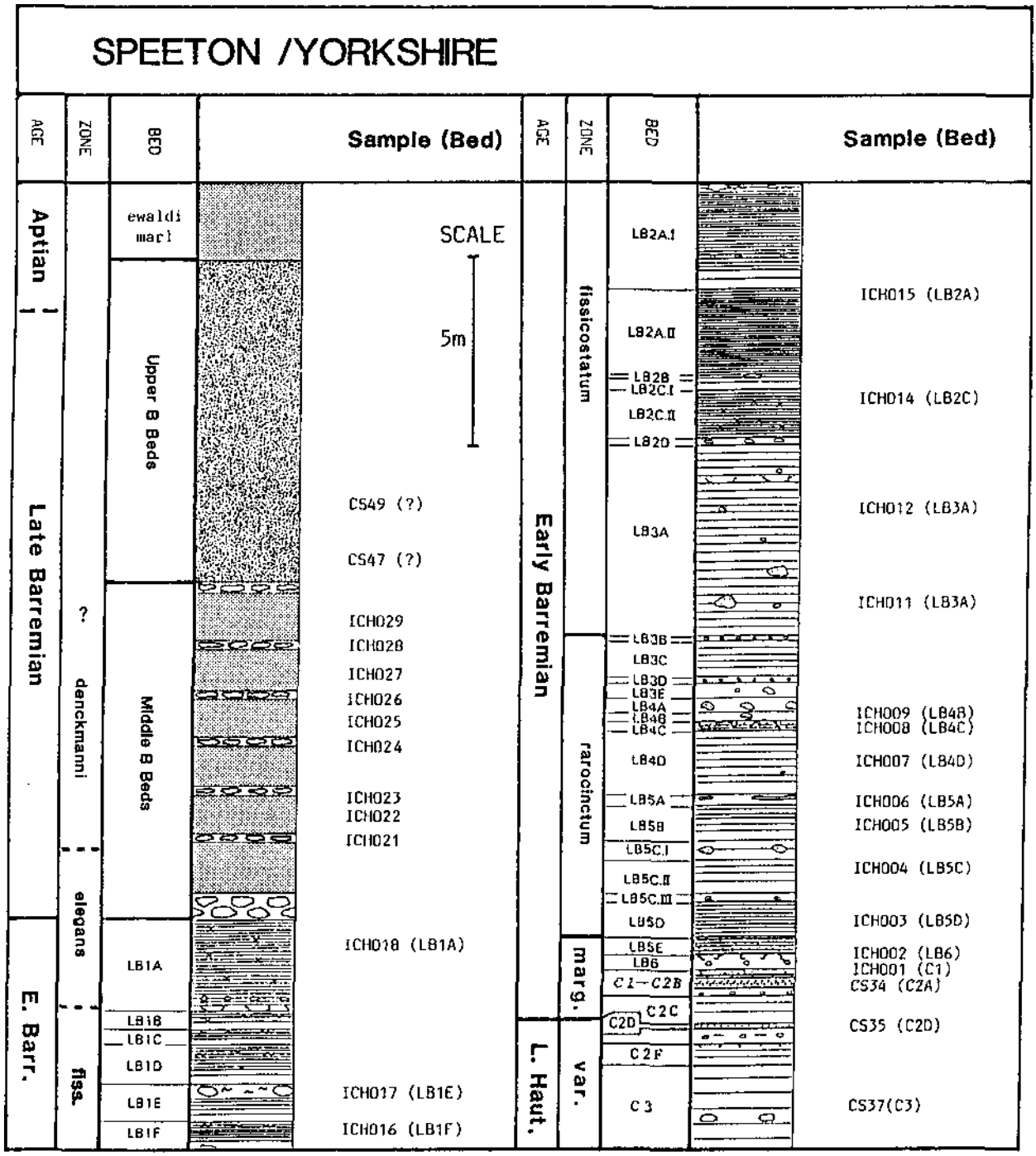

Text-fig. 3. Lithologic log of the Speeton coastal succession, showing ammonite zonation (as far as is known), bed designations and sampled horizons (after KAYE 1964; RAWSON 1971 and Rawson & Mutterlose 1983). Note: The early/late Barremian division is based on belemnite zonations and lithostratigraphic correlation with W. Germany. *C. elegans* has an anomalously early appearance at this locality.

Lower B, Middle B or Cement Beds, and the Upper B Beds. The Lower B Beds and basal Cement Beds have been further detailed by RAWSON & MUTTERLOSE (1983), the C Beds by FLETCHER (1969) and RAWSON (1971b) and the poorly exposed higher B and A Beds by KAYE (1964).

The uppermost C Beds consist of alternating pale and darker clays, often glauconitic and occasionally pyritic.

Of the B Beds, the Lower B are the best exposed and have the most refined lithologic subdivision, consisting of alternations of pale calcareous clays and dark blue-grey clays. Bed LB1 contains abundant pyrite and organic

material in an almost black clay matrix. This horizon (and possibly several below) may be the equivalents of the German Hauptblätterton. The Middle B or Cement Beds consist of dark pyritic clays containing conspicuous calcareous nodule bands or "cementstones". Seven bands have been recognised and are labelled α to η in descending sequence (KAYE 1964). The bed taken as the base of the Middle B is the "double cement bed" of KAYE (1964) (see RAWSON & MUTTERLOSE 1983: 133).

The Upper B Beds are poorly exposed and a detailed subdivision has yet to be made. KAYE (1964) estimated a thickness of 30 ft. for these beds. The top of the Upper B sequence comprises conformable sediments of the Lower Aptian. The Lower Aptian beds are unconformably overlain by the *ewaldi* Marl of the Lower Albian.

Parts of the Speeton Clay are accurately tied in to the various cephalopod zonal schemes, particularly the Hauterivian horizons (e.g. RAWSON (1971a & b). The Hauterivian/Barremian boundary is now taken at the base of Bed C2C (KEMPER et al., 1981), due to the presence of the ammonite *Crioceratites* (*Paracrioceras*) *spathi* at the base of the *variabilis* zone. This ammonite has the characteristic "looped ribs of '*Emericiceras*' from the lowest (sic) Barremian of Tethys" (KEMPER et al., 1981: 307).

Ammonites are less common in the Lower B Beds but zonal boundaries have been designated with a fair degree of certainty up to the *elegans/denckmanni* boundary. Belemnites are common in the Lower B Beds and have enabled correlation to be made with the zonal scheme of MUTTERLOSE (1983; see also RAWSON 1972). The Middle and Upper B Beds are so poorly known that no detailed ammonite biozonation is as yet published. The higher parts of the Upper B Beds have yielded *Aconeceras nisoides* and *Prodeshayesites fissicostatus* of basal Aptian age.

Previous studies of dinocysts from the Speeton Clay have been published by NEALE & SARJEANT (1962), SARJEANT (1966a & b), DAVEY & WILLIAMS (1966a & b) and DAVEY et al. (1966) on material from the West Heslerton borehole. More recently (DAVEY (1974) and DUXBURY (1977, 1979, 1980) have studied the dinocysts from samples collected at outcrop, based on low numbers of samples taken at a relatively low frequency throughout the succession.

2.3 The Hunstanton Borehole, Norfolk

Location: Approximately 1.5 km ESE of Hunstanton pier. Drilled at Lodge Farm, Hunstanton, Norfolk. Nat. grid ref. *TF 6857 4078.*

The Hunstanton borehole was sunk in 1970 by the Institute of Geological Sciences, the cored interval yielded ≅ 130 m of sediment from the Middle Chalk to the Kimmeridge Clay (GALLOIS 1971). The sequence has been related to the outcrops of the Hunstanton beach area by GALLOIS (1973, 1975a, 1984).

The section of the borehole studied comprises the Dersingham Beds (CASEY & GALLOIS 1973) and the Roach of Hauterivian to Barremian age (see Text-fig. 4). Sub-samples from the borehole are in the collection of Dr. N. F. HUGHES (Cambridge), and were kindly provided by the British Geological Survey.

The Dersingham Beds are laterally variable, rhythmic sequences of thinly interbedded, fine-grained sands, ferruginous sandstones, silts and clays represented by ≅ 11.6 m of sediment in this borehole. The upper two rhythms of this sequence in the Hunstanton borehole may represent the Snettisham Clay (GALLOIS 1984: 28).

In the Hunstanton borehole the Snettisham Clay is overlain conformably by ≅ 12.1 m of Roach, also a complex sequence of rhythmic sediments made up of differing amounts of clay, chamosite mud, chamosite (now limonite) ooliths, quartz sand and small quartz and ironstone pebbles. The base of the Roach is taken at a minor erosion surface separating the pebbly oolitic clays of the Roach from the predominantly argillaceous Dersingham Beds.

The Roach/Carstone contact at outcrop was elucidated by GALLOIS (1973, 1975a): the topmost Roach containing two beds of phosphatic ironstone nodules containing *Paracrioceras*. Unconformable above these sediments is an oolitic pebbly clay, a basal bed of the Carstone (GALLOIS 1975a: 26) containing ironstone nodules derived from the Roach below. The bed above this pebbly clay contains derived phosphatised early Aptian ammonites. The succession in the Hunstanton borehole is very similar to this but the Roach lacks the nodules and their ammonite faunas (some core loss was experienced in this section – GALLOIS 1973: fig. 2). About 18.9 m of presumed early Albian Carstone lie unconformably above the Roach.

Certain horizons in the Dersingham Beds are fossiliferous and yield fossils of an early Hauterivian age at the base (species of *Endemoceras*). The Snettisham Clay has yielded two separate faunas, one from the basal parts of the

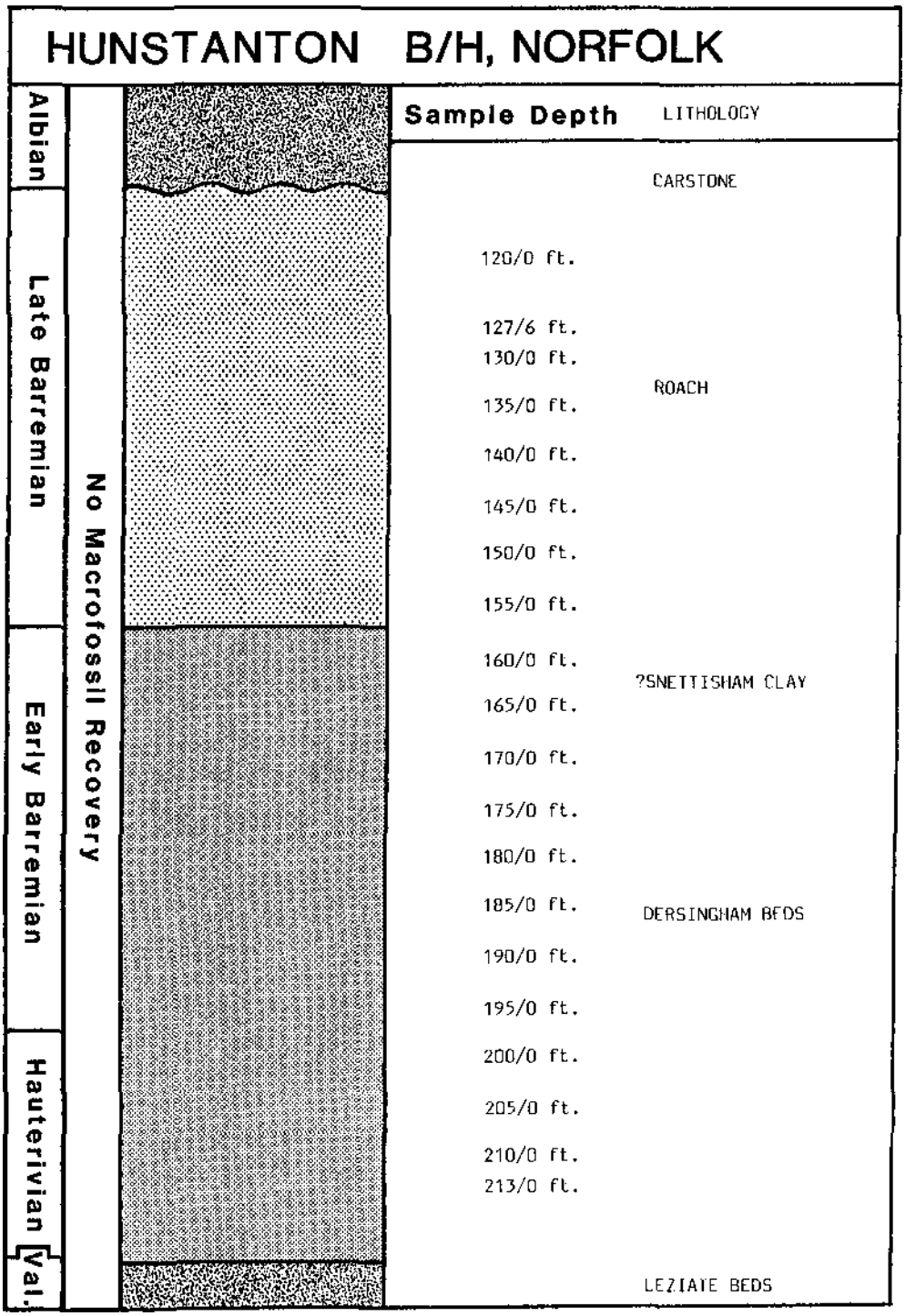

Text-fig. 4. Lithologic log of the Hunstanton borehole. The sequence is a complex series of cyclical sediments. The interpretation of this succession according to GALLOIS (1984), does not agree with the information obtained from palynological studies, the interpretation of which can be seen on the left-hand side of the diagram.

clay containing bivalves, gastropods, crioceratid ammonites and belemnites of the genera *Aulacoteuthis* and *Praeoxyteuthis* indicating an early Barremian age. The upper part of the Snettisham Clay has yielded ammonites indicative of the *elegans* zone (MORTER in GALLOIS 1984: 32). The fauna of the Hunstanton Roach was described by MORTER (1975), compared to the Roach of Lincolnshire and allocated a mid-Barremian age. GALLOIS (1984: 37) suggests the Hunstanton Roach is of late middle to early late Barremian age.

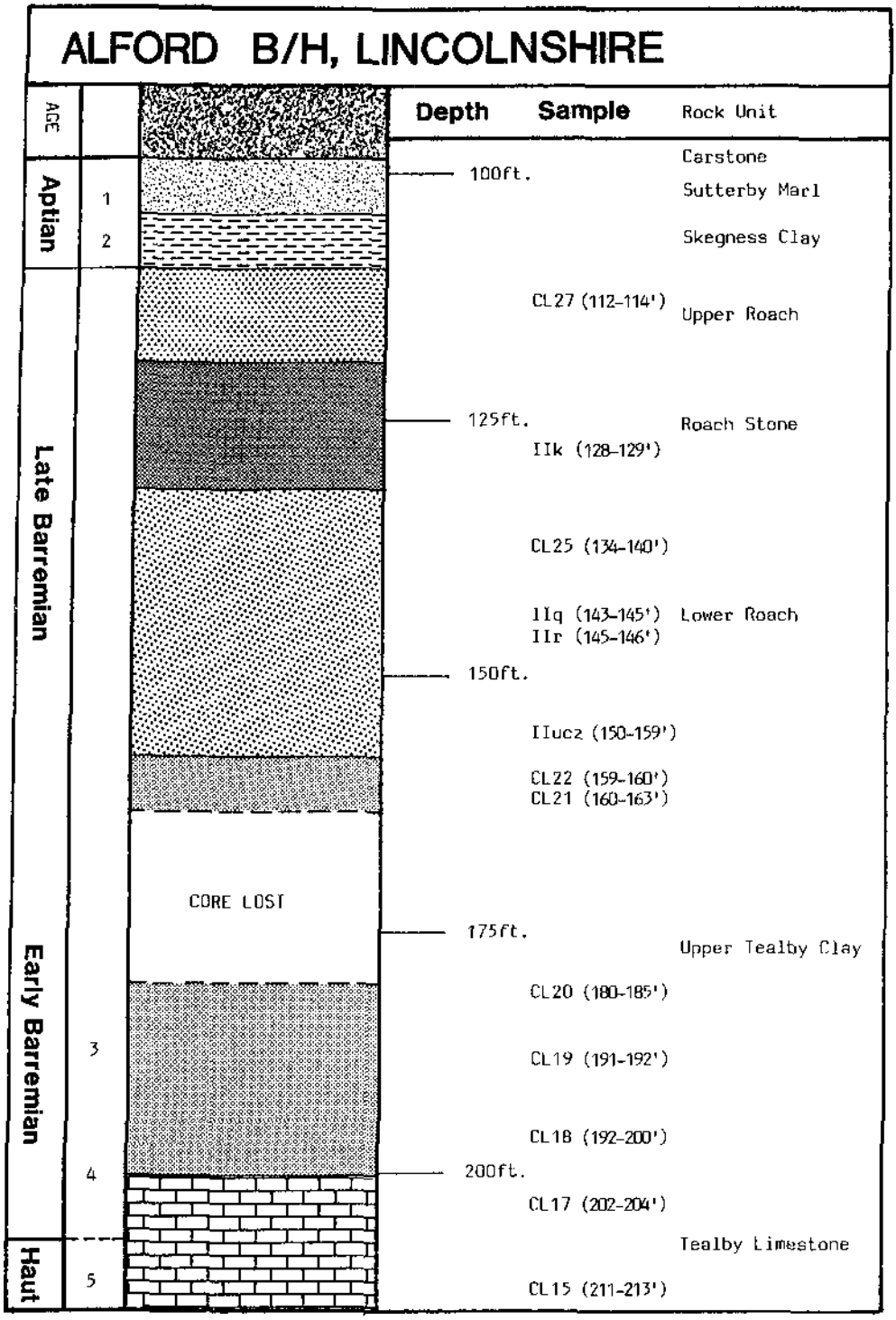

Text-fig. 5. Lithologic log of the succession in the Alford borehole (after SWINNERTON 1935), showing sample horizons and positions of the recovered megafossil zonal indices. 1 = *Neohibolites ewaldi* and *Aconeceras nisoides*; 2 = *Oxyteuthis brunsvicensis*; 3 = *Aulacoteuthis* sp.; 4 = *Hibolites jaculoides*.

2.4 The Alford borehole, Lincolnshire

Location: Bored in the grounds of the Alford pumping station. Nat. grid ref. TF 454757.

This borehole was sunk in 1932 by Alford Town Council, with a core being recovered from a depth of 80 ft. down to 286 ft. Core recovery was incomplete, notably from 98 ft. to 112 ft., where only 2 ft. 9 ins. of core was recovered and 16 ft. of core was lost from between 160–180 ft. A detailed log of the sediments recovered in the cored intervals is provided by SWINNERTON (1935).

Sub-samples from the borehole are in the collection of Dr. N. F. HUGHES (Cambridge) and were kindly made available by the late Prof. H. H. SWINNERTON in 1956 (Text-fig. 5).

The section of the borehole investigated in this work comprises part of the Tealby Beds and the Fulletby Beds. The Tealby Limestone, a light grey, argillaceous or sandy limestone lies from 200–213ft. in the hole. The limestone is overlain by the greenish grey Upper Tealby Clay of about 40ft. thickness.

Overlying the Tealby Beds is ≅45ft. of strata comprising the Fulletby Beds. This unit is split into three members: the Lower Roach (25.5ft.) is a grey-green to buff clay containing abundant chamosite (now limonite) ooliths; the middle member, the Roach Stone (about 13ft. thick) is a ferruginous sandstone; the Upper Roach is a 5ft. horizon of grey-green clay with abundant chamosite ooliths (a detailed lithologic description of the Fulletby Beds is given in OWEN & THURRELL 1968).

Above the Fulletby Beds lies the "Sutterby Marl" of SWINNERTON (1935: 5). This is an 11ft. horizon divisible into two separate beds. The upper 6ft. of this section is a light grey marl and probably represents the Sutterby Marl as now envisaged. The lower 5ft., of dark grey and black clay, although interrupted by poor core recovery, is believed to represent the Skegness Clay (GALLOIS 1975b: 501; RAWSON et al., 1978: 35).

SWINNERTON (1935) gives a list of the fossils found in the core material. *Oxyteuthis brunsvicensis* was found from a depth of 134–209 ft. *Aulacoteuthis* sp. is recorded from the Upper Tealby Clay. *O. pugio* and *Hibolites jaculoides* are recorded from the Tealby Limestone. Further work on these formations has shown that the base of the Tealby Limestone is of late Hauterivian age, the higher parts being Barremian. The Lower Roach has yielded belemnites of the *germanicus* group. The Barremian/Aptian boundary is taken at the base of the Skegness Clay which is of early Aptian age and is apparently unconformable with the Fulletby Beds.

No previous research has been published on the dinocysts of the Alford borehole.

2.5 The Warlingham borehole Surrey

Location: Drilled in a field beside the Woldingham Road, SW of All Saints Church, Warlingham. Nat. grid ref. TQ 3476 5719.

The Warlingham borehole was drilled in 1956–8 and provided the first completely cored section of the Weald Clay. Samples from the cores from a depth of 795–1555 ft. were studied (Text-fig. 6). These 263 samples form part of an unregistered collection of I.G.S. material made available to Dr. N. F. HUGHES in 1956.

A thickness of 577 ft. of Weald Clay was cored (comparing well with the thickness of this formation in boreholes near Maidstone and at outcrop). Four of the seven marker beds recognised by TOPLEY (1875: 102) at outcrop have been recognised in the borehole cores. A detailed lithologic breakdown of the core material is given in WORSSAM & IVIMEY-COOK (1971).

The Aptian Atherfield Clay lies disconformably above the Weald Clay (a break in sedimentation is indicated by horizontal borings filled with silty sand). Shelly bands occurring from 1043 ft. to the Atherfield Clay/Weald Clay junction have been taken to be the '*Perna*' Bed. The base of the Atherfield Clay has been shown to be a diachronous horizon, being of *fissicostatus* age (early Aptian) in the Weald (SIMPSON 1985).

Little is known of the biostratigraphic correlation of the Weald Clay with the standard ammonite zonation schemes. The Atherfield Clay is the lowest formation in the Cretaceous sequence that can be tied in to the European ammonite zonation.

Previous work on Weald Clay dinocysts has been limited (e.g. HUGHES1980; BATTEN 1982). BATTEN (1985) described monospecific dinocyst assemblages from the Weald Clay. More recently, LISTER & BATTEN (1988a & b) have studied the dinocysts of the Weald Clay in the Hurlands Farm borehole, Sussex. HUGHES & HARDING (1985) and HARDING (1986a) described brackish-marine dinocyst assemblages from the Warlingham borehole (data from these papers has been used in the correlation presented later in this work, supplemented by additional work on the dinocyst assemblages of the sediments from across the Barremian/Aptian boundary).

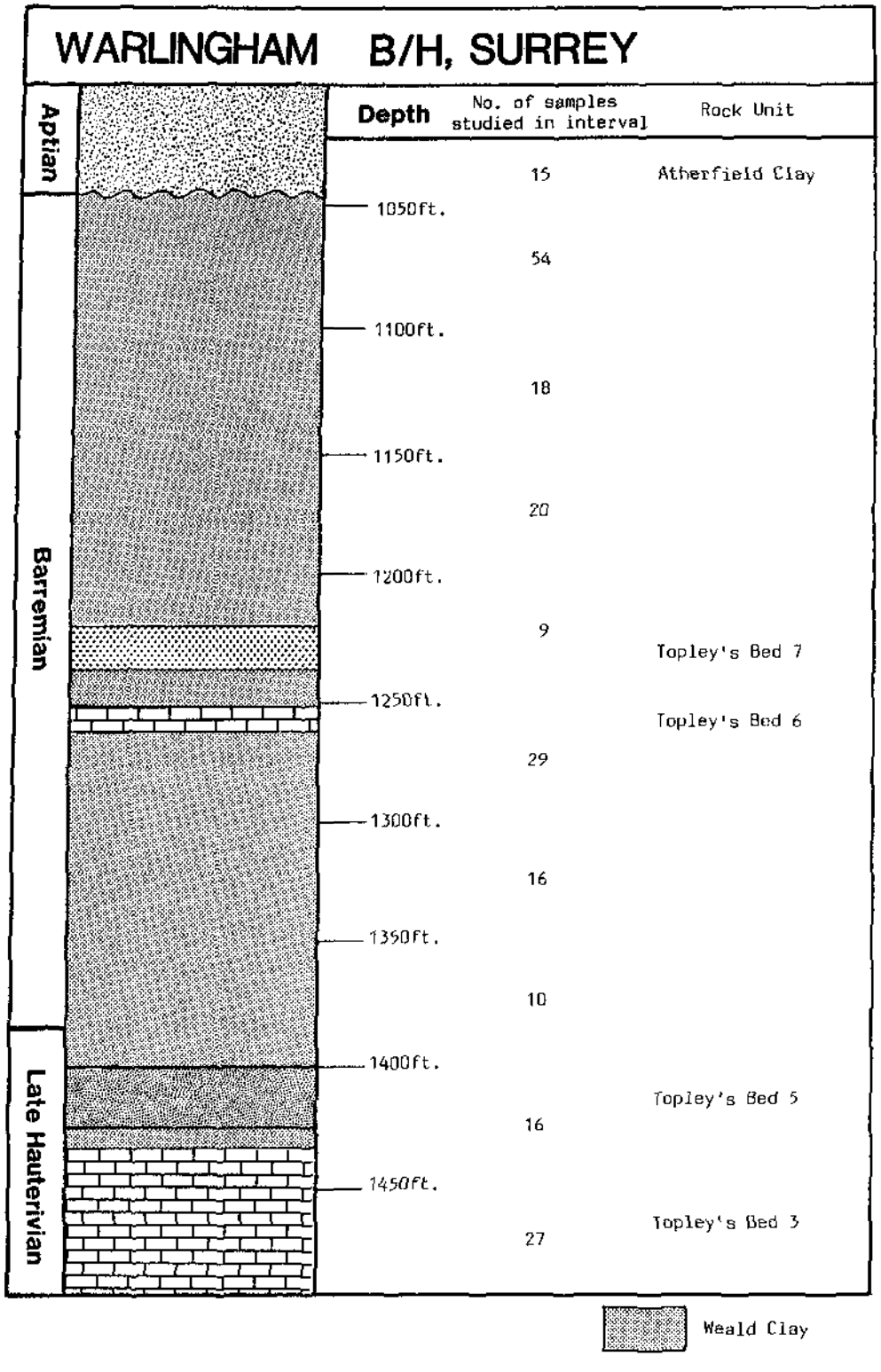

Text-fig. 6. Lithologic log of the Warlingham borehole (after Worssam & Ivimey-Cook 1973), showing the horizons identified with Topley's beds (Topley 1875). The *number of samples studied between each stated interval* is given.

3. Preparation and observation techniques

Standard palynological processing techniques were employed for the maceration of samples used in this study (see PHIPPS & PLAYFORD 1985). Additional methods largely involved the use of different oxidation reagents depending on the character of the organic component of the residue. Oxidation times were kept to a minimum, clearing being performed using NH_4OH, to avoid swelling the palynomorphs. Seiving was not performed as an additional aim of this project was to observe Barremian angiosperm pollen, which is often $\leqq 20$ µm in diameter. Routine observation was performed on strew-mounted residues using a *Philips 501B* scanning electron microscope, photomicrographs being taken on 70 mm Ilford FP4. Rapid location and relocation of specimens was achieved using Cambridge Geology Grids MK. III cemented onto the SEM stubs (see HUGHES et al., 1979).

4. Taxonomic principles

4.1 The species concept

With few exceptions, the prevalent neontological definition of the species concept can be stated as follows: a species consists of a group of interbreeding natural populations that are reproductively (i.e. genetically) isolated from other such groups. A corollary of this has been the observation that a species so defined consits of a group of organisms displaying a normal distribution (i.e. single peak variation) in morphological characteristic(s).

Clearly, the palaeontologist can only describe groups of organisms under a morpho-species concept. The morpho-species can again only be acceptable if the specimens used in the definition all came from the same defined sample, ensuring (assuming a known rate of sedimentation, etc.) that there was at least the possibility that the specimens could have interbred. It is meaningless to base a specific diagnosis on specimens from more than one sample separated either temporally or geographically as no such interbreeding of these specimens could possibly have occurred. However, even such a clustering of morphotypes from a single sample may represent an amalgamation of several morphologically similar but once genetically distinct groups. Conversely a single group of organisms may display significant phenotypic variation to cause 'splitting' of a genetically coherent unit. These possibilities can be well illustrated by examples drawn from studies of recent dinoflagellates (the observations of which are applicable to potentially fossilisable stages in the dinoflagellate life cycle) and fossil dinocysts:

4.1.1 Phenotypic variation within a single species of *Ceratium* may be so great that the morphology of the terminal cells of a vegetative chain would argue for their allocation to separate subgenera (KOFOID 1908).

4.1.2 Variation is also found in tabulation patterns. Some individuals of *Pyrophacus vancampoae* exhibit a 50% increase in the number of hypothecal plates when compared to other individuals (WALL & DALE 1971). Such spectacular variation in this case is accorded subspecific importance. In the case of *Ceratium* paratabulation variation is accorded interspecific status: amongst peridinioid dinoflagellates this feature is used as a generic determinant.

4.1.3 Although it is thought likely that the sporopollenin dinocysts recovered from sediments represent zygotic resting cysts, the possibility that vegetative resting cysts are also represented cannot be overlooked. The range of phenetic variation in the vegetative thecate stage has an as yet unknown relationship to the phenetic variation in the zygotic theca. This leaves the relationship between possible vegetative cysts and zygotic cysts equally obscure.

Taking such factors into account, grouping fossil dinocysts becomes a lottery. The dinocyst taxon should thus be thought of as no more than an artificial grouping of morphotypes which may conceivably encompass several different species and may also include specimens warranting exclusion.

4.2 Current problems

The difficulties experienced by individual workers in assigning the same specific name to identical given specimens are well known (ZACHARIASSE et al. 1978). This situation has arisen because of several factors, of which the following are a few: description of a new species based on a single specimen (allowing no statement of variation), poor illustration of type material, the study of poorly prepared/preserved material. Other problems are briefly discussed below:

4.2.1 The designation of types from different samples: A paratype has often been designated from a sample other than that from which the holotype was described. If the holotype and paratype are isolated from the same sample then there was at least the possibility that the organisms could have interbred. If the paratypes are selected from different samples a misleading impression may be given. The populations of the newly described form may have had different distributions of morphologic variability in each sample. Due to the overlap of these distributions, the paratype (whilst resembling the holotype) may be an end member of a population displaying a *significant evolutionary morphologic shift. This situation has been compounded by the fact that in the great* majority of cases a new species has been erected with no statement of the number of specimens studied.

4.2.2 Synonomies, etc.: Synonymisation and taxonomic transferrals are abused procedures in dinocyst systematics. These procedures should be performed based on the re-examination of type material or the study of *topotype material. Specimens from other localities identified with a previously published taxon from a different* geographical locality (and probably different age) do not constitute reliable data for the emendation of a species originally based on a population from a given palaeontological sample.

4.2.3 Subspecies, etc.: A subspecies is an aggregate of phenotypically similar populations which inhabit geographical subdivisions of the range of a species and which differ taxonomically from other populations of the same species (MAYR 1969). Thus the recording of two or more subspecies from a single sample indicates a misunderstanding of the concept (REYMENT 1980: 21). Equally, varieties and interspecific status can have no meaning when applied to fossils.

4.2.4 "Balloon taxa": Observations on poorly preserved palynomorph assemblages or observations made with low-resolution light microscopes have led to a "best-fit" taxonomy where specimens are "shoe-horned" into existing taxa for want of distinguishing details (PENNY 1986). This results in the "balloon taxa" of HUGHES (1970) which only serves to increase the stratigraphic ranges and decrease the stratigraphic correlation value of a given taxon.

4.3 Taxonomic procedure adopted for this work

The factors discussed above point to the fact that in the past there has been little adherence to any particular set of rules to regulate the quality of new specific designations. The lack of strict guidelines has also enabled vast synonomy listings to build up – often when type material has not been observed. This situation clearly works against ease of data handling and the assimilation of new workers to the field.

The taxonomic methods adhered to in this work when erecting new species conforms with those laid out in the Palaeo Data Handling Code (PDHC – HUGHES 1986). This is essentially a very strict set of working rules to be observed when erecting new taxa and in essence is only a tightening up of the procedures used in Linnean taxonomy. The basic idea of the PDHC is that observations of the material are recorded so that subsequently another worker may read the record and decide for himself the reliability and the degree of comparison of the record with his own material. All the observations forming the record are kept separate so as not to dilute the value of each data item and to enable their individual retrieval. This procedure is entirely compatible with the ICBN.

New morpho-species have been described from a stated number of specimens isolated from a single sample, thus allowing a statement of morphologic variation to be made. The numbers of specimens for which photographic records have been made and the number of these specimens measured for the erection of the new taxon being stated. All these specimen records contribute to the definition of the new morpho-species, and although it is desirable that they should all have equal status syn-type designation, a holotype is nominated to comply with current nomenclatural practise (the remaining specimens effectively becoming paratypes).

Specimens referable to a newly described morpho-species, but isolated from a different sample are recorded using a graded comparison statement of the similarity in the morphologies of the two populations (e.g. CfA). Allowing for a small quantitative deviation from the variation given for the type material, the new specimens are recorded as CfA occurrences. This degree of similarity is deemed sufficient for the records to be of use in stratigraphic correlation. This method has been used in manuscript notes, but these CfA records to newly described species are noted on the range charts as occurrences of the named species. Those specimens which differ from the described taxon in some qualitative aspect have been recorded as CfB occurrences in manuscript notes but are felt

to be significantly different in morphology (and rare in their occurrence) to warrant their exclusion from the taxon for the purposes of accurate stratigraphic definition to minimise ballooning of taxa. Any significant features displayed by specimens from other than the type sample of a new morpho-species, are detailed in the Remarks section at the end of each diagnosis.

The measurements for each species discussed are given in the form (X) Y (Z), being the minimum, mean and maximum values of the measured specimens respectively. The number of specimens for which an SEM record has been made is given, followed by a (usually smaller) figure in brackets which refers to the number of these records which have been used in the determination of the cited dimensions. In the case of new morpho-species, measurements of CfA records have not been included in the diagnosis in order not to dilute the value of the new taxon (but in all cases the measurements of these specimens were similar to those given). Those samples from which CfA records have been identified are given in Appendix A.

Emendations of previously described Linnean taxa have been performed only when holotype/paratype or topotype material has been examined.

4.4 Morphological procedure

The morphological nomenclature used in this work comes from Evitt (1985) which contains excellent definitions of the vocabulary in common usage. Additional terms can be found in Helenes (1986).

When discussing paratabulation, the value of Kofoidian nomenclature is unquestioned when elucidating the paraplate arrangements of peridinioid dinocysts: this is the method used herein when dealing with this group.

The more recently devised Taylor-Evitt nomenclatural system of of (para-)plate designation (e.g. Evitt 1985) has been shown to have distinct advantages over the Kofoidian system when analysing gonyaulacoids. By establishing a coherent method for recognising (para-)plate homology, the Taylor-Evitt system has imparted a new stability to the determination of the relationships between taxa. This system is employed in this paper for the description of gonyaulacoid cyst paratabulation. Using this stablised system the Kofoidian equivalents of the Taylor-Evitt designations have been used to provide a convenient short-hand method of denoting the paratabulation formula. Exhaustive comparisons of the two systems can be found in Evitt (1985) and Jan du Chene et al. (1986).

Archaeopyle nomenclature also follows Evitt (1985), with one small difference. For cavate dinocysts which have been found not to form a perioperculum upon encystment (Eaton 1985; Evitt 1985: 127), the archaeopyle type is listed as –/P. This indicates that the archaeopyle is formed by the removal of a precingular paraplate from the endocyst, there being a preformed opening in the pericyst.

The systematic descriptions have been ordered into the 'major cyst categories' of Evitt (1985), which gives a logical morphological grouping of forms.

5. Dinocyst systematics

5.1 Pp-Cysts (Ascodinium Complex)

Ascodinium fissilum sp. nov.

Plate 2, Figs. 1–8

Etymology: Latin *fissilis* – easy to split, in reference to the disintegration of the periphragm along paraplate sutures.
Holotype: Plate 2, Fig. 6.
Type locality: Gott, Bed 100, sample 100/1/83.

Diagnosis

Shape: Ambitus subcircular to peridinioid. Apical and left antapical horns developed to variable extent. Epicyst and hypocyst of approximately equal length. Greatest width in postcingular region. Strong to moderate dorso-ventral compression.

Phragma: Periphragm extremely thin (≅0.1–0.2 µm thick), laevigate. Scattered intratabular tubercles (≅0.75 µm dia.) indicate paratabulation. Endophragm ≅1 µm thick, surface densely microgranulate. Pericoels restricted to cornucavation of apical and left antapical horns, though occasionally absent.

Paratabulation: As shown by intratabular tubercles and paraplate splitting: ortho-hexa peridinioid. ?pr, 4′, 3a, 7″, ?6c, 5‴, 2⁗, 2s.

Archaeopyle: Type (4A3I), paraplates lost as a free, simple polyplacoid operculum – both periphragm and endophragm remain adpressed and are effectively lost as a single operculum.

Paracingulum: Slightly indented, generally unsculptured or with few tubercles near paraplate margins.

Parasulcus: Suppression of parasutures has reduced paratabulation to two distinguishable regions presumably representing a large *as* and *ps*+*rs*+*ls*.

Dimensions: Length (59) 52.0 (43) µm. Width (51) 44.1 (39) µm. Specimens = 14 (9).

Remarks: This species differs from all the previously described species of the genus by its much reduced cavation and the character of the wall layers. *A. hesperum* (Davey) Helénes 1983 differs in having a much thicker endophragm and being larger. A strange characteristic displayed by specimens of this species is that of partial disintegration along all paraplate boundaries. This feature is not believed due to processing techniques.

5.2 Px-Cysts

Genus *Holmwoodinium* Batten 1985

Remarks: This genus was erected by Batten (1985) to accomodate thin-walled presumed peridinioid dinocysts from the Wealden of Surrey. The single species, *H. notatum*, is stated to have a Type (4A3I) archaeopyle. The specimens described by Hughes & Harding (1985) under the biorecords Cincturo-Judith and Cincturo-Domed can be placed into this Linnean genus. The Type (4A3I) archaeopyle described by Batten (1985) is poorly shown in his illustrations, and may be of Type (3I) or Type (A3I) as that presumed for the previously mentioned biorecords. *H. notatum* may be conspecific with Cincturo-Judith, but SEM observation of this species will need to be carried out before this can be established. Cinturo-Domed is certainly a new form belonging to this genus.

5.3 Gc-Cysts

5.3.1 *Pseudoceratium*-Complex

Genus *Pseudoceratium* Gocht 1957

Remarks: The emendation of this genus by Dörhöfer & Davies (1980) is not accepted as anterior intercalary paraplates have not been observed on any of the several hundreds of specimens of this genus studied. The ventral paratabulation of this genus includes a planate apical margin to paraplate *2* as described by Bint (1986; see also Harding & Hughes, 1990).

Pseudoceratium anaphrissum (Sarjeant) Sarjeant & Stover 1978 emend.

Plate 3, Figs. 10–12; Plate 4, Figs. 1–4

1966c *Doidyx anaphrissa* – Sarjeant, p. 206, Plate 22, Fig. 8, Text-fig. 6. Barremian of the Speeton Clay in the Shell West Heslerton borehole.

1978 *Aptea anaphrissa* – Sarjeant & Stover, p. 51.

1986 *Pseudoceratium anaphrissum* – Bint, p. 145.

Emended Diagnosis

Shape: Ambitus sub-pentagonal to pear-shaped. A short blunt apical horn is usually developed. In addition to this horn a left antapical horn is usually present and may be accompanied by a right antapical horn (often expressed only as a lobe). Two lateral bulges or lobes are developed in an immediately postcingular position. Strong dorso-ventral compression. Epicyst generally larger than hypocyst, may be up to twice the length of the latter.

Phragma: Autophragm ≅1 µm thick. Pitted "orange-peel"-like surface sculpture. Apteate, intratabular processes which flare proximally and distally, exceptionally up to 15 µm in length.

Paratabulation: Tabulation pattern suggested by intratabular processes. Although poorly displayed in most specimens, a study of sufficient numbers yields a paratabulation formula of: 4′, 6′′, ?6c, 6′′′, 1′′′′, 1p, xs. *1i* is characteristically very large with an obscure adcingular boundary.

Archaeopyle: Type (4A) involving all four apicals as a free, simple operculum. Archaeopyle suture offset to the left with small accessory sutures developed adjacent to main suture in pre- and post-cingulars.

Paracingulum: Poorly developed, seen best on dorsal surface where processes are reduced anterior to a line drawn between the pronounced processes on the lateral bulges.

Parasulcus: Again poorly defined, an area of reduced processes, *ai* can be discerned.

Dimensions: Length, plus operculum (139) 119 (91) µm. Width (127) 107 (81) µm
Length, less operculum (94) 87 (79) µm.
Specimens = 40 (28).

Remarks: This species is restricted to the Hauptblätterton and corresponding facies – presumably being first described from the lateral equivalent of Bed LB1 at West Heslerton (SARJEANT 1966c). Reinvestigation of Sarjeant's type material by the present author has shown that no intercalaries are present, DÖRHÖFER & DAVIES (1980) emendation of the genus is not accepted.

Pseudoceratium aulaeum sp. nov.

Plate 1, Figs. 1–6

?1988b *Pseudoceratium pelliferum* – LISTER & BATTEN, Plate 2, Fig. 4.

Etymology: Latin *aulaeum* – embroidered wall hanging, in reference to the interwoven ectophragmal trabeculum.

Holotype: Plate 1, Fig. 1.

Type locality: Warlingham borehole, sample from depth 1044 ft. 5ins.

Diagnosis

Shape: Ambitus typically ceratioid, with long apical horn and shorter antapical and postcingular horns. Epicyst longer than hypocyst by virtue of the long apical horn. Greatest width across post-cingular horn. Strong dorso-ventral compression.

Phragma: Autophragm ≅0.2 µm thick, surface laevigate. Intratabular sculptural elements consist of irregularly distributed processes supporting an ectophragmal trabecular reticulum. Reticulum very variable, may be developed over the whole cyst (rare) or restricted to parts of the intratabular areas. Muri ≅0.4 µm in diameter.

Paratabulation: Paratabulation corniform gonyaulacoid, expressed by parasutural areas devoid of sculpture: 4′, 6′′, Xc, 7′′′, 1′′′′, 1p, Xs.

Archaeopyle: Type (tA), involving apical paraplates as a free, simple, polyplacoid operculum.

Paracingulum: Evidenced by lack of sculpture, individual paraplates not determined.

Parasulcus: Precise paratabulation not known, usually area of reduced sculpture, *ai* offset to the left.

Dimensions: Length, plus operculum (165) 144.1 (130) µm. Width (56) 50.0 (39) µm. Length, less operculum (104) 89.8 (77) µm. Specimens = 29 (21).

Remarks: This species has only been found in the presumed low-salinity assemblages of late Barremian age in the Warlingham borehole. It is distinguished from the other members of the genus by its surface sculpture. Most other species in the genus (including *P. pelliferum*) have intratabular processes of variable nature and of variable height but these are never connected distally by ectophragmal trabeculae as in *P. auleum*. Specimens identified as this new species were recorded by LISTER & BATTEN (1988b) as *P. pelliferum*.

Pseudoceratium pelliferum GOCHT 1957

Plate 1, Figs. 7 and 8

Remarks: The morphology of this species varies in the following ways:

1. Length of the apical, lateral and antapical horns. The length of the three horns may have been related to water temperature (see MUTTERLOSE & HARDING 1987a and b).

2. Expression of paratabulation. The apteate ornamentation of this species may be well developed or almost non-existant, but is generally densely spaced over the cyst surface.

Further discussion of the tabulation of this species can be found in HARDING & HUGHES (1990).

Pseudoceratium solocispinum (DAVEY) LENTIN & WILLIAMS 1975 stat. nov. et emend.

Plate 1, Figs. 9–11

1974 *Pseudoceratium pelliferum* var. *solocispinum* – DAVEY, p. 68, Plate 9, Fig. 6. Barremian Upper B Beds of the Speeton Clay, Speeton.
1975 *P. pelliferum* ssp. *solocispinum* – LENTIN & WILLIAMS, p. 2154.

Emended Diagnosis

Shape: Ambitus typically ceratioid with broad main body (L:W ratio 3:2). Hypocyst and epicyst approximately equal in length. Short, equidimensional horns in apical, postcingular and antapical positions. Pronounced dorso-ventral compression. Greatest width immediately post-paracingulum.

Phragma: Autophragm ≅1–2 μm thick. Microrugulate surface from which arise processes of varying shape. Generally processes taper from the base distally and flare at the distal extremity, rod-like or flattened in cross-section. Processes may be distally antleriform and anastomose in mid-length and rarely be joined by trabeculae. They are reduced or absent from horn extremities.

Paratabulation: Corniform gonyaulacoid. Paratabulation as indicated by intratabular apteate processes: 4′, 6′′, ?6c, 6′′′, 1′′′′, 1p, xs. *Iu* may be incorporated in parasulcus and indicated by two processes). *Y* contacts parasulcus.

Archaeopyle: Type (4A) involving the four apicals as a simple, free opercular piece. Archaeopyle suture zig-zag, sulcal notch offset.

Paracingulum: Poorly developed, more obvious on dorsal surface where anterior and posterior parasutures are delineated. *fi* larger than rest of series.

Parasulcus: Broad lanceolate area of reduced sculpture.

Dimensions: Length – less operculum (85) 73 (66) μm. Width (62) 58 (48) μm. Length – plus operculum (130) 122.6 (108) μm. Specimens = 26 (11).

Remarks: The elevation of this form to species level from subspecies level is justified by its distinct morphology. The short horns and the pronounced, robust nature of the processes set this form apart from *Pseudoceratium pelliferum*, sensu stricto. In addition, this form is smaller and occurs stratigraphically later than *P. pelliferum*.

Genus *Cyclonephelium* (DEFLANDRE & COOKSON) STOVER & EVITT 1978

Remarks: This genus embraces a wide range of cyst morphologies and will no doubt be split into several separate genera as more high resolution observation of the group is performed.

The enormous range of intraspecific variability in body shape and sculpture makes the erection of taxa extremely difficult – as is the unprofitable "shoe-horning" of specimens into previously erected species. As stated by EVITT (1985: 214), the variability is likely to reflect palaeoenvironmental conditions, but too little is known regarding the influence of the environment on these cysts for any meaningful interpretations to yet be made. One factor that has become clear is that paratabulation is better expressed on specimens extracted from sediments deposited in low salinity conditions. According to BINT (1986), this genus is comprises both ceratioid and dorso-ventrally compressed gonyaulacoid cysts. The two types being distinguished by the shape of the first precingular

paraplate. The three main types recognised here all have planate first precingulars and thus fall into the Gc-cyst category:

5.3.1.1 *C. distinctum.* This "balloon" taxon has been used for all the specimens displaying a subcircular ambitus and with coarse, distally flaring processes widely spaced over the cyst surface. There may be antapical bulges formed and the processes are usually reduced or absent from mid-dorsal and mid-ventral regions. (Plate 3, Figs. 1–3).

5.3.1.2 *C.* sp. I. This is a large, thin-walled, uncommon form with very reduced surface sculpture. Processes are short and stubby, with two antapical lobes being developed on the hypocyst. (Plate 3, Figs. 4–6).

5.3.1.3 *C.* sp. II. Again an uncommon form, similar to *C. distinctum,* but with a greater density of more slender processes concentrated in marginate areas. (Plate 3, Figs. 7–9).

5.3.2 *Muderongia* Complex

Remarks: Species of the genera *Muderongia* and *Phoberocysta* display great intraspecific variability. The former genus displays its greatest abundance in brackish-marine sediments and is thus of significant palaeoenvironmental value, whilst the marine examples are few in number but of diverse morphologies. The emendation of the genus *Muderongia* by Jain & Khowaja-Ateequzzaman (1984) is not accepted. Their emendation excludes species placed in the genus which possess five horns, these species are placed in new genus, *Pseudomuderongia.* However, in their examples of *M. mcwhaei* there is clearly a vestigial right antapical horn (in addition to the left antapical, two post-cingular and an apical horn), thus invalidating their emendation.

It appears unlikely that the subspecies of *Phoberocysta neocomica* recognised by Gocht (1957) are distinguishable, being due rather to phenotypic variation.

All the taxa examined herein in this group have been shown to possess planate first precingular paraplates.

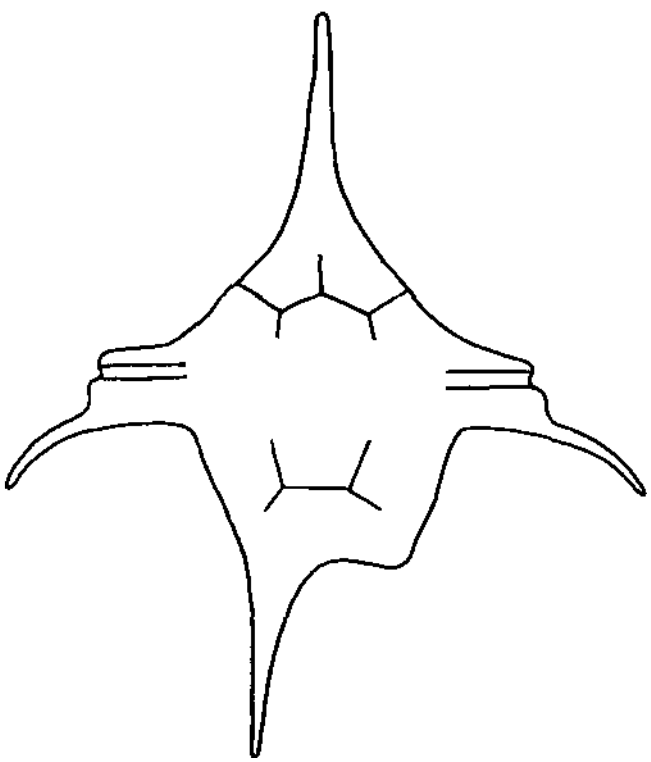

Text-fig. 7. Idealised dorsal reconstruction of a complete specimen of *Vesperopsis longicornis* comb. nov.

Vesperopsis longicornis BATTEN & LISTER 1988 comb. nov. et emend.

Plate 2, Figs. 1–5; Text-fig. 7

?1988b *Australisphaera* sp. A. – LISTER & BATTEN, p. 27, Plate 3, Figs. 10, 14.
1988 *Australisphaera longicornis* – BATTEN & LISTER, p. 340–341, Figs. 1b–e, g.

Emended Diagnosis

Shape: Ambitus typically ceratioid/muderongioid. Main body basically pentagonal in outline modified by apical, two lateral (post-cingular) and two antapical horns. Epicyst and hypocyst of equal length. Greatest width across post-cingular horn extremities. Strong dorso-ventral compression.

Phragma: Autophragm thin (≦1 µm), laevigate to microgranulate. Developed into long tapering horns in apical and left antapical positions. Right antapical position may be occupied by a well developed horn or, more usually by only a bulge. Paracingular bulges in the periphragm are sub-rectangular in shape and bear downward curving horns on their distal antapical extremities.

Paratabulation: As far as can be determined, typically corniform gonyaulacoid. Paratabulation of the epicyst is 4′, 6″ + *ai* indicated by the archaeopyle suture.

Archaeopyle: Type (tA), involving the apical series as an attached, simple, polyplacoid operculum. The operculum is often found to have been mechanically removed (Plate 2, Fig. 5). Parasulcal notch offset to the left.

Paracingulum: Developed between bar-like autophragmal outgrowths of the precingular and postcingular paraplate series, as a parallel sided indentation.

Parasulcus: *ai* offset to left, rest of the tabulation of this area is unknown.

Dimensions: Length, plus operculum (136) 119.5 (100) µm. Width (90) 70.7 (68) µm. Length, less operculum (90) 79.8 (70) µm. Specimens = 23 (15).

Remarks: Following a re-examination of the type material of *Australisphaera fragilis* HARDING 1986a, the emendation of the genus *Australisphaera* (HARDING, 1986a: 100) is questioned. The two closely adpressed wall layers described for the type material of A. fragilis have been found to be an artifact of preservation. By far the majority of specimens of *A. fragilis* are found with an adnate operculum. It is clear that most of the specimens of this species which are found without operculae lost this part of the cyst by mechanical disruption – either post-mortem or during processing (HARDING, 1986a, Pl. 17, Fig. 9, clearly shows a torn ventral archaeoplye margin). Thus it is felt unwise to maintain the generic assignment of *A. fragilis*. Following STOVER & WILLIAMS (1987), all early Cretaceous identifications of the genus *Australisphaera* are treated as suspect.

The species described by BATTEN & LISTER (1988: 340–341) cannot be allocated to *Muderongia* COOKSON & EISENACK or *Nyktericysta* BINT, as both of these genera possess two wall layers. Although *A. longicornis*, as illustrated by BATTEN & LISTER (1988, Figs. 1b–e, g), appears to possess a free operculum, the paratabulation along the principal archaeopyle suture is very difficult to determine. This may also be the result of mechanical damage, as the vast majority of specimens observed during the present study possess adnate operculae (Pl. 2). With these facts in mind, and those already given above, it appears unwise to allocate this species to the genus *Australisphaera* DAVEY. The adnate nature of the operculum of the majority of specimens of this species in the present study would argue for placement into the genus *Vesperopsis* BINT 1986. The species of this genus all possess adnate operculae, however, these are attached ventrally via the parasulcal region, whereas the site of attachment in the present species would appear to be dorsal.

This species is usually found crumpled and in a relatively poor state of preservation due to the diaphanous nature of the autophragm. However, the mounting of individual well-preserved specimens in this study has allowed a clarification of the morphology. This species is distinguished from other members of the genus *Vesperopsis* by the more complicated morphology of the lateral/post-cingular horns. LISTER & BATTEN found this species to be rare in the samples from the Hurlands Farm Borehole (LISTER & BATTEN, 1988b), but no abundance information was given in the specific diagnosis of BATTEN & LISTER (1988) from the Weald Clay of the Isle of Wight. In the present study this species has been found in often flood abundance in the highest parts of the Weald Clay in the Warlingham borehole, associated with *"A." fragilis* (as found by BATTEN & LISTER, 1988: 340).

Generic reallocations:

Following restudy of *Australisphaera fragilis* HARDING 1986a, this species is transferred to *Vesperopsis* BINT 1986, the two wall layers observed by HARDING (1986a) having been found to be artifacts of preservation. *A. pseudovitrea* LISTER & BATTEN 1988b is also transferred to *Vesperopsis* on the basis of its similarity to other species of the genus and its possession of a single wall layer.

Vesperopsis fragilis comb. nov. = *Australisphaera fragilis* HARDING 1986a, p. 100, Plate 16, Figs. 6–9, Plate 17, Fig. 9, Text-fig. 2.

Vesperopsis pseudovitrea comb. nov. = *Australisphaera pseudovitrea* LISTER & BATTEN 1988b, p. 25, Plate 3, Figs. 2–3, Text-fig. 6.

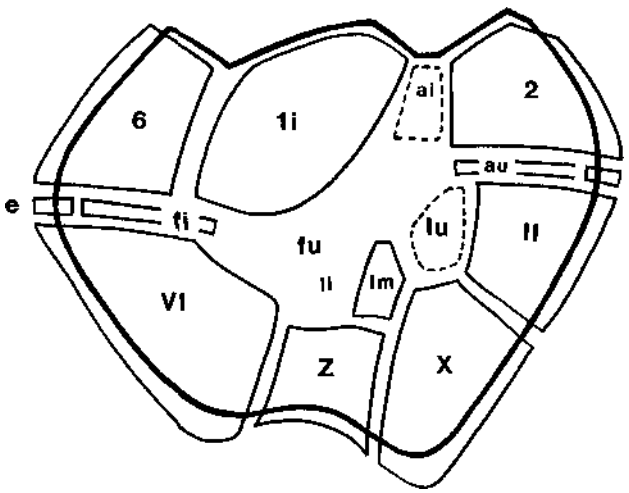

Text-fig. 8. Reconstruction of the ventral paratabulation of *Canningia duxburyi* sp. nov., note that there is often no ectophragmal representation of the *lu* paraplate.

5.4 Gv-Cysts (Areoligera Complex)

Canningia duxburyi sp. nov.

Plate 5, Fig. 1–13; Text-fig. 8

1977 *Canningia* cf. *reticulata* – DUXBURY, p. 26, Plate 8, Fig. 6, Plate 9, Fig. 1. Hauterivian C Beds of the Speeton Clay at Speeton.
1979 *Canningia* cf. *reticulata* – DAVEY, Plate 4, Figs. 11–12.

Etymology: Named after Stanley Duxbury, who first published details of this species.

Holotype: Plate 5, Fig. 1.

Type locality: Hunstanton borehole, Norfolk, sample from depth 195 ft.

Diagnosis

Shape: Ambitus rounded, sub-pentagonal. Pronounced apical horn with lobate antapical region – often developed into two antapical horns of which the left is the most pronounced. Width greatest across paracingular region. Epicyst and hypocyst of approximately equal length. Strong dorso-ventral compression.

Phragma: Ectophragm very thin (≅ 0.3 µm thick), highly perforate and interrupted along parasutures, thus indicating paratabulation. Autophragm (≅ 1 µm thick) has pitted "orange-peel"-like surface sculpture. Ectophragm supported on processes and septa (up to 6 µm high) which form arcuate or linear process complexes. The processes and septa appear to be both intratabular and penitabular in nature depending on situation. Ectocoels are irregularly developed, reduced in dorsal areas and may be absent in ventral areas if ectophragm undeveloped.

Paratabulation: Sexiform gonyaulacoid, paratabulation: 4′, 6″, ?6c, 6‴, 1⁗, 1p, xs. Antapical lobes involve *X/Y/Z* and *VI/Y/Z* triple junctions.

Archaeopyle: Type (4A): loss of apicals as a simple polyplacoid operculum.

Paracingulum: Difficult to discern on many specimens as it is obscured by the disruption of the ectophragm. Individual paraplates are represented by narrow intratabular septa supporting narrow strips of ectophragm. On the ventral surface the septa become discontinuous and may be represented by processes.

Parasulcus: Offset to the left, ectophragmal layer much reduced or absent.

Dimension: Length, less operculum (94) 78.1 (66) µm. Width (120) 93.8 (80) µm. Length of operculum ≅ 35 µm. Specimens = 45 (42).

Remarks: This species was first described by DUXBURY (1977: 26–7) as *Canningia* cf. *reticulata* (also illustrated by DAVEY 1974, Plate 4, Figs. 11–12), and clearly conforms to the recently emended description of *Canningia* (HELBY 1987).

This new species differs from the species described by HELBY (1987): it has an ectophragm which clearly breaks into paraplate related areas (unlike *C. reticulata* COOKSON & EISENACK 1960b and *C. grandis* HELBY 1987), has a much more robust ectophragmal reticulum than *C. pistica* HELBY 1987 and a much wider ectocoel than *C. transitoria* STOVER & HELBY 1987. It differs from *C. senonica* CLARKE & VERDIER 1967 by having a much more robust, angular autophragm and a much narrower ectocoel.

The adcingular margin of paraplate *X*, and the adsulcal margin of *II*, clearly show that *Iu* (which is not always indicated by ectophragmal development) lies outside the parasulcus. This indicates a gonyaulacoid affinity, rather than a ceratioid one, even though the first precingular paraplate is clearly planate (see BINT 1986. See also Plate 5, Figs. 5, 8 and 11 herein).

5.5 Gs-Cysts

5.5.1 *Spiniferites* Complex

Achomosphaera neptunii (EISENACK) DAVEY & WILLIAMS 1966a

Plate 4, Figs. 5–7

Remarks: From the SEM study of this species it has been possible to verify the observations of DUXBURY (1980) and to prove that this easily identifiable form has a Type P_4 precingular archaeopyle. The resulting operculum is reduced. This contrasts with previous misinterpretations of an apical archaeopyle. The processes are clearly parasutural in position (not intratabular as stated by STOVER & EVITT 1978: 139). The surface of the processes is laevigate becoming corrugate proximally where they merge into the rugulate body sculpture. Distally the processes bifurcate or trifurcate (depending on intergonal or gonal postion), and further tri- or bi-furcate respectively.

Avellodinium falsificum DUXBURY 1977

Plate 4, Figs. 8–9

Remarks: A relatively uncommon species which is distinguished from the mass of *Spiniferites* Complex forms by both its Type Ea archaeopyle and its flattened processes. The processes are an extension of the low parasutural septa and are blade-like or Y-shaped in cross-section (intergonal and gonal processes respectively). The paracingulum is distinctive because of its lozenge shaped paraplates. The archaeopyle suture is planar and does not conform to the zig-zag margin of the paracingulum (Plate 4, Fig. 9). The operculum is therefore reduced. The cyst surface is spongy or irregularly reticulate-foveate. The paracingular processes are not tubular and are not of the type found in *Callaiosphaeridium* as suggested by BELOW (1981).

Spiniferites dentatus (GOCHT) DUXBURY 1977

Plate 4, Figs. 10–12

Remarks: The parasutural septa of this species are variable in their development both in height and development of processes (scalloped to vaginate) surmounting them. However, a constant diagnostic feature is that of the bifurcations of these septal processes, as mentioned by DUXBURY (1977: 49). A feature apparently unnoticed by previous workers is the prominent ventral claustrum in the parasulcus (Plate 4, Fig. 10). Operculum reduced.

Spiniferites spumeus sp. nov.

Plate 6, Figs. 1–8

Etymology: Latin *spumeus* – foaming, frothy, in reference to the vacuolar nature of the cyst wall.
Holotype: Plate 6, Fig. 1.
Type locality: Gott, Bed 183.

Diagnosis

Shape: Ambitus prolate ovoid, modified by gonal processes up to 1/3 of body diameter in length. Epicyst and hypocyst of equal lengths. Little or no dorso-ventral compression.

Phragma: 'Differentiated autophragm', up to 2.5 μm thick. Wall consists of a spongy (vacuolar) layer of sporopollenin. Thickness of wall apparently reduced along parasutures. Cyst surface of "orange-peel" texture, pseudo-punctate. Low parasutural crests indented into cyst surface, surmounted by basally hollow gonal processes, angular in section. Processes trifurcate distally and may bifurcate once more.

Paratabulation: Sexiform, weakly S-type gonyaulacoid. Paratabulation formula: 4′, 6″, 6c, 6‴, 1⁗, 1p, ?5s.

Archaeopyle: Type P_4, lost as free monoplacoid operculum.

Paracingulum: Well developed. Paracingular gonal processes may be united across paracingulum up to the point of trifurcation, by the development of an often perforate septum. S-type, most paraplates usually being defined.

Parasulcus: The septa between the paracingular gonal processes may extend into the parasulcus and create a claustrum in the periphragm.

Dimensions: Length (75) 67.6 (63) μm. Width (65) 58.2 (51) μm. Specimens = 6 (6).

Remarks: This species differs from all the other members of the genus in its characteristic surface sculpture and the indented parasutural septa. A similar (ancestral?) species occurs in rocks of early Barremian age at Gott and Speeton, but always has intergonal processes and a thinner cyst wall.

Cannosphaeropsis hughesii sp. nov.

Plate 6, Figs. 9–16

Etymology: named after my supervisor, Dr. Norman Hughes.
Holotype: Plate 6, Figs. 10 and 14.
Type locality: Gott, Bed 50.

Diagnosis

Shape: Ambitus subcircular to prolate ovoidal. Outline modified by parasutural processes and ectophragmal trabeculae. Greatest width across posterior cingular parasuture. Hypocyst slightly longer than epicyst. Apparently no dorso-ventral compression.

Phragma: Ectophragm reduced to rod-like trabeculae (≅ 0.7 μm dia) which appear to be looped from one parasutural process to the next. Trabeculae posses small distal outgrowths or nodes. Autophragm ≅ 1.5 μm thick, cyst surface has "orange-peel" texture with rare hemispherical intratabular tubercles (≅ 1.5 μm dia). Parasutural processes are solid, cylindrical (≅ 1 μm dia) and usually discrete but may anastomose and bifurcate. Height of processes up to 5 μm.

Paratabulation: L-type sexiform gonyaulacoid. Paratabulation as indicated by parasutural processes and trabeculae: 4′, 6″, 6c, 6‴, 1⁗, 1p, 5s. Size and relationships of paraplates difficult to determine in many cases due to compression and displacement of trabeculae. *ai* large with *ai/1u* just posterior to *A/1i*. *1u* elongate and narrow along parasulcus.

Archaeopyle: Type P_4, free, monoplacoid operculum, slightly reduced.

Paracingulum: Marked by parallel trabeculae, laevorotatory, displaced by two cingulum widths.

Parasulcus: L-type, clearly consisting of 5 sulcals and *1u*.

Dimensions: Length (49) 45 (43) µm. Width (42) 38.8 (36) µm. Specimens = 5 (5).

Remarks: A rare species encountered in the oldest samples studied, it lacks parasutural septa and thus does not conform to WILLIAMS & DOWNIE's (1966) diagnosis of the genus *Nematosphaeropsis*. Differs from other species of *Cannosphaeropsis* by its small size and the diminutive extra-trabecular nodes.

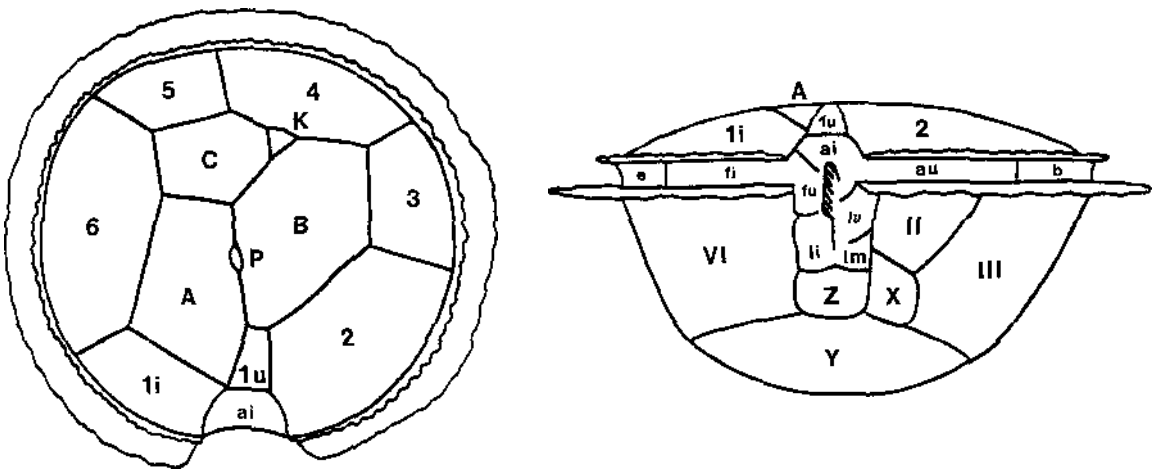

Text-fig. 9. Reconstruction of the apical and ventral paratabulation of *Ctenidodinium complanatum* sp. nov., showing metasert condition.

5.3.2 *Ctenidodinium* Complex

Ctenidodinium complanatum sp. nov.

Plate 7, Figs. 1–12; Text-fig. 9

Etymology: Latin *complanatus* – flattened out in one plane, in reference to the oblate nature of the cyst.
Holotype: Plate 7, Fig. 1.
Type locality: Speeton, Bed LB5B–D.

Diagnosis

Shape: Strongly oblate spheroid, ambitus thus rarely seen, subcircular apical or antapical views being more common. Epicyst is pronouncedly flattened with *P* forming a short apical prominence, hypocyst much larger than epicyst. Pronounced polar compression.

Phragma: Differentiated autophragm ≅ 1 µm thick, consisting of a solid base layer surmounted by a thicker spongy granular layer. The cyst outer surface appears pitted and spongy. The parasutural septa are usually less than 3 µm in height with denticulate margins. However, along the paracingulum the septa are higher, up to 8 µm, varying from distally denticulate to deeply denticulate to fenestrate. Anterior cingular parasutural septum much lower than the posterior one.

Paratabulation: Metasert sexiform gonyaulacoid shown by denticulate septa. Paratabulation formula: 1pr, 4′, 1a, 6″, 6c, 6‴, 1⁗, 1p, 5s. Due to oblate nature of cyst, apicals and antapical are large in relation to other paraplates. *A* is characteristically in contact with *1u* and *B* but not with *2* – metasert condition. *1u* is very small, incidental paraplate *(K)* appears at *B/C/4* triple junction.

Archaeopyle: Type Ea involving all epicystal paraplates. Operculum reduced so that the anterior cingular parasutural septum is left attached to the paracingulum. Simple polyplacoid operculum remains adnate to *ai*.

Paracingulum: Well developed, posterior parasutural septum up to 6 µm wide, may be in the form of a solid septum, distally denticulate, or with ovate fenestrations, or deeply incised into blade-like processes.

Parasulcus: L-type, reduced in size due to large *Y*. Flagellar scar prominent, deep elongate pit.

Dimensions: Diameter (50) 47 (45) µm. Specimens = 4 (4).

Remarks: A rare but distinctive species, differing from the other species placed in the genus by its low denticulate parasutural septa and metasert condition. *C. elegantulum* a much larger form, is the only other member of the genus to be found at such a high stratigraphic level.

According to BENSON (1985) the genus *Ctenidodinium* should be distinguished from *Dichadogonyaulax* by the possession of anterior intercalaries (incidentals of EVITT 1985), and an apically located preapical paraplate. However, BENSON (1985) states that the preapicals of *Dichadogonyaulax* are "displaced ventrally" allowing *A* and *B* to touch each other. Although complying with the description of *Ctenidodinium* in *C. complanatum* paraplates *A* and *B* are in contact, perhaps indicating that this new species may be intermediate in morphology between the two genera. *C. complanatum* has asymmetrical-quadrate antapical and *1u/1i* ventral arrangements, however, the apical arrangement does not conform to any of the schemes given by HELENES (1986). *Dichadogonyaulax irregulare* BENSON 1985 differs from this new species in lacking incidental paraplates, having septal crests of different form and by having a laevigate periphragm.

Dichadogonyaulax irregulare BENSON 1985

Plate 7, Figs. 13–16

Dimensions: Diameter (58) 49.1 (41) μm. Specimens = 18 (13).

Remarks: BENSON (1985) described this species from offshore North America and stated that it was of Neocomian age. The specimens here attributed to this species have only been found in samples of late Hauterivian age from the Hunstanton borehole. The specimens display preapical paraplates but no incidental paraplates, and conform with specimens illustrated by BENSON (1985: Plate 2).

Genus *Heslertonia* (SARJEANT) DUXBURY 1980

Remarks: This genus should be placed in the *Ctenidodinium* Complex of Gs-Cysts, as the type species has a Type Ea archaeopyle (DUXBURY 1980), and not in the *Leptodinium* Complex as stated by EVITT (1985: 222).

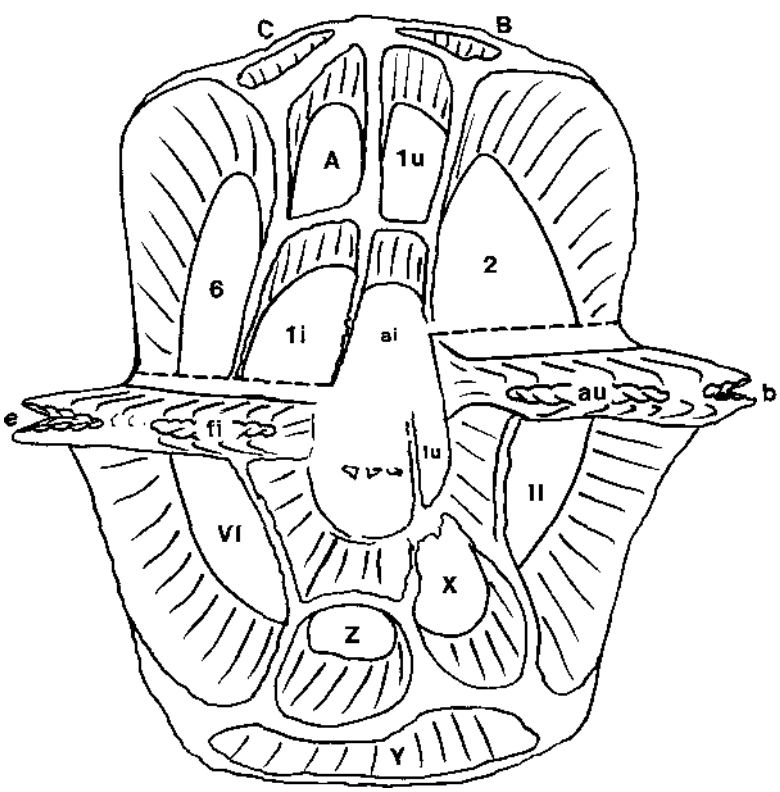

Text-fig. 10. Reconstruction of the ventral paratabulation of *Heslertonia senectus* sp. nov., *H. heslertonensis* is essentially similar, except that *A/1u* is suppressed.

Heslertonia senectus sp. nov.

Plate 8, Figs. 1–11; Text-fig. 10

Etymology: Latin – *senectus* – old age, in reference to the wrinkled nature of the intratabular areas.
Holotype: Plate 8, Fig. 1.
Type locality: Gott Bed 187.

Diagnosis

Shape: Central body spheroidal to prolate ovoidal. Ambitus modified by the high parasutural septa into a more polygonal shape. Greatest width across paracingulum. Hypocyst marginally longer than epicyst. accentuated by the greater development of septa. No dorso-ventral compression.

Phragma: Periphragm extremely thin (≦1 μm), closely adpressed to the endophragm in intratabular areas where it is wrinkled, forming a characteristic rugulate sculpture (rugulae ≅0.25 μm wide). Septa formed by outfolds if the periphragm (causing suturocavation), thus septa are two-layered and usually distally entire (if open the edges are denticulate). Septa covered in parallel, radiating striae or corrugations. Septa may exhibit circular claustra which may develop into septal fenestrations at the base of the septum. Endophragm spheroidal to ovoidal, ≦1 μm thick, surface sculpture not observed.

Paratabulation: Sexiform L-type gonyaulacoid. Paratabulation formula: 4′, 6″, 6c, 6‴, 1⁗, 1p, 5s. Sulcal parasutures partially supressed.

Archaeopyle: Type Ea, simple reduced operculum, adnate via *ai*, but may be removed mechanically.

Paracingulum: Very prominent double layered septum forms a paracingular 'tunnel' which is perforated in intratabular areas, the edges of the perforations being denticulate.

Parasulcus: Rarely observed, parasutures suppressed so that septa reduced or replaced by denticles.

Dimensions: Length (70) 61.6 (53) μm. Width (62) 52.6 (45) μm. Specimens = 13 (11).

Remarks: A late Barremian species of the genus which differs from the other members of the genus by its rugulate sculpture (*H. heslertonensis* the other Barremian species of the genus does not have a rugulate periphragm, see Plate 8, Fig. 12). *H. teichophera* and *H. striata*, Jurassic and late Cretaceous species respectively, both have striate septa but lack the conspicuously rugulate intratabular areas. The latter two species are also stated to possess Type P_4 archaeopyles, but this is uncertain.

5.5.3 *Wanea* Complex

Dissiliodinium sp.

Plate 9, Figs. 1–7

Dimensions: Diameter (62) 54.4 (43) μm. Specimens = 18 (11).

Remarks: It is unlikely that this form is conspecific with *D. globulum* Drugg 1978 (restricted to French Lower Kimmeridgian strata) due to its much higher stratigraphic occurrence. Below (1981) reported the latter form from the Hauterivian to Albian of Morocco. Unfortunately his SEM specimens of this species were somewhat corroded (Below 1981: Plate 15, Figs. 3–4). The size range of the three types is similar but the type found in this study appears much thinner walled. The sculpture of the autophragm, a dense cover of clavate granules/spinules (≅0.2 μm dia), is very distinctive. This form is restricted to rocks of late Barremian age of all the sections studied save for Speeton where two isolated specimens were found in the early Barremian.

Contrary to Evitt's (1985: 142) idea that this genus has a Type 6P archaeopyle, observations made agree with Drugg (1978: 67–8) and Below (1981: 46) that the archaeopyle is formed by the loss of paraplates *2–6*, the apical paraplate series remaining adnate via a 'sulcal' tongue comprising *ai* and *1i*. Accessory archaeopyle sutures are sometimes seen between *1u/A, B, C* but these plates remain attached at the apex of the cyst. Occasionally the precingular series remain attached adcingularly, only accessory archaeopyle sutures forming between these paraplates. *ai/1u* is adcingular to *a/1i*.

Hurlandsia rugarum (Piasecki) Lister & Batten 1988a

Plate 9, Figs. 8–14

Dimensions: Length (80) 71.5 (64) μm. Width (88) 72.7 (57) μm. Specimens = 59 (16). Specimens = 59 (16).

Remarks: Lister & Batten (1988a, p. 507–8) described species of this new genus from rocks of a similar age to those from which the present specimens have been isolated. Their diagnosis is accepted although the paratabulation of the species appears to be entirely consistent with a typical sexiform organisation (i.e. 6 pre- and 6 post-cingular paraplates), this interpretation does however conflict with those of Piasecki (1984) and Lister & Batten (1988a). Epicystal paratabulation shows an elongate *1u*, longer than *A*, with a larger *1i* than interpreted by Piasecki (1984: Fig. 5). Sulcal paratabulation is uncertain, but a flagellar scar is occasionally developed. The discernable paratabulation indicates that this species lies in the *Wanea* Complex of Gs-Cysts of Evitt (1985). The specimens found in this study display the same microrugulate sculpture of the autophragm as that illustrated by Piasecki (1984: Plate 4, Figs. 7–8) and Lister & Batten (1988a, Fig. 4C). The simple epicystal operculum remains attached to the sulcal area via *ai* and is only rarely separated from the hypocyst. Isolated epicysts and hypocysts are therefore uncommon.

This species has been positively identified in the upper Weald Clay from the Warlingham borehole (this study) and from a comparable horizon in the same lithology in the Hurlands Farm borehole, Sussex (Lister & Batten 1988a and b), occurring in flood abundance in both monospecific and low-diversity dinocyst assemblages. In Warlingham, the rocks in which it is found lie above those containing *Cribroperidinium boreas*, a species restricted to the late Barremian. Thus, these specimens are of a late Barremian age. Piasecki (1984), showed that his specimens were of latest Ryazanian to earliest Valanginian age on palynological and ostracod evidence. The discrepancy in the dating of the two occurrences of this species may indicate that *Hurlandsia rugarum* is a stratigraphically long-ranging species restricted to presumed low-salinty environments. Alternatively the age of the Danish material may have been wrongly inferred.

5.5.4 *Leptodinium* Complex

Athigmatocysta glabra Duxbury 1977

Plate 10, figs. 1–3, 5, 6

Remarks: This rare species is not encountered in samples younger than early Barremian in age. The phragma are thin (periphragm ≅ 0.75 μm, endophragm < 0.5 μm) and prone to crushing. S-type sexiform gonyaulacoid paratabulation of: 2pr, 4′, 6″, 6c, 6‴, 1⁗, 1p, 5s, indicated by parasutural ridges. These ridges are semicircular in section ≅ 1 μm in height and width and distally 'nodular'. This latter feature may have been interpreted by Duxbury (1977) as denticulations of the parasutural ridges. *1u* is long and sickle-shaped with a very small *A*, approximating *Q* in size. This morphotype displays a Jurassica-pattern paratabulation, with symmetrical antapical, *Q/B* apical and *1u/1i* ventral arrangements (Helenes 1986). Some specimens however, do show a loss of the *A/1i* contact (Plate 10, Fig. 5) as in *Gonyaulacysta fastigiata* (Helenes 1986: 80).

The transferals of this species to the genera *Endoscrinium* (Below 1981) and *Scriniodinium* (Jan du Chêne et al., 1986b: 315, and Stover & Williams 1987: 27) are not accepted as the paratabulation of the sulcal and apical regions in *Athigmatocysta* is clearly of a different character from that found in any of the species in these genera.

Chlamydophorella trabeculosa (Gocht) Davey 1978

Plate 10, Figs. 4, 8–16

Remarks: This species has been found to display paratabulation compatible with that of the *Leptodinium* Complex. Paratabulation is expressed on the surface of the tenuous ectophragm by rather inconspicuous ridges. The ectophragm is ≅ 0.1 μm thick and highly perforate (although the perforations are < 0.1 μmin dia.). The paratabulation formula is apparently typically L-type sexiform gonyaulacoid, although the apical nature of the

archaeopyle means that *1i* is very elongated and *A* consequently reduced in length. Archaeopyle is Type (tA) involving four apical paraplates. Some specimens display an adnate operculum, but usually this is lost by tearing across *1u*.

Autophragm is laevigate with a dense cover of solid, cylindrical, intratabular processes up to 3 µm long which flare proximally and distally. Each process base is surrounded by an areola of punctae. The point of contact of the process with the ectophragm is marked on the distal surface by a small depression.

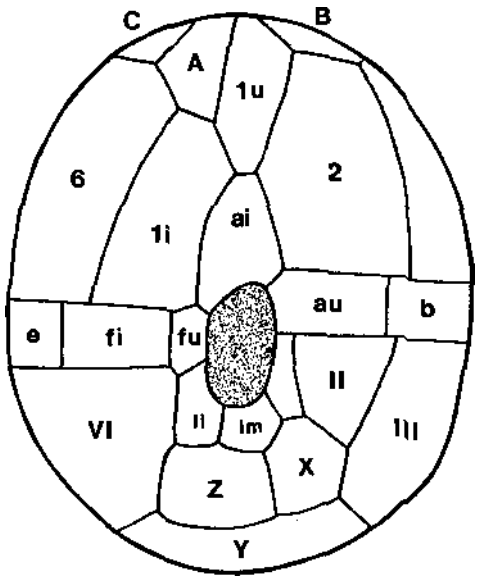

Text-fig. 11. Reconstruction of the ventral paratabulation of *Hystrichostrogylon stolidota* (parasulcal claustrum shown stippled).

Hystrichostrogylon stolidota (Duxbury) Stover & Williams 1987 emend.

Plate 11, Figs. 1–8; Text-fig. 11

1980 *Diphasiosphaera stolidota* – Duxbury p. 116, Plate 1, Figs. 5, 9, Text-fig. 6. Barremian Middle B Beds of the Speeton Clay, Speeton.
1987 *Hystrichostrogylon stolidota* – Stover & Williams, p. 81

Emended Diagnosis

Shape: Ambitus elongate ovoidal, modified by rare development of apical prominence and projecting parasutural processes. Greatest width across paracingulum. Epicyst and hypocyst equal in length. Endocyst ambitus subcircular to ovoidal, barely two thirds the length of the pericyst. Slight dorso-ventral compression.

Phragma: Periphragm thin ≅ 0.3 µm, with 'orange-peel' surface sculpture. Periphragmal claustrum developed in region of flagellar scar. *Spiniferites*-type processes extend distally from low ridges which delineate parasutures. The processes are of variable height depending on the degree of cavation. The greater the cavation the shorter the length of the process stalks. Processes bifurcate (or trifurcate if gonal) and may bifurcate again. In cases of extreme cavation the process terminations only are developed along the parasutural ridges, appearing as a double row of processes. Endophragm has a thick wall with a granular surface. Cavation is often complete, but there may be contact between the two wall layers dorsally.

Paratabulation: L-type sexiform gonyaulacoid. Paratabulation formula: 4′, 6″, 6c, 6‴, 1⁗, 1p, 5s.

Archaeopyle: Type P_4/P_4. Opercula both free, monoplacoid.

Paracingulum: In most cases difficult to determine due to collapse of cyst. No indentation in ambital view, laevorotatory, displaced by ≅ 2 cingulum widths.

Parasulcus: Periphragmal claustrum in flagellar scar region is often of a very large size (up to 18 µm × 18 µm), similar to that of the archaeopyle. L-type ventral paratabulation developed around this claustrum.

Dimensions: Length (62) 55.0 (42) µm. Width (56) 47.6 (40) µm. Specimens = 64 (20).

Remarks: The variability of this species is marked and probably phenotypic. The apical prominence noted by DUXBURY (1980) is an uncommon feature. This cyst type is common in the early Barremian of most sections studied (except for Speeton which may explain why Duxbury believed it to be restricted to the Cement Beds), disappearing in late Barremian time. The L-type ventral organisation of this species is the reason for placing it in this Cyst Complex, almost all of the *Spiniferites* Complex cysts have S-type ventral organisation.

Following the paratabulation patterns of HELENES (1986), the antapical region displays a symmetrical arrangement and the ventral region a *1u/1i* arrangement. The apical pattern has not been determined.

The type species of the genus, *H. membraniphorum* AGELOPOULOS 1964, differs from *H. stolidota* in having only hypocystal cavation. Whereas *H. coninckii* HEILMANN-CLAUSEN 1985 possesses an extremely large mid-ventral claustrum, that in *H. stolidota* is of much smaller dimensions, with paratabulation features clearly indicating it to be developed in a region equivalent to the site of flagellar insertion on the motile cell.

Hystrichostrogylon sp.

Plate 12, Figs. 12–14

Remarks: This distinctive form has only been found in the lowest Barremian rocks of two of the studied sections (Speeton and Hunstanton) and may prove to be a valuable stratigraphic marker. It has an obvious periphragmal claustrum in the flagellar scar region; paratabulation is the same for the preceeding species, but is usually indicated by a double row of crenellate septa. Few well preserved specimens have been observed thus far so the formal description of this form as a new species is not attempted here.

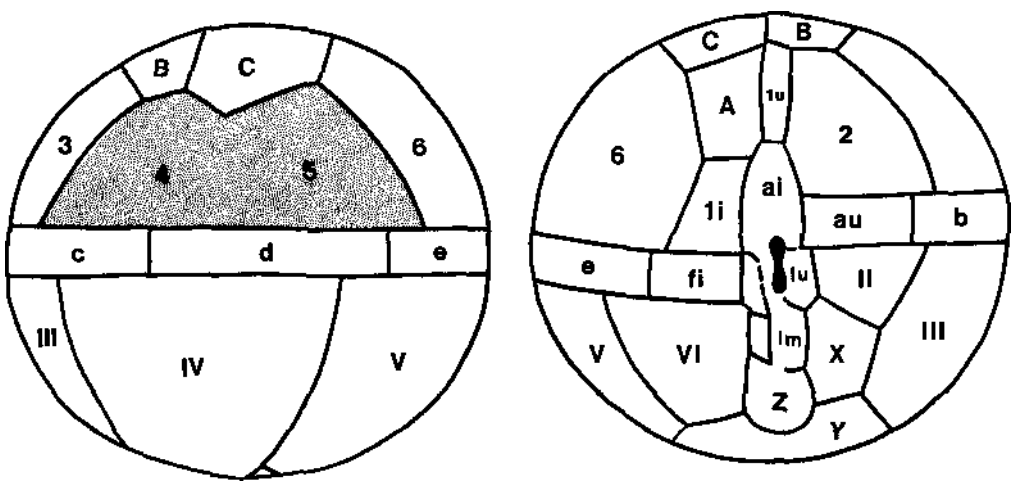

Text-fig. 12. Reconstruction of the dorsal (left) and ventral (right) paratabulation of *Exiguisphaera phragma*, the $2P_{4,5}$ archaeopyle is stippled.

Exiguisphaera phragma (DUXBURY) JAN DU CHÊNE et al. 1988a

Plate 12, Figs. 1–11; Text-fig. 12

Dimensions: Diameter (49) 43 (38) µm. Specimens = 68 (22).

Remarks: This spheroidal cyst type is frequently encountered in late Hauterivian and early Barremian samples. The paratabulation formula is L-type sexiform gonyaulacoid: 4′, 6′′, 6c, 6′′′, 1′′′′, 1p, 5s. No preapical paraplate has been observed. *1u* is narrow and apparently in contact with *C* along its anterior margin. *A/1i* is posterior to *1u/ai*. *A* is rectangular and apparently does not reach up to the apex of the cyst*(?1u/B/C)*. Archaeopyle is Type 2P, involving paraplates *4* and *5* which are lost in the form of a free, compound biplacoid operculum (Plate 12, Fig. 5).

DUXBURY (1979: 199) and JAN DU CHÊNE et al. (1986a: 11) state that the cyst has a perforate wall. In actual fact the interior surface of the non-vacuolate autophragm is unbroken and the distal surface of the cyst consists of densely packed granules (≅ 0.1 μm dia.) which may be elongated giving a setose appearance. Autophragm thickness ≅0.3 μm. The parasutural septa are composed of short, solid processes (elongated setae) up to 3 μm long which may furcate and anastomose and be connected distally by a trabeculum. The regular fence-like parasutural septa described by DUXBURY (1979) are rarely well developed. These parasutural features vary from evenly spaced processes all connected by a trabeculum to examples which display an erratic distribution of uneven processes with no connecting trabeculum whatsoever (Plate 12, Fig. 2). Intratabular tubercles are common and appear to be elongated setae (Plate 12, Fig. 6).

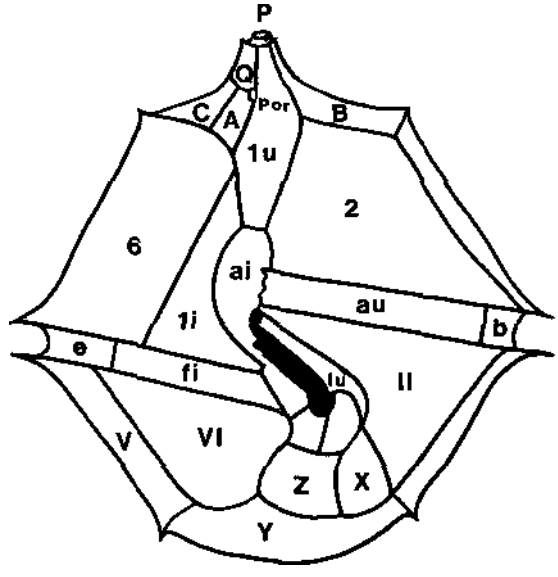

Text-fig. 13. Reconstruction of the ventral paratabulation of *Gonyaulacysta exsanguia* emend., perforate pandasutural bands are omitted for clarity.

Gonyaulacysta exsanguia DUXBURY 1977 emend.

Plate 13, Figs. 4, 7–10; Text-fig. 13

1977 *Gonyaulacysta exsanguia* – DUXBURY, p. 35, Plate 1, Figs. 6–7, Text-fig. 10. Bed C6 of the Speeton Clay, Speeton.

Emended Diagnosis

Shape: Pentagonal ambitus, markedly angular. Apex produced into short, blunt, broad apical horn. Convex antapex. Greatest width across anterior cingular parasuture. Moderate dorso-ventral compression. Cyst extremely thin walled.

Phragma: Periphragm up to 0.3 μm thick, laevigate to very finely granulate, no intratabular tubercles. Parasutural septa low (4–5 μm), distally variable from crenellated to bearing bifurcate spines. The characteristic feature of this species is the wide band of minute perforations along either side of each parasutural septum. These 'pandasutural' bands are up to 6 μm wide, the individual perforations (effectively claustra) are < 0.1 μm in diameter. Endophragm is also very thin (0.1–0.2 μm thick), laevigate to faintly granular. Cavation is restricted to the apical horn *with local suturocavation*.

Paratabulation: Sexiform gonyaulacoid (S-type) formula: 2pr, 4′, 1a, 6″, 6c, 6‴, 1⁗, 1p, 5s. Inconspicuous incidental paraplate on dorsal surface; prominent porichnion on *Q/1u/A* triple junction; *A* small and bordering 6 which contacts *1u*.

Archaeopyle: Type P_4, perioperculum and endoperculum lost as one unit, archaeopyle free.

Paracingulum: Strongly indented, laevorotatory, overhanging, displaced by 2½ cingulum widths.

Parasulcus: S-type, prominent, parasutures subdued. Claustrum developed in position of flagellar scar.

Dimensions: Length (60) 51.4 (43) µm. Width (59) 51.4 (41) µm. Specimens = 32 (21).

Remarks: This species is emended (after study of new topotype and additional material from each of the studied sections) to include full details of its paratabulation, to elucidate the variation in septal processes and to describe the diagnostic perforate 'pandasutural' bands bordering the parasutural septa. This is a very thin walled species and is often found distorted, identification is however simple on the recognition of the perforate bands. No mention of this peculiar feature was made by DUXBURY (1977) as the feature is of too small a size to be resolved by LM.

This species displays a Jurassica paratabulation pattern, the apical *Q/B* arrangement including a single incidental paraplate. The ventral *1u/1i* arrangement shows a contact between *6* and *1u* (HELENES 1986: 80).

Gonyaulacysta fastigiata DUXBURY 1977

Plate 13, Figs. 11–13

Remarks: This species is common in the oldest samples studied, becoming less frequent through the early Barremian and dying out by late Barremian time. In contrast to DUXBURY's (1977) specimens, many of those observed in this study show bifurcations of the parasutural septal denticles. The periphragm is interrupted in the parasulcal area, being undeveloped over *1m, 1u* and the flagellar scar region. Paratabulation formula: 2pr, 4′, 6′′, 6c, 6′′′, 1′′′′, 1p, 5s. *1i* is very elongated and is only in contact with five paraplates, this results in the loss of the *A/1i* contact as noted by HELENES (1986: 80; text-fig. 4a and d). This is the only modification of the Jurassica paratabulation pattern. A porichnion is developed at the *Q/A/1u* triple junction. No dorsal incidental paraplates have been discerned.

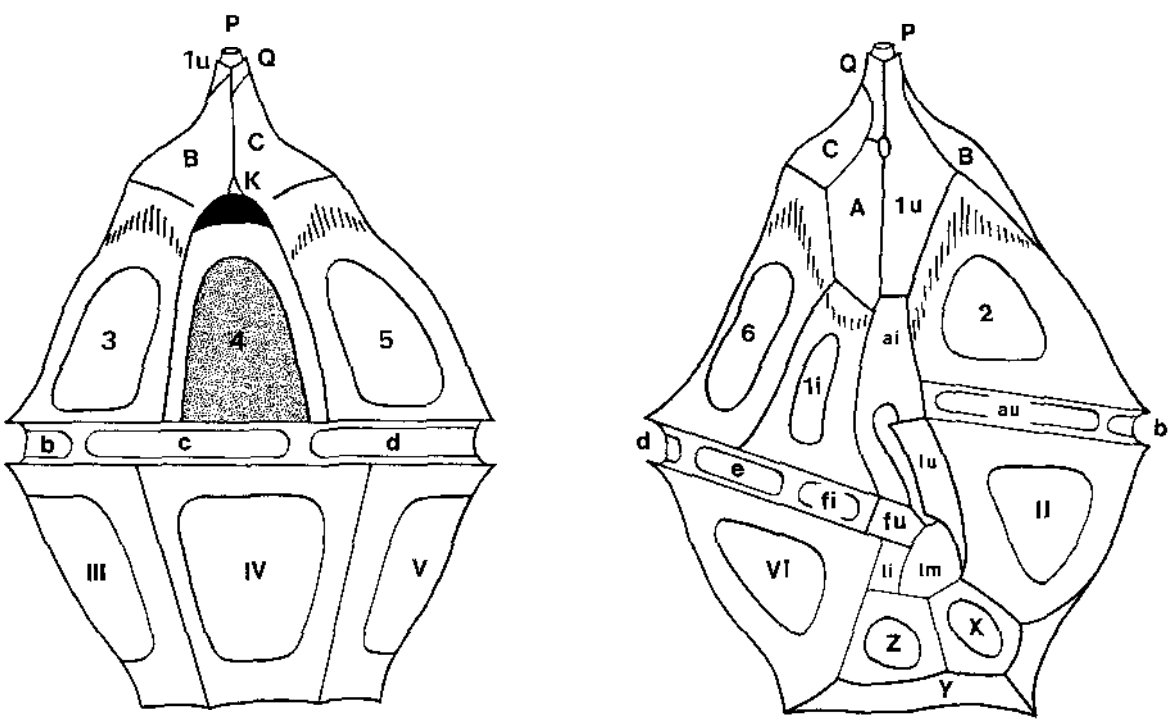

Text-fig. 14. Reconstruction of the dorsal (left) and ventral (right) paratabulation of *Gonyaulacysta speciosus* sp. nov., showing -/P_4 archaeopyle stippled.

Gonyaulacysta helicoidea (Eisenack & Cookson) Sarjeant 1966b

Plate 13, Figs. 1–3, 5–6

Remarks: This taxon is probably a species plexus as the shape, size, degree of intratabular tuberculation and length of the apical horn are all variable. Some representative specimens are illustrated. No dorsal incidental paraplates have been observed. These cysts display a Spinifera paratabulation pattern (Helenes 1986) with a ventral *A/ai* contact. Specimens with a high density of intratabular tubercles appear in late Barremian time.

Gonyaulacysta speciosus sp. nov.

Plate 14; Plate 15, Figs. 12–14; Text-fig. 14

Etymology: Late *speciosus* – handsome, in reference to the striking appearance of the cyst.
Holotype: Plate 14, Fig. 1.
Type locality: Gott, Bed 78.

Diagnosis

Shape: Slightly elongate pentagonal ambitus. Greatest width across posterior paracingular suture. Epicyst (less apical horn) and hypocyst of approximately equal length. An elongate apical horn is developed. Slight dorso-ventral compression.

Phragma: The periphragm is only partially developed. Two distinct wall layers are present in the parasutural areas but no periphragm is developed over the central parts of the paraplates of the hypocystal or the cingular or precingular series. Thus the periphragm forms a 'roof' over the parasutures of all but the apical series, where it is complete, forming a 'tent' over the apex of the endocyst. The periphragm (0.4 µm thick), is laevigate with rare tubercles. Paratabulation is delineated by periphragmal septa which are distally denticulate. The denticles vary in shape from phylloidal to acuminate. The denticles are absent from the reduced septa in the apical and parasulcal regions. The endophragm is ≅0.6 µm thick, subspherical with the entire surface covered in clumped, fused granules (which are sometimes developed into solid cylindrical setae). The cyst is delphicavate (involving a pericoel between the apical and the anterior part of the precingular series), with localised suturocavation.

Paratabulation: Sexiform gonyaulacoid (S-type), formula: 2pr, 4′, 1a, 6′′, 6c, 6′′′, 1′′′′, 1p, 5s. Two preapicals are present, *1u* is slender and contacts *Q* dorsally and ventrally. Porichnion at *A/Q/1u* triple junction.

Archaeopyle: Type –/P4, apparently paraplate *4* in the periphragm was not formed on encystment, operculum consists of endophragmal plate *4* alone.

Paracingulum: Prominent, strongly laevorotatory, overhanging, displaced by ≅3 cingulum widths. Strongly indented due to the suturocavate nature of the bounding parasutures. The parasutural septa which delineate the paracingulum bear a single line of rounded tubercles along the plane of the septum (Plate 14, Figs. 7 and 11).

Parasulcus: S-type, sulcal parasutures reduced. Periphragm developed over all the sucal paraplates save for the intratabular areas of *X* and *Z*.

Dimensions: Length (65) 54.2 (46) µm. Width (45) 41.0 (37) µm. Specimens = 11 (9).

Remarks: This is an easily recognised species due to the striking sculpture of the exposed endophragm. It differs from *Gonyaulacysta centriconnata* Riding 1983, which is also suturocavate, in its partial development of the periphragm, the strong sculpture, and the S-type (not L-type) ventral organisation. *G. teicha* Davey 1974 has the inflated apical pericoel of this new species and rare suturocavation, however, it also has a complete periphragm and an unsculptured endophragm.

Paratabulation pattern following Helenes (1986) is of the Spinifera type, there being a contact between paraplates *A* and *ai*.

This species has proved to be have a very restricted time range, being a good marker for the Hauterivian/Barremian boundary.

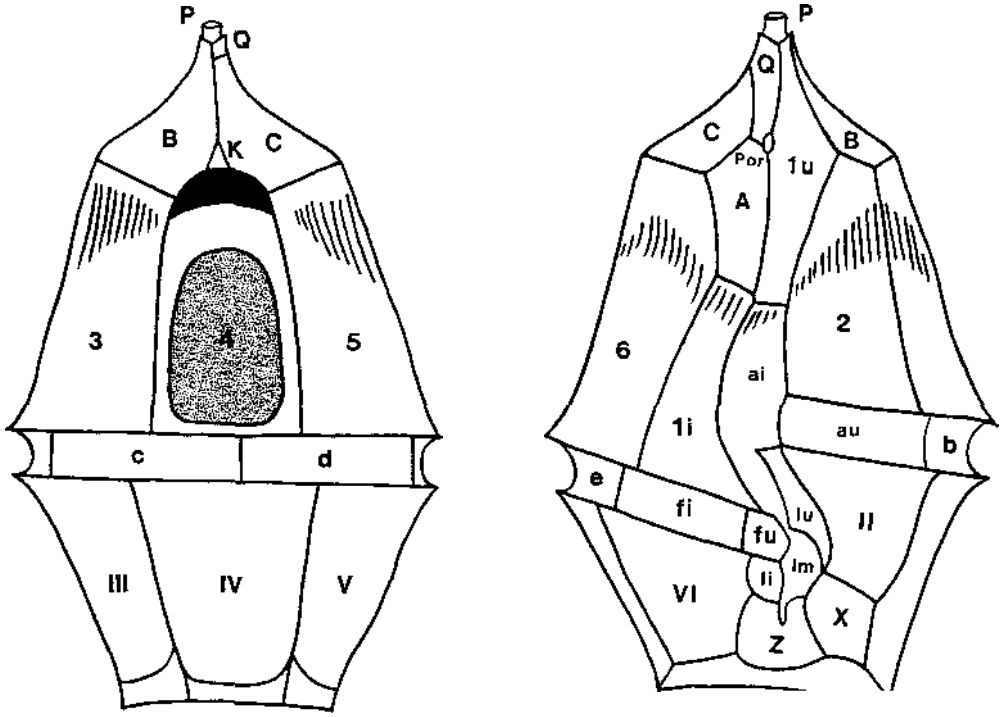

Text-fig. 15. Reconstruction of the dorsal (left) and ventral (right) paratabulation of *Gonyaulacysta teicha* sp. nov., showing -/P4 archaeopyle stippled.

Gonyaulacysta teicha Davey 1974 emend.

Plate 15, Figs. 1–11, 15; Text-fig. 15

1974 *Gonyaulacysta teicha* – Davey, p. 53, Plate 4, Figs. 5–7. Bed LB4D of the Speeton Clay, Speeton.

Emended Diagnosis

Shape: Ambitus elongate pentagonal. Greatest width across posterior cingular parasuture. Epicyst about 1.3 times the length of the hypocyst. Short broad apical horn is developed. Slight dorso-ventral compression.

Phragma: Periphragm ambitus elongate pentagonal, up to 0.5 µm thick, laevigate. Rare intratabular tubercles. Apical paraplates characteristically bear rugulate ridges. Parasutural septa bear cordate/phylloidal denticles although these do vary greatly and may degenerate into distally serrate fenestrate septa. Endophragm is subspherical to ellipsoidal, ≅ 1.5 µm thick with an 'orange-peel' type of sculpture. Cyst is delphicavate (pericoel developed beneath the apical horn and the anterior parts of the precingular paraplates), with local suturocavation.

Paratabulation: Sexiform gonyaulacoid (S-type), formula: 2pr, 4′, 1a, 6′′, 6c, 6′′′, 1′′′′, 1p, 5s. Paraplate *1u* contacts *Q* ventrally but not dorsally. Porichnion on paraplate *A* just posterior to *A/Q/1u* triple junction.

Archaeopyle: Type –/P4, apparently periphragmal paraplate *4* not formed during encystment.

Paracingulum: Prominent, strongly laevorotatory, overhanging, displaced by ≅ 3 cingulum widths, strongly indented.

Parasulcus: S-type, sulcal parasutures reduced but not suppressed entirely.

Dimensions: Length (70) 58.2 (46) µm. Width (56) 44.0 (35) µm. Specimens = 41 (28).

Remarks: This species is emended after the study of topotype material from Bed LB4D at Speeton. The emendation emphasises the variability of the septal denticles, revises the paratabulation formula and describes the non-operculate nature of the periarchaeopyle (i.e. a claustrum). Paratabulation follows the Jurassica type of Helenes (1986). The possession of a strongly inflated apical pericoel probably indicates a close relationship with *Gonyaulacysta speciosus* sp. nov. and the *G. cassidata* lineage.

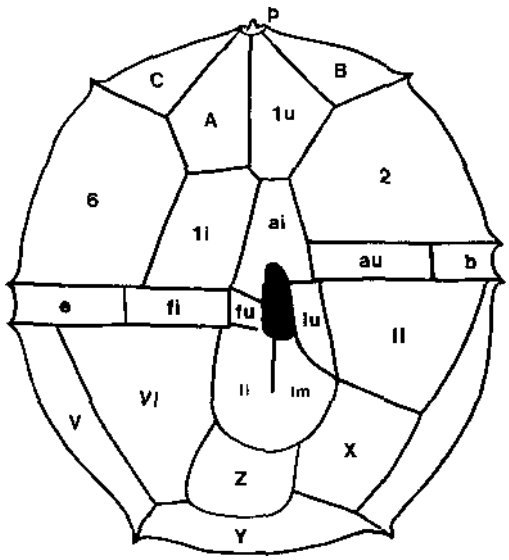

Text-fig. 16. Reconstruction of the ventral paratabulation of Meiourogonyaulax sagena emend. nov.

Meiourogonyaulax sagena (DUXBURY) LENTIN & WILLIAMS 1981 emend.

Plate 16, Figs. 10–14; Text-fig. 16

1980 *Lithodina sagena* – DUXBURY, p. 127. Plate 3, Figs. 6, 9, 12–13. Barremian Middle B Beds of the Speeton clay, Speeton.
1981 *Meiourogonyaulax sagena* – LENTIN & WILLIAMS, p. 182.

Emended Diagnosis

Shape: Ambitus subcircular to subhexagonal. Both apex and antapex flattened. Greatest width across paracingulum. An apical prominence is sometimes developed. Epicyst and hypocyst of equal length. Moderate dorso-ventral compression.

Phragma: Autophragm up to 4 μm thick. Microgranular surface (granulae partly fused) has rugulate sculptural elements forming a low nontabular reticulum. The rugulae may be prominent (up to 2 μm high and ≅5 μm wide) or virtually undeveloped. The rugulate reticulum supports a very delicate ectophragm (≦0.1 μm thick) which is prone to removal during the oxidation process. The parasutures are delineated by single rows of pointed and occasionally ribbed denticles (≅1 μm wide by 3 μm long) – although exceptionally these may be absent.

Paratabulation: L-type sexiform gonyaulacoid. Paratabulation formula interpreted from the parasutural denticles: pr, 4′, 6′′, 6c, 6′′′, 1′′′′, 1p, 5s.

Archaeopyle: Type (tA). Operculum free, simple polyplacoid. Archaeopyle suture deeply indented on the ventral surface forming a U-shaped notch as *A* and *1u* are almost equal in length.

Paracingulum: Well developed, weakly laevorotatory, displaced by ½–1 cingulum width.

Parasulcus: Narrow on epicyst but a broad conspicuous on the hypocyst – up to 10 μm wide. *Ii/Im* suppressed. *Z* characteristically displaced to the right.

Dimensions: Length, + operculum (60) 48.3 (41) μm. Width (60) 47.9 (41) μm. Specimens = 46 (18).

Remarks: Study of new topotype material (and additional material from the other localities studied) of this species has clarified some of the more poorly known morphological features. DUXBURY's (1980: 127) interpretation of an endocyst and a pericyst in this species is incorrect as the outer wall layer is supported on the nontabular rugulate reticulum. This makes the wall layers involved the autophragm and ectophragm (sensu EVITT 1985) resulting in a very similar morphology to *Cassiculosphaeridia* as interpreted in this work. Paratabulation pattern for the apical area has not been determined, but *Y* is symmetrical and the ventral area possesses a *1u/1i* arrangement (HELENES 1986).

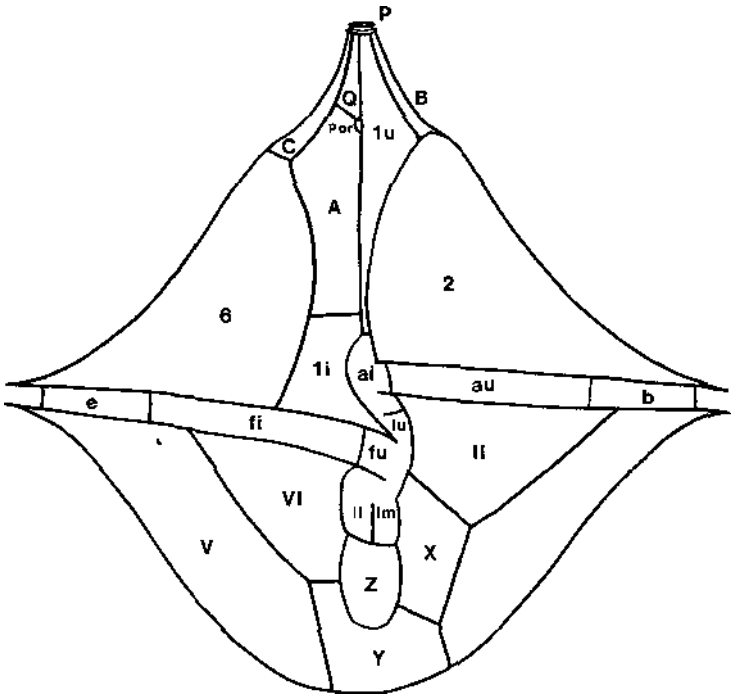

Text-fig. 17. Reconstruction of the ventral paratabulation of *Occisucysta duxburyi*, showing long and narrow *1u*.

Occisucysta duxburyi JAN DU CHÊNE et al. 1986a

Plate 16, Figs. 1–9; Text-fig. 17

Remarks: A most striking species with very distinctive microreticulate pitting on the distal surface of the periphragm (which is ≅ 0.3 µm thick). This sculpture extends over the surface of the intratabular tubercles (which are most prominent on paraplates *B, Y* and the postcingulars). The endophragm is thicker (≅ 0.75 µm), granular in cross section and has a rough rugulate/pitted surface sculpture. Cavation is restricted to the region of the apical horn and the paracingulum.

Paratabulation pattern as cited by JAN DU CHÊNE et al. (1986a) consists of asymmetrical-oblong antapical, *P/C* apical and *1u/1i* (with paraplate *ai* contacting paraplate *2*) ventral arrangements. Parasutural septa (up to 10 µm high) delineate a paratabulation formula of 2pr, 4′, 6′′, 6c, 6′′′, 1′′′′, 1p, 5s. *A* and *1u* are very elongated, the latter plate being very narrow. Porichnion lies on *Q/A/1u* triple junction. Reduced Type 2P archaeopyle involving paraplates *3* and *4* as a compound biplacoid operculum (Plate 16, Fig. 1). Parasulcus is deeply indented.

In contrast to the description given in JAN DU CHÊNE et al. (1986: 16–17), this species has been found, in this study, to be the sole species of the genus present in Barremian time. Fenestration of the paracingular septa have been noted in some specimens.

Pentadinium omasum sp. nov.

Plate 17

Etymology: Latin *omasum* – paunch, in reference to the large dorsal pericoel.
Holotype: Plate 17, Fig. 1.
Type locality: Gott, Bed 197.

Diagnosis

Shape: Ambitus subpentagonal to ovoid. Small apical prominence. Outline modified by camocavate nature of the equatorial region (the periparacingulum is separated from the endocyst in all but the parasulcal region). Greatest width across paracingulum. Epicyst and hypocyst of equal dimensions. No dorso-ventral compression.

Phragma: Periphragm ≅0.75 µm thick, weakly granular sculpture. Paratabulation indicated by undulate septa of variable height (low in parasulcal region – ≦2 µm, up to 5 µm in antapical region). Endophragm up to 1 µm thick, of spheroidal shape with a pseudopunctate/'orange-peel' type surface sculpture. Camocavate: entire dorsal part of the paracingulum is separated from the endocyst by up to 15 µm. Suturocavation developed to varying degrees along the parasutures adjacent to the paracingulum.

Paratabulation: S-type sexiform gonyaulacoid paratabulation as shown by the parasutural septa: 4′, 6′′, 6c, 6′′′, 1′′′′, 1p, 5s. *A* and *1u* very small, with the parasuture dividing them often suppressed. Suppression of the parasulcal sutures also occurs. A porichnion is rarely observed, when present lies on *A/1u*.

Archaeopyle: Type –/P_4 – fourth precingular paraplate is lost from the endocyst in archaeopyle formation as a free, monoplacoid operculum. It appears that there was no fourth precingular periphragmal paraplate formed on encystment.

Paracingulum: Displayed as a pronounced outbulging of the periphragm. Laevorotatory, displaced by 1½–2 cingulum widths.

Parasulcus: S-type, parasutures often suppressed.

Dimensions: Length (56) 48.1 (44) µm. Width (55) 47.4 (42) µm. Specimens = 14 (13).

Remarks: This new species is restricted to rocks of late Barremian age. It differs from *Stephodinium* in that the separation of periphragm and endophragm is merely paracingular and not dorsal (Stover & Evitt 1978). It differs from *Pentadinium polypodum* Edwards 1982, to which it appears superficially similar (Edwards 1982: Plate 3, Fig. 5), as it lacks gonal processes.

Trichodinium calvus sp. nov.

Plate 19, Figs. 7–12

Etymology: Latin *calvus* – bald, in reference to the lack of tuberculation characteristic of the other members of this genus.
Holotype: Plate 19, Fig. 7.
Type locality: Gott, Bed 192.

Diagnosis

Shape: Ambitus subspherical to prolate ovoidal. Apex produced into a narrow apical horn. Greatest width across paracingulum. Epicyst (less apical horn) and hypocyst of equal length. No dorso-ventral compression.

Phragma: Differentiated autophragm up to 2.5 µm thick. Surface sculpture pseudoreticulate to microrugulate. Network of sporopollenin rugulae amastomoses into short, fibrous tubercles (up to 2 µm long). The distribution of the tubercles is intratabular. Short, narrow apical horn reaches 12 µm in length in some specimens.

Paratabulation: Parasutures are delineated by 'scarp'-like ridges and by the orientation of the tubercles. Paratabulation appears to be L-type sexiform gonyaulacoid, but the details of the apical paratabulation have not been worked out as yet.

Archaeopyle: Type P_4 – operculum free, monoplacoid.

Paracingulum: Indicated by alignment of tubercles or by 'scarp'-like ridges. Laevorotatory, displaced by ≅1½ cingulum widths.

Parasulcus: L-type, slightly indented. Flagellar scar developed. Precise paratabulation indistinct.

Dimensions: Length (84) 69 (56) µm. Width (66) 58 (43) µm. Specimens = 28 (18).

Remarks: The narrow, true apical horn distinguishes this species from *Trichodinium speetonense* which has a false apical horn in the form of a tuft of fused spinules. The sparse tuberculation distinguishes this new species the other species of the genus, which have evenly distributed tuberculate/spinose sculptural elements. Restricted to deposits of late Barremian age.

Trichodinium ciliatum (Gocht) Eisenack 1964

Plate 18, Figs. 1–6

Dimensions: Length (72) 63 (48) µm. Width (68) 60 (50) µm. Specimens = 32 (18).

Remarks: The specimens illustrated by Gocht (1957: Plate Figs. 9–10; 1959: Plate 8, Figs. 5–6) as *Trichodinium ciliatum,* are clearly different from *T. castanea* (with which *T. ciliatum* has been synonomised by Clarke & Verdier 1967) as they possess no indications of paratabulation other than the archaeopyle, and have a dense, even cover of tubercles.

This species is of great stratigraphic value as it occurs in rocks of Hauterivian and earliest Barremian age, but disappears before the advent of the Hauptblätterton and equivalent facies. It is easily distinguished from other species of the genus by its subcircular ambitus and dense, even cover of evexate tubercles (1–2 µm long) formed by the fusion of the fibres forming an open reticulum on the distal surface of the differentiated autophragm. An apical tuft of longer tubercles is occasionally present but no true horn develops. Paratabulation is obscure but is consistent with an L-type sexiform gonyaulacoid format as far as can be discerned. Paracingulum often expressed by rows of longer tubercles. Parasulcal area and *IV* are sometimes less densely spinose. Flagellar scar present.

Trichodinium discus sp. nov.

Plate 18, Figs. 7–13

Etymology: Latin – *discus* – a quoit, in reference to the subcircular ambitus.
Holotype: Plate 18, Fig. 7.
Type locality: Gott, Bed 100.

Diagnosis

Shape: Ambitus cubcircular to prolate ovoidal. Greatest width across posterior of paracingulum. Epicyst generally shorter than hypocyst (may be only ½ the length in exceptional circumstances). Strong dorso-ventral compression.

Phragma: Differentiated autophragm ≅ µm thick. Distal surface composed of pseudoreticulum of sporopollenin fibres which anastomose to form acuminate tubercles up to 4 µm long. Tubercles are evenly distributed save for bald areas corresponding to paraplate *IV* and the parasulcus. Occasionally the parasutures are indicated by low ridges, usually along the paracingulum. No apical process.

Paratabulation: Obscure, consistent with L-type sexiform gonyaulacoid in as far as can be determined.

Archaeopyle: Type P_4 – free, monoplacoid operculum, anterior archaeopyle margin is distinctly rounded.

Paracingulum: Occasionally defined by aligned tubercles. Laevorotatory, displaced by 1–1½ cingulum widths.

Parasulcus: L-type. Area of reduced tuberculation. Flagellar scar pronounced.

Dimensions: Length (63) 57.5 (51) µm. Width (60) 56.0 (47) µm. Specimens = 15 (10).

Remarks: *Trichodinium discus* sp. nov. is probably the form recorded by previous workers on Barremian dinocysts as *T. castanea.* However, this new species is clearly not the same as the latter named species, due to its lack of an apical prominence and its more circular ambitus. The lack of an apical horn and the character of the tuberculation serve to differentiate this new species from the other members of the genus.

Trichodinium speetonense Davey 1974

Plate 19, Figs. 1–6

Dimensions: Length (98) 78 (58) µm. Width (95) 70 (44) µm. Specimens = 40 (23).

Remarks: Easily distinguished from the other members of the genus studied due to a variety of features. The ıracingulum characteristically bulges outwards and is delineated by rows of acuminate spinules longer than those)und over the rest of the cyst (up to 5 µm long). The spinules occur over the whole of the surface of the ifferentiated autophragm, but are concentrated in apical, antapical and paracingular areas. The apical 'horn' is ally no more than a fused cluster of longer spinules at the apex of the cyst and may reach a length of 8 µm. aratabulation can be partially discerned on many specimens, outlined by aligned spinules (e.g. Plate 19, Fig. 2) and ppears to be consistent with an L-type sexiform gonyaulacoid arrangement. Archaeopyle Type P_4. A pronounced agellar scar is often present.

5.5.5 *Hystrichodinium* Complex

Genus *Hystrichodinium* (Deflandre) Clarke & Verdier 1967

Remarks: Species of this genus are thin-walled, fragile and thus rarely well preserved. Observation is often difficult due to the long processes becoming entangled with debris or breaking off during drying of the strew mounted residues.

Several forms exhibiting variations in process distribution and termination have been observed in this study:

Hystrichodinium voigtii (Alberti) Davey 1974 (Plate 20, Figs. 1–6, 11) – this may be a phenotypically variable species as the length and distribution of the processes and the degree of expression of paratabulation all vary widely.

H. furcatum Alberti 1961 (Plate 20, Fig. 9) – an early Barremian form characterised by furcate process extremities. Furcation is simple, the terminations splitting into two or three parts, each of which may branch once again.

H. ramoides Alberti 1961 (Plate 20, Fig. 10) – a late Barremian form with more complicated process terminations. There may be up to four successive terminal furcations of each process (always more than two furcations occur), each furcation is generally a bifurcation.

H. compactum Alberti 1961 (Plate 20, Figs. 7–8) – a form with a vast number of simple tapering processes which may be gonal, intergonal and apparently intratabular.

The first three species all show weakly S-type sexiform gonyaulacoid paratabulation, with as far as can be determined, dorso-ventrally compressed symmetrical antapical and *A/ai* ventral arrangements. The intratabular 'pores' are not an internal wall feature as proposed for some specimens by Evitt (1985: 223–4), but genuine perforations of the periphragm (Plate 20, Figs. 4, 5 and 11). The perforations are up to 1 µm in diameter (usually ≅0.5 µm) and surrounded by a raised border in most instances. The endophragm can be observed through these claustra and is usually microgranular. The 'pores' may bear a relationship to the position of trichocyst pores on the motile thecate organism.

Index list to species discussed in Part I

PART II: SYSTEMATICS, BIOSTRATIGRAPHY

Summary

This is the second and concluding part of a study of dinocysts extracted from sediments of Barremian age from Boreal western Europe. A calibration based on a sequence of dinocyst events is detailed and integrated with the already exisiting cephalopod zonation for the Boreal Barremian.

Two new monotypic dinocyst genera are described in this part of the paper (*Resticulasphaera* gen. nov. and *Vexillocysta* gen. nov.). In addition, four new dinocyst species are established and two species are emended following the study of type and new topotype material.

This detailed morphological data has enabled the extraction of the maximum stratigraphic information possible at this juncture. The vertical ranges of many of the studied taxa have been refined, making possible the determination of a sequence of appearance/disappearance events. The selection of particular events has resulted in the creation of a calibration scheme for the Late Hauterivian and the Barremian, which is shown to have a wide geographic application. This scheme is a 'state-of-of-the-art' calibration rather than a zonation. The concept of a biostratigraphic zonation is believed too rigid for what should be a constantly evolving process of successive refinements of biostratigraphic events used to determine the time-correlation of one rock unit with another.

Systematic section. Part II

5.6 Gi-Cysts

5.6.1 *Hystrichosphaeridium* Complex

Discorsia nanna (Davey) Khowaja-Ateequzzaman et al. 1985

Plate 23, Figs. 1–4

Dimensions: Body length (26) 23.8 (21) µm. Body width (22) 19.0 (16) µm. Length across processes (45) 41.9 (37) µm. Width across processes (45) 38.0 (27) µm. Specimens = 26 (11).

Remarks: A small, distinctive species and an uncommon constituent of residues studied. The elongate main body comprises an endophragm of ≦1 µm thickness which is laevigate with scattered rugulae. The periphragm (≅0.2 µm thick) covers the endocyst and forms the processes. The processes are tubular and corrugated distally (the corrugation is developed to a variable extent along the process length). Distally, the processes flare outwards and end in a very characteristic 'ruffle' as the periphragm thickens and becomes more complex in structure (Plate 23, Fig. 4). Proximally the corrugations may extend across the main body from process to process (as in *Kleithriasphaeridium corrugatum*) or be restricted to the process bases. This corrugation becomes discontinuous and vermiform in late Barremian specimens. The Type (tA) archaeopyle indicated by Khowaja-Ateequzzaman et al. (1985) could not be confirmed due to collapse of the thin-walled cyst, although the archaeopyle is undoubtably apical.

Hystrichosphaeridium arborispinum Davey & Williams 1966b

Plate 23, Figs. 5, 6, 8

Dimensions: Body length (52) 42.6 (33) µm. Width (38) 30.3 (25) µm. Process length (22) 15 (12) µm. Specimens = 33 (15).

Remarks: This species makes its first appearance in samples of latest early Barremian age (the Hauptblätterton and equivalent facies). The species has an extremely erratic distribution in late Barremian time, usually occurring in low abundance in great contrast to its importance in the Hauptblätterton and its equivalents.

The distinctive ornate, ragged ended processes (Plate 23, Fig. 8) of this species vary in both their length and diameter (11–23 µm and 2–5 µm, respectively). The smaller processes are often proximally perforate, sometimes to such an extent that only part of the cylinder is formed and gives the appearance of an annulate process complex (common in the parasulcal region). Archaeopyle Type (tA), the four apicals form a free, simple polyplacoid operculum. Paratabulation formula is indicated by the intratabular processes but requires further study because the thin-walled species collapses unfavourably for observation.

Genus *Kleithriasphaeridium* Davey 1974

Remarks: *K. corrugatum* (Plate 22, Figs. 1–9) and *K. simplicispinum* (Plate 22, Figs. 10–15) have been recognised in this study, both forms possessing rugulate endocysts (Plate 22, Figs. 9 and 15).

A form attributable to *K. fasciatum* has only been found in Hauptblätterton sediments. The forms of several species of dinocyst are abberrant in this facies adding new weight to the view held by Duxbury (1977: 41) that the only difference between this species and *K. corrugatum* is one of process length. It appears likely that the differences between these two 'species' is due to phenotypic variation.

Two variants of *K. simplicispinum* have been found, the first with very reduced processes (Plate 22, Fig. 14), the second with microgranular sculpture of the periphragm around the process bases.

Oligosphaeridium pseudoabaculum sp. nov.

Plate 24, Figs. 1–7

Etymology: *Pseudo* from the Greek, meaning "supposed but not real", in reference to the superficial similarity to *O. abaculum* Davey 1979.

Holotype: Plate 24, Fig. 1.

Type locality: Gott, Bed 100.

Diagnosis

Shape: Main cyst body is spheroidal to prolate (may be accentuated by the development of axial compression folds). Greatest width in equatorial region. Epicyst and hypocyst ≅ dimensions. No dorso-ventral compression. Ambitus modified by tubiform processes about 2/3 main cyst body diameter in length. Processes developed on apical, pre- and post-cingular, *X*, *Y* and *Z* paraplates.

Phragma: Imperforate endophragm ≦ 1 µm thick has a pitted external surface (Plate 24, Fig. 6) Periphragm is ≧ 1 µm thick. Over the main cyst body the periphragm takes the form of a 'spongy' textured layer, externally having a 'porous' appearance caused by the partial fusion of the sporopollenin globules constituting this layer. Around the process bases (often partially fenestrate) the sculpture develops into shallow striations. The periphragmal processes are externally laevigate, generally parallel sided and distally slightly flared. Process terminations are variable but not often strongly aculeate. The cyst is apiculocavate.

Paratabulation: Process formula: 0pr, 4′, 6″, 0c, 5‴, 1p, 1⁗, 1s. Inferred paratabulation is typically *sexiform gonyaulacoid (see Evitt 1985: 56, 250–256, for discussion of other members of this genus).*

Archaeopyle: Type (4A), *1u, A–C* lost as a free, simple, polyplacoid operculum. Accessory archaeopyle sutures dedveloped between precingular paraplates.

Paracingulum: Devoid of processes, often shows up as a band of reduced periphragmal sculpture in the equatorial region of the main cyst body.

Parasulcus: Devoid of processes save for *Z*, *ai* can be distinguished along the archaeopyle suture.

Dimensions: Maximum diameter across processes = (142) 118.8 (85) µm. Main body diameter = (63) 55.4 (48) µm. Specimens = 19 (18).

Remarks: This species can be distinguished from other members of the genus by the combination of tubiform processes and the distinctive surface sculpture. The surface sculpture bears some resemblance to that of *O. abaculum* (Davey 1979: Plate 48, fig. 3). The latter species, however, also possesses low ridges delineating a complete sexiform paratabulation. The endophragm of *O. abaculum* appears to be laevigate (Davey (1979: Plate 48, Fig. 5). Although the cingulum is sometimes discernible in *O. pseudoabaculum,* a complete paratabulation is never developed. This new species has only been isolated from the Hauptblätterton and its equivalents (i.e. restricted to late early Barremian time).

5.6.2 *Systematophora* Complex

Hystrichosphaerina schindewolfii Alberti 1961

Plate 21, Figs. 1–3, 5–6

Remarks: L-type sexiform gonyaulacoid paratabulation as indicated by processes and process groups: 4′, 6″, 6c, 6‴, 1⁗, 1p, 5s. Cingular paraplates are each represented by two simple, distally bifurcating, tapering processes, often connected proximally or arising from a common base. Sulcal paraplates are also represented by simple, tapering (often distally blunt) intratabular processes: *Z*, *Ii* and *Im* plates are represented by a cluster of such processes. The remaining paraplates are represented by intratabular annulate process groups of varying diameter, each group connected distally by a continuous trabeculum. Evitt (1985: Fig. 4.4 J, K, N) shows such process groups arising from a basal ridge. In this study the process group (or complex process) has been observed to consist of an outgrowth of the periphragm formed into a tube, the base of which is a continuous layer of periphragm – i.e. there is no direct connection between the endocyst and the environment via a pericoel. The proximal diameter of the process group is so reduced in some specimens as to give the impression of a distally fenestrate complex process. Periphragmal surface texture is pseudo-punctate.

Genus *Callaiosphaeridium* (Davey & Williams) Below 1981

Plate 21, Figs. 4, 7–11

Remarks: When many specimens of this genus are observed it becomes increasingly difficult to split them into recognisable species. Furthermore, it appears that the morphology of the specimens varies phenotypically. A species plexus can be recognised with end members resembling *C. asymmetricum* (having individual epi- and hypocystal parasutural processes) and *C. trycherium* (parasutural processes connected by parasutural crests). Paraplate *Y* is very large and quadrate. Sulcal paratabulation is clear (Plate 21, Fig. 9), *X* being twice the size of *Z*.

Paratabulation formula as indicated by parasutural crests/processes and paracingular intratabular processes: 4′, 6″, 6c, 6‴, 1⁗, 1p, 5s.

5.7 Gn-Cysts (*Operculodinium* Complex)

Cleistosphaeridium fungosus sp. nov.

Plate 25, Figs. 1–9

Etymology: Latin fungosus – with a fur-like covering, referring to the setose surface of the cyst.
Holotype: Plate 25, Fig. 1.
Type locality: Gott, Bed 100.

Diagnosis

Shape: Ambitus subspherical. Even distribution of equidimensional tubiform processes. Epicyst and hypocyst not differentiated. No dorso-ventral compression.

Phragma: Autophragm ≅ 0.5 µm thick, distally covered in densely packed filamentous fibres up to 1 µm long and 0.2 µm in diameter (Plate 25, Figs. 7 and 8). Numerous solid, tubiform processes (?periphragm) up to 4 µm long are evenly distributed over the cyst surface in an apparently non-tabular fashion. The processes flare slightly distally and may have a central perforation at the end.

Paratabulation: Epicystal paratabulation identified from the accessory archaeopyle sutures: 4′, 6″, + *ai*. Hypocystal paratabulation unknown.

Archaeopyle: Type (tA), involving four apicals as free, simple, polyplacoid operculum. Accessory archaeopyle sutures formed between the precingular paraplate series.

Paracingulum: Undifferentiated.

Parasulcus: Undifferentiated.

Dimensions: Diameter (45) 37.8 (32) µm. Process length (5) 3 (2) µm. Specimens = 19 (14).

Remarks: Occurring in flood abundance in the Hauptblätterton samples, but a fairly common constituent of many of the samples studied. Differs from the previously described species in its distinctive setose surface sculpture combined with the short, solid processes. Late Barremian specimens appear to be slightly larger and have fewer processes (e.g. Plate 25, Fig. 4).

Genus *Dapsilidinium* Bujak et al. 1980

Remarks: A genus represented by two common species in Hauterivian and Barremian time:

Sp. I (Plate 26, Figs. 6–8). Main cyst body has low, partially fused, granular sculptural elements (≦ 1 µm in dia.), combined with long, hollow, non-tabular processes (about half the body diameter in length and ≅ 1 µm in dia.). Process terminations may flare slightly with an entire margin. Archaeopyle is Type (tA).

Sp. II (Plate 26, Figs. 1–5). Main body covered in short spinules (≦ 1 µm long, ≅ 0.25 µm dia.) surmounted by an uneven fibrous layer (? = ectophragm), through which the processes project. Processes are hollow, parallel-sided or slightly narrowed distally (half body diameter in length, ≅ 1.5–2.0 µm dia.). Archaeopyle is Type (tA) with accessory sutures developed along precingular parasutures. This cyst-type is similar to *D. warreni* (Habib) Lentin & Williams.

Genus *Resticulasphaera* gen. nov.

Etymology: Latin *resticula* – string, and *sphaera* – a ball. In reference to the structure of the cyst surface and the nature of the processes.

The diagnosis of this new monospecific genus is the same as that for the single species discovered in this study.

Resticulasphaera medusae gen. et sp. nov.

Plate 27, Figs. 1–8

Etymology: From Medusa – one of the three Gorgons who had snakes for hair, in reference to the form of the processes.
Holotype: Plate 27, Fig. 1.
Type locality: Gott, Bed 185.

Diagnosis

Shape: Ambitus subcircular to prolate ovoidal. Epicyst about 1/3 of cyst length, the remaining 2/3 consisting largely of hypocyst (paracingulum narrow). Greatest width immediately post-cingulum. Strong dorso-ventral compression.

Phragma: Autophragm ≅ 0.3–0.5 µm thick. Surface sculpture of fine interwoven, matted fibres up to 2 µm long, forming a dense cover over the whole cyst save for the paracingulum which often verges on laevigate (Plate 27, Fig. 4). Acuminate processes in the form of long (up to 10 µm), solid, hair-like fibres. These are apparently partially non-tabular and partially sutural (along the borders of the paracingulum) in location.

Paratabulation: Not discernable save for the differentiation of the paracingulum.

Archaeopyle: Type E, entire epicyst lost as simple, free, polyplacoid operculum, which may rarely remain attached to the parasulcal region.

Paracingulum: Indicated by the subdued nature of the sculpture as a narrow equatorial band. Anterior edge of paracingulum becomes rolled over towards the antapex after archaeopyle formation.

Parasulcus: Undifferentiated, only determinable when the epicyst remains attached to this region.

Dimensions: Body length (22) 18.7 (17) µm. Body width (18) 16.9 (15) µm. Process length (14) 7 (5). Specimens = 10 (10).

Remarks: The small size of this form and its distinctive morphology warrant the erection of a new genus. Archaeopyle type distinguishes this form from other spherical cysts with long nontabular processes (e.g. *Cleistosphaeridium, Dapsilidinium* and *Polysphaeridium*. Other genera with Type E archaeopyles (e.g. *Ctenidodinium, Dichadogonyaulax* and *Heslertonia*) do not possess elongated processes and display clear paratabulation over the whole cyst surface.

Genus *Vexillocysta* gen. nov.

Etymology: Latin *vexillum* – a banner or pennant, in reference to the distinctive form of the processes.

The diagnosis of this new monospecific genus is the same for that of the single species discovered in this study.

Vexillocysta retis sp. nov.

Plate 24, Figs. 8–14

Etymology: Latin *retis* – a net, referring to the characteristic surface sculpture of the periphragm.
Holotype: Plate 24, Fig. 8.
Type locality: Gott, Bed 100.

Diagnosis

Shape: Ambitus subcircular to prolate ovoidal, modified by numerous processes. Epicyst and hypocyst of about equal dimensions. Greatest width in equatorial region. Moderate dorso-ventral compression.

Phragma: Endophragm ≅ 0.75 μm thick, seemingly almost laevigate where visible (Plate 24, Fig. 13). Periphragm ≅ 0.3–0.5 μm thick, consists of a base layer overlain by interconnected sporopollenin fibrils forming a pseudo-reticulum (max. lumina diameter 1 μm). Many of the fibrils terminate perpendicular to the plane of the periphragm, giving a globular appearance to the reticulum. The numerous, flat, blade-like processes (intra- and peni-tabular) are proximally hollow, distally solid and often bifurcate. The processes are faintly striate in appearance. Process width (1–3.5 μm) is inversely proportional to length (6–12 μm), both long and short processes may be found on one specimen (shorter processes in mid-dorsal and mid-ventral areas). Both cyst wall layers are closely adpressed except for the process bases.

Paratabulation: The complex distribution of the processes makes the determination of the paratabulation difficult, but it appears to be compatible with a gonyaulacoid type. Apical paratabulation determined from archaeopyle sutures: 4′, 6′′ + *ai*.

Archaeopyle: Type (4A), free, simple polyplacoid operculum. Short accessory archaeopyle sutures formed between precingular paraplates.

Paracingulum: Occasionally recognisable due to alignment of process blades delineating a process-free band.

Parasulcus: Difficult to detect save for on excysted specimens where *ai* can be distinguished along the *archaeopyle margin*.

Dimensions: Length = (60) 51 (40) μm. Width = (50) 44 (35) μm. Specimens = 25 (20).

Remarks: This new species is easily distinguished from other dinocysts having a similar type and arrangement of processes (e.g. in the genera *Pervosphaeridium, Operculodinium, Exochosphaeridium* and *Lingulodinium*) by the nature of the archaeopyle (apical as opposed to precingular in all the latter genera). The genus *Vexillocysta* gen. nov. differs from *Epiplosphaera* Klement 1960 (which also has an apical archaeopyle), in the nature of the processes developed on the external cyst surface. In the new genus the processes may, in some instances, be aligned with adjacent ones. However, in *Epiplosphaera,* the processes arise from a complex reticular network of septa. Of the specimens of *Cleistosphaeridium* described by McIntyre & Brideaux (1980) from Canada, the morphotype referred to as *C.* sp. KE bears a strong resemblance to *Vexillocysta retis,* although it should be noted that the Canadian material is of Valanginian age.

This form is a common constituent of the floras studied – especially in the Hauptblätterton facies. Later Barremian forms have a more subdued reticulation and fewer, more slender processes.

5.8 Gx-Cysts

5.8.1 *Batioladinium* Complex

Batioladinium longicornutum (Alberti) Brideaux 1975

Plate 28, Figs. 1–4

Dimensions: Length, plus operculum (three examples) – 310 µm, 190 µm. Length, less operculum (150) 116.4 (80) µm. Length of operculum (112) 96.5 (70) µm. Width (31) 26.8 (22) µm. Specimens = 12 (12).

Remarks: This species is uncommon and erratic in its distribution. The cyst surface is laevigate, sculpture being entirely absent. The only features on the cyst surface are pits or claustra along the apical and antapical horns indicating the position of internal vacuoles. Paratabulation as indicated by Evitt (1985: Fig. 11.3). Horn lengths extremely variable.

Batioladinium jaegeri (Alberti) Brideaux 1975

Plate 28, Figs. 5–11

Dimensions: Length, plus operculum (92) 72.6 (58) µm. Width (37) 28.7 (22) µm. Specimens = 41 (24).

Remarks: This species has a variable morphology. The overall shape and the size of the horns vary between two extremes:

1. Short, dumpy specimens (≅ 60 µm long) with prolate ovoidal ambitus and vestigial horns, prominent microgranular sculpture.
2. Longer specimens (up to 85 µm long), with a more rectangular ambitus and prominent apical horn, subdued microgranular sculpture.

The latter form is by far the most common. All forms exhibit a differentiated autophragm consisting of a solid, imperforate base layer. On top of this base is a layer consisting of a multitude of sporopollenin globules partially fused together. The outer surface thus appears to be microgranular (Plate 28, Fig. 11). The variability in the structure of the cyst wall would appear to unite those species illustrated by Alberti (1961) from the German Barremian as *Broomea jaegeri* and *B. pellifera* (both now *Batioladinium*). The former species was only recorded from one locality and the latter was based on 5 specimens. The morphologies of these two types, on the basis of the material studied herein, may form the two end members of a species plexus. These types bear a strong resemblance to the Australian species. *B. micropodum* (Eisenack & Cookson) Brideaux, which has a coarsely and closely granular sculpture.

Some specimens show traces of paratabulation other than the archaeopyle suture, but these are infrequent and difficult to interpret.

5.8.2 *Prolixosphaeridium* Complex

Prolixosphaeridium deirense Davey et al. 1966 emend.

Plate 29, Figs. 1–8

1966 *Prolixosphaeridium deirense* – Davey et al., p. 171. Plate 3, Fig. 2. Text-fig. 45. Lateral equivalent of the Speeton Clay, from a depth of 39 m in the West Heslerton borehole, presumed Middle Barremian strata.
1974 *Prolixosphaeridium parvispinum* – Davey & Verdier, p. 636.

Emended Diagnosis

Shape: Ambitus prolate ovoidal, length: width ratio ≅ 2:1. hypocyst apparently longer than epicyst. Apical paraplates greatly reduced in size with respect to total cyst dimensions. Strong dorso-ventral compression unlikely as cyst found in variety of orientations.

Phragma: Differentiated autophragm ≅ 1 µm thick. Surface sculpture is essentially comprised of a pseudoreticulum, through the lumina of which protrude clavulae (≅ 0.5 µm dia.), giving rise to a granular aspect under the light microscope. In certain places the clavulae are elongated and fuse with neighbouring ones to form solid cylindrical processes. The processes are nontabular and acuminate. Those specimens with a less dense covering of processes (< 50) possess wider processes (> 2 µm dia.), those more densely covered (> 60) have narrower processes (< 2 µm dia.).

Paratabulation: Unknown but consistently shows only 5 precingular paraplates and an *ai* all separated by accessory sutures. This may indicate fusion of two precingular paraplates (see Evitt 1985).

Archaeopyle: Type (tA), presumably involving four apicals as a free, simple polyplacoid operculum. Accessory archaeopyle sutures developed in precingular paraplate series.

Paracingulum: Undifferentiated.

Parasulcus: Only shown by position of *ai* after archaeopyle formation and by slight reduction of process length.

Dimensions: Body length, less operculum (59) 49.4 (42) µm. Body width (32) 25.5 (22) µm. Process length (15) 9 (7) µm. Specimens = 21 (15).

Remarks: The synonomy of *Prolixosphaeridium deirense* with *P. parvispinum* is questioned. Wetzel (1933: 44) erected *Hystrichosphaeridium xanthiopyxides* on "about" six specimens. Deflandre (1937: 77) subsequently described two varieties of this species – var. *granulosum* (on one specimen now lost), and var. *parvispinum*. Both of these types were only illustrated with line drawings. Cookson & Eisenack (1958: 45) elevated the latter variety to specific rank after studying specimens of an Australian form which was a degree of magnitude greater in size than Deflandre's original material. Davey et al. (1969: 17) transferred *H. parvispinum* to *Prolixosphaeridium*. Subsequently, Davey & Verdier (1974: 636–7) synonomised *P. deirense*, the original type of the genus, with *P. parvispinum*, making the latter the new type species.

P. parvispinum is thus a very poorly defined species and pending possible reexamination of Deflandre's type material and the study of topotype material, may not even be referrable to *Prolixosphaeridium*. Thus, *P. deirense*, the original type of the genus is emended, after restudying the holotype and observing additional material from the late Barremian Speeton Clay, and is reinstated as the type of the genus.

The type of sculpture exhibited by this species is very similar to *Tanyosphaeridium*, these genera appear closely related, being distinguished only by the solid processes of the former and the hollow ones of the latter.

Prolixosphaeridium deirense has been recorded in residues from Angles. However, these specimens are more elongate and possess a much more dense cover of shorter processes (e.g. Millioud 1969; Below 1982; Srivastava 1984; see also Duxbury 1980: 138–9): SEM observation of Angles specimens has revealed that the construction of the features of the cyst surface is identical to that of the Boreal specimens, with solid processes formed from fusion of extended papillae. This may indicate that these two morphs are merely two phenotypic variants.

Genus *Tanyosphaeridium* Davey & Williams 1966

Plate 29, Figs. 9–15

Remarks: The specimens referrable to this genus observed in this work have axially elongated cyst bodies (length: width ratio ≧ 2) and > 30 long, hollow processes. Process termination is variable, as is process distribution – the paracingular area rarely being devoid of processes. Archaeopyle is of Type (tA), involving four apicals. As in *Prolixosphaeridium*, accessory archaeopyle sutures between the precingular paraplate series indicate an *ai* plate and only 5 precingulars. This may indicate fusion of two precingular paraplates. Surface sculpture is also very like that found in the genus *Prolixosphaeridium*, but of a rather more subdued nature. The processes appear to arise from swollen, modified papillae.

Intraspecific variation is important in this genus. Forms with very elongate cyst bodies are the predominant type, but forms with lower length : width ratios are not uncommon. However, the two morphotypes are never found within the same residue so this may be a phenotypic variation.

Genus *Wallodinium* Loeblich & Loeblich 1968

Plate 23, Figs. 7, 12

Remarks: Both *W. krutzschii* and *W. lunum* display a sulcal tongue *(ai)* along the periarchaeopyle margin. This implies the loss of all the epicystal paraplates in archaeopyle formation. Thus the epicyst is much reduced in size in relation to the rest of the cyst. In the case of *W. lunum*, the position of the sulcal tongue *(ai)* implies strong lateral compression of the cyst (Plate 23, Fig. 12).

5.8.3 *Apteodinium* Complex

Batiacasphaera mica sp. nov.

Plate 25, Figs. 10–19

Etymology: Latin *mica* – grain or crumb, in reference to the cyst sculpture.
Holotype: Plate 25, Fig. 10.

Type locality: Gott, Bed 100.

Diagnosis

Shape: Ambitus subcircular, varying from slightly oblate to slightly prolate in shape. Epicyst and hypocyst of approximately equal lengths. Greatest width across paracingular region. Moderate to strong dorso-ventral compression.

Phragma: Autophragm up to 1 μm thick, surface microgranular. Granules vary in size on individual specimens – often coarser along paracingular margins and at the antapex.

Paratabulation: Complete paratabulation unknown, but epicystal tabulation as shown by archaeopyle sutures: 4′, 6′′, *ai. A/1i* parasuture anterior to *1u/ai.*

Archaeopyle: Type (tA), involving four apical paraplates as a free, simple, polyplacoid operculum sometimes adherent. Accessory archaeopyle sutures formed in precingular series.

Paracingulum: Rarely expressed, but may be present as an equatorial band conspicuous for its reduced ornamentation.

Parasulcus: Rare specimens show flagellar scar, more usually the only indication is the position of *ai.*

Dimensions: Diameter (60) 47.5 (30) μm. Specimens = 29 (20).

Remarks: The granulation of the cyst body varies from being equidimensional over the whole cyst surface, to being much coarser along parasutures. Those specimens with coarse granulation have thicker walls.

This species is distinguished from *Kallosphaeridium* by the free rather than adnate nature of the operculum. It differs from *B. macrogranulata* Morgan 1975 in having a more subcircular ambitus and having less evenly distributed granulation and from *B. saidensis* Below 1981 in being smaller and having smaller granulae.

5.8.4 *Chlamydophorella* Complex

Genus *Cassiculosphaeridia* Davey 1969

Remarks: Evitt (1985) placed this genus into his Gx-Miscellaneous category, a catchall group for Gx-cysts which did not have a wall capable of being resolved into two distinct layers. SEM investigation of the genus has shown that specimens consist of an autophragm (bearing nontabular muri or septa in the form of a pseudo-reticulum) supporting an ectophragm, the latter layer being very susceptible to degradation by oxidation. The ectophragmal layer may be a clearly separable outer lamella, or in the form of fragile, sheet-like extensions of the distal parts of the muri.

Cassiculosphaeridia magna Davey 1974 emend.

Plate 30, Figs. 1–7

1974 *Cassiculosphaeridia magna* – Davey, p. 46, Plate 1, Figs. 3–7. Bed LB5B of the Speeton Clay, Speeton.

Emended diagnosis

Shape: Ambitus oblate to subcircular. Thick-walled, robust cyst, greatest width in paracingular region. Hypocyst half as long again as the epicyst. Moderate dorso-ventral compression.

Phragma: Differentiated autophragm robust, up to 3 μm thick. In cross section consists of an imperforate internal layer, the main part of the wall is composed of partially fused sporopollenin granulae (up to 0.75 μm in dia.). Distally the granulae fuse more completely leaving a punctate surface layer which is developed into 'septa' up to 8 μm high. The septa are flared proximally and distally and may be fenestrate. The septa are prone to oxidation damage which rounds off their distal extremities. The septa are generally non-tabular, in the form of a pseudoreticulation. Ectophragm is rarely preserved, though when present is ≅ 0.2–0.5 μm thick and is a distal extension of the septa (Plate 30, Fig. 3. The ectocoel is partitioned, an ectocoelar area enclosed in each lumen of the pseudoreticulum.

Paratabulation: Only determined for the epicyst by studying the nature of the archaeopyle suture: pr, 4′, 6′′, *ai*.

Archaeopyle: Type (tA), involving the apicals as a free, simple polyplacoid operculum.

Paracingulum: Usually undifferentiated, but sometimes delineated by quasi-parallel orientation of septa.

Parasulcus: Shown occasionally by slightly offset parasulcal notch.

Dimensions: Diameter (105) 95.6 (85) μm. Specimens = 31 (10).

Remarks: The presence of an ectophragm in this species has not previously been reported. However, study of new topotype material from Bed LB5B at Speeton and abundant specimens of this striking species from other localities has shown that this is a consistent feature if very mild oxidising agents are used (or oxidation is not performed) to prevent digestion of the ectophragm.

Cassiculosphaeridia tunicata sp. nov.

Plate 27

Etymology: Latin *tunicatus* – having a thin separable covering, in reference to the thin ectophragm.
Holotype: Plate 27, Figs. 9 and 11.
Type locality: Gott, Bed 67.

Diagnosis

Shape: Ambitus subcircular to slightly oblate. Greatest width posterior to archaeopyle margin (≅ paracingulum). Epicyst and hypocyst difficult to distinguish. Moderate to strong dorso-ventral compression.

Phragma: The autophragm is up to 1 μm thick with a laevigate surface texture. The distal surface of the autophragm bears an uneven reticulum of solid muri/septa (up to 2.5 μm wide and 1–2 μm high) which are nontabular in arrangement. The reticulation is variable, the lumina range from 3–18 μm in diameter. The ectophragm (≅ 0.1 μm thick) forms a continuous, highly perforate layer over the whole cyst surface. This layer is supported on the reticulum but subsides into the lumina and appears draped over the cyst surface. Perforations in the ectophragm are random, densely distributed and usually less than 1 μm in diameter. The ectophragm is often seen to 'blister' over the lumina, this may be due to distortion caused by authigenic pyrite growing to the ectocoels.

Paratabulation: Hypocystal paratabulation unknown, but rare specimens show an angular archaeopyle margin giving the following epicystal paratabulation formula: 4′, 6′′, + *ai*.

Archaeopyle: Type (tA), involving the loss of the apical paraplate series as a simple, polyplacoid operculum.

Paracingulum: Only distinguished on a few specimens which show alignment of the muri in the equatorial region.

Parasulcus: May show as an area of reduced reticulation, or may be evidenced by the parasulcal notch.

Dimensions: Diameter (55) 48.9 (42) µm. Specimens = 10 (10).

Remarks: A distinctive species of *Cassiculosphaeridia* due to the more coherent nature of the ectophragm. In most of the species of this genus that have been studied the ectophragm is a much more diaphanous layer formed of aggregations of granular material, rather than a solid lamellum. *C. tazadensis* Below, has an ectophragm which is either imperforate or perforated on a very small scale (Below 1981: Plate 12, Fig. 16).

Genus *Chlamydophorella* (Cookson & Eisenack) Duxbury 1983

Remarks: The paratabulation of most members of this genus is unknown. However, during the present study, one member of this genus – *C. trabeculosa* (ex-*Gardodinium*) – has been found to exhibit L-type sexiform gonyaulacoid tabulation (Harding, 1989. Also see *Leptodinium* Complex of Gs-Cysts herein).

Chlamydophorella nyei Cookson & Eisenack 1958

Plate 26, Figs. 9–16

Remarks: Whilst the specimens all display certain characters in common, body shape (spheroidal to axially elongate), horn length and size of ectophragmal perforations vary considerably. Many of these variations appear to be of a phenotypic nature. This species is much smaller than *C. trabeculosa*, and unlike that species, has no expression of paratabulation on the ectophragm. Apical archaeopyle (Type (tA) suture indicates four apical and six precingular paraplates + *ai*. Autophragm up to 0.5 µm thick, bears densely packed, solid, intratabular processes (3–6 µm long and ≅ 1 µm dia.), which may be perforate but do not bifurcate distally as suggested by Davey (1978: 893). Ectophragm ≅ 0.2 µm thick, granular surface is highly perforate. The perforations vary in size (up to 1.5 µm dia.) and are of an irregular shape.

5.9 Rp-Cysts

Genus *Angustidinium* Goodman & Evitt 1981

Plate 30, Figs. 13–14

Remarks: A few, very rare specimens referable to this genus have been found throughout the Barremian. The specimens are not conspecific with *A. acribes*, but do possess the five apical paraplates, the camarate *2a* and the peridinioid hypocyst paratabulation characteristic of this species. One peculiar feature of these specimens is the preferential digestion of the paraplate sutures by the oxidising agent used in preparation.

6. Ranges of dinocyst taxa

This chapter gives details of the biostratigraphic ranges of all the species identified in the palynologic residues studied. A range chart is given for each of the successions examined (Tables 3–7). The ranges of the dinocysts isolated from the Warlingham borehole between 1500 ft. can be found in Hughes & Harding (1985) and Harding (1986a). The presence of a particular species in a particular sample has been quantified, based on counts of not less than 500 specimens per stub, additional records of rare species being added from observation of slides where appropriate. This serves both to illustrate the importance of an individual species within a sample, its importance throughout geologic time and to quantify the yield of each particular sample. These facts are of great importance as they compose the raw data on which conclusions are based and allows the reader to assess the conclusions reached.

The ranges of the new species described in this work are stated on the range charts included in this chapter. It is necessary at this point to discuss the ranges of those more stratigraphically important species already decribed from these and other localities.

Pseudoceratium anaphrissum: has an extremely restricted stratigraphic distribution. In this study the range of this species has been found to be coincident with the early Barremian Hauptblätterton event. Thus records of this

form from the Middle B Beds of the Speeton Clay (DAVEY 1974) must be questioned (see DUXBURY 1980: 137). THUSU (1978) correctly identified this species (as *Tenua anaphrissa*) from Kong Karls Land (Spitsbergen), further extending its range within the Boreal realm. The precise age of the sample from which the specimens were recovered was not stated any more accurately than "Barremian".

BELOW (1981: Plate 2, Fig. 5) illustrated *P. anaphrissum* (as *Aptea*) from the Hauterivian of Morocco where it occurs in only one sample in flood abundance but is morphologically within the range of variation seen in Boreal material for this species. The sample may possibly be wrongly dated as there appears to be little in the way of biostratigraphic control on this part of the Moroccan succession. Alternatively, the restricted occurrence of *P. anaphrissum* in Boreal successions may represent an isolated incursion of the Tethyan seas into Boreal Europe (MUTTERLOSE & HARDING 1987b), thus giving an artificially short stratigraphic range for the Boreal occurrence of the species. However, as this species is more widely reported from Boreal successions, it may be unwise to interpret its occurrence in this latter manner, although *P. anaphrissum* may prove to be an important inter-province marker species.

Other illustrated records of this species in WILLIAMS (1975) and POCOCK (1976), from material from offshore southeastern and Arctic Canada respectively, are not of conspecific specimens.

Cassiculosphaeridia magna: both DAVEY (1974) and DUXBURY (1980) recorded this species as occurring throughout Barremian time. This study has found that the species is restricted to early Barremian time, becoming extinct during Hauptblätterton event times. DE RENEVILLE & RAYNAUD (1980) also recorded the disappearance of this species at the end of early Barremian time at the Angles locality. The anomalous ranges cited by Davey and Duxbury may well refer to records of a similar large reticulate dinocyst which occurs sporadically from the end of the Hauptblätterton event into late Barremian time. This form also has an apical archaeopyle (tA), but is also characterised by a prominent paracingular bulge and a noticeable sulcal groove. This form is the subject of continuing study.

Cerbia tabulata: A common species in late Barremian time, first appearing at the end of the Hauptblätterton event, seemingly 'replacing' *Pseudoceratium anaphrissum* in the palynological assemblages. The inception of this species at this point is corroborated by DAVEY (1979, as *Cyclonephelium*) and by DUXBURY (1980, as *Canninginopsis*?). Similar ranges are reported from Morocco by BELOW (1981), from late Barremian to Aptian time (although on his Fig. 87 there is a record of 1–3 specimens in the Hauterivian which is not confirmed in the text). This form has also been recorded, but not illustrated, from rocks of latest Barremian age in the Angles section by DE RENEVILLE & RAYNAUD (1980).

Cribroperidinium confossum: DUXBURY (1977) gave a range from Bed C4B to LB6 in the Speeton Clay when describing this species. The present study has not found this species in rocks of late Hauterivian age as presently defined at Speeton (or elsewhere by interpretation). This discrepancy may be due to very low abundance in these lower samples, but DUXBURY (1977) gave no abundance data.

Cribroperidinium sepimentum: restudy of the NEALE & SARJEANT (1962) type material has resulted in the recognition of this species in samples from Hunstanton of a late Hauterivian age and of a ?reworked specimen in the earliest Barremian of Gott. DAVEY (1974) gave a range up into the Middle B Beds of Speeton, but did not illustrate any of these specimens. DUXBURY (1977) on the other hand, found only three specimens restricted to the late Hauterivian Beds C6 and C9A at Speeton. It appears that this species (the type of the genus) occurs rarely and is most common in samples deposited in conditions of somewhat reduced salinity (although DAVEY – 1979 – states that it composes up to 5% of assemblages in Beds C4B to C2D at Speeton).

FOUCHER (in ROBASZYNSKI et al., 1980) erected a "*Cribroperidinium sepimentum* Partial Range Zone" for the late Aptian of the Boulonnais (France), but without illustrations this identification must be regarded as dubious.

Cribroperidinium tensifiense: the range of mid-Barremian to Albian given by BELOW (1981) for the Tethyan type material from Morocco is in agreement with the ranges presently found. The species first appears in Hauptblätterton times in low abundance, but becomes an important component of late Barremian assemblages and of Aptian assemblages at Warlingham.

Exiguisphaera phragma: an often abundant species for which no complete stratigraphic range has been published. First described by DUXBURY (1979) from Bed C10 at Speeton, it has also been recorded in the Haldager No. 1 borehole, Denmark in the "early-?late Hauterivian" (DAVEY 1982). Present work indicates that it ranges into earliest Barremian time.

Canninginopsis duxbryi sp. nov.: recorded as *Canningia* cf. *reticulata* by DUXBURY (1977) from Beds C7 to C3 at Speeton. DAVEY (1979) gave a range of Beds C4B/C to C2C/D. Bed by bed sampling has now shown that this range should be extended into the earliest Barremian Bed LB5D at Speeton and Bed 61 at Gott.

Alaskadinium wigginsii: DUXBURY (1977) found this species (as *Gonyaulacysta kostromiensis*) to range from Bed D2D to Bed C1A at Speeton; it has also been found in the "?late Hauterivian" of the Haldager No. 1 borehole, Denmark (as *Nelchinopsis kostromiensis* – DAVEY 1982). THUSU (1978) reported it from the Ryazanian and Valanginian sediments of Spitsbergen.

VOZZHENNIKOVA (1967) first described *G. kostromiensis* from the Valanginian deposits of the USSR. The forms illustrated from rocks of Valanginian to ?early Hauterivian age of Alaska by WIGGINS (1972) and DUXBURY (1977) are probably not of conspecific forms (LENTIN, pers. comm., HARDING, in prep.). The species here referred to as *Alaskadinium wigginsii* DUXBURY 1977, may prove to be an excellent inter-province marker due to its wide geographic distribution (Alaska to Boreal Europe). In the present study the range of this species has been found to extend into very earliest Barremian time.

Gonyaulacysta teicha: a range from bed C4 to LB4D was given by DAVEY (1974, 1979). The present study has yielded specimens from as high as Bed LB4C at Speeton and comparable horizons at the other localities studied.

Hystrichodinium furcatum: a species with a very short stratigraphic range, being restricted to earliest Barremian time from the samples studied here, although ALBERTI (1961) also recorded it from late Hauterivian sediments of Germany in possibly unreliably dated borehole material.

Hystrichodinium ramoides: this species also has an extremely short vertical range within latest Barremian time, comparable with the range given to this species by ALBERTI (1961) in German borehole samples. DUXBURY (1980) is believed to have quoted an excessively long range for this species.

Hystrichosphaeridium arborispinum: originally described from the presumed mid-Barremian Speeton Clay of the West Heslerton borehole. This study has found that the species first appears in Hauptblätterton event times at Gott, Speeton and Hunstanton. The species is not represented at the equivalent level at Alford due to poor dinocyst yield. Although an extremely common component of the assemblages in the Hauptblätterton at the former three localities, it becomes rare and erratic in its distribution in upper Barremian sediments. These ranges agree with those of DAVEY (1974) and DUXBURY (1980).

Kleithriasphaeridium corrugatum: this form becomes extinct at the end of early Barremian time, dying out during the Hauptblätterton event. This is corroborated by DAVEY (1974, who recorded it no higher than Bed LB1 at Speeton. DUXBURY (1980) recorded it in the lowest of his samples from the Middle B Beds of the Speeton Clay, but gave no abundance data. Reworked specimens have been found in the late Barremian samples of the Alford borehole and local reworking may account for the anomalous record given by Duxbury.

Meiourogonyaulax sagena: first described by DUXBURY (1980), this species was believed restricted to the Middle B Beds of the Speeton Clay. Whilst the occurrence of this species outside the Middle B Beds at this locality is uncommon, it ranges into early and late Barremian time of the other localities studied; it is most common in the early Barremian of Gott.

Nexosispinum vetusculum: DAVEY (1974) gave the range of this species as Bed LB5B to LB2D at Speeton, later extending this range down to Bed C11 (DAVEY 1979). DUXBURY (1977), in his range chart recorded the species from Bed C3 to LB3. Although the species becomes uncommon through early Barremian time, it has been found in abundance in some samples from Bed 100 at Gott (100/11/83) and thus must be taken as ranging almost to the top of the early Barremian.

Odontochitina operculata: the present author agrees with DUXBURY (1980) in that the reported pre-late Barremian occurrences of this species appear to have been misidentifications of forms with similar morphologies, such as the isolated opercula of species of *Muderongia*. This species was not recorded earlier than the late Barremian by SARJEANT (1966b) or DUXBURY (1980) or in this study.

Palaeoperidinium cretaceum: this species was restricted to nearshore environments as the assemblages in which it occurs contain high percentages of terrestrial palynomorphs, including the large early angiosperm pollen genus *Afropollis* (pers. obs. & PENNY, 1989). It is extremely common in some late Barremian samples (e.g. Hunstanton 130/0), but is otherwise rare in most samples of this age studied (only two specimens have been isolated from Gott material). Thus, this species may be used as a palaeoenvironmental index, but does not satisfy the requirements of a zonal index species (see DAVEY 1979, 1982).

Pseudoceratium pelliferum and *P. solocispinum*: the disappearance of *Pseudoceratium pelliferum* has been noted in samples of earliest late Barremian age of all the localities studied. It is effectively 'replaced' by *P. solocispinum*, which persists into the later late Barremian, but disappears before the end of the age. *P. solocispinum* has only been previously reported from late Barremian time (Davey 1974; Duxbury 1980), as a subspecies of *P. pelliferum*. The two forms have not been found to occur together in any sample studied for this work and are here recognised as distinct species.

Records of either species from post-Barremian strata should be treated with caution, as they are probably reworked examples or erroneous identifications (perhaps of the very similar *P. interiorense* Bint 1986 or *P. aulaeum* sp. nov.).

Subtilisphaera terrula and *S. perlucida*: the first named species was described by Davey (1974, as *Deflandrea*) in samples from Bed LB5B through to the ζ cementstone band of the Middle B Beds of the Speeton Clay. Duxbury (1980) gave a range from Bed C1B up to the δ cementstone band. Davey (1979) revised his earliest appearance of the species down to Bed C4B/C. The present study has shown that this species, although subject to palaeoenvironmental control (it occurs in nearshore sediments only, being absent from the offshore sediments of the Hauptblätterton at Gott), becomes extinct early in late Barremian time. It is effectively 'replaced' by the appearance of *S. perlucida*, which does not occur earlier than the disappearance of *S. terrula*.

Trabeculidinium quinquetrum: this species has only been described from the Middle B Beds of Speeton (Duxbury 1980) and has been found to have a similarly restricted distribution in the Gott and Alford successions.

Trichodinium ciliatum: a species which has been observed to disappear in early Barremian time, it is not recorded higher than Bed LB5B at Speeton by Davey (1974), although Duxbury (1977) records it from the Middle B Beds. In the present study this form has been recorded up to Bed LB4C at Speeton, Bed 83 at Gott, a depth of 170 ft. in the Hunstanton borehole and a depth of 202–204 ft. in the Alford borehole.

Trichodinium speetonense: the first appearance of this species is in early Barremian time, as a 'replacement' in the dinocyst flora for *Trichodinium ciliatum* (no morphological intermediates have been observed). Davey (1974) records a range beginning in Bed LB4D at Speeton, whereas Duxbury (1980) records it no lower than the Middle B Beds. *The range of this species can now be envisaged as beginning in Bed LB2C at Speeton, Bed 83 at Gott, a* depth of 155 ft. in the Hunstanton borehole and a depth of 191–192 ft. in the Alford borehole. The specimens identified by Pocock (1976) as *T.* cf. *speetonense*, possess true apical horns and therefore are not referable to this species.

7. Biostratigraphy

7.1 Introduction

Coquand (1862) proposed the Barremian stage of the Lower Cretaceous as a stratigraphic unit. It was not until Busnardo (1965a) that a stratotype section for the Barremian was designated. The Barremian age is now a division of the Early Cretaceous epoch of the global geologic time scale and is designated by a marker point at its beginning. Historically, the Barremian reference sections have always been in the Tethyan province, a potentially advantageous situation which, theoretically means that it may be possible to correlate the area with both the northern Boreal province and the southern Austral province.

Previous studies of the dinocyst assemblages present in the Angles section have been carried out by several authors in varying degrees of detail and varying accuracy of specific assignments. The samples collected for the present study have proved difficult to examine due to the vast amounts of organic debris present in the residues. For this reason it has not been possible to include data from this succession in the results presented here. It is hoped that the material will be studied at a later date in order to achieve the same degree of accuracy as that attained for the Boreal sections already studied. The previous works concerning the dinocysts of Angles (Millioud 1969; De Reneville & Raynaud 1980; Zahiri 1981; Srivastava 1984), and the few samples already analysed by the present author, have proved to be of value for comparative purposes in order to assess the potential of various species for stratigraphic correlation.

Work has been concentrated on the Boreal successions as they have been found to yield readily observable, high diversity and well preserved dinocyst floras.

7.2 Calibration and correlation

Using closely spaced samples and SEM observation it has been possible to refine the stratigraphic distribution of many of the observed species. Few of the species identified have had their stratigraphic range extended (the main exception to this being *Meiourogonyaulax sagena*).

The selection of events from the range charts to create a calibration scheme suitable to be applied to any western European Boreal succession of Barremian age, has been made with the following observations in mind. The precise time-correlation of one succession with another cannot be realised as a certain amount of diachroneity is to be expected with biological events at separate geographical localities. In order to reduce the possibility of diachroneity of events, the close spacing of sampling and thus the decreased stratigraphical spacing of events, will raise the chances of detecting a strongly diachronous event (Scott 1985). Such events can then be weeded out as they represent slow dispersal events and are therefore not the best points available on which to erect a calibration. Because of this fact such correlations should only be viewed as a correlation of biological event ordering in one area with the events of another area and not of a true time-correlation (the process of "bracket-correlation" of Hughes & Moody-Stuart 1969 and Hughes 1976). The aim of a biostratigrapher must be to identify those events which are the most reliable for the erection of a calibration scheme. From a geochronological point of view the migration of a planktonic species is a 'virtually' instantaneous event (Berggren & Van Couvering 1978).

The calibration presented here to permit correlation of other successions with the reference successions has been based on first appearances of taxa wherever possible. The taxa used in the calibration have been chosen because of their restricted stratigraphic distribution and, where possible, because of their known occurrence in Tethyan deposits. The calibration scheme can be seen in Text-fig. 18, where it is set against the Boreal cephalopod zonations of Kemper (1976) and Mutterlose (1983).

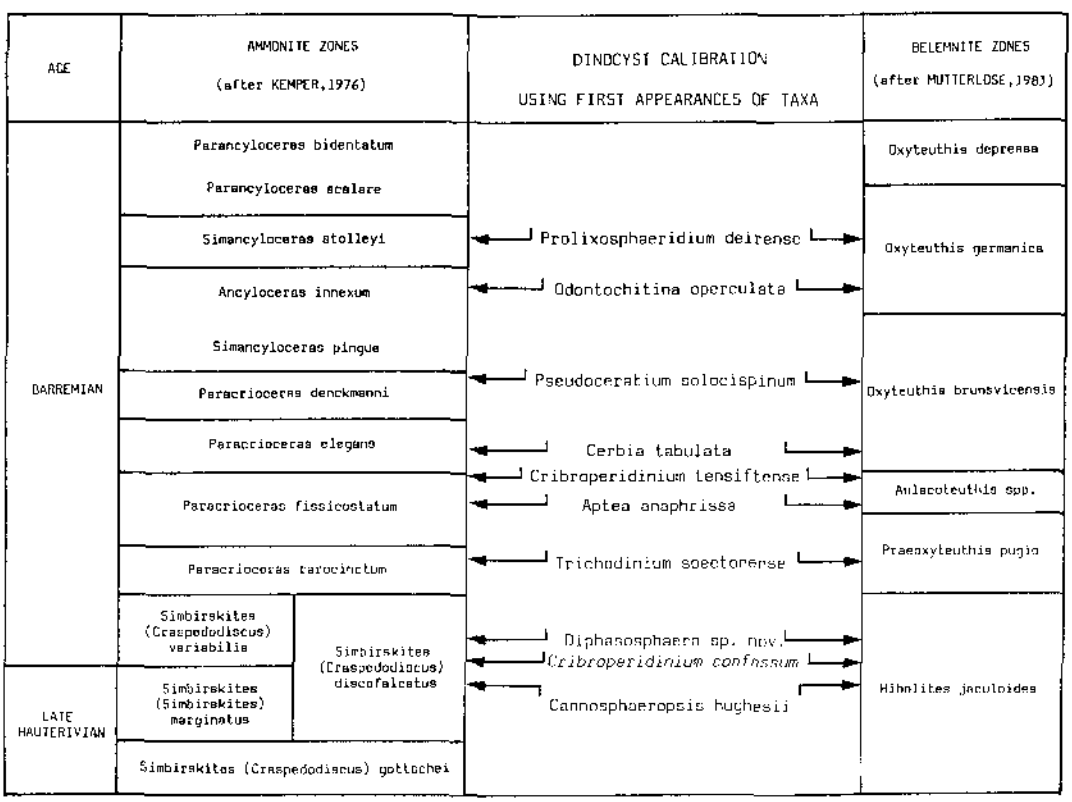

Text-fig. 18. Dinocyst calibration for the NW European Late Hauterivian and Barremian, correlated with the standard cephalopod zonations. All arrows mark species appearance datums in the successions, except for *Cannosphaeropsis hughesii*, which is an extinction datum. The early/late Barremian division would be drawn between the *fissicostatum* and *elegans* ammonite zones and the *Aulacoteuthis* and *brunsvicensis* belemnite zones.

The concept of a 'zonation' is felt to be too rigid for what should be a constantly evolving process of biostratigraphical refinement. Such zonations are only useful at the time of their erection, thereafter the scheme becomes more and more destabilised as new data is added (see below). Instead of a formalised zonation, I have presented the data amassed in the form of an informal series of events (a calibration), which is capable of being updated at any time in the future. This removes the need constantly to redefine zonal boundaries and even to rename zonal taxa as the systematics of the groups involved changes.

There is no completely exposed section of late Hauterivian through to early Aptian age strata in the Boreal of NW Europe at the present time. Thus any study of this period must rely on a composite section, compiled from separate localities in order to cover the required time span. The Speeton succession has long been the subject of academic study; the lithologic subdivision of the strata at this locality, although disturbed, has been worked out in great detail (e.g. Rawson 1971; Rawson & Mutterlose 1983). This lithostratigraphy has been used as the base onto which to refer cephalopod zonations. Kemper et al. (1981) were able to correlate the 'Boreal Barremian' of Speeton with the Tethyan Barremian on ammonite evidence better than at any other known locality in NW Europe. The Hauterivian/Barremian boundary is now placed at the base of Bed C2C on the basis of ammonite evidence. For

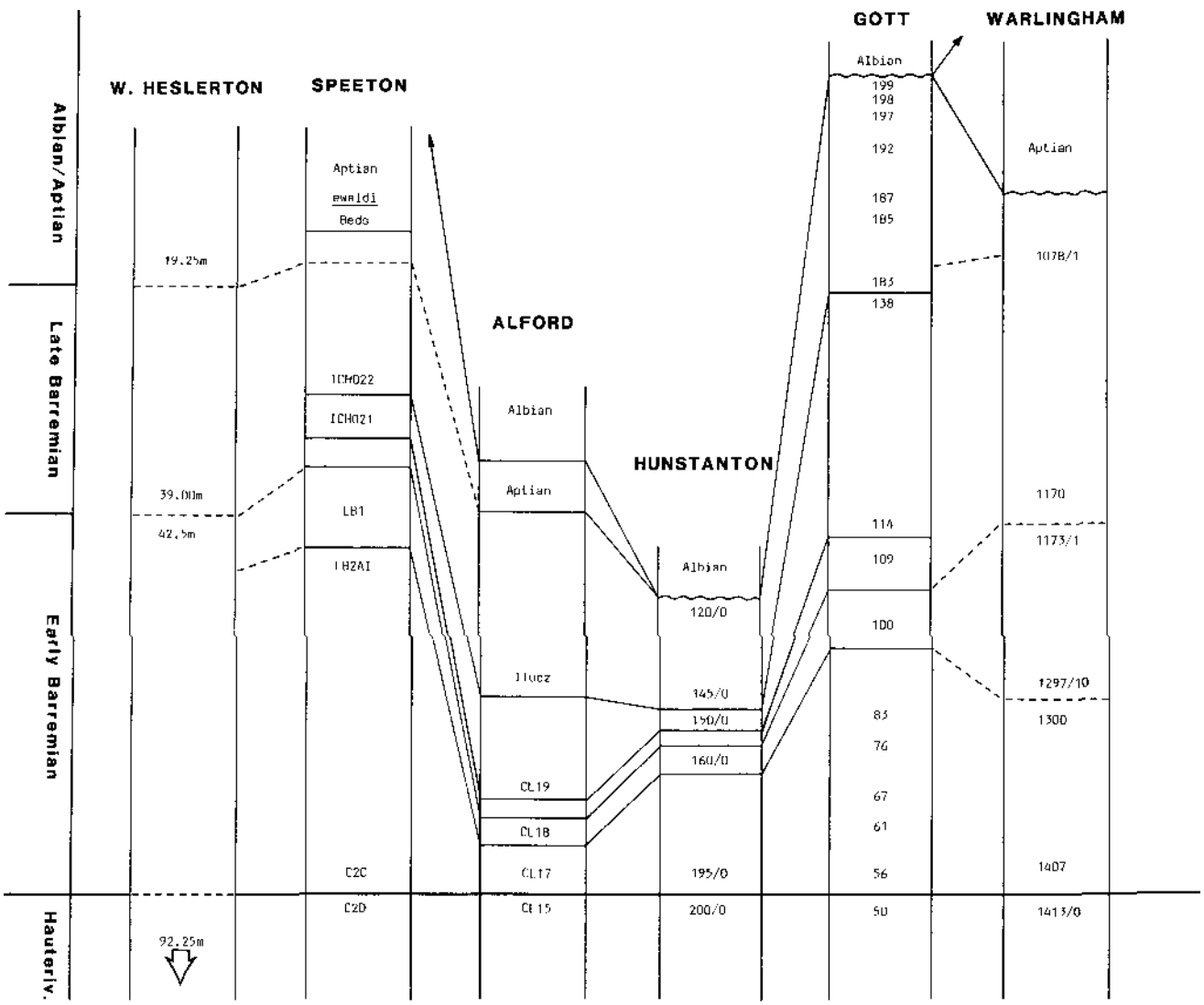

Text-fig. 19. Proposed correlation of the successions dealt with in the text, based on palynological examination. All sections are to scale, except that of Warlingham which is half the scale of the others.

these reasons I have chosen the Speeton succession as the standard reference section for the early Barremian to which to refer the data accumulated from the other localities studied in this work.

Deposits of later Barremian age at Speeton are poorly known (Middle and Upper B Beds), due to incomplete exposure. Because of the difficulties of precise stratigraphic positioning of samples in the late Barremian at Speeton, this section of the calibration relies more on data from the well exposed and accurately lithologically subdivided Gott succession, which is tied in well to the cephalopod zonations of both KEMPER (1976) and MUTTERLOSE (1983).

Unfortunately, the Aptian and topmost Barremian sediments at Gott have been removed by erosion, although the erosive contact with sediments of Albian age appears to have resulted in the loss of very little of the topmost Barremian (J. MUTTERLOSE, pers. comm.). A continuous succession of late Barremian through to early Aptian age is known in the Alford borehole, but poor dinocyst recovery from the Skegness Clay and Sutterby Marl in this section has meant that the Barremian/Aptian boundary has not yet been characterised. This is the subject of current research.

A correlation, using this calibration scheme, of the localities studied, is presented in Text-fig. 19. A refinement of this correlation and a detailed discussion of the methods used in the compilation of this scheme will appear at a later date.

7.3 Comparisons with previously erected zonations

There have been few detailed dinocyst zonation schemes published which attempt any better refinement than one or two dinocyst zones per age. The utility of dinocysts in stratigraphic subdivision has thus not approached the apparent resolution of cephalopod zonations. However, the present study has shown that this need not always be the case. Closely spaced sampling coupled with high resolution observation techniques show that dinocysts are extremely useful organisms for fine-resolution biostratigraphic purposes, especially in those successions which are impoverished with respect to megafossils.

One of the published dinocyst zonations which attains a much greater degree of accuracy than those mentioned above is that of DAVEY (1979, 1982), for the Portlandian-Barremian of NW Europe. However, the ranges of some of the named zonal indices given by Davey have been questioned (DUXBURY 1980; this work). Several datum events established by DAVEY (1979, 1982) such as the earliest appearance of *Odontochitina operculata* and the extinctions of *Canningia duxburyi* sp. nov. and *Pseudoceratium pelliferum* and used as zonal or subzonal boundaries, cannot in the light of new information be maintained. Thus the established zonal scheme is now somewhat destabilised and would necessitate a redefinition of several of the zonal and subzonal boundaries if the scheme was to be maintained. However, the zonations erected by DAVEY (1979, 1982) have provided a very valuable framework, indicating that dinocyst calibrations of the geologic column can be constructed with a better resolution than previously believed and has provided the impetus for further research.

DUXBURY (1977) erected five zones labelled A to E (in ascending order) for the Speeton Clay (this designation is felt to have been unwise as the Speeton Clay has already been divided into Beds labelled A to E in descending sequence which creates unnecessary complications). Of these zones, Duxbury's 'E' zone falls within the scope of the present survey. The base of the zone is characterised by the first appearances of *Hystrichosphaerina schindewolfii* and *Subtilisphaera terrula*, the top by the latest occurrences of *Cribroperidinium confossum* (as *Gonyaulacysta*) and *Spiniferites dentatus*. The first appearance of *H. schindewolfii* has been found in the present survey to be an unreliable event as the first appearance seems to occur at different horizons at several of the localities studied (i.e. not a homotaxial event). The last occurrences of the two species characterising the top of the zone have not been found to occur at the same horizon in any of the localities examined. DUXBURY (1977: 60) also states that "a distinctive change in assemblage character between SPE2 and SPE 3 (both of early Barremian age) is probably unimportant as far as species range considerations are concerned and is probably due to lithological variation rather than any other single factor". This transition from Duxbury's sample SPE2 to SPE3 actually marks the transition to Hauptblätterton conditions at Speeton, this event has important influences on the biostratigraphic ranges of some species but is not due merely to a change in lithology.

Duxbury (1980) proposed no zonation for the higher beds of the B division of the Speeton Clay, only listing the species confined to the Lower B Beds, the Middle B Beds and the Upper B Beds. Some of these ranges have now been increased.

A survey of other zonations established for Boreal successions shows that they all have little in common with the calibration scheme now envisaged. Both Williams (1975) and Pocock (1976) gave zonations for Canadian material, the former for Eastern Canada and the latter for Arctic Canada. These zonations include species also described in this work, but the illustrations given by the aforementioned authors are clearly not of conspecific material (two examples being *Aptea* (now *Pseudoceratium*) *anaphrissa* and *Trichodinium* aff. *speetonense*). Several of the species common in the samples studied in this survey are listed as occurring in the Canadian material, but the ranges of these species are different.

The Tethyan assemblages from Angles studied by De Reneville & Raynaud (1980) show some similarity in species content with those of NW Europe. The ranges of some species also tie in well with some of those from the Boreal Realm – the extinction of *Cassiculosphaeridia magna* and *Kleithriasphaeridium corrugatum* at the end of the early Barremian and the first appearance of *Prolixosphaeridium deirense* (as *P. parvispinum*) in late Barremian time.

Other studies of the dinocysts of the Tethyan Province include those of Antonescu & Avram (1980) on Romanian material. In the zonal scheme erected in that work, zonal rank is given to *Prolixosphaeridium parvispinum* (*P. deirense* in this work) which is stated to appear in late Barremian time, as it does in the Boreal Province.

Perhaps the most detailed work on Tethyan dinocyst zonations has been performed on DSDP material from the western Atlantic by Habib (1975, 1977, 1978). However, the results from these studies show that the species composition in this region is rather different from both the Tethyan of the Mediterranean region and the Boreal of NW Europe. The zonal indices used by Habib largely comprise species of the genus *Druggidium*. Although the genus is well represented in the Boreal region (Harding 1986b) it appears that the acme of the genus was earlier in the Cretaceous in the Tethyan Province than that seen in NW Europe. Habib (1975, 1977, 1978) gives zonal status to *Odontochitina operculata*, which he records from late Hauterivian time onwards. This very early record of this species may be due to a true earlier occurrence of the species in Tethys followed by a later migration into the Boreal Province, or due to the problems of specific misidentification mentioned earlier (see p. 52).

The differences in species composition between the French/Romanian/Atlantic and NW European material can be partly explained by the fact that the former assemblages are of an oceanic nature compared to the shelf sea nature (showing greater species diversity) of the assemblages reported from NW Europe Bujak & Williams (1985). It appears that the assemblages from NW Europe have several species in common with the Tethyan assemblages of southern France and Romania. The Romanian material bears closest comparison with the Valangian to Hauterivian zonation of the western Atlantic. Zonations for the Austral Province (which are of little relevance to the present study) are detailed in Bujak & Williams (1989).

Index list to species dicussed in Part II

References

For those references to authors of systematic descriptions not in the following bibliography, the reader is referred to Lentin & Williams (1989).

Alberti, G. (1961): Zur Kenntnis Mesozoischer und Alttertiärer Dinoflagellaten und Hystrichosphaerideen von Nord- und Mitteldeutschland sowie einigen anderen europäischen Gebieten. – Palaeontographica, Abt. A, **116:** 1–58.

Alimirzaie, D. (1972): Horizontale Veränderung der Foraminiferen-Fauna in einer Mergeltonbank des Mittel-Barrême von Sarstedt bei Hannover (Mit einer Vermessung und Kartierung der Ziegeleigrube Otto Gott). – Dipl.-Arbeit, Kiel, 41p. Unpublished.

Antonescu, E. & Avram, E. (1980): Corrélation des dinoflagellés avec les zones d'ammonites et de calpionelles du Crétacé Inférieur de Svinita-Banat. – Annuarul Institutului de Geologie si Geofizica, Bucharest, **56:** 97–132.

Batten, D. J. (1982): Palynofacies and salinity in the Purbeck and Wealden of southern England. – In Banner, F. T & Lord, A. R. (eds.) Aspects of micropalaeontology, 278–308. Allen & Unwin.

–,– (1985): Two new dinoflagellate cyst genera from the non-marine Lower Cretaceous of southeast England. – N. Jb. Geol. Paläont. Mh., **1985** (7): 427–437.

Batten, *D. J. & Lister, J. K. (1988):* Early Cretaceous dinoflagellate cysts and chlorococcalean algae from freshwater and low salinity palynofacies in the Englisch Wealden. Cretaceous Research, **9:** 337-367

Below, R. (1981): Dinoflagellaten-Zysten aus dem oberen Hauterive bis unteren Cenoman Süd-West Marokkos. Palaeontographica, Abt. B, **176:** 1–145.

–,– (1982a). Zur Kenntnis der Dinoflagellaten-Zysten-Populationen im Ober Apt der Tongrube "Otto Gott" in Sarstedt/Norddeutschland. – N. Jb. Geol. Paläont. Abh., **164:** 339–363.

–,– (1982b): Scolochorate Zysten der Gonyaulacaceae (Dinophyceae) aus der Unterkreide Marokkos. – Palaeontographica, Abt. B, **182:** 1–51.

Benson, D. G. Jnr. (1985): Observations and recommendations on the fossil dinocyst genera *Ctenidodinium, Dichadogonyaulax* and *Korystocysta.* – Tulane Studies in Geology and Paleontology, **18:** 145–155.

Berggren, W. A. & Van Couvering, J. A. (1978): Biochronology. – In Cohee, G. V., Glaessner, M. F. & Hedberg, H. D. (eds.) – The Geologic Time Scale. AAPG, Tulsa, Oklahoma. 39–55.

Bint, A. N. (1986): Fossil Ceratiaceae: a restudy and new taxa from the mid-Cretaceous of the Western Interior, U.S.A. Palynology, **10:** 135–180.

Busnardo, N. (1965a): Le stratotype du Barrémian. I. Lithologie et macrofaune. – Mém. B.R.G.M., **34:** 101–116.

–,– (1965b): Rapport sur l'étage Barrémian. – Mém. B.R.G.M., **34:** 161–169.

Casey, R. & Gallois, R. W. (1973): The Sandringham Sands of Norfolk. – Proc. Yorks. geol. Soc., **40:** 1–22.

Casey, R. & Rawson, P. F. (eds.) (1973): The Boreal Lower Cretaceous. – Geol. Inl. Spec. Issue, 5, 448p. Seel House Press, Liverpool.

Clarke, R. F. A. & Verdier, J.-P. (1967): An investigation of microplankton assemblages from the Chalk of the Isle of Wight, England. – Verhandelingen der Koninklijke Nederlandsche Akademie van Wetenschappen, Afdeeling Natuurkunde, Eerste Reeks, **24:** 1–96.

Cookson, I. C. & Eisenack, A. (1958): Microplankton from Australian and New Guinea Upper Mesozoic sediments. – Proc. Roy. Soc. Victoria, **70:** 19–79.

–,– (1960): Upper Mesozoic microplankton from Australia and New Guinea. – Palaeontology, **2:** 243–261.

Coquand, H. (1862): Sur la covenance détablir dans le groupe inférieur de la formation crétacée un nouvel étage entre le néocomien proprement dit (couches à *Toxaster complanatus* et à *Ostrea Couloni*) et le néocomien supérieur (étage urgonien dÁlc. d'Orbigny). – Bull. Soc. géol. France, **19:** 531–541.

Cotillon, P. (1984): Tentative world-wide correlation of Early Cretaceous strata by limestone-marl cyclicities in pelagic deposits. – Bull. geol. Soc. Denmark, **33:** 91–102.

Davey, R. J. (1974): Dinoflagellate cysts from the Barremian of the Speeton Clay, England. – Birbal Sahni Inst. Paleobotany Spec Publ., **3:** 41–76.

–,– (1978): Marine Cretaceous palynology of Site 361, DSDP Leg 40, off southwestern Africa. – In Bolli, H. M., Ryan, W. B. F., et al., Init. Reps. DSDP, **40:** 883–914.

–,– (1982): Dinocyst stratigraphy of the latest Jurassic to Early Cretaceous of the Haldager No. 1 borehole, Denmark. – Danmarks Geologiske Undersøgelse, Ser. B, Nr. 6, 57p.

Davey, R. J., Downie, C., Sarjeant, W. A. S. & Williams, G. L. (1969): Appendix to "Studies on Mesozoic and Cainozoic dinoflagellate cysts". – Bull. B.M. (N.H.) Geol. Appendix to Supplement, **3:** 24p.

–,– (1966): Fossil dinoflagellate cysts attributed to *Baltisphaeridium.* – In Davey, R. J., Downie, C., Sarjeant, W. A. S. & Williams, G. L.: Studies on Mesozoic and Cainozoic dinoflagellate cysts. Bull. B.M. (N.H.) Geol. Supplement, **3:** 157–175.

Davey, R. J. & Verdier, J.-P. (1974): Dinoflagellate cysts from the Aptian type sections at Gargas and La Bedoule, France. Palaeontology , **17:** 623–653.

Davey, R. J. & Williams, G. L. (1966a): The genera *Hystrichosphaera* and *Achomosphaera.* In Davey, R. J., Downie, C., Sarjeant, W. A. S. & Williams, G. L. – Studies on Mesozoic and Cainozoic dinoflagellate cysts. Bull. B.M (N.H.) Geol. Supplement, **3:** 28–52.

–,– (1966b): The genus *Hystrichosphaeridium* and its allies. In Davey, R. J., Downie, C., Sarjeant, W. A. S. & Williams, G. L. Studies on Mesozoic and Cainozoic dinoflagellate cysts. Bull. B.B. (N.H.) Geol. Supplement, **3:** 53–106.

Deflandre, G. (1937): Microfossiles des silex crétacés. Deuxième partie. Flagellés *incertae sedis* Hystrichosphaeidés. Sarcodinés. Organisms divers. – Ann. de paléontologie, **26:** 51–103.

De Reneville, P. & Raynaud, J.-F. (1981): Palynologie du stratotype du Barrémien. Bull. Centres Rech. Explor.-Prod. Elf-Aquitaine, **5:** 1–29.

Dettmann, M. E. (1973): Angiosperm pollen from Albian to Turonian sediments of Eastern Australia. – Geol. Soc. Australia, Spec. Publ., **6:** 3–34.

Dörhöfer, G. & Davies, E. H. (1980): Evolution of archaeopyle and tabulation in Rhaetogonyaulacacinean dinoflagellate cysts. – Royal Ontario Museum, Life Sciences Misc. Publs., 91p.

Drugg, W. S. (1978): Some Jurassic dinoflagellate cysts from England, France and Germany. – Palaeontographica, Abt. B, **168:** 61–79.

Duxbury, S. (1977): A palynostratigraphy of the Berriasian to Barremian of the Speeton Clay of Speeton, England. – Palaeontographica, Abt. B, **160:** 17–67.

–,– (1979): Three new genera of dinoflagellate cysts from the Speeton Clay (Early Cretaceous) of Speeton, England. – Micropaleontology, **25:** 198–205.

–,– (1980): Barremian phytoplankton from Speeton, east Yorkshire. – Palaeontographica, Abt. B, **173:** 107–146.

–,– (1983): A study of dinoflagellate cysts and acritarchs from the Lower Greensand (Aptian to Lower Albian) of the Isle of Wight, southern England. – Palaeontographica, Abt. B, **186:** 18–80.

Eaton, G. L. (1985): Structure and encystment in some fossil cavate dinoflagellate cysts. – Jnl. Micropalaeontology, **3:** 53–64.

Evitt, W. R. (1985): Sporopollenin dinoflagellate cysts: Their morphology and interpretation. – AASP Foundation. Hart Graphics Inc., Austin, Texas. 333p.

Ferry, S. & Schaaf, A. (1981): The early Cretaceous environment at Deep Sea Drilling Project Site 463 (mid-Pacific mountains), with reference to the Vocontian trough (French sub-Alpine ranges). – In Init. Reps. DSDP, **62:** 669–682.

Fletcher, B. N. (1969): A lithological subdivision of the Speeton Clay C Beds (Hauterivian), East Yorkshire. – Proc. Yorks. geol. Soc., 37: 323–327.

Gaida, K. H., Kemper, E. & Zimmerle, W. (1978): Das Oberapt von Sarstedt und seine Tuffe. – Geol. Jb., **A45:** 43–123.

Gallois, R. W. (1971): The log of the Hunstanton borehole. – Ann. Rep. Inst. Geol. Sci., **1971:** 116.

–,– (1973): The base of the Carstone at Hunstanton. – Bull. geol. Soc. Norfolk, **23:** 25–34.

–,– (1975a): The base of the Carstone at Hunstanton. – Bull. geol. Soc. Norfolk, **27:** 21–27.

–,– (1975b): A borehole section across the Barremian-Aptian boundary (Lower Cretaceous) at Skegness, Lincolnshire. – Proc. Yorks. geol. Soc., **40:** 499–503.

–,– (1984): The late Jurassic to mid Cretaceous rocks of Norfolk. – Bull. geol. Soc. Norfolk, **34:** 3–64.

Gocht, H. (1957): Mikroplankton aus dem nordwestdeutschen Neokom. (Teil I) – Paläont. Z., **31:** 163–185.

–,– (1959): Mikroplankton aus dem nordwestdeutschen Neokom (Teil II). – Päont. Z., **33:** 50–89.

Goodman, D. K. & Evitt, W. R. (1981): The dinoflagellate *Angustidinium acribes* (Davey & Verdier) gen. et comb. nov. from the mid-Cretaceous of the northern California Coast Ranges. – Grana, **20:** 43–54.

Habib, D. (1975): Neocomian dinoflagellate zonation in the western North Atlantic. – Micropaleontology, **21:** 373–392.

–,– (1977): Comparison of Lower and Middle Cretaceous palynostratigraphic zonations in the western North Atlantic. – In Swain, F. W. (ed.) – Stratigraphic micropaleontology of Atlantic Basin and Borderlands. Elsevier Scientific Publishing, Amsterdam. 341–367.

–,– (1978): Palynostratigraphy of the Lower Cretaceous section at Deep Sea Drilling Project Site 391, Blake-Bahama Basin, and its correlation in the North Atlantic. – Init. Reps. DSDP, **44:** 887–897.

Hallam, A., Hancock, J. M., La Breque, J. L., Lowrie, W. & Channell, J. E. T. (1985): Jurassic to Paleogene: Part 1. Jurassic to Cretaceous geochronology and Jurassic to Paleogene magnetostratigraphy. In Snelling, N. J. (ed.). The Chronology of the geological record. – Geol. Soc. Memoir, **10:** 118–140. Blackwells, Oxford.

Harding, I. C. (1986a): An early Cretaceous dinocyst assemblage from the Wealden of southern England. – Spec. Papers in Palaeontology, **35:** 95–109.

–,– (1986b): Archaeopyle variability in early Cretaceous dinocysts of the partiform gonyaulacoid genus *Druggidium* Habib. – Inl. Micropalaeontology, **5 (2):** 17–26.

–,– (1986c): A dinocyst calibration of the northwest European Barremian. – Unpublished Ph. D. Thesis, University of Cambridge. 325pp.

–,– (1989): A comparison of three early Cretaceous sexiform gonyaulacoid dinocysts. Abstracts of the 4th International Conference on Modern an Fossil Dinoflagellates, Woods Hole, April 1989, p. 51.

–,– (in press): *Picodinium fallax,* a new dinocyst showing 'AA' type tabulation.

Harding, I. C. & Hughes, N. F. (1990): A revision of *Endoceratium dettmannae* from the Cambridge Greensand, with observations on the ceratioid dinocysts. – Rev. Palaeobot. Palynol. **60.**

Helenes, J. (1985): Morphological analysis of Mesozoic-Cenozoic *Cribroperidinium* (Dinophyceae), and taxonomic implications. – Palynology, **8:** 107–137.

Hughes, N. F. (1970): The need for agreed standard of recording in palaeopalynology and palaeobotany. – Paläont. Abh., **B111:** 357–364.

–,– (1973): Palynological time-correlation of the English Wealden with boreal marine successions. In Casey, R. & Rawson, P. F. (eds.). The Boreal Lower Cretaceous. – Geol. Inl. Spec. Issue, **5:** 185–192. Seel House Press, Liverpool.

–,– (1976): Palaeobiology of angiosperm origins. – CUP, Cambridge. 242 p.

–,– (1987): The problems of data-handling for early angiosperm-like pollen. – In Spicer, R. A. & Thomas, B. A (eds.) Systematic and taxonomic approaches to palaeobotany. – Systematic Assocn. Series, no. **31:** 235–253. Clarendon Press, Oxford.

Hughes, N. F., Drewry, G. E. & Laing, J. F. (1979): Barremian earliest angiosperm pollen. – Palaeontology, **22:** 513–535.

Hughes, N. F. & Harding, I. C. (1985): Wealden occurrence of an isolated Barremian dinocyst facies. Palaeontology, **28:** 555–565.

Hughes, N. F. & Moody-Stuart, J. S. (1969): A method of stratigraphic correlation using early Cretaceous miospores. Palaeontology, **12:** 84–111.

Jain, K. P. & Khowaja-Ateequzzaman (1984): Reappraisal of the genus *Muderongia* Cookson & Eisenack, 1958. – Inl. Palaeontological Soc. India, **29:** 34–42.

Jan du Chêne, R., Becheler, I., Helenes, J. & Masure, E. (1986): Les genres *Diacanthum, Exiguisphaera, Occisucysta* et *Tehemadinium* gen. nov. (kystes fossiles de Dinoflagellés). Cahiers de Micropaléontologie, 1 (3/4), 38 pp.

Judd, J. W. (1868): On the Speeton Clay. – Q. Inl. geol. Soc. Lond., **24:** 218–250.

–,– (1870): Additional observations on the Neocomian strata of Yorkshire and Lincolnshire. – Q. Inl. geol. Soc. Lond., **26:** 326–345.

Kaye, P. (1964): Observations on the Speeton Clay (Lower Cretaceous). – Geol. Mag., **101:** 340–356.

Kelly, S. R. A. & Rawson, P. F. (1983): Some late Jurassic-mid-Cretaceous section on the East Midlands Shelf, England, as demonstrated on a field meeting, 18–20 May, 1979. – Proc. Geol. Ass., **94:** 65–73.

Kemper, E. (1976): Geologischer Führer durch die Grafschaft Bentheim und die angrenzenden Gebiete mit einem Abriß der emsländischen Unterkreide. – Nordhorn-Bentheim. 206 p.

Kemper, E., Rawson, P. F. & Thieuloy, J.-P. (1981): Ammonites of Tethyan ancestry in the early Lower Cretaceous of north-west Europe. – Palaeontology, **24:** 251–311.

Kennedy, W. J. & Odin, G. S. (1982): The Jurassic and Cretaceous time scale in 1981. In Odin, G. S. (ed.). – Numerical dating in stratigraphy, **1:** 557–592. John Wiley & Sons Ltd., London.

Khowaja-Ateequzzaman, Jain, K. P. & Manum, S. B. (1985): Dinocyst genus *Discorsia*: a reinterpretation. – Palynology, **9:** 95–103.

Kilian, W. (1888): Description géologique de la Montagne de Lure (Basses-Alpes). – Ann. Sci. géol., **19–20:** 458 p.

Koenen, A. von (1902): Die Ammonitiden des Norddeutschen Neocom. – Abh. preuss. geol. Landesanst., N. F. **24:** 451 p.

Kofoid, C. A. (1908): Exuviation, autotomy and regeneration in *Ceratium* – Univ. California Publs. Zoology, **4:** 345–386.

Lamplugh, G. W. (1889): On the subdivisions of the Speeton Clay. – Q. Inl. geol. Soc. Lond., **45:** 575–618.

–,– (1896): On the Speeton Series of Yorkshire and Lincolnshire. – Q. Inl. geol. Soc. Lond., **62:** 179–218.

–,– (1924): A review of the Speeton Clays. – Proc. Yorks. geol. Soc., **20:** 1–31.

Leckenby, J. (1859): Note on the Speeton Clay of Yorkshire. – The Geologist, **2:** 9–11.

Lentin, J. K. & Williams, G. L. (1989): Fossil dinoflagellates: Index to genera and species, 1989 edition. – AASP Contributions Series, No. **20,** 473 p.

Lister, J. K. & Batten, D. J. (1988a): *Hurlandsia*, a new non-marine Early Cretaceous dinocyst genus. – N. Jb. Geol. Paläont. Mh., **1988**(8): 505–516.

–,– (1988b): Stratigraphic and palaeoenvironmental distribution of Early Cretaceous dinoflagellate cysts in the Hurlands Farm Borehole, West Sussex, England. – Palaeontographica, Abt. B, **210:** 9–89.

McIntyre, D. J. & Brideaux, W. W. (1980): Valanginian miospore and microplankton assemblages from the Richardson Mountains, District of Mackenzie, Canada. – Geological Survey Canada, Bulletin 320. 57 pp.

Mayr, E. (1969): Principles of systematic zoology. McGraw-Hill, New York.

Mehrotra, N. C. & Sarjeant, W. A. S. (1984): *Dingodinium*, a dinoflagellate cyst genus exhibiting variation in archaeopyle character. – Micropaleontology, **30:** 292–305.

Michael, E. (1964): Microplankton und sporomorphe aus dem norddeutschen Barrême. – Mitt. Geol. Inst. T. H. Hannover, **2:** 22–48.

–,– (1979): Mediterrane Faunenein flüsse in den borealen Unterkreide-Becken Europas, besonders Nordwestdeutschlands. – In Wiedmann, J. (ed.) Aspekte der Kreide Europas IUGS Series A, **6:** 305–321.

Millioud, M. E. (1969): Dinoflagellates and acritarchs from some western European Lower Cretaceous type localities. – In Bronniman, P. & Renz, H. H. (eds.) – Procs. First Intl. Conf. planktonic microfossils, Geneva, 1967, **2:** 420–434.

Morter, A. A. (1975): A Barremain fauna from excavations at Hunstanton beach. – Bull. geol. Soc. Norfolk, **27:** 29–32.

Moullade, M. (1966): Etude stratigraphique et micropaléontologique du Crétacé Inférieur de la "Fosse Vocontienne". – Doc. Lab. Géol. Fac. Sci. Lyon, **15:** 1–369.

Mutterlose, J. (1983): Phylogenie und Biostratigraphie der Unterfamilie Oxyteuthinae (Belemnitida) aus dem Barrême (Unter-Kreide) NW-Europas. – Palaeontographica, Abt. A, **180:** 1–90.

–,– (1984): Die Unterkreide-Aufschlüsse (Valangin-Alb) im Raum Hannover-Braunschweig. – Mitt. Geol. Inst. Univ. Hannover, **24:** 61 p.

Mutterlose, J. & Harding, I. C. (1987a): Phytoplankton from the anoxic sediments of the Barremain (Lower Cretaceous) of NW-Germany. – Abh. Geol. B.-A., **39:** 177–215. Vienna.

–,– (1987b): The Barremian Blätterton: an anoxic warm water sediment of the Lower Saxony Basin. – Geol. Jb., **A96:** 187–207.

Neale, J. W. & Sarjeant, W. A. S. (1962): Microplankton from the Speeton Clay of Yorkshire. – Geol. Mag., **99:** 439–458.

Odin, G. S. (1985): Concerning the numerical ages proposed for the Jurassic and Cretaceous geochronology. In Snelling, N. J. (ed.). The Chronology of the geological record. – Geol. Soc. Memoir, **10:** 196–198. Blackwells, Oxford.

Orbigny, A. d' (1847): Paléontologie français. Terrains Crétacés. IV. – Brachiopodes.

Owen, E. F. & Thurrell, R. G. (1968): British Neocomian rhynchonelloid brachiopods. – Bull. B. M. (N. H.) Geology, **16:** 99–123.

Penny, J. H. J. (1986): An early Cretaceous angiosperm pollen assemblage from Egypt. – Spec. Papers in Palaeontology, **35:** 121–134.

–,– (1989) New early Cretaceous forms of the pollen *Afropollis* from England and Egypt. – Rev. Palaeobotany & Palynology, **58:** 289–299.

Phillips, J. (1829): Illustrations of the Geology of Yorkshire. – Thomas Wilson & Sons, York, 254 p.

Phipps, D. & Playford, G. (1984): Laboratory techniques for extraction of palynomorphs from sediments. – Pap. Dep. Geol. Univ. Queensland, **11:** 1–23.

Piasecki, S. (1984): Dinoflagellate cyst stratigraphy of the Lower Cretaceous Jydegård Formation, Bornholm, Denmark. – Bull. geol. Soc. Denmark, **32:** 145–161.

Pocock, S. A. (1976): A preliminary dinoflagellate zonation of the uppermost Jurassic and lower part of the Cretaceous, Canadian Arctic, and possible correlation in the Western Canadian Basin. Geoscience and Man, **15:** 101–114.

Rawson, P. F. (1971a): Lower Cretaceous ammonites from north-east England: the Hauterivian genus *Simbirskites*. – Bull. B. M. (N. H.) Geol., **20**: 25–86.

–,– (1971b): The Hauterivian (Lower Cretaceous) biostratigraphy of the Speeton Clay of Yorkshire, England. – Newsl. Stratigr., **1**: 61–76.

–,– (1972): A note on the biostratigraphical significance of the Lower Cretaceous belemnite genus *Aulacoteuthis* in the B Beds of the Speeton Clay, Yorkshire. – Proc. Yorks. geol. Soc., **39**: 89–91.

–,– (1973): Lower Cretaceous (Ryazanian-Barremian) marine connections and cephalopod migrations between the Tethyan and Boreal Realms. – In Casey, R. & Rawson, P. F. (eds.). The Boreal Lower Cretaceous. – Geol. Inl. Spec. Issue, **5**: 131–144. Seel House Press, Liverpool.

–,– (1980): Early Cretaceous ammonite biostratigraphy and biogeography. – In House, M. R. & Senior, J. R. – The Ammonoidea. Systematics Assocn. Spec. Volume, **18**: 499–529. Academic Press, London.

–,– (1983): The Valanginian to Aptian stages – current definitions and outstanding problems. – Zitteliana, **10**: 493–500.

Rawson, P. F., Curry, D., Dilley, F. C., Hancock, J. M., Kennedy, W. J., Neale, J. W., Wood, C. J. & Worssam, B. C. (1978): A correlation of *Cretaceous rocks in the British Isles*. – *Spec. Rep. Geol. Soc. Lond.*, **9**: 70 p.

Rawson, P. F. & Mutterlose, J. (1983): Stratigraphy of the Lower B and basal Cement Beds (Barremian) of the Speeton Clay, Yorkshire, England. – Proc. Geol. Ass., **94**: 133–146.

Reyment, R. A. (1980): Morphometric methods in biostratigraphy. – Academic Press, London. 175 p.

Riding, J. B. (1983): *Gonyaulacysta centriconnata* sp. nov., a dinoflagellate cyst from the Late Callovian and Early Oxfordian of Eastern England. – Palynology, **7**: 197–204.

Robazsynski, F., Amedro, F., Foucher, J. C., Gaspard, D. Magniez-Jannin, F., Manivit, H. & Sournay, J. (1980): Synthèse biostratigraphique de l'Aptien au Santonien du Boulonnais à partir de spet groupes paléontologiques: foraminifères, nannoplancton, dinoflagellés et macrofaunes. – Rev. de Micropaléontologie, **22**: 195–321.

Roger, J. (1980): Barrémian. In Cavelier, C. & Roger, J. (eds.): Les étages français et leurs stratotypes. Mém. B. R. G. M., **109**: 106–111.

Sarjeant, W. A. S. (1966a): Dinoflagellate cysts with *Gonyaulax*-type tabulation. – In Davey, R. J., Downie, C., Sarjeant, W. A. S. & Williams, G. L. – Studies on Mesozoic and Cainozoic dinoflagellate cysts. Bull. B. M. (N. H.) Geol. Supplement **3**: 107–156.

–,– (1966b): Further dinoflagellate cysts from the Speeton Clay. – In Davey, R. J., Downie, C., Sarjeant, W. A. S. & Williams, G. L. Studies on Mesozoic and Cainozoic dinoflagellate cysts. – Bull. B. M. (N. H.) Geol. Supplement, **3**: 199–214.

Schott, W. et al. (1969): Paläogeographischer Atlas der Unterkreide von Nordwestdeutschland, mit einer Übersichtsdarstellung des nördlichen Mitteleuropa. Bundesanstalt für Bodenforschung, Hannover. 315 pp.

Scott, G. H. (1985): Homotaxy and biostratigraphic theory. – Palaeontology, **28**: 777–782.

Sedgwick, A. (1826): On the classification of the strata which appear on the Yorkshire coast. – C. Baldwin, London. 26 p.

Simpson, M. I. (1985): The stratigraphy of the Atherfield Clay Formation (Lower Aptian, Lower Cretaceous) at the type and other localities in southern England. – Proc. Geol. Ass., **96**: 23–45.

Srivastava, S. K. (1984): Barremian dinoflagellate cysts from southeastern France. – Cahiers de Micropaléontologie, 2–1984, 90 p.

Stover, L. E. & Evitt, W. R. (*1978*): *Analyses of pre-Pleistocene organic-walled dinoflagellates*. – *Stanford Univ. Publ. Geol. Sci.*, ***15***: *300* p.

Swinnerton, H. H. (1935): The rocks below the Red Chalk of Lincolnshire, and their cephalopod faunas. – Q. Inl. Geol. Soc., Lond., **91**: 1–46.

Tarkian, M. (1968): Bericht über die feinstratigraphische Profilaufnahme und biostratigraphische Aufsammlungen im Barrême und Apt der Gott'schen Ziegelei bei Sarstedt. – Ber. NLfB Hannover. 10 p. Unpublished.

Thieuloy, J.-P. (1977): Les ammonites boréales des formations néocomiens du Sud-Est français (Province subméditerranéenne). – Géobios, **10** (3): 395–461.

Thusu, B. (1978): Aptian to Toarcian dinoflagellate cysts from Arctic Norway. – In Thusu, B. (ed.) Distribution of biostratigraphically diagnostic dinoflagellate cysts and miospores from the NW European continental shelf and adjacent areas. – I. K. U. Publication, No. **100**: 61–95.

Topley, W. (1875): The geology of the Weald. – Mem. geol. Surv. Gt. Br., 503 p.

Vozzhennikova, T. F. (1967): Iskopaemye peridinei Yuskikh, Melvykh i Paleogenovkh otlozhen i SSSR. – Izdatel "Nauka" Moscow. 347 p. [Fossilized peridinid algae in the Jurassic, Cretaceous and Palaeogene deposits of the USSR. Transl. by Less, E. and published by the *National Lending Library for Science and Technology*, Boston Spa, Yorks., England, 1971].

Wall, D. & Dale, B. (1971): A reconsideration of living and fossil *Pyrophacus* Stein, 1883 (Dinophyceae). – Inl. Phycology, **7**: 221–235.

Wetzel, O. *(1933): Die in organischer Substanz erhaltenen Mikrofossilien des baltischen Kreide-Feuersteinsphischen und stratigraphischen* Anhang. – Palaeontographica, Abt B, **77**: 141–186 und **78**: 1–110.

Wiggins, V. D. (1972): Two new Lower Cretaceous dinoflagellate genera from southern Alaska (USA). – Rev. Palaeobot. Palynol., **14**: 297–308.

Williams, G. L. (1975): Dinoflagellate and spore stratigraphy of the Mesozoic-Cenozoic, offshore eastern Canada. – Geol. Surv. Canada, Paper 74–30, **2**: 107–161.

Williams, G. L. & Bujak, J. P. (1986): Mesozoic and Cenozoic dinoflagellates. In Bolli, H. M., Saunders, J. B. & Perch-Nielsen, K. (eds.) – Plankton stratigraphy. CUP, Cambridge. 847–964.

Williams, G. L. & Downie, C. (1966): Further dinoflagellate cysts from the London Clay. – In Davey, R. J., Downie, C., Sarjeant, W. A. S. & Williams, G. L. Studies on Mesozoic and Cainozoic dinoflagellate cysts. Bull. B. M. (N. H.) Geol. Supplement, **3**: 215–236.

Worssam, B. C. & Ivimey-Cook, H. C. (1971): The stratigraphy of the Geological Survey borehole at Warlingham, Surrey. – Bull. Inst. geol. Surv. Gt. Br., **36**: 1–176.

Zachariasse, W. J., Reidel, W. R., Sanfilippo, A., Schmidt, R. R., Brolsma, M. J., Schrader, H. J., Gersonde, R., Drooger, M. M. & Broekman, J. A. (1978): Micropalaeontological counting methods and techniques – an exercise on an eight metres section of the Lower Pliocene of Capo Rosselle, Sicily. – Utrecht Micropal. Bull., **17**: 1–265.

Zimmerle, W. (1979): Lower Cretaceous tuffs in northwest Germany and their geotectonic significance. – In Wiedmann, J. (ed.) Aspekte der Kreide Europas. IUGS Series A, **6**: 385–402.

Appendix 1

Samples in which CfA records to new species have been found.

Ascodinium fissilum sp. nov.
Gott: 50/1/79, 61/1/79 to c98/1 inclusive, 109, 114. Speeton: CS37, ICH001, ICH007, ICH008, ICH014, to ICH016, ICH022, ICH023, ICH024, CS47, CS49. Hunstanton: 185/0, 175/0, 160/0, 150/0, 145/0, 120/0. Alford: IIq, IIr. Warlingham: 1044 to 1025 inclusive.

Canningia duxburyi sp. nov.
Gott: 50/1/79 to 61/1/79 inclusive. Speeton: CS37, CS35, ICH001, ICH004, ICH005. Alford: CL15.

Cannosphaeropsis hughesii sp. nov.
Speeton: CS35. Alford: CL15.

Cassiculosphaeridia tunicata sp. nov.
Gott: 56/1/79 to c76/1 inclusive, c83/1. Speeton: CS37, CS34, ICH001, ICH003.

Cleistosphaeridium fungosus sp. nov.
Gott: 50/1/79, 56/1/79, 71/1/79 to c83/1 inclusive, c98/1, 109 to 197/1/83 inclusive, 199/1/83. Speeton: CS37 to ICH001 inclusive, ICH003 to ICH008 inclusive, ICH011, ICH016, ICH018, ICH024 to CS47 inclusive. Hunstanton: 205/0, 200/0, 185/0, 165/0, 160/0, 150/0, 145/0, 135/0, 130/0, 120/0. Alford: CL17 to CL19 inclusive, IIucz, IIr, IIk, CL27.

Ctenidodinium complanatum sp. nov.
Gott: 56/1/79, c78/1 to c88/1 inclusive, 100/3/83, 100/7/83, and reworked in 187 x/5. Speeton: ICH003, ICH015. Hunstanton 195/0. Alford: IIq.

Gonyaulacysta speciosus sp. nov.
Gott: 61/1/79, 71/1/79 to c78/1 inclusive and reworked in 197/3/83, 199/1/83. Speeton: CS37, ICH001, ICH003, ICH005. Hunstanton 200/0, 185/0. Alford: CL17.

Heslertonia senectus sp. nov.
Gott: 185 x/5, 197/4/83, 197/1/83. Speeton: ICH022. Alford: IIr, IIq, IIk, GL27.

Pentadinium omasum sp. nov.
Gott: 187 x/5 to 197/4/83 inclusive, 197/2/83, 199/1/83. Speeton: CS47, CS49. Alford: IIr, IIucz.

Pseudoceratium aulaeum sp. nov.
Warlingham: 1065/4, 1060/3, 1060/0, 1057/9, 1052/3, 1051/2, 1050/1.

Resticulasphaera medusae gen. et sp. nov.
Gott: 61/1/79, 100/12/83, 138, 183 x/4, 187 x/5 to 197/3/83 inclusive, 198/1/83, 199/1/83. Speeton: ICH003, ICH014, ICH017, ICH025 to ICH027 inclusive, CS47, CS49. Hunstanton: 120/0. Alford: IIr.

Spiniferites spumeus sp. nov.
Gott: 185 x/5, 187 x/5. Speeton: ICH025. Hunstanton: 145/0, 130/0. Alford: IIr, IIk, IIq.

Trichodinium calvus sp. nov.
Gott: 197/4/83. Speeton: CS47. Alford: CL27.

Trichodinium discus sp. nov.
Gott: 67/1/79, c74/1 to c98/1 inclusive, 109, 185 x/5, 197/2/83, 197/1/83. Speeton: CS37, CS34, ICH001, ICH008, ICH014, ICH015, ICH017, ICH021, ICH022, ICH025, ICH027, CS47, CS49. Hunstanton: 213/0, 180/0, 170/0, 155/0.

Explanation of Plates

Plate 1

μm bar = 10 μm, except Figs. 4, 8 and 11 = 1 μm

Figs. 1–6. *Pseudoceratium aulaeum* sp. nov. All from Stub IC194; Prep. Z247; Sample WM1044/5 and ×800 otherwise stated.
Fig. 1. Holotype; Ref. No. 67; Neg. 1030/34. dv, specimen with short antapical horn. ×600.

Fig. 2. Ref. No. 68; Neg. 1031/34. dv, operculum lost. ×600.

Fig. 3. Stub IC195; rest of data as for Fig. 1; Ref. No. 4; Neg. 3004/27. vv, operculum lost.

Fig. 4. Stub IC527; rest of data as for Fig. 1; Ref. Spec. 2; Neg. 3003/65. Detail of surface sculpture (paracingulum runs top to bottom on righthand side of fig.). ×3000.

Fig. 5. Data as for Fig. 4; Ref. Spec. 2; Neg. 3002/64. Detail of dorsal side of main cyst body, showing archaeopyle suture, paracingulum and fragile nature of horns. × 1450.
Fig. 6. Ref. No. 66; Neg. 1034/34. Detached operculum.

Figs. 7, 8. *Pseudoceratium pelliferum.*
Fig. 7. Stub IC387; Prep. CH042; Sample ICH014; Ref. 239/768; Neg. 3005/18. vv, longhorned morph. × 400.
Fig. 8. Stub IC278; Prep. CH099; Sample G100/7/83; Ref. 316/790; Neg. 3010/65. Detail of surface sculpture on dorsal surface (archaeopyle suture runs top to bottom on lefthand side of fig.). × 3000.

Figs. 9–11. *Pseudoceratium solocispinum* stat. nov. et emend.
Fig. 9. Stub GD189; Prep. X232; Sample CS47; Ref.; Neg. 3005/29. vv, minus operculum. × 800.
Fig. 10. Stub GD229; Prep. X413; Sample Hun130/0; Ref.; Neg. 3003/31. dv, minus operculum. × 800.
Fig. 11. Stub IC353; Prep. CH114; Sample G192x/2; Ref. 382/844; Neg. 2006/98. detail of periphragm sculpture. × 3000.

Plate 2

μm bar = 10 μm, except for Figs. 13 and 14 = 1 μm

Figs. 1–5. *Vesperopsis longicornis* All figures from Prep. Z193; Sample WM 1051/2.
Fig. 1. Stub IC484; Ref. Spec. 1; Neg. 3001/52. vv, × 400.
Fig. 2. Stub IC484; Ref. Spec. 6; Neg. 3006/52. Lateral horn, detail, × 1200.
Fig. 3. Stub IC496; Ref. Spec. 1; Neg. 3024/53; dv, × 400.
Fig. 4. Stub IC496; Ref. Spec. 3; Neg. 3026/53. vv, × 400.
Fig. 5. Stub IC496; Ref. Spec. 2; Neg. 3025/53. vv, minus operculum, × 400.

Figs. 6–11, 13. *Ascodinium fissilum* sp. nov. All × 800 except where otherwise stated.
Fig. 6. Holotype, Stub IC320; Prep. CH1889; Sample G100/1/83; Ref. 358/773; Neg. 2047/18. vv, showing partially detached operculum.
Fig. 7. Data as for Fig. 6; Ref. 249/889; Neg. 2023/18. vv, specimen showing well developed apical and left antapical horns.
Fig. 8. Stub IC317; Prep. CH190; Sample G100/2/83; Ref. 324/689; Neg. 2040/29. vv, showing splitting along paraplate boundaries.
Fig. 9. Stub IC; rest of data as for Fig. 8; Ref. 266/822; Neg. 2054/29. vv, showing partially attached operculum.
Fig. 10. Data as for Fig. 6; Ref. 368/785; Neg. 2006/18. odv, specimen showing combination apical archaeopyle.
Fig. 11. Data as for Fig. 6; Ref. 245/782; Neg. 2024/18. oav.
Fig. 13. Data as for Fig. 6; Ref. 342/791; Neg. 2041/18. detail showing granulate endophragm and laevigate periphragm with intratabular tubercles. × 3000.

Figs. 12, 14, 15. *Phoberocysta neocomica.* All × 600 except where stated.
Fig. 12. Stub IC415; Prep. X459; Sample HUN190/0; Ref. 330/824; Neg. 3017/23. vv.
Fig. 14. Stub IC325; Prep. CH105; Sample Gc83/1; Ref. 319/828; Neg. 2032/43. detail of periphragm along paraplate boundary. × 3000.
Fig. 15. Stub IC145; Prep. CH073; Sample ICH 021; Ref. 374/747; Neg. 3001/25. vv.

Fig. 13. *Phoberocysta* sp. Stub IC375; Prep. X488; Sample CS 37; Ref. 307/728; Neg. 3041/13. vv, uncommon form with sparse processes.

Plate 3

μm bar = 10 μm in all cases

Figs. 1–3. *Cyclonephelium distinctum, all* × 800.
Fig. 1. Stub IC310; Prep. CH103; Sample G100/11/83; Ref. 298/ 833; Neg. 2010/17. dv.
Fig. 2. Stub IC334; Prep. Z226; Sample G67/1/79; Ref. 399/791; Neg. 2006/56. dv.
Fig. 3. Stub IC344; Prep. CH110; Sample G138; Ref. 287/883; Neg. 2001/83. vv.

Figs. 4–6. *Cyclonephelium* sp. I., all × 800.
Fig. 4. Stub IC265; Prep. Davey; Sample G100/6/83; Ref. 268/856; Neg. 1030/72. dv.
Fig. 5. Stub IC281; Prep. CH097; Sample G100/5/83; Ref. 241/885; Neg. 1004/86. vv.
Fig. 6. Stub IC284; Prep. CH097; Sample G100/5/83; Ref. 213/719; Neg. 1029/81. dv.

Figs. 7–9. *Cyclonephelium* sp. II., all Prep. CH113; Sample G187x/5; all × 800.
Fig. 7. Stub IC350; Ref. 351/868; Neg. 2030/92. dv.
Fig. 8. Stub IC351; Ref. 363/753; Neg. 2006/94. dv.
Fig. 9. Stub IC351; Ref. 364/901; Neg. 2032/93. vv.

Figs. 10–12. *Pseudoceratium anaphrissum*, emend. all × 400.
Fig. 10. Data as for Fig. 4; Ref. 293/910; Neg. 1001/72. dv.
Fig. 11. Stub IC272; Prep. CH099; Sample G100/7/83; Ref. 232/877; Neg. 1031/91. vv.
Fig. 12. Stub IC303; Prep. CH101; Sample G100/9/83; Ref. 343/843; Neg. 2005/20. vv.

Plate 4

μm bar = 10 μm in all cases

Figs. 1–4. *Pseudoceratium anaphrissum.* emend.
Fig. 1. Stub IC302; Prep. CH101; Sample G100/9/83; Ref. 248/722; Neg. 2033/10. vv, isolated operculum. ×800.
Fig. 2. Data as for Fig. 1; Ref. 236/811; Neg. 2027/10. vv, showing paratabulation. ×400.
Fig. 3. Stub IC282; Prep. CH097; Sample G10005/83; Ref. 227/704; Neg. 1006/83. vv, detail of archaeopyle suture. ×1600.
Fig. 4. Data as for Fig. 1; Ref. 253/893; Neg. 2016/10. dv. ×400.

Figs. 5–7. *Achomosphaera neptuni.*
Fig. 5. Stub IC310; Prep. CH103; Sample G100/11/83; Ref. 396/795; Neg. 2038/16. dv, showing displaced operculum with double plate-centred process. ×560.
Fig. 6. Stub IC356; Prep. Z230; Sample G197/2/83; Ref. 402/748; Neg. 3008/05. detail of archaeopyle showing accessory sutures. ×1600.
Fig. 7. Stub IC309; rest of data as for Fig. 5; Ref. 253/747; Neg. 2035/11. detail of surface sculpture. ×1600.

Figs. 8, 9. *Avellodinium falsificum.*
Fig. 8. Stub IC346; Prep. CH111; Sample G183x/4; Ref. 343/703; Neg. 2005/81. llv. ×800.
Fig. 9. Data as for Fig. 8; Ref. 209/835; Neg. 2009/82. llv, showing epicystal archaeopyle. ×800.

Figs. 10–12. *Spiniferites dentatus.*
Fig. 10. Stub IC334; Prep. Z226; Sample G67/1/79; Ref. 361/769; Neg. 2008/56. vv, showing sulcal claustrum. ×800.
Fig. 11. Stub IC285; Prep. CH096; Sample G100/4/83; Ref. 261/881; Neg. 1020/80. dv, showing precingular archaeopyle. ×800.
Fig. 12. Stub IC343; Prep. Z228; Sample Gc78/1; Ref. 316/792; Neg. 2023/65. detail of parasutural processes, showing bifurcate nature. ×1600.

Plate 5

μm bar = 10 μm in all cases

Canningia duxburyi sp. nov. All from Prep. X423; Sample HUN195/0, except where otherwise stated.

Fig. 1. Stub GD226; Ref. 317/807; Neg. 3008/31. dv, operculum lost. ×600.
Fig. 2. Stub IC375; Prep. X488; Sample CS37; Ref. 299/865; Neg. 3012/13. dv, complete specimen. ×600.
Fig. 3. Stub IC486; Ref. Specimen 10; Neg. 3037/52. dv, minus operculum, ×600.
Fig. 4. Data as for Fig. 2, Ref. 353/834; Neg. 3016/13. dv. ×600.
Fig. 5. Holotype. Stub IC486; Ref. Specimen 14; Neg. 3002/53. vv, ectophragm developed over *lu*, but not *ai*. ×600.
Fig. 6. Stub IC487; Ref. Specimen 6; Neg. 3018/53. vv, operculum still attached. ×600.
Fig. 7. Stub GD226; Ref. 373/742; Neg. 3029/22. dv. ×520.
Fig. 8. Stub IC486; Ref. Specimen 13; Neg. 3001/53. vv, no ectophragm developed over *lu*. ×600.
Fig. 9. Stub GD226; Ref. 317/807; Neg. 3026/22. detail of Fig. 1. ×1200.
Fig. 10. Stub IC486; Ref. Specimen 6; Neg. 3033/52. Detail of granular periphragm, ectophragm shows predominantly penitabular supports, paraplate *lu* to left of picture. ×1200.
Fig. 11. Stub IC483; Ref. Specimen 1; Neg. 3001/54. vv, ectophragm developed over *ai*, but not on *lu* ×600.
Fig. 12. Stub GD225; Ref. 258/832; Neg. 3018/22. dv detached operculum. ×800.
Fig. 13. Stub IC486; Ref. Specimen 2; Neg. 3029/52. vv, ectophragm developed over *lu* and partially over *1i* and *ai*. ×600.

Plate 6

μm bar: Figs. 4, 5 and 13 = 1 μm, all others = 10 μm

Figs. 1–8. *Spiniferites spumeus* sp. nov. All ×800 unless otherwise stated.
Fig. 1. Holotype, Stub IC347; Prep. CH111; Sample G183x/4; Ref. 302/813; Neg. 2013/84. llv.
Figs. 2 and 4. Data as for Fig. 1; Ref. 325/766; Negs. 2037/84 and 2001/85. dv, showing archaeopyle, Fig. 4 = detail of process and surface sculpture. ×3000.
Fig. 3. Stub IC346; rest of data as for Fig. 1; Ref. 313/915; Neg. 2046/80. rlv.
Fig. 5. Data as for Fig. 1; Ref. 368/754; Neg. 2025/84. cross-section of cyst wall, showing vacuoles. ×3000.
Fig. 6. Stub IC346; rest of data as for Fig. 1; Ref. 372/873; Neg. 2044/80. rlv.
Fig. 7. Stub IC348; Prep. CH112; Sample G185x/5; Ref. 353/763; Neg. 2027/86. oaav.
Fig. 8. Data as for Fig. 1; Ref. 382/793; Neg. 2038/84. vv, showing S-type ventral arrangment.

Figs. 9–16. *Cannosphaeropsis hughesii* sp. nov. All ×800 unless otherwise stated.
Fig. 9. Stub IC328; Prep. Z223; Sample G50/1/79; Ref. 283/812; Neg. 2008/44. llv.

Fig. 10 and 14. Holotype, data as for Fig. 9; Ref. 316/802; Negs. 2002/44 and 2005/44, vv, showing S-type ventral arrangment, 14 = aav.
Fig. 11 and 12. Stub IC376; Prep. X486; Sample CS35; Ref. 351/780; Negs. 3002/14 and 3003/14. orlv and 12 = dv, showing precingular archaeopyle.
Fig. 13. Stub AM194; rest of data as for Fig. 11; Ref 279/756; Neg. 0040/93. detail of surface sculpture and trabeculae. ×7000.
Fig. 15 and 16. Data as for Fig. 1; Ref. 356/818; Negs. 2006/44 and 2007/44. rlv and Fig. 16 = odv, showing precingular archaeopyle.

Plate 7

µm bar: Figs. 4, 8 and 13 = 1 µm, all other Figs. = 10 µm

Figs. 1–10, 12–13. *Ctenidodinium complanatum* sp. nov., all ×800 except where otherwise stated.
Fig. 1. Holotype, Stub GD208; Prep. X226; Sample CS 40; Ref. 250/723; Neg. 2028/30. av, parasulcus to top.
Fig. 2. Stub IC373; Prep. CH031; Sample ICH 003; Ref. 355/751; Neg. 3013/16. oaav.
Fig. 3. Stub IC374; rest of data as for Fig. 2; Ref. 275/894; Neg. 3013/15. aav.
Fig. 4. Stub IC382; Prep. CH036; Sample ICH 008; Ref. 260/718; Neg. 3021/19. detail of sulcal paratabulation. ×3000.
Fig. 5. Stub IC342; Prep. Z228; Sample Gc78/1; Ref. 350/789; Neg. 2004/66. av.
Fig. 6. Stub IC324; Prep. CH106; Sample Gc88/1; Ref. 249/805; Neg. 2010/40. av.
Fig. 7. Data as for Fig. 3; Ref. 268/736; Neg. 3002/15. vv.
Fig. 8. Data as for Fig. 4; Ref. 300/764; Neg. 3018/19. detail of apical region and incidental paraplate (bottom). ×3000.
Fig. 9. Stub GD255A; Prep. X458; Sample HUN 185/0; Ref. 302/833; Neg. 3005/23. oaav.
Fig. 10. Stub IC343 rest of data as for Fig. 5; Ref. 263/844; Neg. 2011/65. detail of parasulcus. ×1600.
Fig. 12. Stub IC330; Prep. Z224; Sample G56/1/79; Ref. 269/897; Neg. 2014/47. aav. ×1600.
Fig. 13. Data as for Fig. 11; Ref. 195/757; Neg. 2030/48. cross-section of cyst wall. ×7000.

Figs. 11, 14–16. *Dichadogonyaulax irregulare.*
Fig. 11. Stub GD223; Prep. X439; Sample HUN 205/0; Ref. 232/827; Neg. 3038/21. detail of parasulcus. ×1600.
Fig. 14. Stub IC412; Prep. X424; Sample HUN 200/0; Ref. 187/838; Neg. 3017/21. av, parasulcus to left.
Fig. 15. Data as for Fig. 14; Ref. 252/784; Neg. 2021/21. aav, parasulcus to right.
Fig. 16. Data as for Fig. 13; Neg. 2037/21. aav.

Plate 8

µm bar: Figs. 4, 10 and 11 = 1 µm; all other Figs. = 10 µm

Figs. 1–11. *Heslertonia senectus* sp. nov. All ×800 except where otherwise stated.
Fig. 1. Holotype, Stub IC351; Prep. CH113; Sample G 187x/5; Ref. 220/781; Neg. 2008/93. odv, showing epicystal archaeopyle.
Fig. 2 and 3. Stub IC347; Prep. CH111; Sample G183x/4; Ref. 267/873; Negs. 1028/85 and 1029/85. vv, showing epicystal archaeopyle and detail of sulcal paratabulation Fig. 3 = ×1600.
Fig. 4. Stub IC350; rest of data as for Fig. 1; Ref. 300/910; Neg. 2013/75. detail of periphragm sculpture. ×3000.
Fig. 5. Stub IC351; rest of data as for Fig. 1; Ref. 328/715; Neg. 2008/94. llv.
Fig. 6. Data as for Fig. 2; Ref. 355/700; Neg. 2028/84. odv.
Fig. 7. Stub IC348; Prep. CH112; Sample G185x/5; Ref. 325/764; Neg. 2031/86. av of detached operculum.
Fig. 8. Stub IC358; Prep. CH116; Sample G197/3/83; Ref. 193/773; Neg. 3022/10. dv.
Fig. 9. Stub IC350; Prep. CH113; Sample G187x/5; Ref.; Neg. 2027/90. aav.
Fig. 10. Stub IC349; rest of data as for Fig. 7; Ref. 346/697; Neg. 2025/87. detail of paracingular septum (running top to bottom of picture) ×3000.
Fig. 11. Stub IC350; rest of data as for Fig. 1; Ref. 295/806; Neg. 2029/89. detail of fenestration in parasutural septum. ×3000.

Fig. 12. *Heslertonia heslertonensis.* Stub IC324; Prep. CH106; Sample Gc88/1; Ref. 241/841; Neg. 2042/40. llv, showing archaeopyle suture

Plate 9

µm bar: Figs. 7, 12–14 = 1 µm; all other Figs. = 10 µm

Figs. 1–7. *Dissiliodinium* sp. All ×800 except where otherwise stated.
Fig. 1. Stub IC303; Prep. CH101; Sample G100/9/83; Ref. 369/809; Neg. 2006/20. av, note apical series remains joined via sulcal 'isthmus'.

Fig. 2 and 5. Stub IC381; Prep. CH035; Sample ICH007; Ref. 291/757; Negs. 3010/19b and 3011/19b. vv, showing break up of opercular pieces and flagellar scar. 5 = ×1600.
Fig. 3. Data as for Fig. 2; Ref. 389/897; Neg. 3007/19b. vv, showing tabulation.
Fig. 4 and 7. Stub IC350; Prep. CH113; Sample G187x/5; Ref. 384/869; Negs. 2018/75 and 2019/75. ?vv, flagellar scar to top in 4, detail of sculpture in 7. Fig. 7 = ×3000.
Fig. 6. Data as for Fig. 4; Ref. 351/866; Neg. 2029/92. ovv.

Figs. 8–14. *Hurlandsia rugarum.* All ×600 except where otherwise stated.
Fig. 8 and 14. Stub IC193; Prep. Z241; Sample WM1050/1; Ref. No. 1; Negs. 1002/31 and 1015/32. llv. 14 = ×7000.
Fig. 9 and 13. Data as for Fig. 8; Ref. No. 4; Negs. 1003/32 and 1007/32. vv, showing epicystal archaeopyle and sulcal paratabulation. 13 = ×7000.
Fig. 10. Stub IC189; Prep. CH016; Sample WM1056/6; Ref. 228/778; Neg. 1014/35. dv, showing epicystal archaeopyle.
Fig. 11. Data as for Fig. 8; Ref. No. 17; Neg. 1016/32. vv.
Fig. 12. Data as for Fig. 10; Ref. 214/773; Neg. 1010/35. detail of sculpture. ×7000.

Plate 10

μm bar: Figs. 3, 4, 8, 12 and 16 = 1 μm; all others = 10 μm

Figs. 1–3, 5–6. *Athigmatocysta glabra.*
Fig. 1 and 6. Stub IC330; Prep. Z224; Sample G56/1/79; Ref. 303/734; Negs. 2021/46 and 2022/46. Fig. 1 = dv showing archaeopyle, ×600; Fig. 6 = detail showing endocyst, ×1600.
Fig. 2 and 3. Stub IC341; Prep. Z240; Sample Gc76/1; Ref. 287/841; Negs. 2022/69 and 2023/69. Fig. 2 = vv, S-type, ventral organisation, Fig. ×600; 3 = detail of apical horn, ×3000.
Fig. 5. Stub IC333; Prep. Z225; Sample G61/1/79; Ref. 244/848; Neg. 2027/52a. av of apical horn. ×1600.

Fig. 7. *Chlamydophorella ordinale* Stub IC364; Prep. Z233; Sample G199/1/83; Ref. 344/723; Neg. 2027/03. ?dv, showing diaphanous ectophragm ×800.

Figs. 4, 8–16. *Chlamydophorella trabeculosa.* All ×800 unless otherwise stated.
Fig. 4. Stub IC320; Prep. CH189; Sample G100/1/83; Ref. 228/866; Neg. 2021/18. damaged specimen showing autophragmal processes and perforate ectophragm. ×3000.
Fig. 8. Stub IC373; Prep. CH031; Sample ICH003; Ref. 300/806; Neg. 3015/16. detail of autophragmal showing basal perforations. ×3000.
Fig. 9. Stub IC379; Prep. CH033; Sample ICH005; Ref. 340/775; Neg. 3008/19a. dv showing apical archaeopyle suture. ×800.
Fig. 10. Stub IC382; Prep. CH036; Sample ICH008; Ref. 252/800; Neg. 3023/19b. vv.
Fig. 11. Stub IC343; Prep. Z228; Sample Gc78/1; Ref. 276/779; Neg. 2040/65. vv.
Fig. 12. Stub IC340; rest of data as for Fig. 2; Ref. 282/850; Neg. 2026/54. detail of flagellar scar on ectophrag. ×7000.
Fig. 13. Data as for Fig. 12; Ref. 249/731; Neg. 2010/64. vv, detail of specimen less operculum showing paratabulation. ×1600.
Fig. 14. Stub IC335; Prep. Z226; Sample G67/1/79; Ref. 240/888; Neg. 2004/59. as for Fig. 13. ×1600.
Fig. 15. Stub IC358; Prep. CH116; Sample G197/3/83; Ref. 228/850; Neg. 3029/009. vv.
Fig. 16. Stub IC350; Prep. CH113; Sample G187x/5; Ref. 347/788; Neg. 2031/90. detail of perforate ectophragm showing attachment points of autophragmal processes. ×3000.

Plate 11

μm bar: Figs. 8, 11–12, 14 = 1 μm; all others = 10 μm

Figs. 1–8, 12. *Hystrichostrogylon stolidota* emend. All ×800 unless otherwise stated.
Fig. 1. Stub IC323; Prep. CH107; Sample Gc98/1; Ref. 233/814; Neg. 2012/39. dv, showing precingular archaeopyle.
Fig. 2. Stub IC332; Prep. Z225; Sample G61/1/79; Ref. 300/712; Neg. 2028/51. odv, specimen with reduced pericoels.
Fig. 3. Stub IC284; Prep. CH097; Sample G100/5/83; Ref. 319/718; Neg. 1006/82. vv, showing parasulcal claustrum.
Fig. 4. Stub IC338; Prepä. Z239; Sample Gc74/1; Ref. 258/725; Neg. 2019/63. vv, showing parasulcal claustrum.
Fig. 5. Stub IC342; Prep. Z228; Sample Gc78/1; Ref. 245/776; Neg. 2009/68. dv, specimen showing prominent parasutural processes and well developed pericoels.
Fig. 6 and 7. Stub IC322; Prep. CH108; Sample G109; Ref. 263/792; Negs. 2037–2038/35. Fig. 6 = aav. Fig. 7 = detail of parasulcal tabulation, claustrum partially obscured due to folding. ×1600.
Fig. 8. Stub IC387; Prep. CH042; Sample ICH014; Ref. 375/716; Neg. 3009/18. detail showing displaced perioperculum. ×3000.
Fig. 12. Stub IC290; Prep. CH095; Sample G100/3/83; Ref. 338/782; Neg. 1039/97. detail of surface sculpture of endophragm (left) and periphragm (right), ×3000.

Fig. 9. Acritarch gen. et sp. nov. I. Stub IC297; Prep. CH100; Sample G100/8/83; Ref. 204/793; Neg. 2009/71. ×3000.
Fig. 10. Acritarch ring-dot. Stub IC282; CH097; Sample G100/5/83; Ref. 188/848; Neg. 1033/82. ×1600.
Fig. 11. Acritarch mam-dot. Stub IC350; Prep. CH113; Sample G187 x/5; Ref. 325/751; Neg. 2033/90. ×3000.
Figs. 12 and 17. Acritarch gen. et sp. nov. II.
Fig. 12. Stub IC373; Prep. CH031; Sample ICH003; Ref. 327/772; Neg. 3014/16. ×1600.
Fig. 17. Stub IC333; Prep. Z225; Sample G61/1/79; Ref. 274/867; Neg. 2035/52a. ×1600.
Figs. 13 and 14. *Mychristridium* sp. II. Both Stub IC230; Prep. Z193; Sample WM1051/2.
Fig. 13. Ref. 311/734; Neg. 1039/48. ×3000.
Fig. 14. Ref. 222/779; Neg. 1038/48. ×3000.
Fig. 15. *Veryhachium* sp. Stub IC047; Prep. CH001; Sample WM1153/2–8; Ref. 411/762; Neg. 0039/23. ×1600.
Fig. 16. *Mychristridium* sp. I. Stub IC059; Prep. CH027; Sample WM1110/9–10; Ref. 241/746; Neg. 0064/24. ×3000.
Fig. 18. Acritarch square-holes. Stub IC341; Prep. Z240; Sample Gc76/1; Ref. 329/798; Neg. 2027/70. ×1600.

Plate 12

μm bar: Figs. 6 and 8 = 1 μm; others = 10 μm

Figs. 1–11. *Exiguisphaera phragma.* All ×1600 unless otherwise stated.
Fig. 1. Stub IC340; Prep. Z240; Sample Gc76/1; Ref. 300/713; Neg. 2001/64. dv, showing two-plate archaeopyle. ×800.
Fig. 2. Stub IC374; Prep. CHO 31 Sample ICH003; Ref. 177/783; Neg. 3006/15. vv, showing paratabulation. ×1200.
Fig. 3. Stub IC333; Prep. Z225; Sample G61/1/79; Ref. 322/850; Neg. 2027/52b. detail of ventral epicystal paratabulation.
Fig. 4. Stub IC341; rest of data as for Fig. 1; Ref. 334/775; Neg. 2031/70. detail of archaeopyle showing that two paraplates are involved.
Fig. 5. Data as for Fig. 1; Ref. 414/813; Neg. 2035/64. detail of displaced operculum, showing the breakup of the compound biplacoid operculum.
Fig. 6. Stub IC339; Prep. Z239; Sample Gc74/1; Ref. 402/878; Neg. 2009/55. detail of ventral hypocystal paratabulation, showing intratabular spinules. ×3000.
Fig. 7. Stub IC342; Prep. Z228; Sample Gc78/1; Ref. 392/867; Neg. 2035/66. detail of apical paratabulation.
Fig. 8. Stub IC341; rest of data as for Fig. 1; Ref. 342/813; Neg. 2024/70. detail of surface sculpture and parasutural processes. ×3000.
Fig. 9. Data as for Fig. 3; Ref. 312/839; Neg. 2030/52b. detail of ventral hypocystal paratabulation.
Fig. 10. Data as for Fig. 7; Ref. 222/813; Neg. 2028/60. ovv.
Fig. 11. Stub IC330; Prep. Z224; Sample G56/1/79; Ref. 226/813; Neg. 2039/48. aav. ×1200.
Figs. 12–14. *Hystrichostrogylon* sp. All ×800.
Fig. 12. Stub IC373; rest of data as for Fig. 2; Ref. 367/797; Neg. 3002/16. oav, showing precingular archaeopyle and double row of crennelated parasutural septa.
Fig. 13. Data as for Fig. 2; Ref. 279/738; Neg. 3003/15. aav, sulcal claustrum visible at top.
Fig. 14. Data as for Fig. 2; Ref. 246/8472 Neg. 3010/15. odv, crushed specimen.

Plate 13

μm bar: Figs. 4, 7 and 9 = 1 μm; all others = 10 μm

All ×800 except where otherwise stated

Figs. 1–3, 5, 6. *Gonyaulacysta helicoidea.*
Fig. 1. Stub GD123; Prep. W350; Sample ALF IIre; Ref. 278/817; Neg. 3023/30. dv, showing precingular archaeopyle.
Fig. 2. Stub IC292; Prep. CH095; Sample G100/3/83; Ref. 253/8802; Neg. 2004/01. rlv.
Fig. 3. Stub GD125; Prep. W415; Sample ALF IIrg; Ref. 319/730; Neg. 3031/30. vv. ×1200.
Fig. 5. Stub IC376; Prep. X486; Sample CS35; Ref. 324/889; Neg. 3018/14. aav.
Fig. 6. Stub IC329; Prep. Z223; Sample G50/1/79; Ref. 228/753; Neg. 2004/26. detail of displaced perioperculum. ×1600.
Figs. 4, 7–10. *Gonyaulacysta exsanguia* emend.
Fig. 4. Stub IC328; rest of data as for Fig. 6; Ref. 342/754; Neg. 2017/44. detail of parasutural septa and processes, showing perforate bands. ×3000.
Fig. 7. Stub IC350; Prep. CH113; Sample G187x/5; Ref. 313/873; Neg. 2034/91. detail of apical horn, archaeopyle, also showing endophragm. ×3000.
Fig. 8. Stub IC265; Prep. DAVAY; Sample G100/6/83; Ref. 299/739; Neg. 1025/74. vv, showing S-type ventral organisation. ×1280.

Fig. 9. Stub IC299; Prep. CH100; Sample G100/8/83; Ref. 328/758; Neg. 2025/02. detail of perforate 'pandasutural bands' on epicystal part of parasulcus. ×3000.
Fig. 10. Stub IC358; Prep. CH116; Sample G197/3/83; Ref. 269/866; Neg. 3026/09. aav.

Figs. 11–13. *Gonyaulacysta fastigiata.*
Fig. 11. Stub IC375; Prep. X488; Sample CS37; Ref. 384/738; Neg. 3024/13. vv.
Fig. 12. Stub IC376; Prep. X486; Sample CS35; Ref. 259/708; Neg. 3025/14. vv.
Fig. 13. Stub IC384; Prep. CH097; Sample G100/5/83; Ref. 203/772; Neg. 1032/81. vv.

Plate 14

μm bar: Figs. 6–9, 11 and 15 = 1 μm; all others = 10 μm

Gonyaulacysta speciosus sp. nov. All ×800 except where otherwise stated

Fig. 1 and 5. Holotype, Stub IC340; Prep. Z240; Sample Gc76/1; Ref. 291/731; Negs. 2005/64 and 2007/64. dv, plus detail of archaeopyle and apical periphragm. Fig. 5 = ×1600.

Fig. 2 and 6. Stub IC342; Prep. Z228; Sample Gc78/1; Ref. 288/863; Negs. 2014/67 and 2015/67. dv, plus detail of apical horn. Fig. 6 = ×3000.

Fig. 3 and 4. Stub IC364; Prep. Z223; Sample G199/1/83; Ref. 289/724; Negs. 3036/03 and 3037/03. dv, plus detail of epicyst, note endo-operculum inside cyst. Fig. 4 = ×1600.

Fig. 7 and 9. Stub IC341; rest of data as for Fig. 1; Ref. 252/738; Negs. 2035/69 and 2037/69. detail of paracingular septum and cross-section through endophragm and partial periphragm. Both ×7000.

Fig. 8. Stub IC341; rest of data as for Fig. 1; Ref. 332/862; Neg. 2030/64. detail of apical horn. ×3000.

Fig. 10. Stub IC424; Prep. X305; Sample CL17; Neg. 3014/31. oav.

Fig. 11. Stub IC341; rest of data as for ig. 1; Ref. 331/894; Neg. 2007/70. detail of surface sculpture. ×3000.

Fig. 12. Stub IC379; Prep. CH033; Sample ICH005; Ref. 264/699; Neg. 3005/19a. odv.

Fig. 13. Stub IC373; Prep. CH031; Sample ICH003; Ref. 223/747; Neg. 3009/16. rlv.

Fig. 14. Stub IC374; rest of data as for Fig. 12; Ref. 376/764; Neg. 3023/15. dv.

Fig. 15. Stub IC333; Prep. Z225; Sample G61/1/79; Ref. 389/771; Neg. 2019/53. detail of surface sculpture. ×3000.

Plate 15

μm bar: Figs. 4, 9 and 11 = 1 μm; all others = 10 μm

Figs. 1–11, 15. *Gonyaulacysta teicha* emend. All ×800 except for where otherwise stated.
Fig. 1. Stub IC343; Prep. Z228; Sample Gc78/1; Re. 275/887; Neg. 2002/65. dv.
Fig. 2. Stub IC340; Prep. Z240; Sample Gc76/1; Ref. 188/762; Neg. 2044/64. dv.
Fig. 3. Data as for Fig. 1; Ref. 297/733; Neg. 2034/65. dv.
Fig. 4. Stub IC338; Prep. Z239; Sample Gc74/1; Ref. 288/853; Neg. 2017/62. detail of denticulate septa and endophragm in region of archaeopyle. ×3000.
Figs. 5 and 11. Data as for Fig. 4; Ref. 364/821; Negs. 2004/62 and 2006/62. rlv and detail of apical horn showing porichnion. 11 = ×3000.
Fig. 6. Stub IC374; Prep. CH031; Sample ICH003; Ref. 237/863; Neg. 3011/15. vv, showing S-type ventral organisation. ×1200.
Fig. 7. Stub IC342; rest of data as for Fig. 3; Ref. 323/721; Neg. 2007/66. llv.
Fig. 8. Data as for Fig. 6; Ref. 286/753; Neg. 3032/15. showing endoperculum in place and presumed primary absence of perioperculum. ×1600.
Figs. 9 and 10. Stub IC337; Prep. Z227; Sample G71/1/79; Ref. 302/752; Negs. 2036/78 and 2037/78. ovv and detail of rugulae on apical series. 9 = ×3000.
Fig. 15. Data as for Fig. 4; Ref. 236/752; Neg. 2016/63. oaav.

Figs. 12–14. *Gonyaulacysta speciosus* sp. nov. All ×800.
Fig. 12. Data as for Fig. 2; Ref. 406/812; Neg. 2036/64. vv.
Fig. 13. Data as for Fig. 1; Ref. 229/717; Neg. 2049/65. ovv.
Fig. 14. Data as for Fig. 7; Ref. 276/730; Neg. 2012/68. rlv.

Plate 16

μm bar: Figs. 6, 8–10 = 1 μm; all others = 10 μm

Figs. 1–9. *Occisucysta duxburyi*.

Fig. 1. Stub GD229; Prep. X413; Sample HUN130/0; Ref. 314/727; Neg. 2037/07. ollv, showing partially displaced compound biplacoid operculum. ×800.

Fig. 2. Stub IC337; Prep. Z227; Sample G71/1/79; Ref. 379/774; Neg. 2041/73. vv. ×680.

Fig. 3. Stub IC334; Prep. Z226; Sample G67/1/79; Ref. 245/767; Neg. 2022/56. ovv, detail of apical horn showing porichnion. ×1600.

Fig. 4. Stub IC342; Prep. Z228; Sample Gc78/1; Ref. 402/820; Neg. 2021/66. detail of parasulcal tabulation. ×1600.

Figs. 5 and 8. Data as for Fig. 3; Ref. 336/768; Negs. 2009/56 and 2011/56. aav. Fig. 5 = ×800; Fig. 8 = detail of surface sculpture on antapical paraplate showing tuberculation. ×3000.

Fig. 6. Data as for Fig. 4; Ref. 404/819; Neg. 2020/66. detail of cross-sections of 'reticulate' periphragm and coarsely sculptured endophragm. ×7000.

Fig. 7. Stub IC350; Prep. CH113; Sample G187x/5; Ref. 25–/77–; Neg. 2037/89. vv, detail of apical horn and porichnion. ×1600.

Fig. 9. Stub IC333; Prep. Z225; Sample G61/1/79; Ref. 277/772; Neg. 2019/52a. detail of cingular parasutural septum showing fenestration. ×3000.

Figs. 10–14. *Meiourogonyaulax sagena* emend.

Fig. 10. Stub IC335; rest of data as for Fig. 5; Ref. 370/852; Neg. 2033/58. detail of autophragm surface sculpture and parasutural denticles (ectophragm removed by acid digestion). ×3000.

Fig. 11. Data as for Fig. 10; Ref. 268/884; Neg. 2013/59. vv. ×800.

Fig. 12. Data as for Fig. 2; Ref. 322/847; Neg. 2021/79. vv. ×800.

Fig. 13. Stub GD119; Prep. W348; Sample ALF IIq; Ref. 222/758; Neg. 3013/30. detail showing laevigate ectophragm. ×1600.

Fig. 14. Stub IC340; Prep. Z240; Sample Gc76/1; Ref. 245/704; Neg. 2043/64. vv, detail of parasulcal tabulation. ×1600.

Plate 17

μm bar: Fig. 3 = 1 μm; all others = 10 μm

Pentadinium omasum sp. nov. All ×800 except where otherwise stated.

Fig. 1 and 3. Holotype, Stub IC358; Prep. CH116; Sample G197/3/83; Ref. 404/768; Neg. 3028/10. oav and detail of two wall layers and the fusion between them. Fig. 3 = ×3000.

Fig. 2. Stub IC346; Prep. CH111; Sample G183x/4; Ref. 309/752; Neg. 2038/80. oav.

Fig. 4. Stub IC353; Prep. CH114; Sample G192x/2; Ref. 222/744; Neg. 2036/98. ollv.

Fig. 5. Data as for Fig. 1; Ref. 402/880; Neg. 3009/10. odv.

Fig. 6. Stub IC354; Prep. Z229; Sample G197/1/83; Ref. 251/812; Neg. 3008/06. vv.

Fig. 7. Data as for Fig. 1; Ref. 184/777; Neg. 3023/10. oav.

Fig. 8. Data as for Fig. 2; Ref. 416/841; Neg. 2005/80. dv.

Fig. 9. Stub IC359; rest of data as for Fig. 1; Ref. 354/735; Neg. 3008/09. av.

Fig. 10. Data as for Fig. 1; Ref. 265/839; Neg. 3034/09. vv.

Fig. 11. Stub IC357; Prep. Z230; Sample G197/2/83; Ref. 246/752; Neg. 3035/05. vv.

Fig. 12. Stub IC359; rest of data as for Fig. 1; Ref. 295/716; Neg. 3001/08. dv, with displaced endocyst.

Fig. 13. Stub IC347; rest of data as for Fig. 2; Ref. 315/838; Neg. 2012/84. aav.

Fig. 14. Data as for Fig. 11; Ref. 246/750; Neg. 3036/05. rlv.

Plate 18

μm bar: Figs. 6, 11 and 12 = 1 μm; all others = 10 μm

Trichodinium ciliatum. All ×800 except where otherwise stated

Fig. 1. Stub IC342; Prep. CH106; Sample Gc88/1; Ref. 244/784; Neg. 2007/40. dv, showing archaeopyle.

Fig. 2. Stub IC370; Prep. CH029; Sample ICH001; Ref. 216/747; Neg. 3010/11. dv.

Fig. 3. Stub IC333; Prep. Z225; Sample G61/1/79; Ref. 304/8652; Neg. 2011/52b. detail of flagellar scar. ×1600.

Fig. 4. Data as for Fig. 3; Ref. 212/804; Neg. 2023/52a. dv.

Fig. 5. Data as for Fig. 1; Ref. 268/812; Neg. 2023/40. vv.
Fig. 6. Stub IC325; Prep. CH105; Sample Gc83/1; Ref. 325/844; Neg. 2017/43. detail of surface sculpture. ×3000.

Trichodinium discus sp. nov. All ×800 except where otherwise stated

Fig. 7. Holotype, Stub IC283; Prep. CH097; Sample G100/5/83; Ref. 268/806; Neg. 1002/84. dv, showing archaeopyle.
Fig. 8. Stub IC281; rest of data as for Fig. 7; Ref. 288/723; Neg. 1019/87. dv.
Fig. 9. Stub IC314; Prep. CH104; Sample G100/12/83; Ref. 379/804; Neg. 2043/12. vv.
Fig. 10. Stub IC387; Prep. CH042; Sample ICH014; Ref. 301/826; Neg. 3004/18. dv.
Fig. 11 and 12. Stub IC338; Prep. Z239; Sample Gc74/1; Ref. 184/794; Negs. 2001/63–2003/63. vv. 11. detail of surface sculpture, 12. detail of flagellar scar. Both ×3000.
Fig. 13. Stub IC349; Prep. CH112; Sample G185x/5; Ref. 403/836; Neg. 2002/88. dv.

Plate 19

μm bars = 10 μm, except Fig. 11 = 1 μm

Trichodinium spectonense. All ×600 unless otherwise stated

Fig. 1. Stub IC265; Prep. Davey; Sample G100/6/83; Ref. 318/893; Neg. 1011/73. dv, showing precingular archaeopyle. ×800.
Fig. 2. Data as for Fig. 1; Ref. 305/764; Neg. 1020/77. vv, showing flagellar scar. ×720.
Fig. 3. Stub IC427; Prep. Z334; Sample ALF CL20; Ref. 301/828; Neg. 3017/31. vv. ×800.
Fig. 4. Stub IC426; Prep. Z333; Sample ALF CL21; Ref. 270/800; Neg. 3019/31. dv, showing precingular archaeopyle.
Fig. 5. Stub GD189; Prep. X232; Sample CS47; Ref. 213/832; Neg. 3002/29. vv. ×800.
Fig. 6. Data as for Fig. 1; Ref. 321/723; Neg. 1016/74. vv; 6, detail of apical 'tuft' of partially fused spines, not a true horn, ×1600.

Trichodinium calvus sp. nov. All ×800 except where otherwise stated

Fig. 7. Holotype, Stub IC353; Prep. CH114; Sample G192x/2; Ref. 401/722; Neg. 2042/98. ovv.
Fig. 8 and 11. Stub IC352; rest of data as for Fig. 7; Ref. 371/773; Negs. 2033/96 and 2034/96. rlv, operculum in place and detail of surface of differentiated autophragm. Fig. 9 = ×3000.
Fig. 9. Stub IC352; rest of data as for Fig. 7; Ref. 194/748; Neg. 2029/95. dv, showing archaeopyle.
Fig. 10. Data as for Fig. 7; Ref. 254/798; Neg. 2005/99. ovv.
Fig. 12. Data as for Fig. 1; Ref. 284/850; Neg. 2010/99. av, specimen showing traces of paratabulation.

Plate 20

μm bar: Figs. 4–5, 8–9 = 1 μm; all others = 10 μm

Figs. 1–6, 11. *Hystrichodinium voigtii.*
Fig. 1. Stub IC417; Prep. CH097; Sample G100/5/83; Ref. none; Neg. 3001/26. dv. ×560.
Fig. 2. Stub GD125; Prep. W415; Sample ALF llrg; Ref. 353/759; Neg. 3032/30. vv, specimen with high parasutural septa and reduced processes. ×800.
Fig. 3. Stub IC333; Prep. Z225; Sample G61/1/79; Ref. 362/850; Neg. 2002/53. detail of parasulcal tabulation, showing flagellar scar. ×1600.
Fig. 4. Stub IC325; Prep. CH105; Sample Gc83/1; Ref. 302/796; Neg. 2036/41. detail of thecamorphic expression of 'trichocyst pores'. *×3000.*
Fig. 5. Stub IC265; Prep. Davey; Sample G100/6/83; Ref. 211/724; Neg. 1019/75. as for Fig. 4. ×3000.
Fig. 6. Stub IC352; Prep. CH114; Sample G192x/2; Ref. 389/759; Neg. 2028/96. detail of parasulcal tabulation, showing overhanging cingulum. ×1600.
Fig. 11. Stub IC347; Prep. CH111; Sample G183x/4; Ref. 313/732; Neg. 2035/84. detail of parasulcal tabulation, note pores. ×1600.
Figs. 7–8. *Hystrichodinium compactum.* Stub IC330; Prep. Z224; Sample G56/1/79; Ref. 354/771; Negs. 2007/46 and 2008/46. 7, vv = ×800; 8 = detail, ×300.
Fig. 9. *Hystrichodinium furcatum.* Stub IC339; Prep. Z239; Sample Gc74/1; Ref. 335/881; Neg. 2039/55. detail of process termination, showing single furcation. ×3000.
Fig. 10. *Hystrichodinium ramoides.* Stub IC361; Prep. CH115; Sample G197/4/83; Ref. 310/795; Neg. 3020/00. detail of process terminations, showing multiple furcations. ×1600.

Plate 21

μm bar: Figs. 4, 15 = 1 μm; all others = 10 μm

Figs. 1–3, 5–6. *Hystrichosphaerina schindewolfii.*
Fig. 1. Stub IC336; Prep. Z227; Sample G71/1/79; Ref. 232/716; Neg. 2038/78. dv, specimen has lost operculum and shows the simple, double process corresponding to each cingular paraplate. ×600.
Figs. 2 and 3. Data as for Fig. 1; Ref. 354/850; Neg. 2032–2033/79. Fig. 2 = vv, ×600. Fig. 3 = detail of sulcal paratabulation, accessory archaeopyle sutures can be seen around *ai,* ×1600.
Fig. 5. Stub IC405; Prep. CH077; Sample ICH025; Ref. 273/827; Neg. 3017/25. oavv, showing apical archaeopyle and accessory sutures. ×800.
Fig. 6. Stub IC334; Prep. Z226; Sample G67/1/79; Ref. 310/726; Neg. 2013/56. isolated four-paraplate operculum with accessory sutures. ×800.

Figs. 4, 7–11. *Callaiosphaeridium* spp. All ×800 unless otherwise stated.
Figs. 4 and 8. Stub IC338; Prep. Z239; Sample Gc74/1; Ref. 346/704; Neg. 2025–2026/61. Fig. 4 = detail of fenestration at base of parasutural septa. ×3000. Fig. 8 = aav, two dorsal paracingular processes broken off.
Fig. 7. Stub GD255A; Prep. X458; Sample HUN185/0; Ref. 316/744; Neg. 3010/23. rlv.
Fig. 9. Stub IC373; Prep. CH031; Sample ICH003; Ref. 227/837; Neg. 3006/16. detail of sulcal paratabulation. ×1600.
Fig. 10. Stub IC281; Prep. CH097; Sample G100/5/83; Ref. 253/731; Neg. 1008/87. vv of specimen with little development of parasutural septa.
Fregion to top left.

Figs. 12–15. *Exochosphaeridium* spp. All ×800 unless otherwise stated.
Fig. 12. Stub IC332; Prep. Z225; Sample G61/1/79; Ref. 337/769; Neg. 2033/51. dv, showing precingular archaeopyle.
Figs. 13 and 15. Stub Y; Prep. Z228; Sample Gc78/1; Ref. None; Neg. 0009–0010/93. dv. Fig. 15 = detail of surface sculpture. ×3000.
Fig. 14. Stub IC374; rest of data as for Fig. 9; Ref. 372/731; Neg. 3006/12. rlv.

Plate 22

μm bar: Figs. 5, 9–10, 15 = 1 μm; all others = 10 μm

Figs. 1–9. *Kleithriasphaeridium corrugatum.*
Fig. 1. Stub GD265; Prep. X465; Sample CS55; Ref. 190/753; Neg. 3007/31. vv, showing precingular archaeopyle. ×600.
Fig. 2. Stub X; Prep. Z226; Sample G67/1/79; Ref. 389/795; Neg. 0017/85. dv, showing precingular archaeopyle. ×600.
Fig. 3. Stub IC342; Prep. Z228; Sample Gc78/1; Ref. 318/894; Neg. 2023/67. detail of archaeopyle. ×1600.
Fig. 4. Stub IC341; Prep. Z240; Sample Gc76/1; Ref. 254/778; Neg. 2032/69. isolated operculum. ×1600.
Fig. 5. Stub IC328; Prep. Z223; Sample G50/1/79; Ref. 323/706; Neg. 2014/44. detail of typical process termination. ×3000.
Fig. 6. Stub IC333; Prep. Z225; Sample G61/1/79; Ref. 355/743; Neg. 2033/53. detail of surface sculpture in the region of the parasulcus. ×1600.
Fig. 7. Stub IC325; Prep. CH105; Sample Gc83/1; Ref. 347/857; Neg. 2033/42. detail, showing partially displaced operculum with single, plate-centred process. ×1600.
Fig. 8. Data as for Fig. 3; Ref. 263/885; Neg. 2038/67. detail of archaeopyle. ×1600.
Fig. 9. Stub IC339; Prep. Z239; Sample Gc74/1; Ref. 243/820; Neg. 2031/60. detail of broken process base revealing sculpture of enophragm beneath. ×7000.

Figs. 10–15. *Kleithriasphaeridium simplicispinum.*
Fig. 10. Stub IC362; Prep. Z231; Sample G198/1/83; Ref. 341/757; Neg. 3018/02. claustra in parasulcal region. ×3000.
Fig. 11. Stub IC380; Prep. CH034; Sample ICH006; Ref. 372/844; Neg. 3013/19a. isolated operculum. ×1600.
Fig. 12. Data as for Fig. 3; Ref. 392/848; Neg. 2039/66. dv, showing precingular operculum. ×600.
Fig. 13. Data as for Fig. 3; Ref. 253/741; Neg. 2025/68. oaav. ×600.
Fig. 14. Stub IC359; Prep. CH116; Sample G197/3/83; Ref. 330/759; Neg. 3003/09. llv of specimen with processes much reduced in length. ×800.
Fig. 15. Stub IC347; Prep. CH111; Sample G183x/4; Ref. 235/805; Neg. 2009/85. detail of broken process base revealing sculpture of endophragm beneath. ×7000.

Plate 23

μm bar: Figs. 3–4, 8 and 16 = 1 μm; others = 10 μm

All × 800 unless otherwise stated

Figs. 1–4. *Discorsia nanna.*
Fig. 1. Stub GD313; Prep. X420; Sample HUN170/0; Ref. 270/864; Neg. 3009/31. view uncertain. × 1200.
Fig. 2. Stub GD255A; Prep. X458; Sample HUN185/0; Ref. 338/859; Neg. 3016/23. view uncertain of specimen with baggy periphragm.
Fig. 3. Stub IC333; Prep. Z225; Sample G61/1/79; Ref. 394/809; Neg. 2014/53. detail of broken process base showing surface sculpture of peri- and endophragm. × 7000.
Fig. 4. Stub IC334; Prep. Z226; Sample G67/1/79; Ref. 242/793; Neg. 2027/56. detail of typical process terminations. × 7000.

Figs. 5, 6, 8. *Hystrichosphaeridium arborispinum.*
Fig. 5. Stub IC278; Prep. CH099; Sample G100/7/83; Ref. 230/788; Neg. 1033/90. dv showing apical archaeopyle suture.
Fig. 6. Stub IC299; Prep. CH100; Sample G100/8/83; Ref. 245/760; Neg. 2038/02. view uncertain.
Fig. 8. Stub IC037; Prep. CH007; Sample CS46; Ref. 270/849; Neg. 0038/12. detail of typical process termination. × 3000.

Fig. 7. *Wallodinium krutzschii.* Stub IC361; Prep. CH115; Sample G197/4/83; Ref. 359/775; Neg. 3046/00. vv, showing parasulcal tongue, operculum lost. × 600.

Figs. 9–11, 13–16. *Protoellipsodinium* sp.
Fig. 9. Stub IC338; Prep. Z239; Sample Gc74/1; Ref. 196/737; Neg. 2018/63. odv, showing precingular archaeopyle.
Fig. 10. Stub IC339; rest of data as for Fig. 9; Ref. 248/733; Neg. 2011/60. dv.
Fig. 11. Data as for Fig. 10; Ref. 400/828; Neg. 2014/55. dv.
Fig. 13. Stub IC364; Prep. Z233; Sample G199/1/83; Ref. 298/908; Neg. 3008/03. odv of stratigraphically later example with fewer processes.
Fig. 14. Data as for Fig. 7; Ref. 307/766; Neg. 3038/00. odv, see Fig. 13.
Fig. 15. Stub IC359; Prep. CH116; Sample G197/4/83; Ref. 338/723; Neg. 3013/09. odv, see Fig. 13.

Fig. 16. Data as for Fig. 5; Ref. 328/772; Neg. 1004/90. detail of archaeopyle suture, operculum still in place. × 3000.

Fig. 12. *Wallodinium luna.* Stub IC341; Prep. Z240; Sample Gc76/1; Ref. 291/772; Neg. 2031/69. rlv, parasulcal tongue to top right of cyst, operculum lost.

Plate 24

μm bar: Figs. 6, 11 and 13 = 1 μm, all others = 10 μm

Figs. 1–7. *Oligosphaeridium pseudoabaculum* sp. nov. All from Prep. CH103; Sample G100/11/83 except where otherwise stated.
Fig. 1. Holotype. Stub IC481; Ref. Specimen 3; Neg. 3009/52. odv, × 400.
Fig. 2. Stub IC482; Ref. Specimen 1; Neg. 3019/52. dv, × 400.
Fig. 3. Stu IC482; Ref. Specimen 3; Neg. 3021/52. ovv, showing parasulcal notch. × 400.
Fig. 4. Stub IC312; Ref. 305/715; Neg. 2009/15. detail of partially detached operculum showing parasulcal notch. × 1600.
Fig. 5. Stub IC311; Ref. 311/795; Neg. 2045/14. vv, detail showing *X* and *Z* processes, and bases of *2, 1i, II, III* and *Y*. × 1066.
Fig. 6. Stub IC282; Prep. CH097; Sample G100/5/83; Ref. 225/755; Neg. 1003/83. detail of broken process base showing difference in sculpture of endophragm and periphragm. × 3000.
Fig. 7. Stub IC311; Ref. 300/829; Neg. 2041/13. rlv, faint trace of paracingulum where periphragmal sculpture is diminished. × 800.

Figs. 8–14. *Vexillocysta retis* gen. et sp. nov. All from Stub IC265; Prep. Davey; Sample G100/6/83 and × 800 except where otherwise stated.
Fig. 8. Holotype. Ref. 292/758; Neg. 1024/78. vv, showing apical archaeopyle.
Fig. 9. Ref. 312/837; Neg. 1009/77. view uncertain, operculum to top left, paracingulum running top right to bottom left.
Fig. 10. Ref. 252/863; Neg. 1024/72. view uncertain, orientation uncertain.
Fig. 11. Stub IC350; Prep. CH113; Sample G187 x/5; Ref. 383/868; Neg. 2020/75. detail showing reticulate nature of periphragmal sculpture and the bifurcating blade-like processes bearing globular striations. × 3000.
Fig. 12. Ref. 282/778; Neg. 1029/78. view uncertain, archaeopyle suture visible.
Fig. 13. Stub GD229; Prep. X413; Sample Hun130/0; Ref. 359/770; Neg. 3001/20. detail showing separation of thick laevigate endophragm from thin periphragm along margin of operculum. *× 7000.*
Fig. 14. Stub IC337; Prep. Z227; Sample G71/1/79; Ref. 323/874; Neg. 2001/78. vv, clearly showing margin of apical archaeopyle, form with more gracile processes (similar to 'antapical' region of Fig. 10).

Plate 25

μm bar: Figs. 7–8, 15 = 1 μm; all others = 10 μm

All ×800 except where otherwise stated

Figs. 1–9. *Cleistosphaeridium fungosus* sp. nov.

Fig. 1. Holotype, Stub IC300; Prep. CH100; Sample G100/8/83; Ref. 318/732; Neg. 2003/03. view uncertain, showing apical archaeopyle suture.

Fig. 2. Stub IC284; Prep. CH097; Sample G100/5/83; Ref. 227/841; Neg. 1036/81. view uncertain, showing apical archaeopyle suture.

Fig. 3. Stub IC278; Prep. CH099; Sample G100/7/83; Ref. 355/880; Neg. 1012/88. view uncertain, showing apical archaeopyle suture.

Fig. 4. Stub IC353; Prep. CH114; Sample G192x/2; Ref. 380/780; Neg. 2021/98. specimen minus operculum, showing accessory archaeopyle sutures.

Fig. 5. Stub IC297; rest of data as for Fig. 1; Ref. 214/788; Neg. 2010/71. detail showing archaeopyle suture. ×1600.

Fig. 6. Stub IC265; Prep. Davey; Sample G100/6/83; Ref. 303/864; Neg. 1004/73. showing displaced apical operculum.

Fig. 7. Stub IC303; Prep. CH101; Sample G100/9/83; Ref. 185/806; Neg. 2010/00. detail of surface sculpture. ×3000.

Fig. 8. Stub IC350; Prep. CH113; Sample G187x/5; Ref. 176/800; Neg. 2022/76. cross-section of cyst wall, showing processes and filaments. ×7000.

Fig. 9. Data as for Fig. 8; Ref. 274/788; Neg. 2020/76. as for Fig. 4.

Figs. 10–19. *Batiacasphaera mica* sp. nov.

Fig. 10. Holotype, Stub IC282; rest of data as for Fig. 2; Ref. 238/718; Neg. 1005/83. ?dv, displaced apical operculum visible. ×1600.

Fig. 11. Data as for Fig. 2; Ref. 309/813; Ne. 1019/82. ovv, with sulcal 'groove'. ×1600.

Fig. 12. Data as for Fig. 2; Ref. 261/753; Neg. 1001/82. ?vv, complete specimen. ×1600.

Fig. 13. Stub IC316; Prep. CH104; Sample G100/12/83; Ref. 293/897; Neg. 2002/19. view uncertain, operculum lost.

Fig. 14. Data as for Fig. 5; Ref. 212/763; Neg. 2012/71. as for Fig. 13.

Fig. 15. Data as for Fig. 5; Ref. 264/847; Neg. 2004/71. detail of flagellar scar and surface sculpture. ×3000.

Fig. 16. Stub IC323; Prep. CH107; Sample Gc98/1; Ref. 228/766; Neg. 2038/39. specimen showing traces of paratabulation.

Fig. 17. Data as for Fig. 5; Ref. 372/874; Neg. 2011/05. showing archaeopyle.

Fig. 18. Stub IC334; Prep. Z226; Sample G67/1/79; Ref. 405/798; Neg. 2005/56.

Fig. 19. Stub IC332; Prep. Z225; Sample G61/1/79; Ref. 286/873; Neg. 2007/51. specimen with well developed paracingulum.

Plate 26

μm bar: Figs. 4, 8, 13–14 = 1 μm; all others = 10 μm

All ×800 except where otherwise stated

Figs. 1–5. *Dapsilidinium* sp. II.

Fig. 1. Stub IC285; Prep. CH096; Sample G100/4/83; Ref. 198/731; Neg. 1021/80. oav, showing apical archaeopyle.

Fig. 2. Stub IC316; Prep. CH104; Sample G100/12/83; Ref. 400/785; Neg. 2010/19. complete specimen, orientation uncertain.

Fig. 3. Stub IC361; Prep. CH115; Sample G197/4/83; Ref. 262/832; Neg. 3006/00. vv of axially elongate specimen showing narrow parasulcal processes.

Fig. 4. Stub IC325; Prep. CH105; Sample Gc83/1; Ref. 307/796; Neg. 2034/43. cross-section of cyst wall showing large tubular processes and small processes with matted fibrous endings. ×7000.

Fig. 5. Data as for Fig. 3; Ref. 269/878; Neg. 3007/00. view uncertain, showing displaced apical operculum.

Figs. 6–8. *Dapsilidinium* sp. I.

Fig. 6. Stub IC297; Prep. CH100; Sample G100/8/83; Ref. 308/768; Neg. 2004/06. showing apical archaeopyle suture.

Fig. 7. Stub IC281; Prep. CH097; Sample G100/5/83; Ref. 328/719; Neg. 1025/85. showing displaced apical operculum.

Fig. 8. Stub IC265; Prep. Davey; Sample G100/6/83; Ref. 268/689; Neg. 1010/75. detail of surface sculpture. ×3000.

Figs. 9–16. *Chlamydophorella nyei.*

Fig. 9. Stub IC364; Prep. Z223; Sample G199/1/83; Ref. 269/767; Neg. 3001/04. ?dv of typical specimen.

Fig. 10. Stub IC337; Prep. Z227; Sample G71/1/79; Ref. 323/876; Neg. 2039/77. view uncertain, atypical globular specimen.

Fig. 11. Stub IC354; Prep. Z229; Sample G197/1/83; Ref. 252/828; Neg. 3013/06. ?dv of elongate specimen.
Fig. 12. Stub X; Prep. Z226; Sample G67/1/79; Ref. 252/826; Neg. 0002/88. view uncertain, operculum lost.
Fig. 13. Stub IC334; *rest of data as for Fig. 12; Ref. 301/803; Neg. 2042/56. detail of cyst cross-section, showing fenestrate* ectophragm. ×3000.
Fig. 14. Stub IC362; Prep. Z231; Sample G198/1/83; Ref. 299/792; Neg. 3009/02. detail of ectophragm surface, showing autophragmal processes. ×3000.
Fig. 15. Stub IC335; rest of data as for Fig. 12; Ref. 375/788; Neg. 2016/58. detail of ectophragmal apical horn. ×1600.
Fig. 16. Data as for Fig. 6; Ref. 284/710; Neg. 2017/71. vv, detail of ectophragmal apical horn. ×1600.

Plate 27

μm bar: Figs. 3, 4 and 8 = 1 μm; all others = 10 μm

Resticulasphaera medusae gen. et sp. nov. All ×1600 unless otherwise stated

Fig. 1. Holotype, Stub IC348; Prep. CH112; Sample G185x/5; Ref. 222/774; Neg. 2044/86. vv, showing flagellar scar.
Fig. 2. Stub IC156; Prep. CH078; Sample ICH026; Ref. 332/745; Neg. 3018/25. dv, showing displaced epicystal operculum.
Fig. 3. Data as for Fig. 1; Ref. 246/800; Neg. 2004/86. dv.
Fig. 4. *Stub IC346; Prep. CH111; Sample G183x/4; Ref. 309/803; Negs. 2033/80 and 2034/80. 4 – detail of surface sculpture* along archaeopyle suture, ×7000. 16 – showing epicystal archaeopyle.
Fig. 5. Stub IC347; rest of data as for Fig. 1; Ref. 222/802; Neg. 2007/85. vv, showing epicystal archaeopyle suture.
Fig. 6. Data as for Fig. 4; Ref. 293/768; Neg. 2022/81. dv.
Fig. 7. Stub IC351; Prep. CH113; Sample G187x/5; Ref. 308/896; Neg. 2026/93. dv.
Fig. 8. Stub IC384; Prep. X240; Sample CS52; Ref. 288/738; Neg. 3023/18. detail of surface sculpture. ×7000.

Cassiculosphaeridia tunicata sp. nov. All ×800 except where otherwise stated

Figs. 9 and 11. Holotype, Stub IC334; Prep. Z226; Sample G67/1/79; Ref. 316/801; Neg. 2003/56 and 2004/56. ?vv and detail of perforate ectophragm. 3 = ×3000.
Fig. 10. Data as for Fig. 1; Ref. 241/771; Neg. 2021/56. orientation uncertain.
Fig. 12. Data as for Fig. 1; Ref. 311/805; Neg. 2002/56. orientation uncertain.
Fig. 13. Data as for Fig. 1; Ref. 282/757; Neg. 2017/56. orientation uncertain.
Fig. 14. Stub IC335; rest of data as for Fig. 1; Ref. 335/769; Neg. 2019/58 orientation uncertain.

Plate 28

μm bar: Fig. 11 = 1 μm; all others = 10 μm

Figs. 1–4. *Batioladinium longicornutum.*
Figs. 1 and 4. Stub IC347; Prep. CH111; Sample G183x/4; Ref. 288/864; Negs. 2017/85 and 2040–2042/85. vv of specimen with broken left antapical horn, ×800. Fig. 4 – detail of archaeopyle suture, ×1600.
Fig. 2. Stub IC336; Prep. Z227; Sample G71/1/79; Ref. 332/760; Neg. 2002/79. vv of specimen with reduced apical horn. ×400.
Fig. 3. Stub IC333; Prep. Z225; Sample G61/1/79; Ref. 263/713; Neg. 2007/52a. isolated operculum. ×800.
Figs. 5–11. *Batioladinium jaegeri.* All ×800 unless otherwise stated.
Fig. 5. Data as for Fig. 3; Ref. 376/844; Neg. 2003/53. vv, showing apical archaeopyle.
Fig. 6. Stub IC335; Prep. Z226; Sample G67/1/79; Ref. 251/705; Neg. 2023/58. vv, specimen showing archaeopyle suture.
Fig. 7. Stub IC338; Prep. Z239; Sample Gc74/1; Ref. 255/806; Neg. 2020/62. llv.
Fig. 8. Stub IC277; Prep. CH099; Sample G100/7/83; Ref. 405/858; Neg. 1001/79. vv of 'short, fat' morph.
Fig. 9. Stub IC341; Prep. Z240; Sample G76/1; Ref. 412/824; Neg. 2017/70. dv, showing archaeopyle suture.
Fig. 10. *Stub IC337; rest of data as for Fig. 2; Ref. 277/802; Neg. 2002/77.* dv.
Fig. 11. Stub IC289; Prep. CH095; Sample G100/3/83; Ref. 304/757; Neg. 1013/93. detail of surface sculpture. ×7000.

Plate 29

μm bar: Figs. 6–8, 12, 14, 15 = 1 μm, all others = 10 μm

Figs. 1–8. *Prolixosphaeridium deirense* emend.
Fig. 1. Stub IC351; Prep. CH113; Sample G187x/5; Ref. 276/825; Neg. 2020/93. dv.
Fig. 2. Stub IC350; rest of data as for Fig. 1; Ref. 301/792; Neg. 2009/91. odv.
Fig. 3 and 8. Data as for Fig. 2; Ref 298/899; Negs. 2029/76 and 2030/76. ?dv and detail of surface sculpture. 8 = Fig. 4. Data as for Fig. 1; Ref. 314/793; Neg. 2019/94. specimen showing greater density of processes.
Fig. 5 and 6. Stub IC271; Prep. CH185; Sample ANG199B; Ref. 376/825; Negs. 3001/24 and 3003024. vv, Tethyan specimen, more elongate and with shorter processes but displaying same type of surface sculpture. 6 = × 3000.
Fig. 7. Stub IC349; Prep. CH112; Sample G185x/5; Ref. 349/904; Neg. 2005/88. detail of surface sculpture. × 3000.

Figs. 9–15. *Tanyosphaeridium* spp.
Fig. 9. Stub IC355; Prep. Z229; Sample G197/1/83; Ref. 361/872; Neg. 3027/06. dv.
Fig. 10. Stub IC348; rest of data as for Fig. 7; Ref. 374/742; Neg. 2024/86. dv.
Fig. 11 and 14. Stub IC323; Prep. CH107; Sample Gc98/1; Ref. 237/787; Negs. 2004/39 and 2005/39. ovv, and detail showing apical archaeopyle and accessory sutures in precingular paraplate series.
Fig. 12. Stub IC325; Prep. CH105; Sample Gc83/1; Ref. 267/877; Neg. 2031/42. detail of surface sculpture. × 3000.
Fig. 13. Stub IC333; Prep. Z225; Sample G61/1/79; Ref. 337/705; Neg. 2002/54. specimen lacking paracingular processes.
Fig. 15. Stub IC346; Prep. CH111; Sample G183x/4; Ref. 273/799; Neg. 2027/81. detail of surface sculpture. × 3000.

Plate 30

μm bar: Figs. 4–5, 11–12 = 1 μm; all others = 10 μm

Figs. 1–7. *Cassiculosphaeridia magna* emend.
Fig. 1. Stub IC340; Prep. Z240; Sample Gc76/1; Ref. 247/882; Neg. 2023/64. ?vv, operculum lost. × 400.
Fig. 2. Stub IC341; rest of data as for Fig. 1; Ref. 314/849; Neg. 2016/70. ?dv, operculum lost. × 400.
Fig. 3. Data as for Fig. 2; Ref. 239/849; Neg. 2019/64. complete specimen showing partial preservation of ectophragm. × 400.
Fig. 4. Stub IC337; Prep. Z227; Sample G71/1/79; Ref. 308/742; Neg. 2035/78. cross-section of cyst wall supporting ectophragm. × 3000.
Fig. 5. Stub IC332; Prep. Z225; Sample G61/1/79; Ref. 372/771; Neg. 2020/51. cross-section of cyst wall showing granular sporopollenin. × 7000.
Fig. 6. Stub IC325; Prep. CH105; Sample Gc83/1; Ref. 327/742; Neg. 2015/41. detail of autophragm surface, ectophragm almost completely removed by oxidation. × 1600.
Fig. 7. Stub IC33; rest of data as for Fig. 5; Ref. 347/884; Neg. 2013/52b. isolated operculum. × 800.

Figs. 8–12. *Cassiculosphaeridia* spp.
Fig. 8. Stub IC310; Prep. CH103; Sample G100/11/83; Ref. 207/734; Neg. 2015/16. vv, showing sulcal notch. × 800.
Fig. 9. Data as for Fig. 6; Ref. 297/729; Neg. 2039/41. orlv, operculum lost. × 800.
Fig. 10. Data as for Fig. 6; Ref. 257/777; Neg. 2013/42. av, showing archaeopyle, paraplate ai to left. × 1600.
Fig. 11. Stub IC330; Prep. Z224; Sample G56/1/79; Ref. 352/836; Neg. 2029/46. detail of ectophragm. × 7000.
Fig. 12. Stub GD117; Prep. W407; Sample ALF IIk; Ref. 344/876; Neg. 3007/30. detail of ectophragmal covering supported by non-tabular septa. × 3000.

Figs. 13–14. *Angustidinium* sp.
Fig. 13. Stub IC382; Prep. CH036; Sample ICH008; Ref. 328/726; Neg. 3016/19b. vv. × 1600.
Fig. 14. Data as for Fig. 7; Ref. 304/783; Neg. 2014/54. vv, showing differential dissolution of paraplate boundaries. × 1600.

Plate 31

μm bar = 10 μm on all Figs., except Fig. 10 = 1 μm

Figs. 1 and 2. *Nexosispinum vetusculum.*
Fig. 1. Stub IC337; Prep. Z227; Sample G71/1/79; Ref. 268/863; Neg. 2025/77. dv, showing 2P archaeopyle and traces of paratabulation. × 800.

Fig. 2. Stub IC381; Prep. CH035; Sample ICH007; Ref. 269/894; Neg. 3006/19b. detail showing operculum splitting into two separate pieces. × 1600.

Fig. 3. *Odontochitina operculata.* Stub GD180; Prep. F137; Sample F137; Ref. 349/841; Neg. 3007/60. dv, specimen shows claustra in horns. × 534.

Fig. 4. *Trabeculidinium quinquetrum.* Stub IC349; Prep. CH112; Sample G185 x/5; Ref. 302/698; Neg. 2020/74. view uncertain. × 800.

Figs. 5 and 6. *Sirmiodinium grossi.*
Fig. 5 Stub IC355; Prep. Z229; Sample G197/1/83; Ref. 326/875; Neg. 3017/06. dv, showing (tA)aP3a archaeopyle. × 800.
Fig. 6. Stub IC334; Prep. Z226; Sample G67/1/79; Ref. 325/844; Neg. 2033/57. vv, claustra in paracingulum visible. × 800.

Figs. 7, 9, 10. *Cerbia tabulata.*
Fig. 7. Stub GD249; Prep. X416; Sample HUN 145/0; Ref. 749/389; Neg. 3001/60. vv. × 600.
Fig. 9. Stub IC321; Prep. CH109; Sample G114; Ref. 362/728; Neg. 2037/36. dv. × 800.
Fig. 10. Stub GD117; Prep. W407; Sample ALF IIk; Ref. 240/868; Neg. 3001/30. detail of microreticulate sculpture. × 3000.

Fig. 8. *Pterodinium premnos.* Stub IC350; Prep. CH113; Sample G187 x/5; Ref. 264/711; Neg. 2006/76. dv, detail showing reduced nature of archaeopyle and the characterisic intratabular projections. × 1600.

Fig. 11. *Ellipsodinium reticulatum.* Stub IC361; Prep. CH115; Sample G197/4/83; Ref. 376/840; Neg. 3026/00. dv, operculum displaced inside the cyst. × 1600.

The English title is to be followed by an English "Abstract". Up to 5 key words should appear at the end of the "Abstract". These should facilitate correct classification in subject areas for data processing (e.g. key words = Sporomorphae, Thallophyta, Bryophyta, Gymnospermae, Angiospermae; Ecology, Plant Geography, Phylogeny; Devonian; North America). This should be followed by a Table of Contents; its sections and subtitles must correspond to those in the main text. The Table of Contents should be followed by an Introduction, including a general description of the problems, references to earlier work done by other authors, explanation of special features and abbreviations in the text, the objective methodology, and techniques applied in the particular investigation, acknowledgements or recognition of research assistance.

5. Description of species: observe the International Rules of Botanical Nomenclature when presenting new species. In open nomenclature abbreviations cf., aff., n. sp. n. gen. et sp. are to be used without further additions. Analogously: subsp., subgen.
In the synonymy list, species names and literature references should be separated by a dash in cases where the author of the bibliographical passage is not the original author of the species name. Examples:

1855 *Populus balsamoides* GOEPP., Tertiäre Flora von Schoßnitz in Schlesien, S. 23, Taf. 15, Fig. 5, 7.
1856 *Populus glandulifera* — HEER, Flora tertiaria Helvetia II, S. 17, Taf. 5, Fig. 5—11, Taf. 68, Fig. 7.

In referring to types and typoids indicate location of collection (abbreviated) and catalogue number.

6. Illustrations: Illustrations in the text are to be labelled as "Text-fig." and those on plates as "Fig.". For plate-figures, the adding of the plate number is necessary. Submit black Indian ink originals of drawings (no hachures with coloured or lead pencils). If millimeter graph paper is used, avoid red grid lines! Keep in mind that any lettering might be reduced for reproduction. Photographs must be sharp with clear contours and lighting of the object from the left front. If possible, they should be printed on high-gloss white paper. Scales of figures are to be included and specified in the explanatory text.

Photo plates should be mounted on stiff cardboard with plain white or black background. Photoreproductions of whole plates cannot be accepted. The individual figures on a plate should correspond with one another in terms of dark/light contrast so that the whole plate appears as a unit. Indicate the desired degree of reduction as a fraction on the reverse side of each illustration.

If an inscription cannot be clearly and neatly placed on a plate, please use a pencil to put it in; the publishers will then have it drawn in.

The area for plates is 17.5 × 23 cm and should not be exceeded.

Only a limited number of photo plates, maximum 15 even for large contributions, can be accepted for each paper without printing charges. The appropriate number of plates will be determined by the editor, whose decision will be final.

Figure legends and plate explanations are to be submitted together on separate manuscript sheets. These legends and explanations should be both in German and English, if the article is not in English.

7. Reference list: When citing journal titles, we request the author to use the German standards for journal abbreviations DIN 1502. For example:

EISENACK, A. (1961): Einige Erörterungen über fossile Dinoflagellaten nebst Übersicht über die zur Zeit bekannten Gattungen. — N. Jb. Geol. Paläont., Abh., 112: 281—324.

SCHINDEWOLF, O. H. (1950): Grundfragen der Paläontologie. — 1. Aufl. (E. Schweizerbart'sche Verlagsbuchhandlung), Stuttgart.

Please use broken underlining to mark all persons' names and double underlining for volume numbers.

All publications referred to in the paper must be included in the reference list.

8. Proofreading: The authors (in case of co-author papers only the first-named author) will receive:

a) 2 sets of galley proofs
b) 2 sets of page proofs prior to final printing.

We request immediate return to the publishers of one set of the carefully corrected galley proofs and, subsequently, of the page proofs. If the page proofs are not returned in time, the paper will be published exactly as it appears in the uncorrected page proofs.

Author's corrections in proofs must not exceed 5 % of the typesetting costs; above that, the authors shall be charged for the costs.

© 1990 by E. Schweizerbart'sche Verlagsbuchhandlung (Nägele u. Obermiller), Johannesstraße 3A, D-7000 Stuttgart 1, F.R.G.

All rights reserved.

For users in USA: According to the code at the bottom of the first page of an article copies may be made if the copier pays the

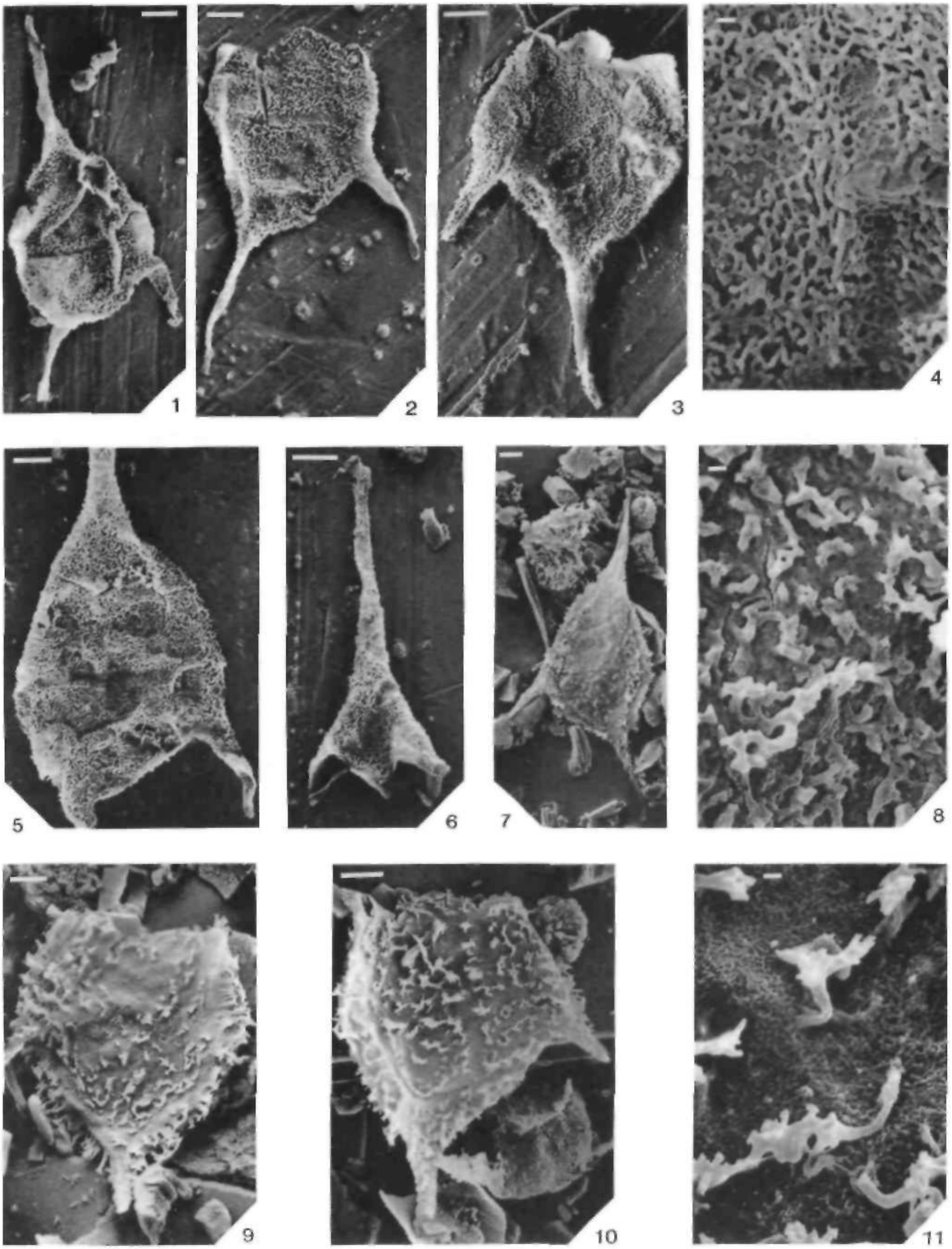
1
2
3
4
5
6
7
8
9
10
11

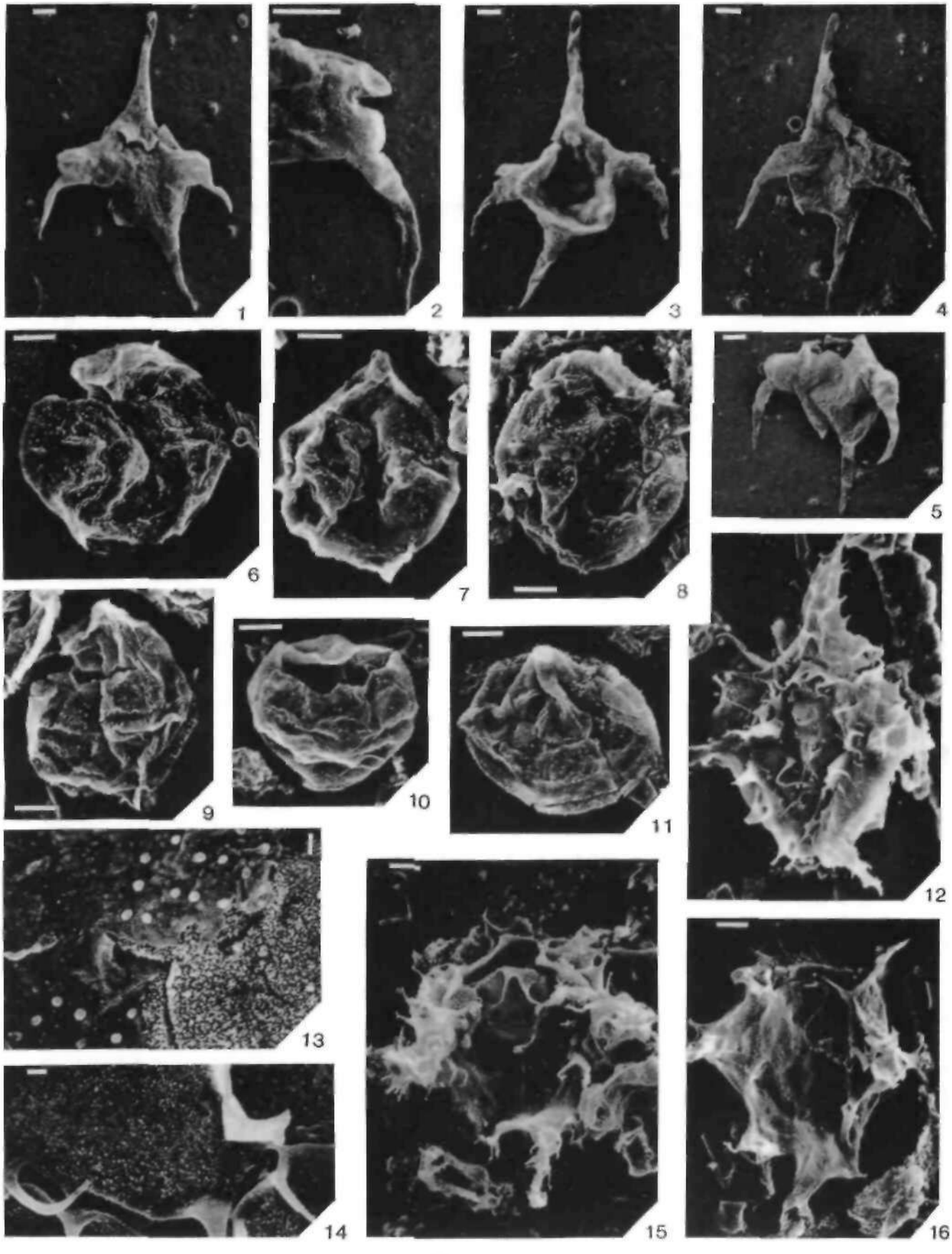
1
2
3
4
5
6
7
8
9
10
11
12
13
14
15
16

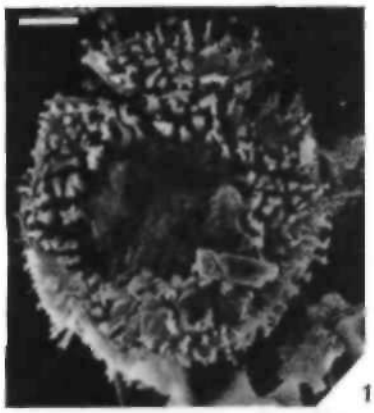
1

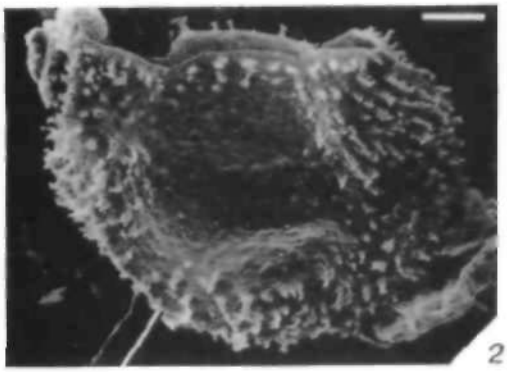
2

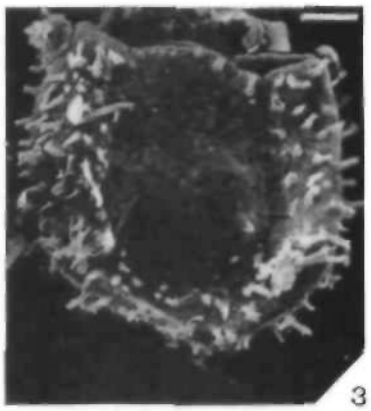
3

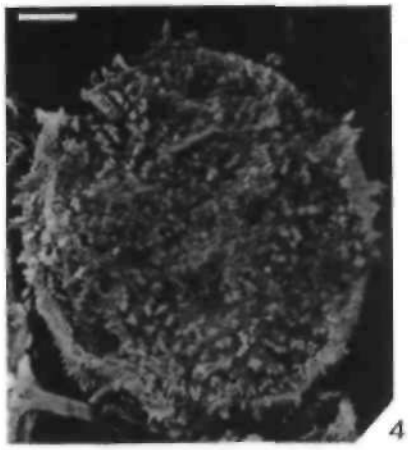
4

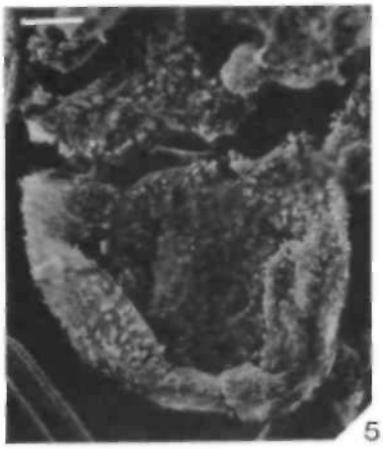
5

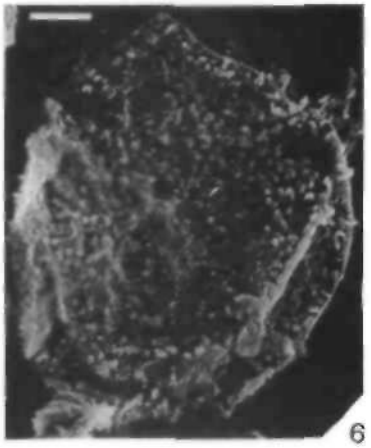
6


7

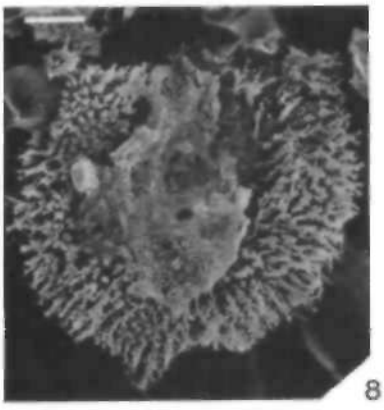
8

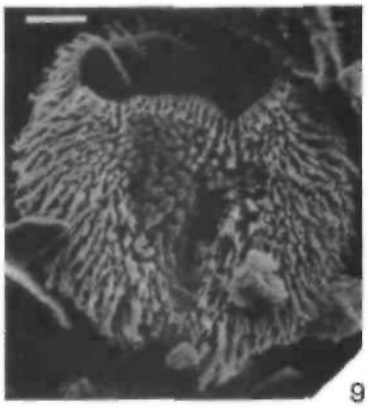
9

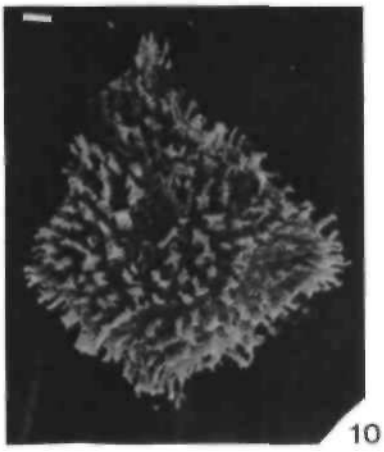
10

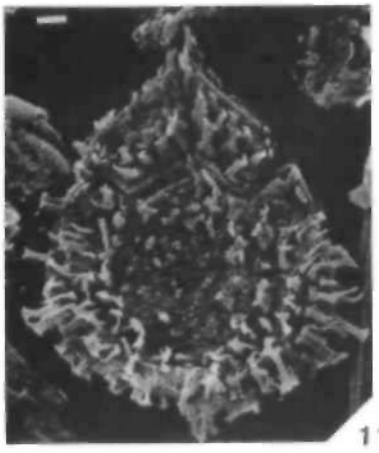
11

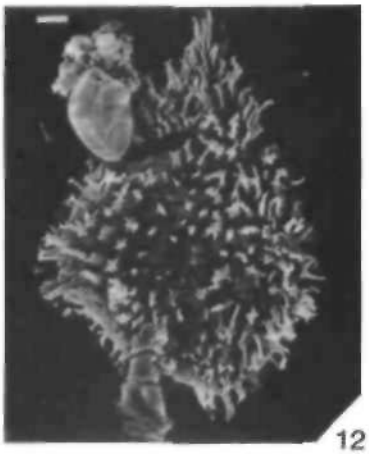
12

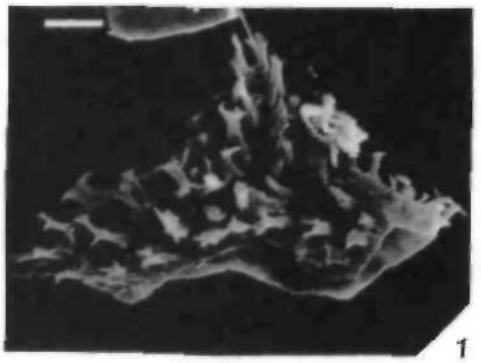
1

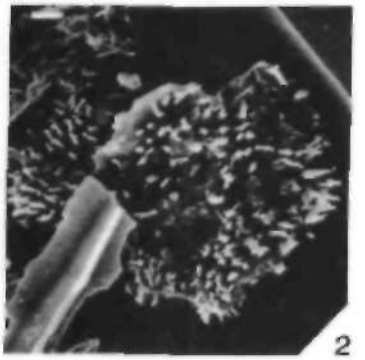
2

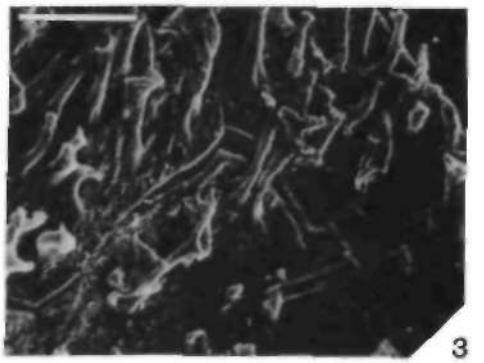
3

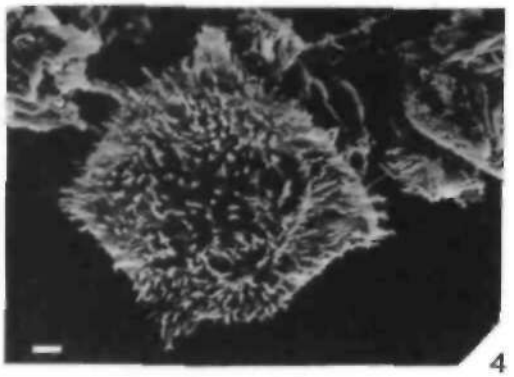
4

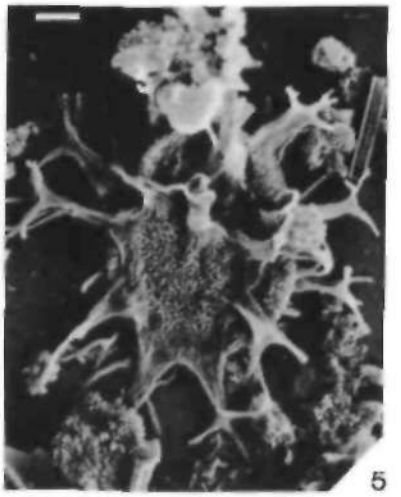
5

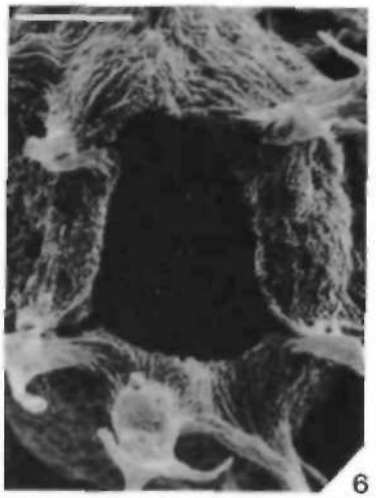
6

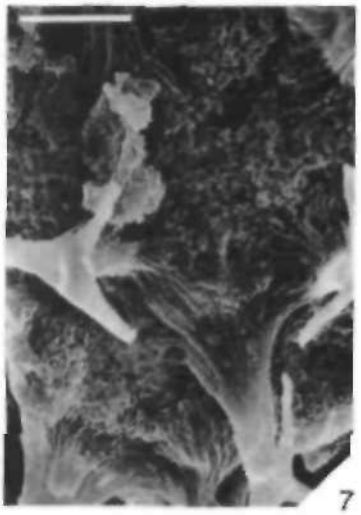
7

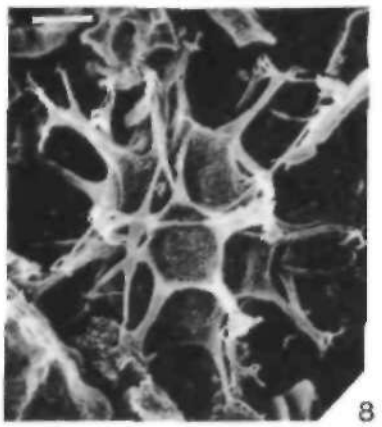
8

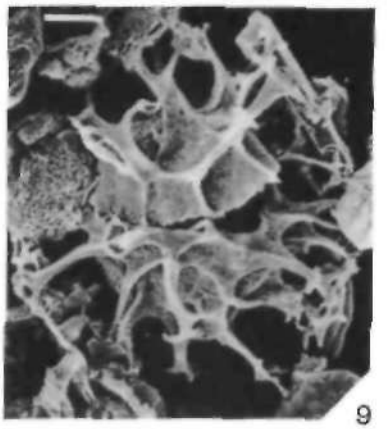
9

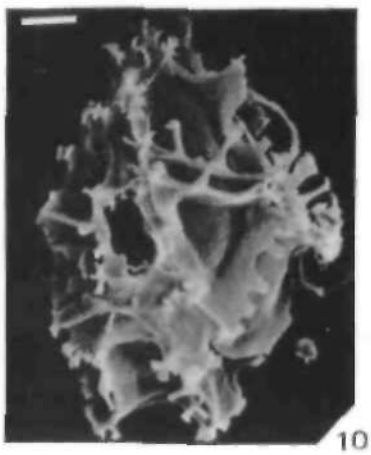
10

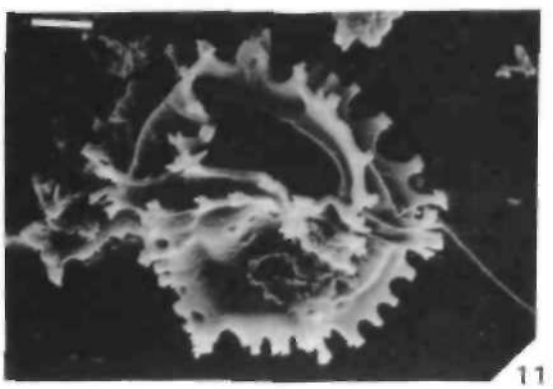
11

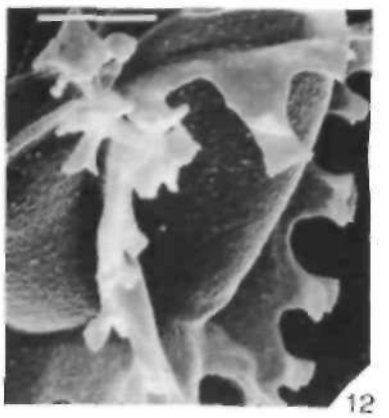
12

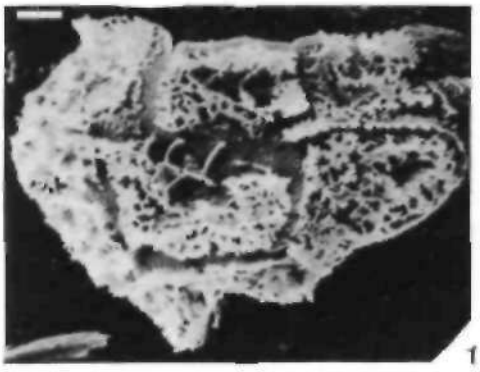
1

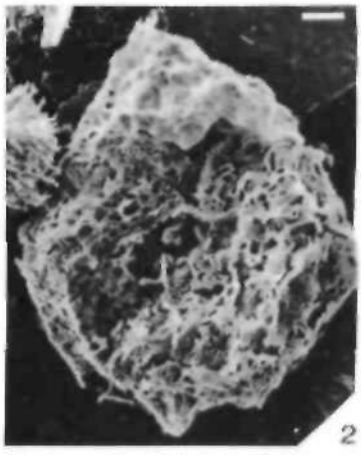
2

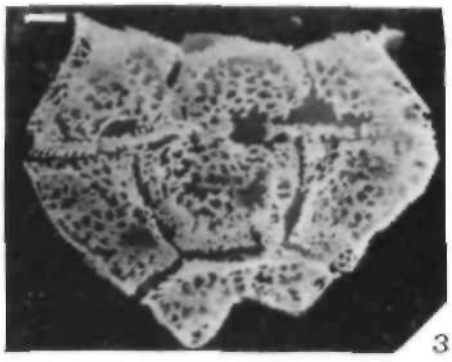
3

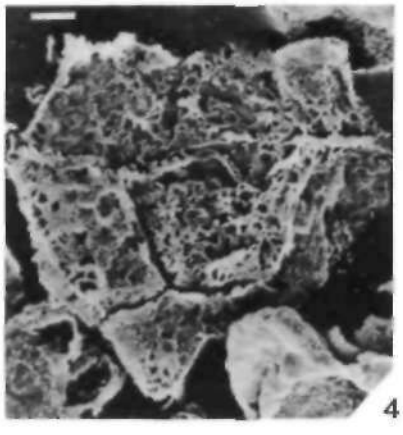
4

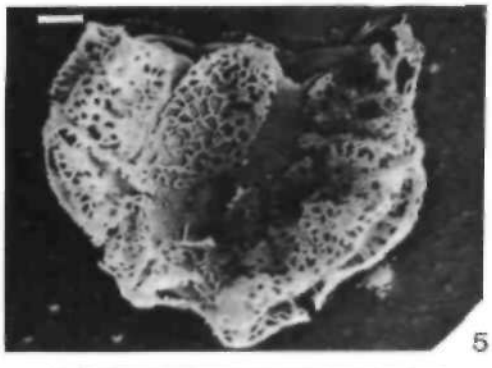
5


6

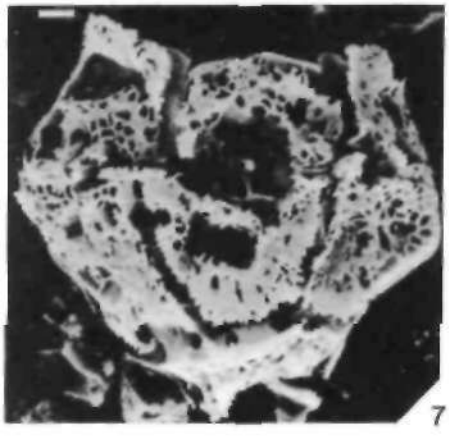
7

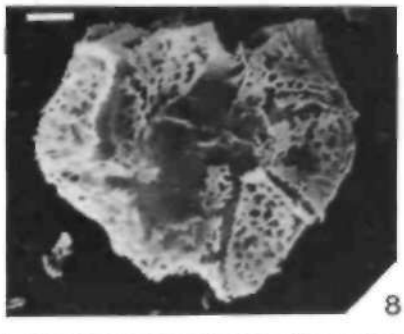
8

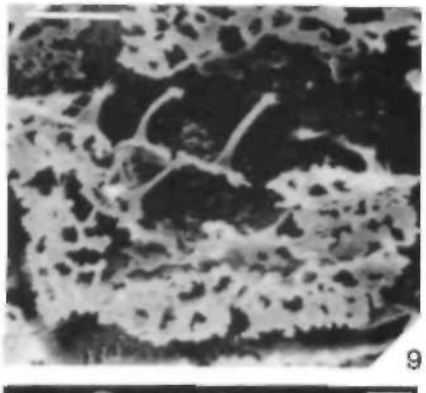
9

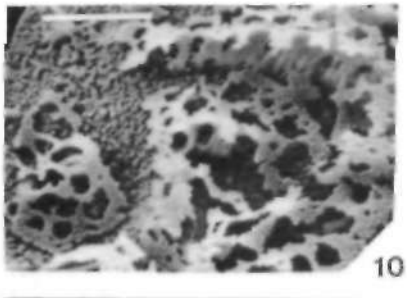
10

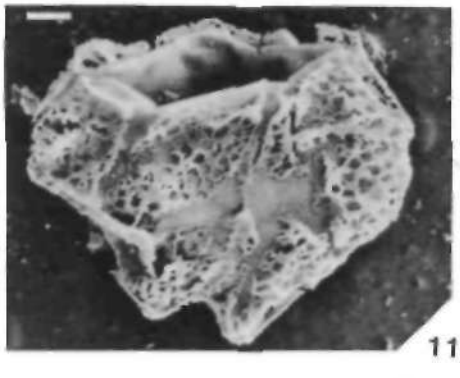
11

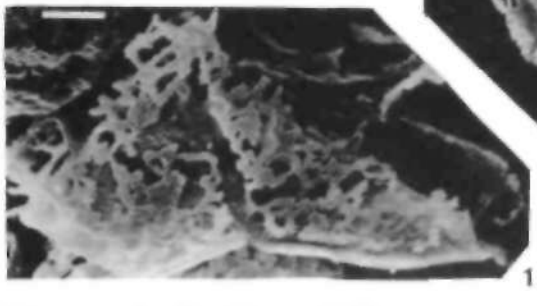
12

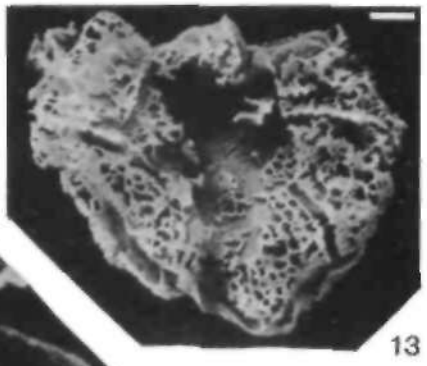
13

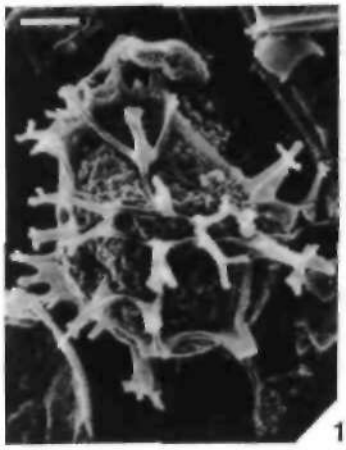
1

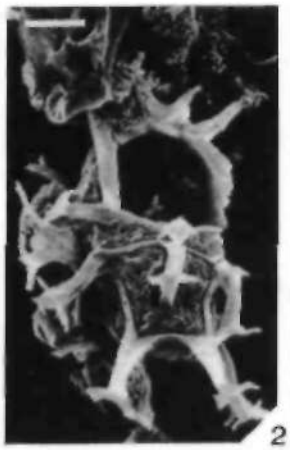
2

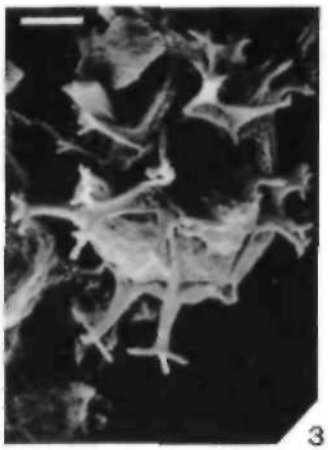
3


4

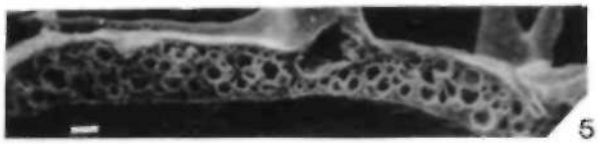
5


6

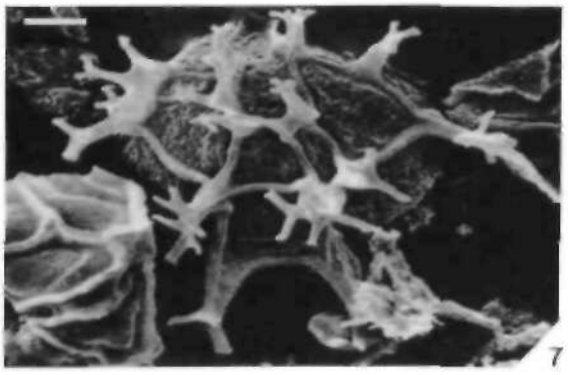
7

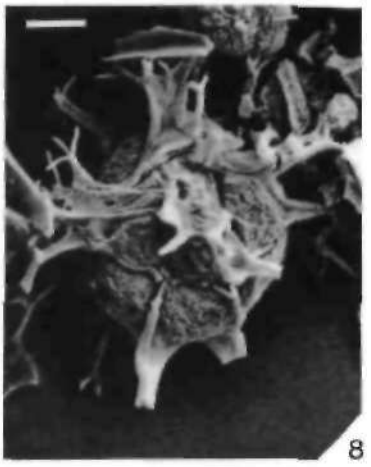
8

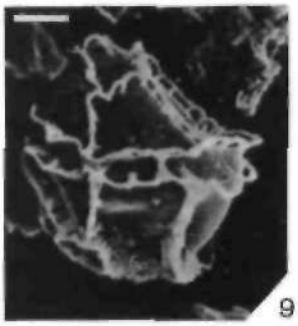
9

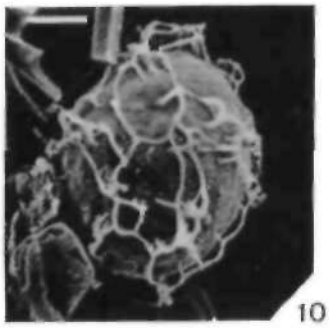
10

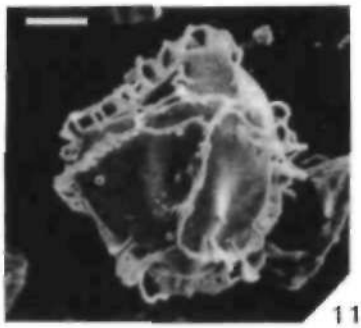
11


12

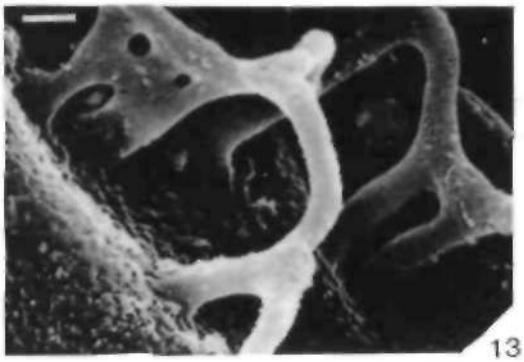
13


14

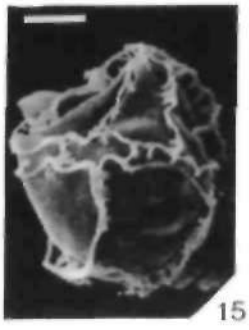
15


16

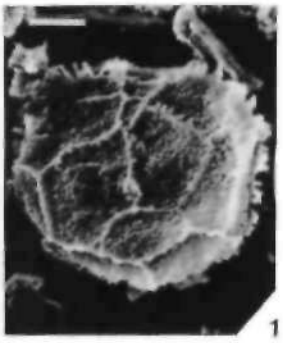
1

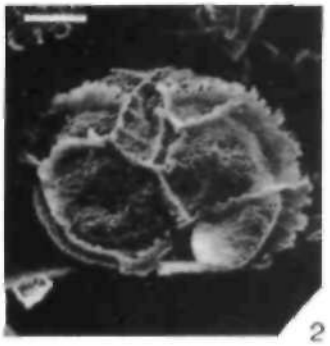
2


3


4

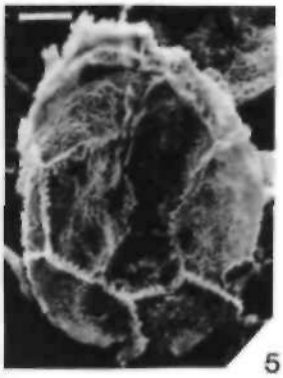
5

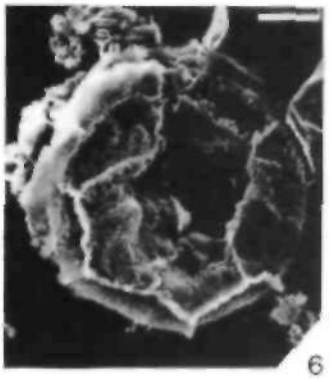
6

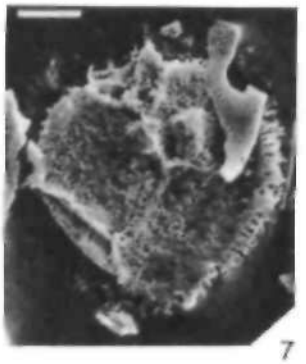
7

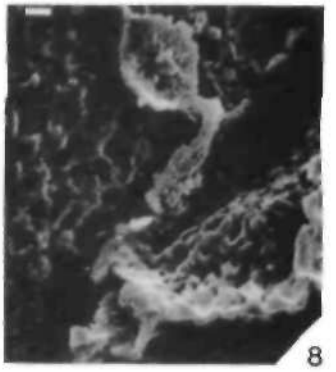
8

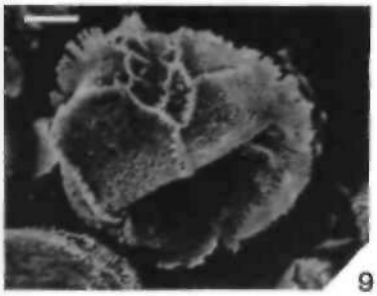
9

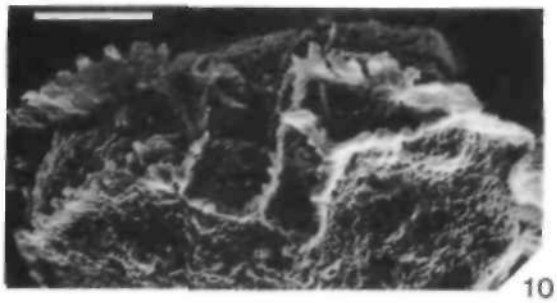
10


11

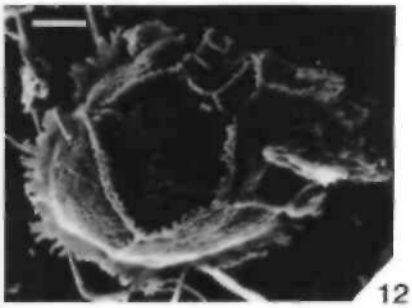
12

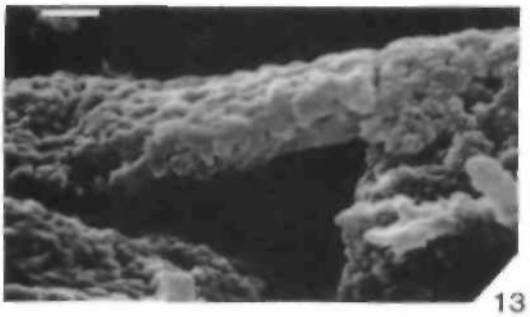
13

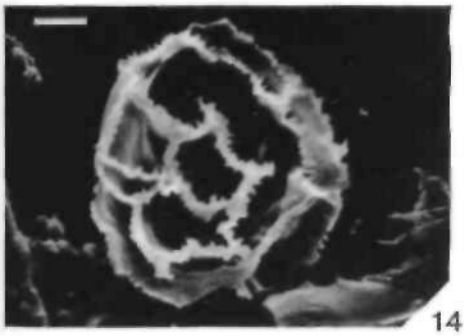
14

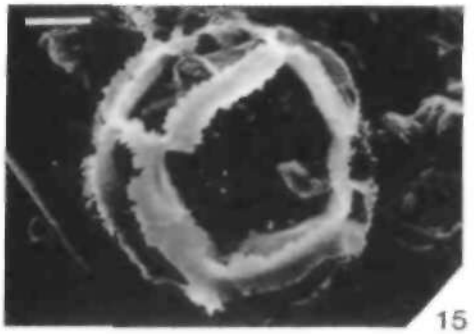
15

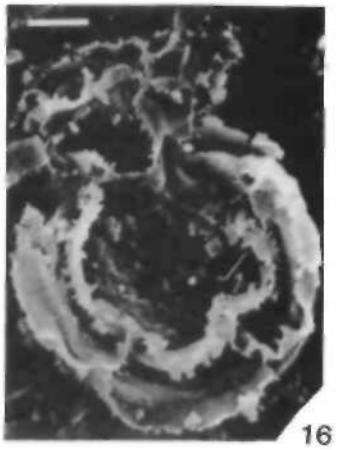
16

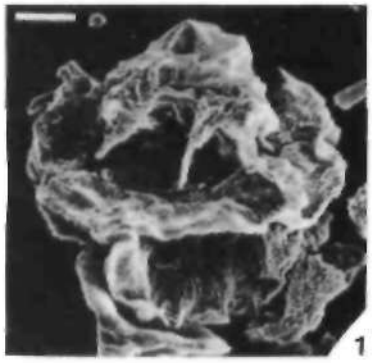
1

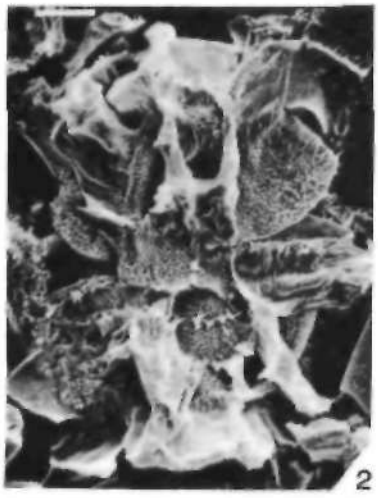
2

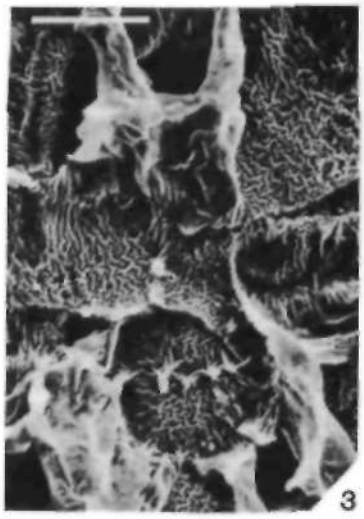
3

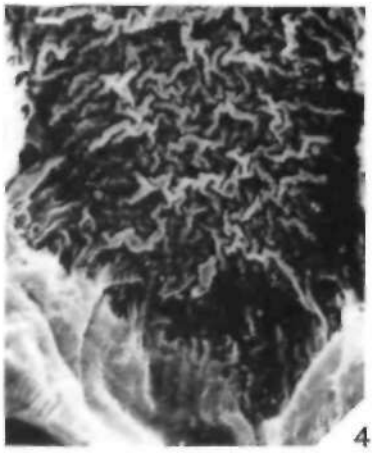
4

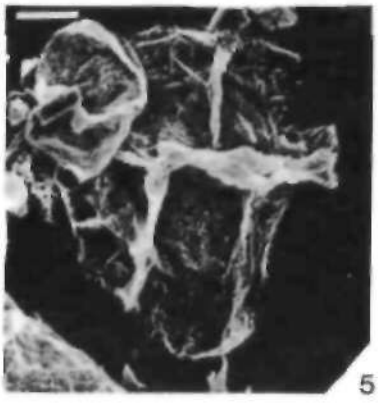
5

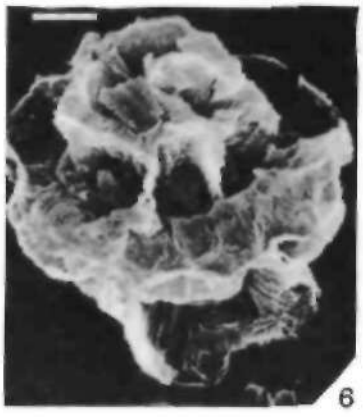
6

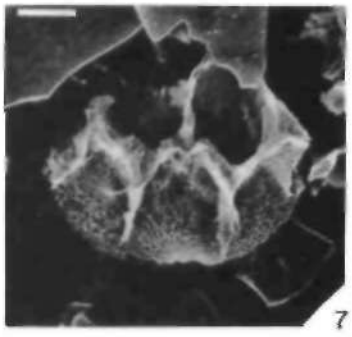
7

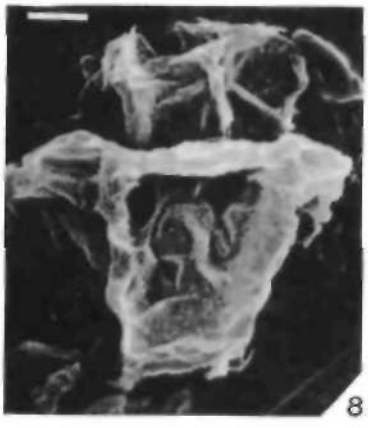
8

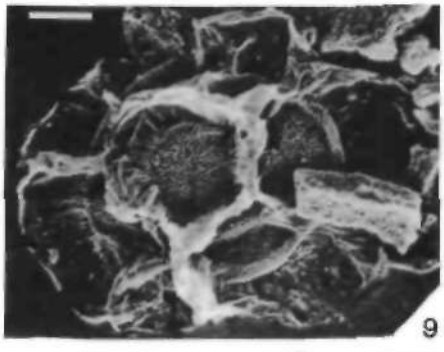
9

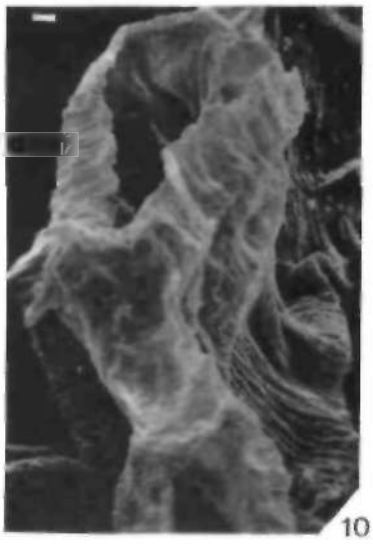
10

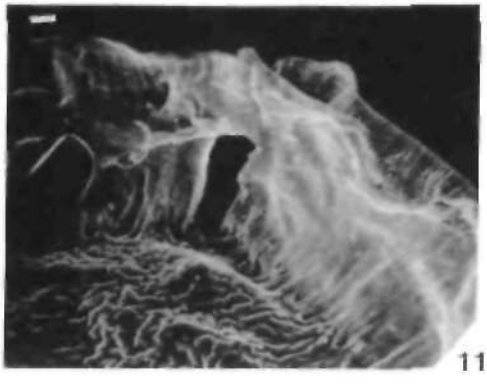
11

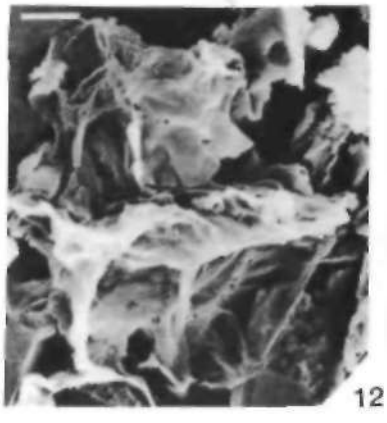
12


1


2


3


4


5

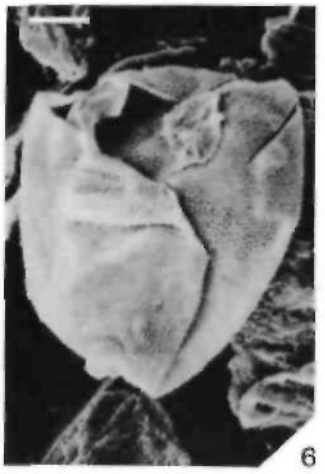
6


7


8

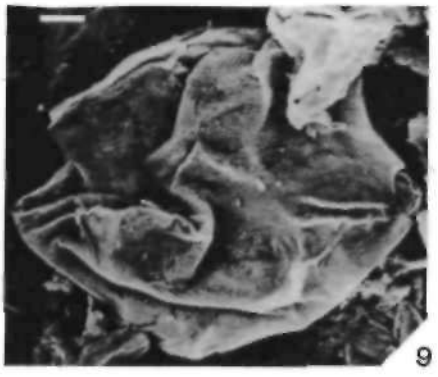
9

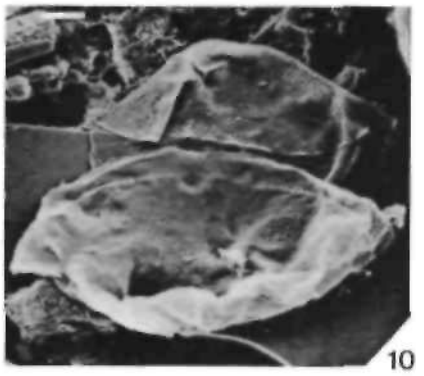
10

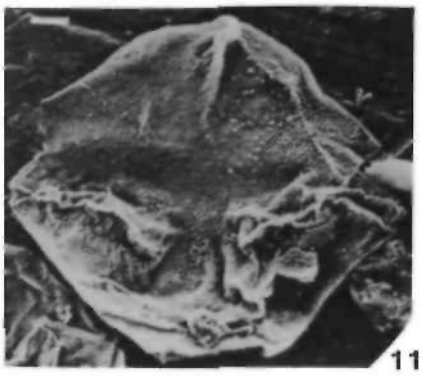
11

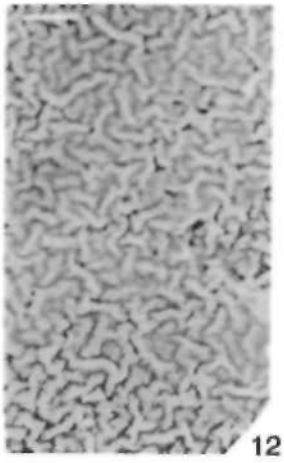
12

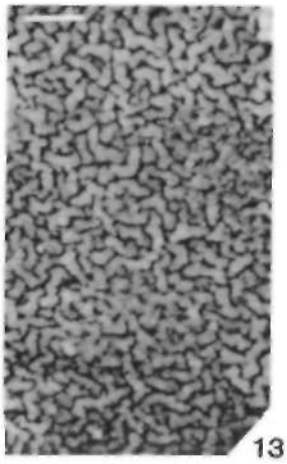
13

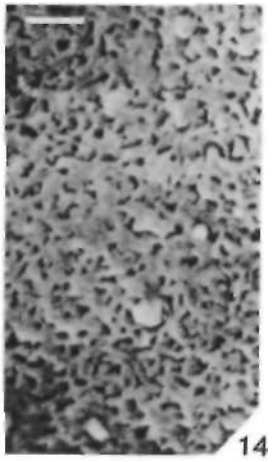
14


1


2


3


4

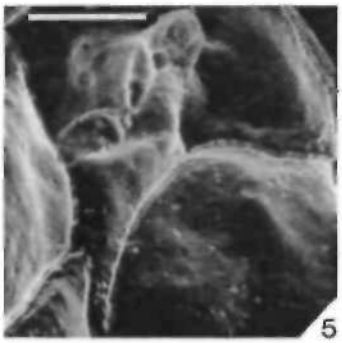
5

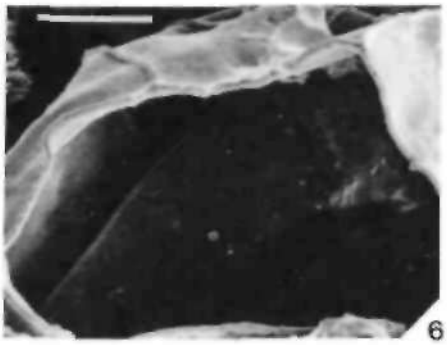
6

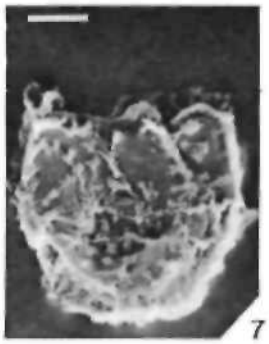
7


8

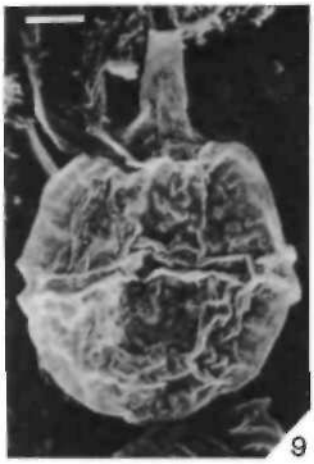
9

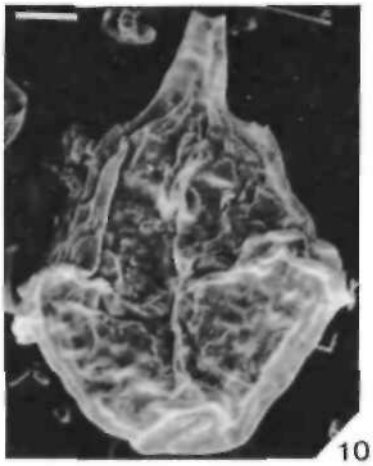
10

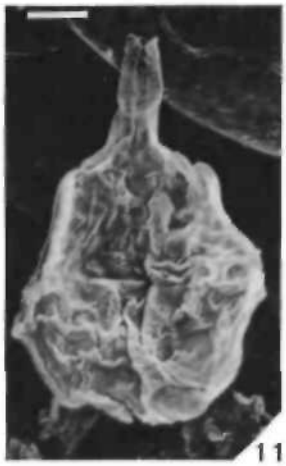
11


12

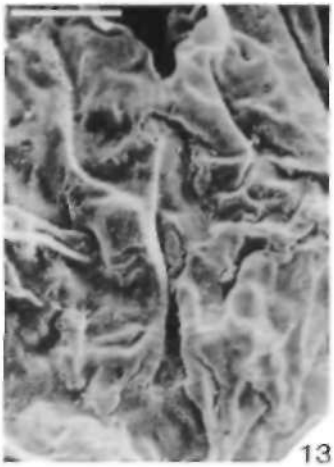
13


14


15

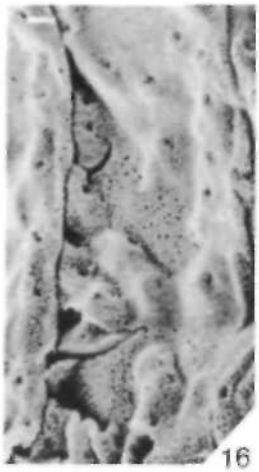
16

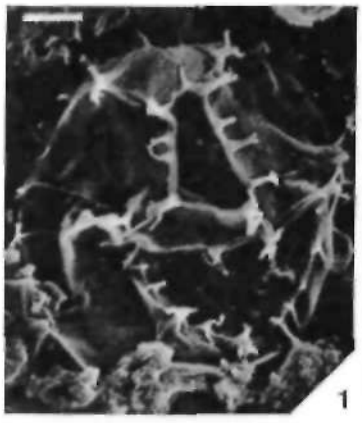
1

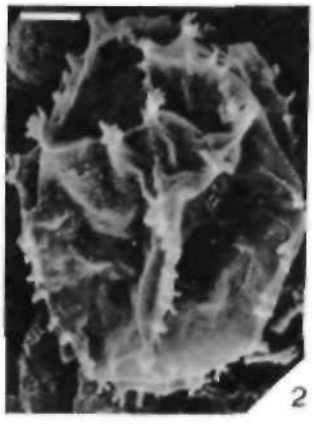
2

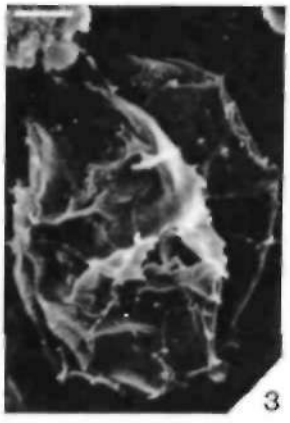
3

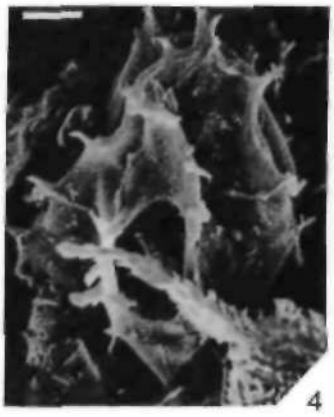
4

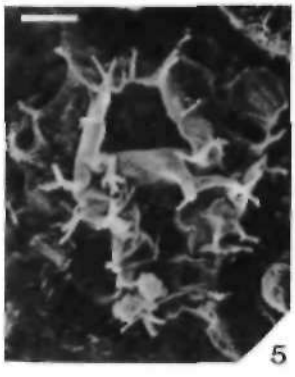
5

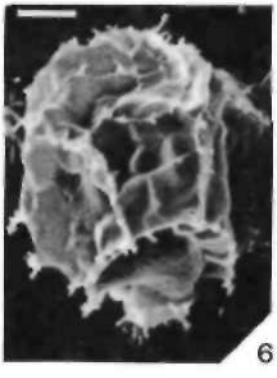
6

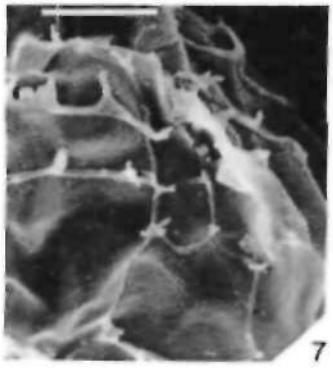
7

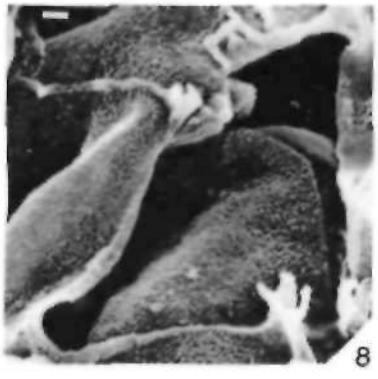
8

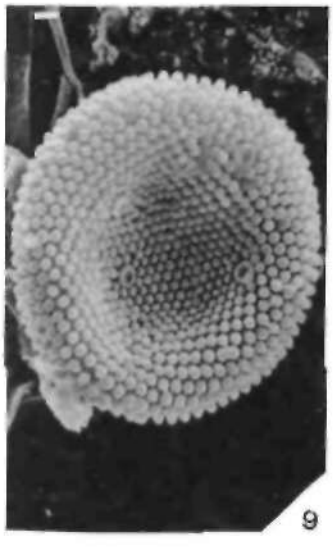
9


10

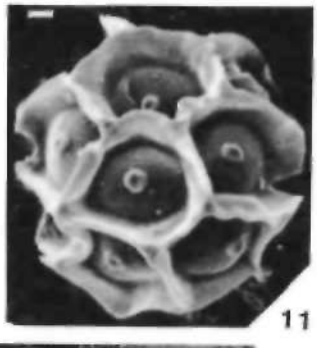
11

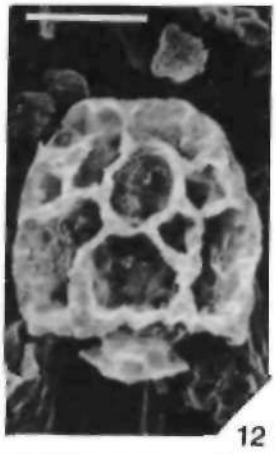
12

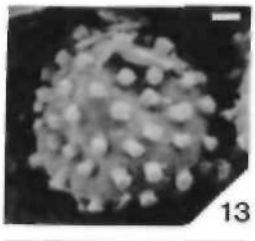
13

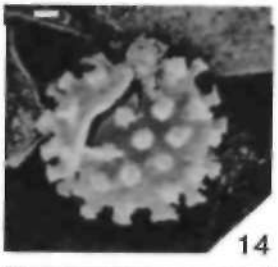
14

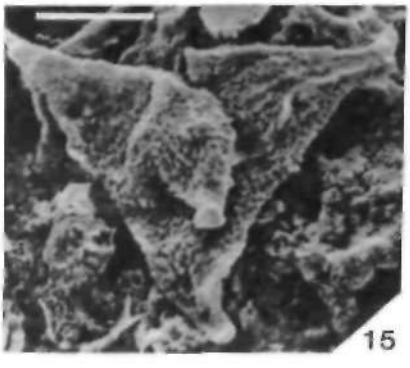
15

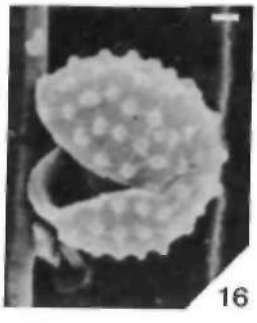
16


17


18

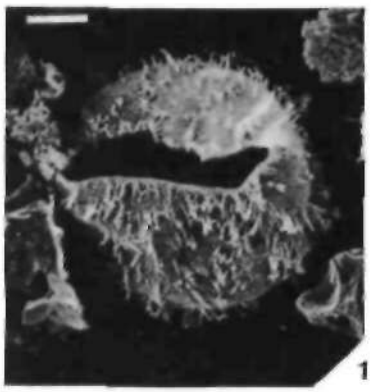
1

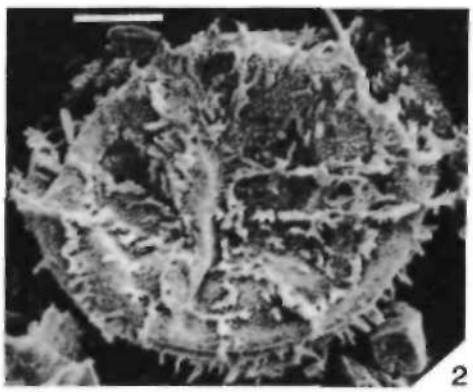
2

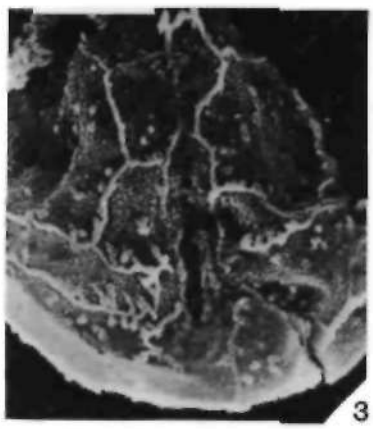
3

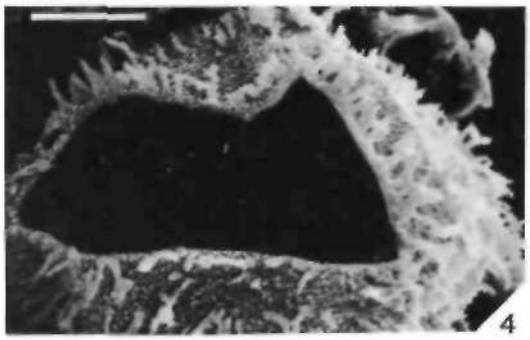
4

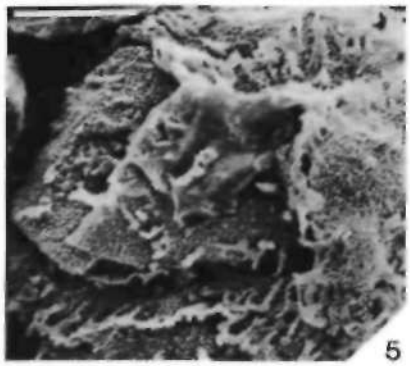
5


6

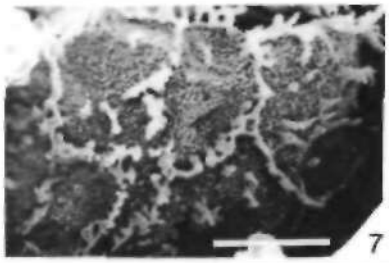
7


8

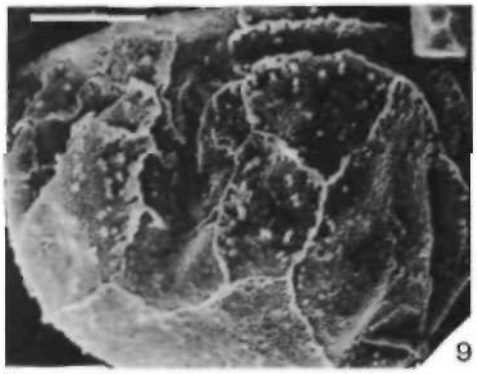
9

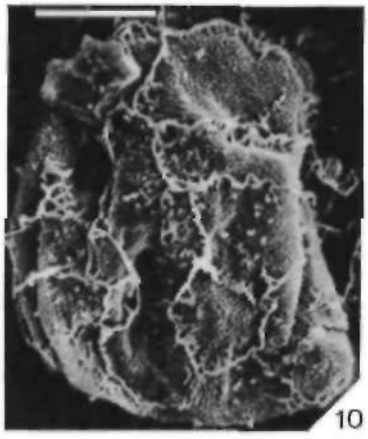
10

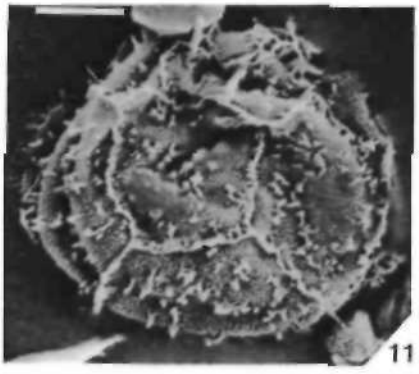
11

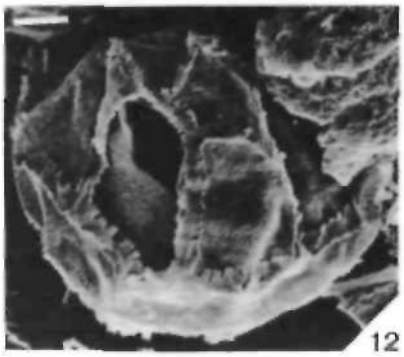
12

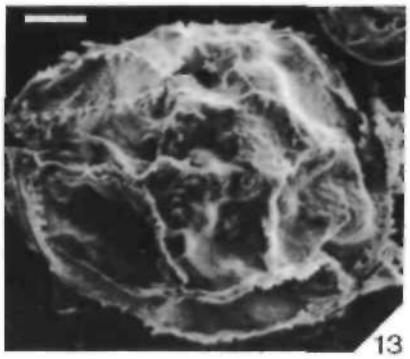
13

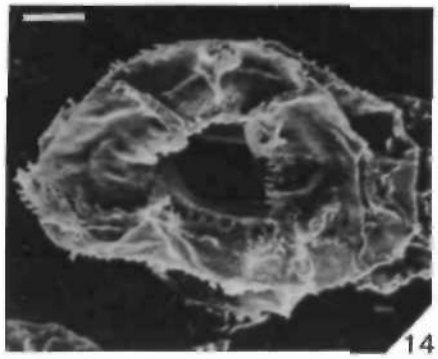
14

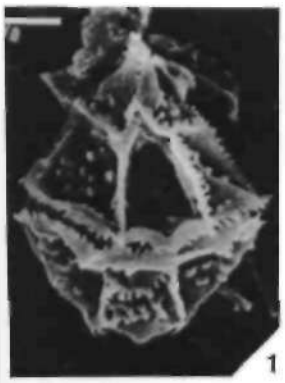
1


2


3

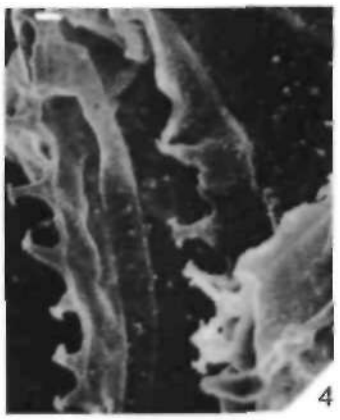
4

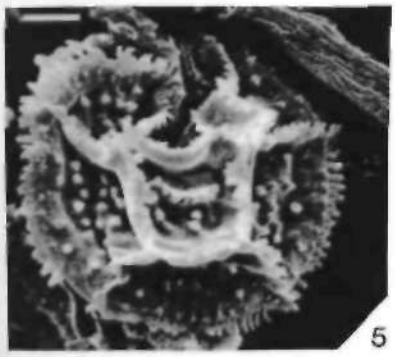
5

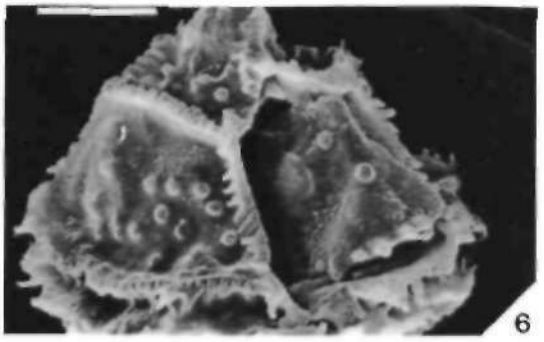
6

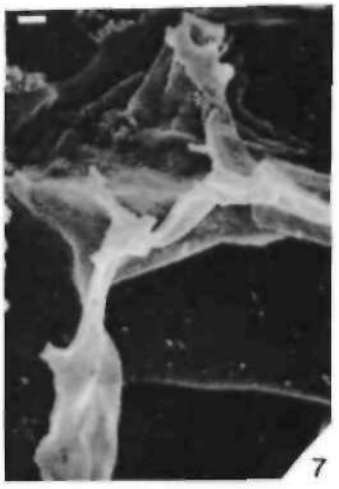
7

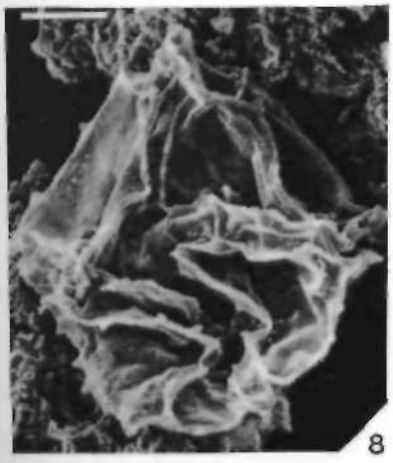
8

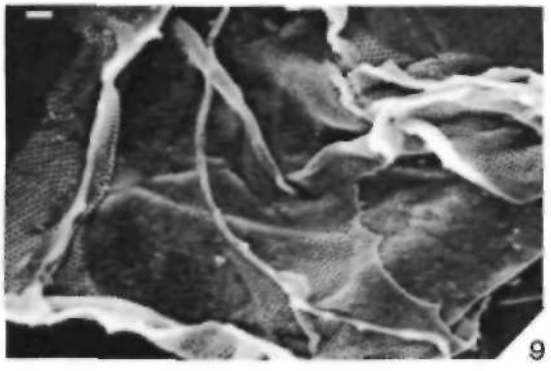
9

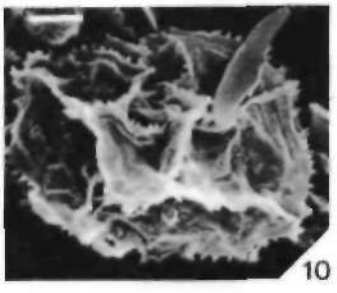
10


11

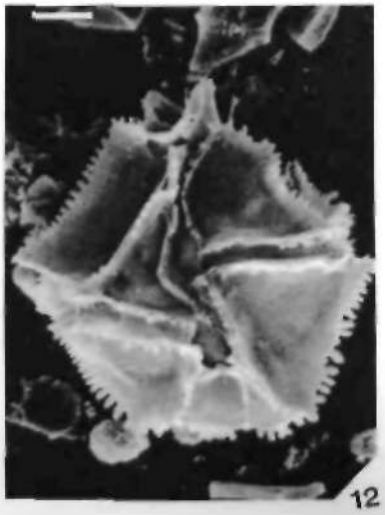
12


13

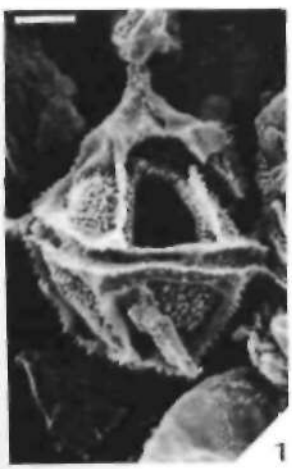
1

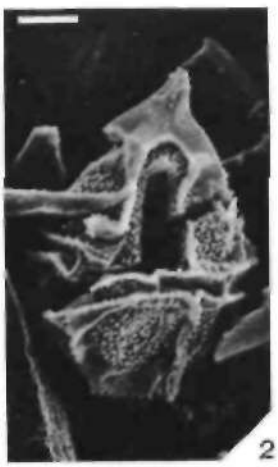
2

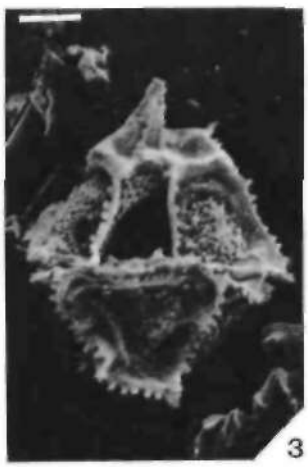
3


4

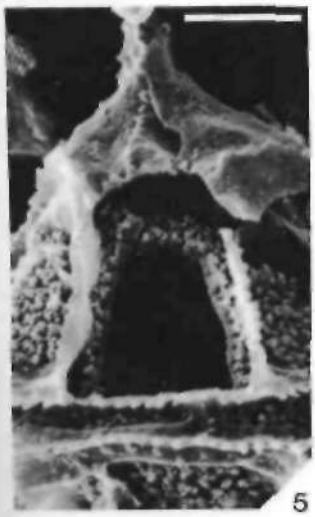
5

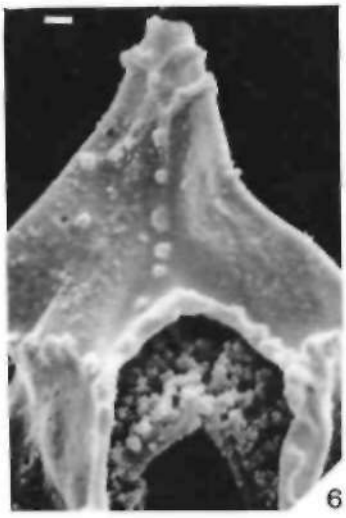
6

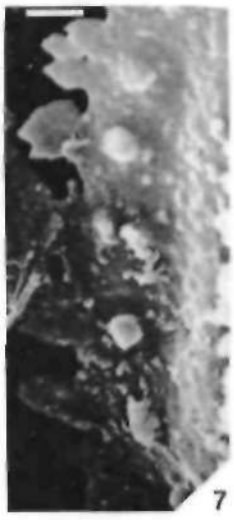
7

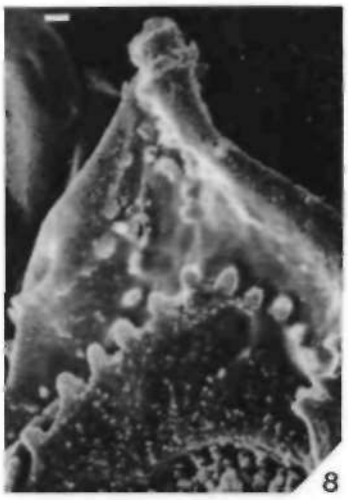
8

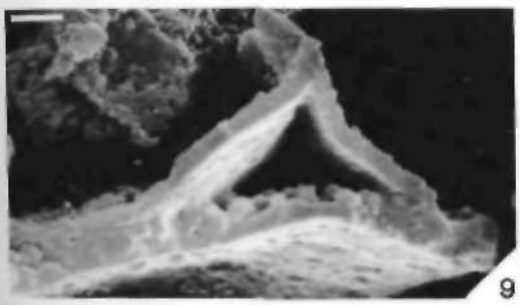
9

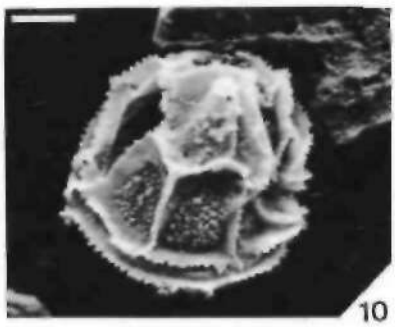
10

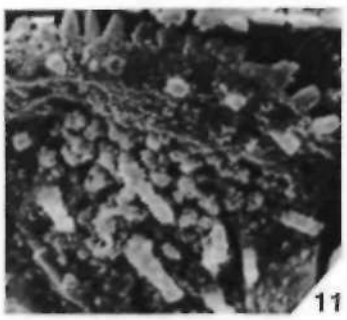
11


12

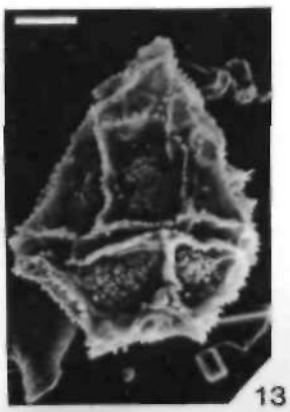
13

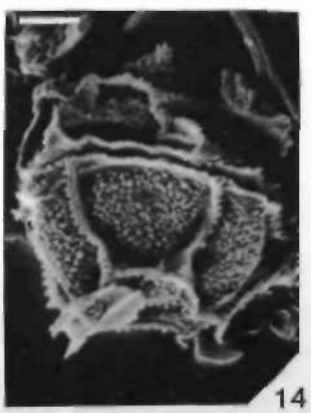
14

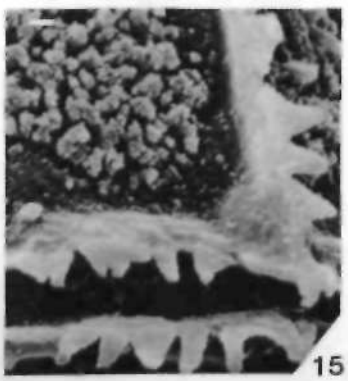
15


1

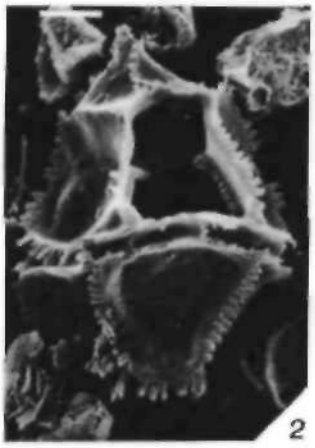
2

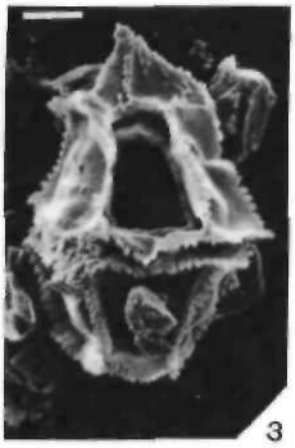
3

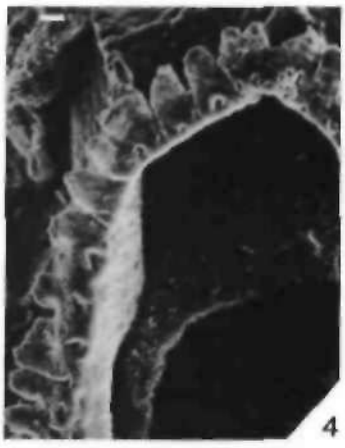
4

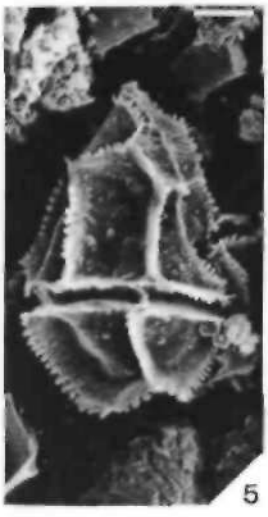
5

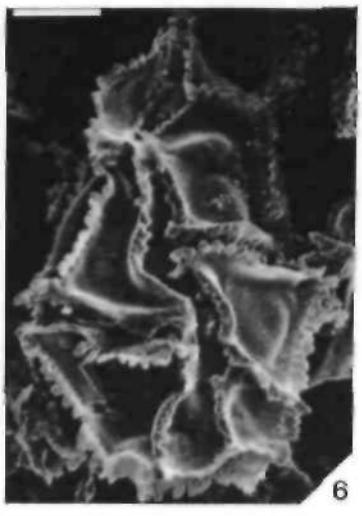
6


7

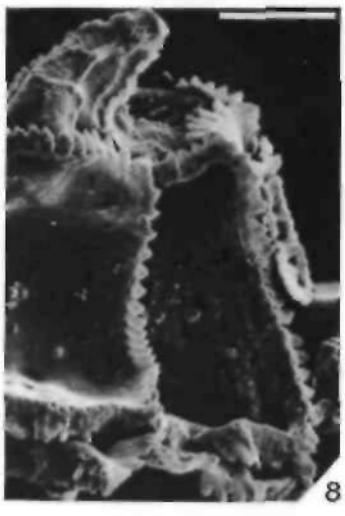
8

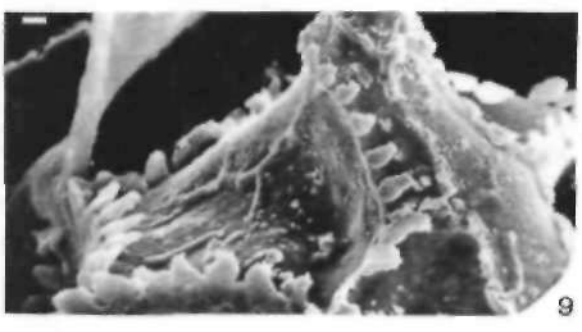
9

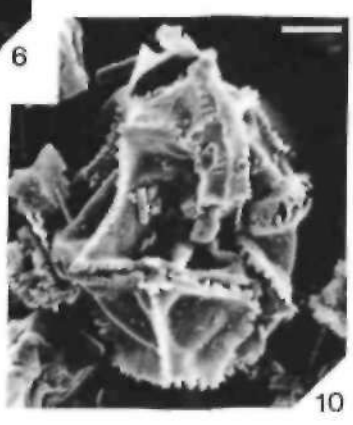
10

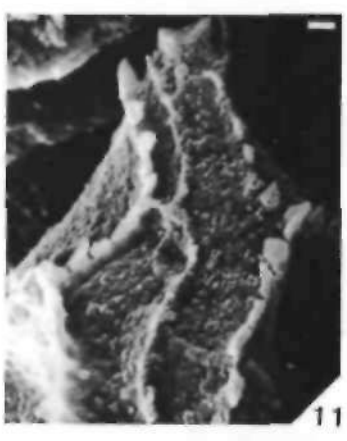
11

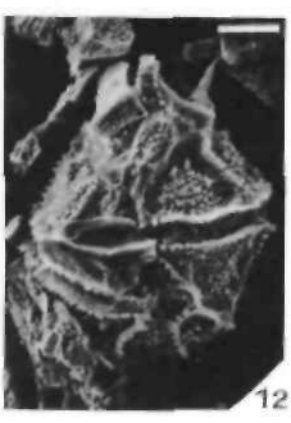
12

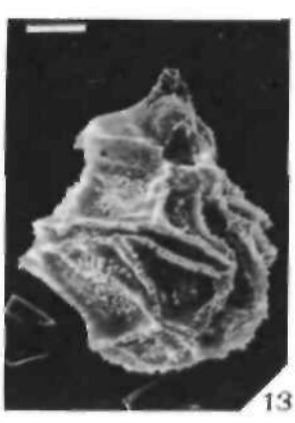
13

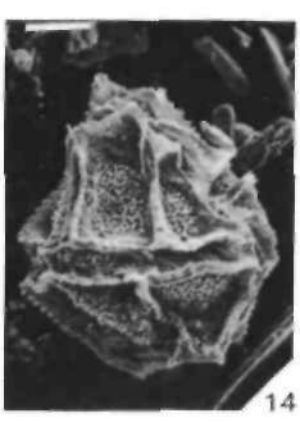
14

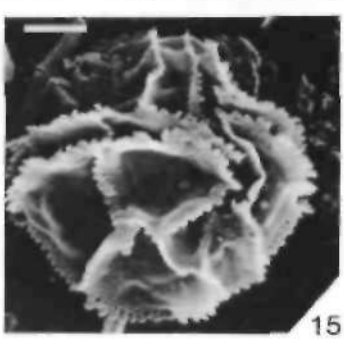
15

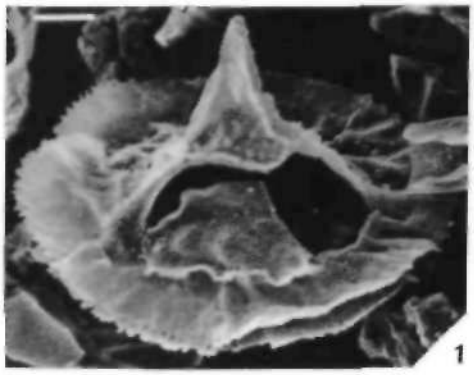
1

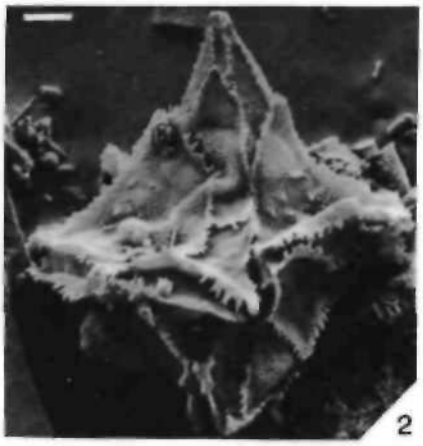
2

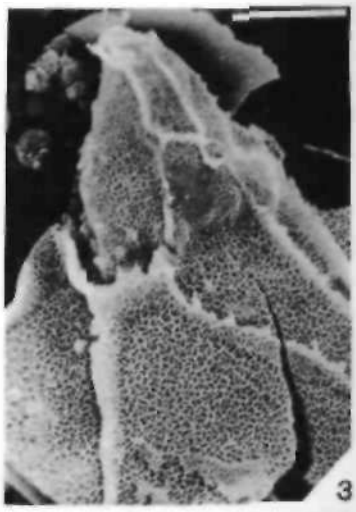
3

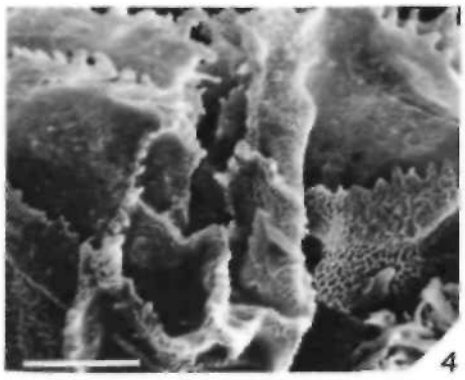
4

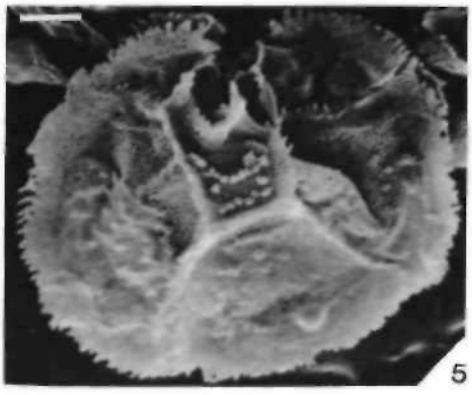
5

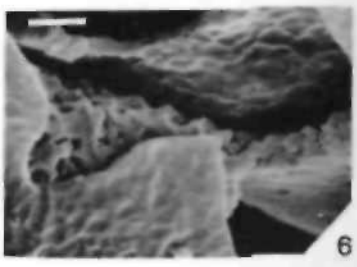
6

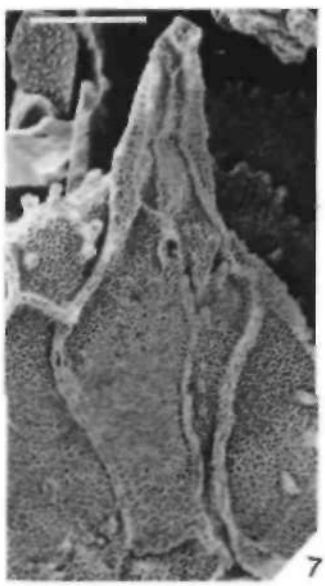
7


8

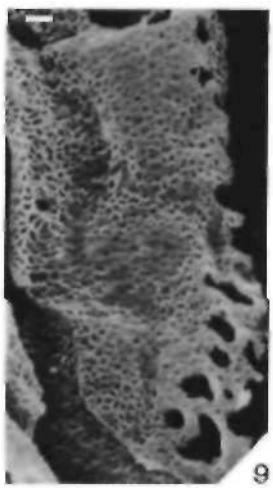
9

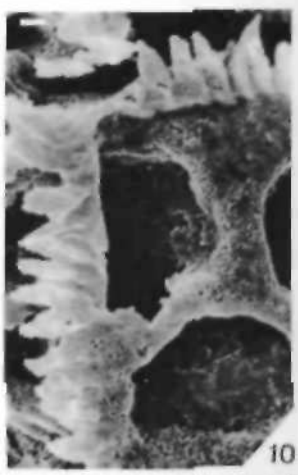
10


11

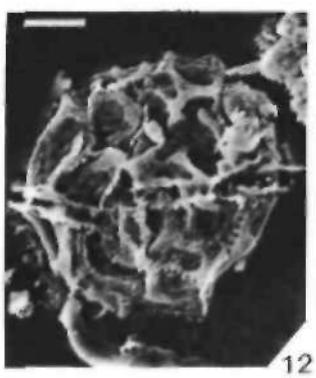
12

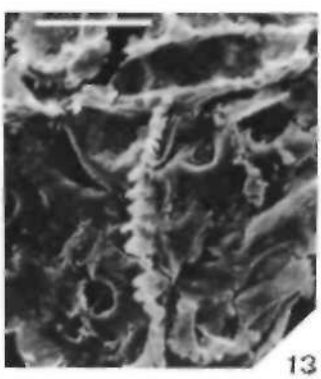
13

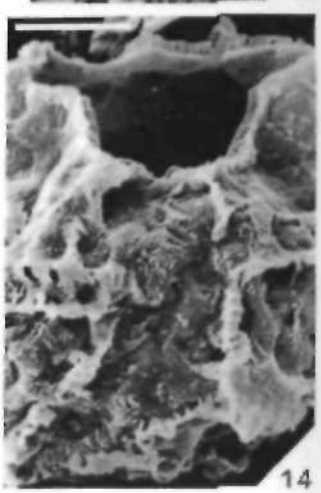
14

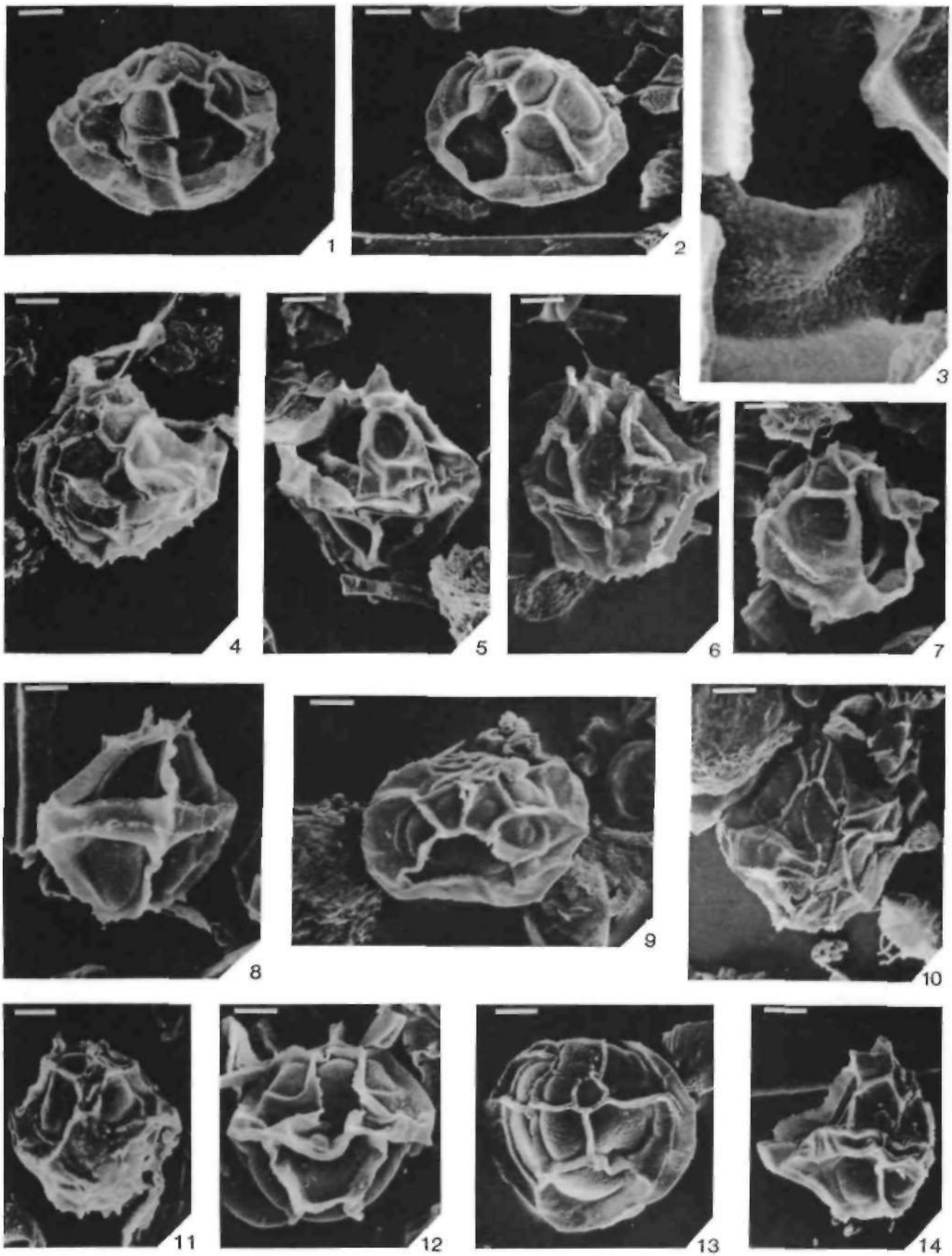

Jan C. Harding: Ankyrocyst calibration.

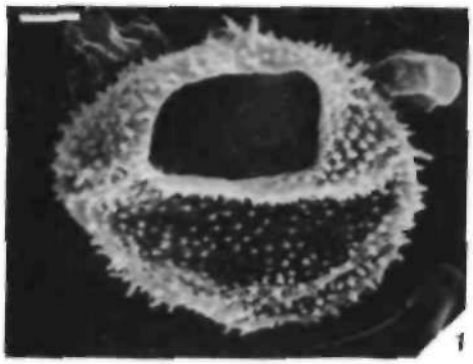
1

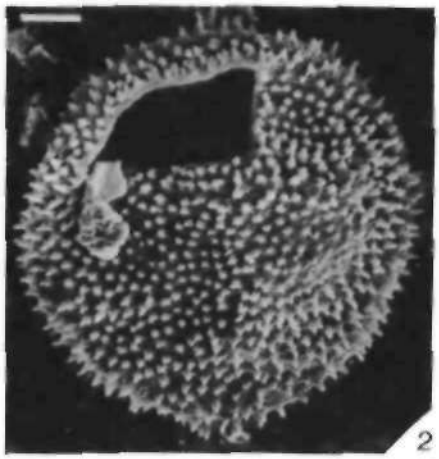
2

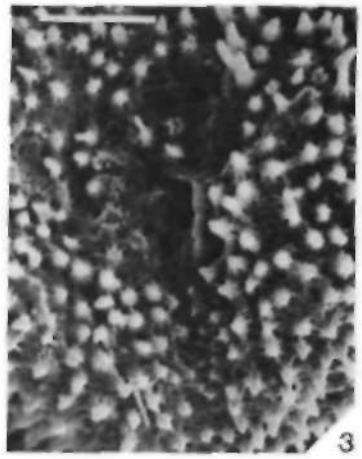
3

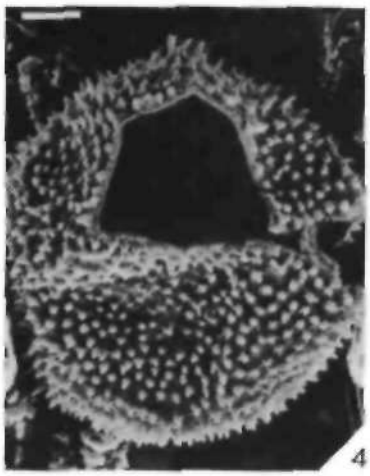
4

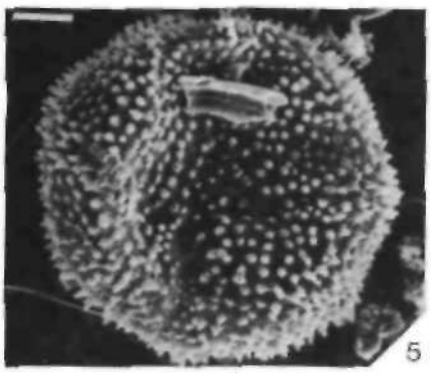
5

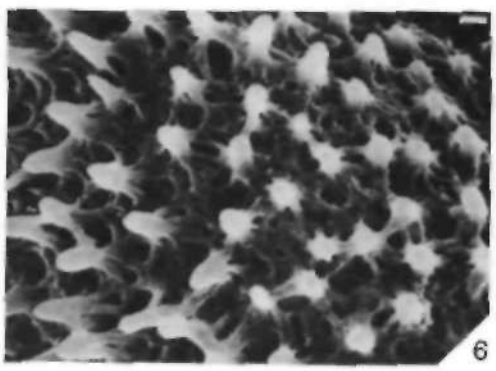
6

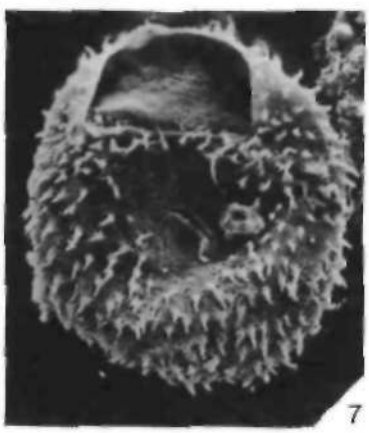
7

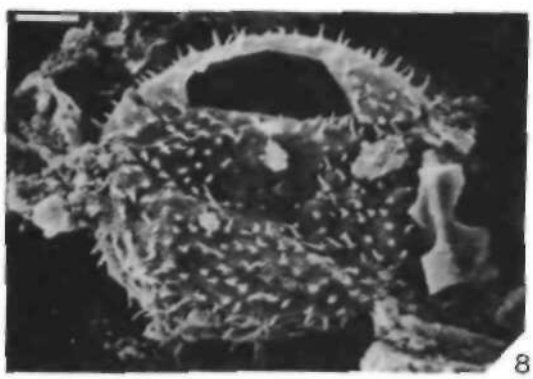
8


9

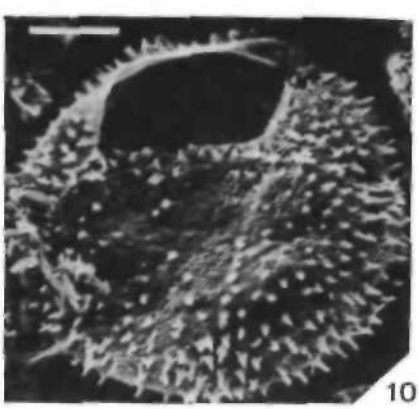
10


11

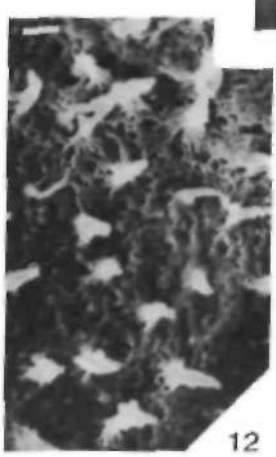
12

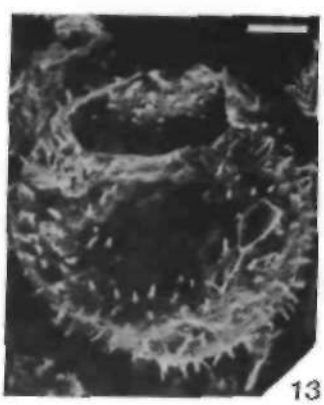
13

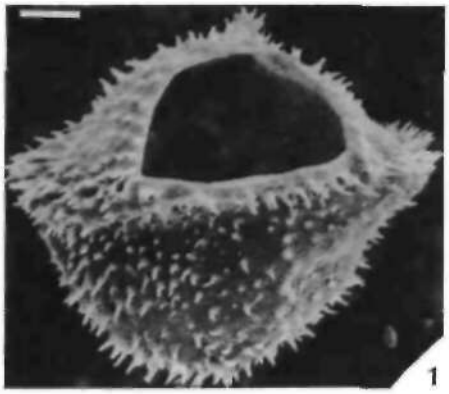
1


2

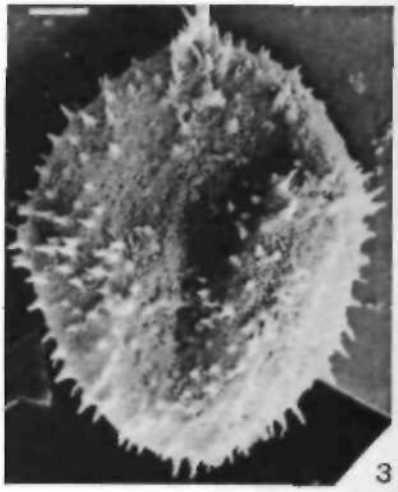
3


4

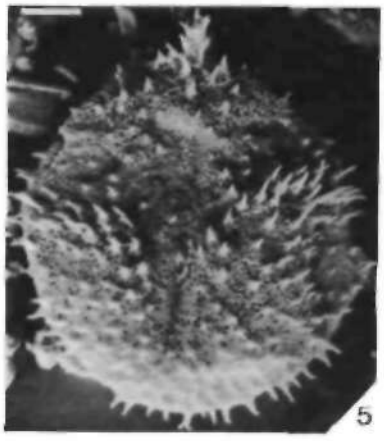
5

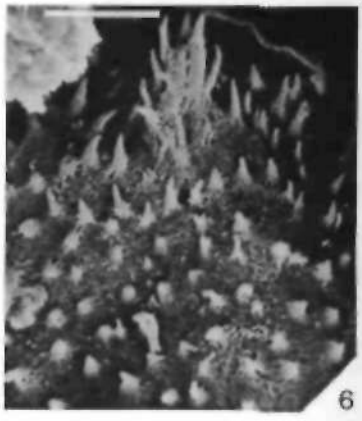
6

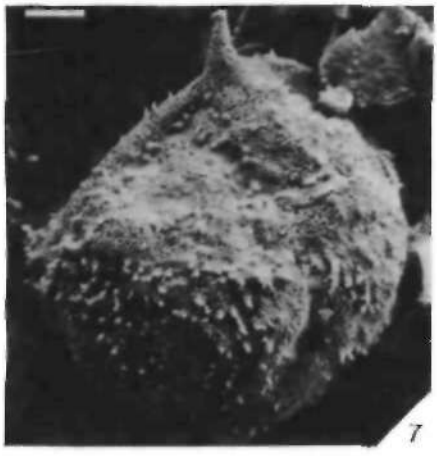
7

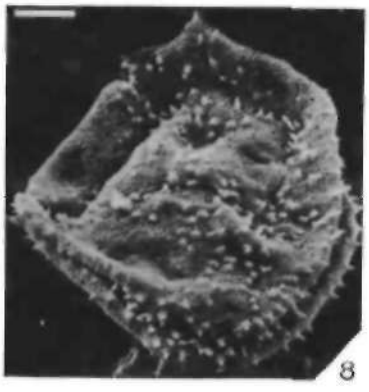
8

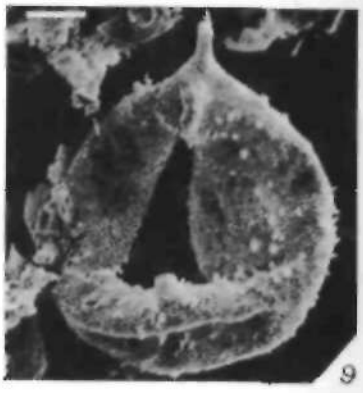
9

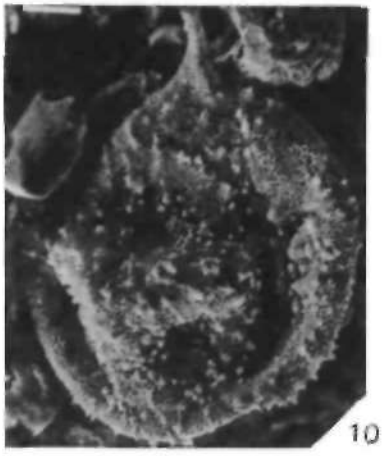
10

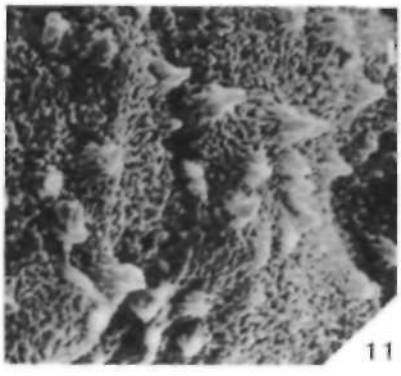
11

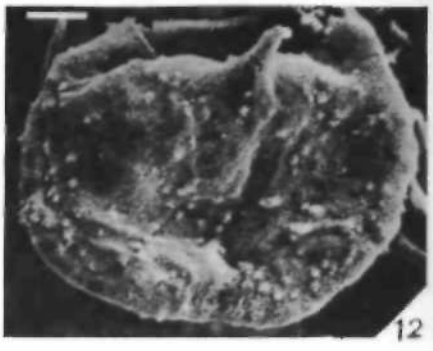
12

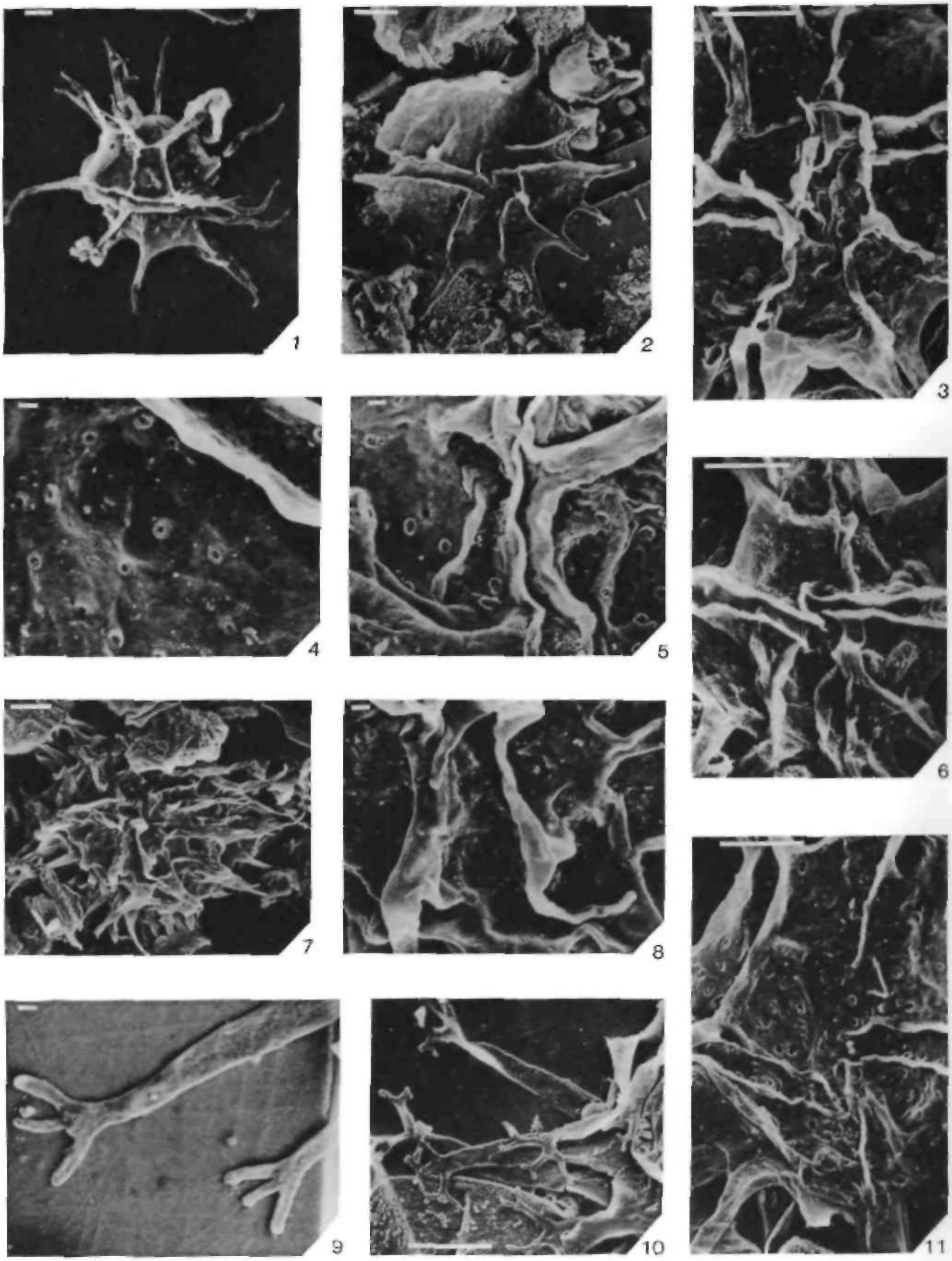
1
2
3
4
5
6
7
8
9
10
11

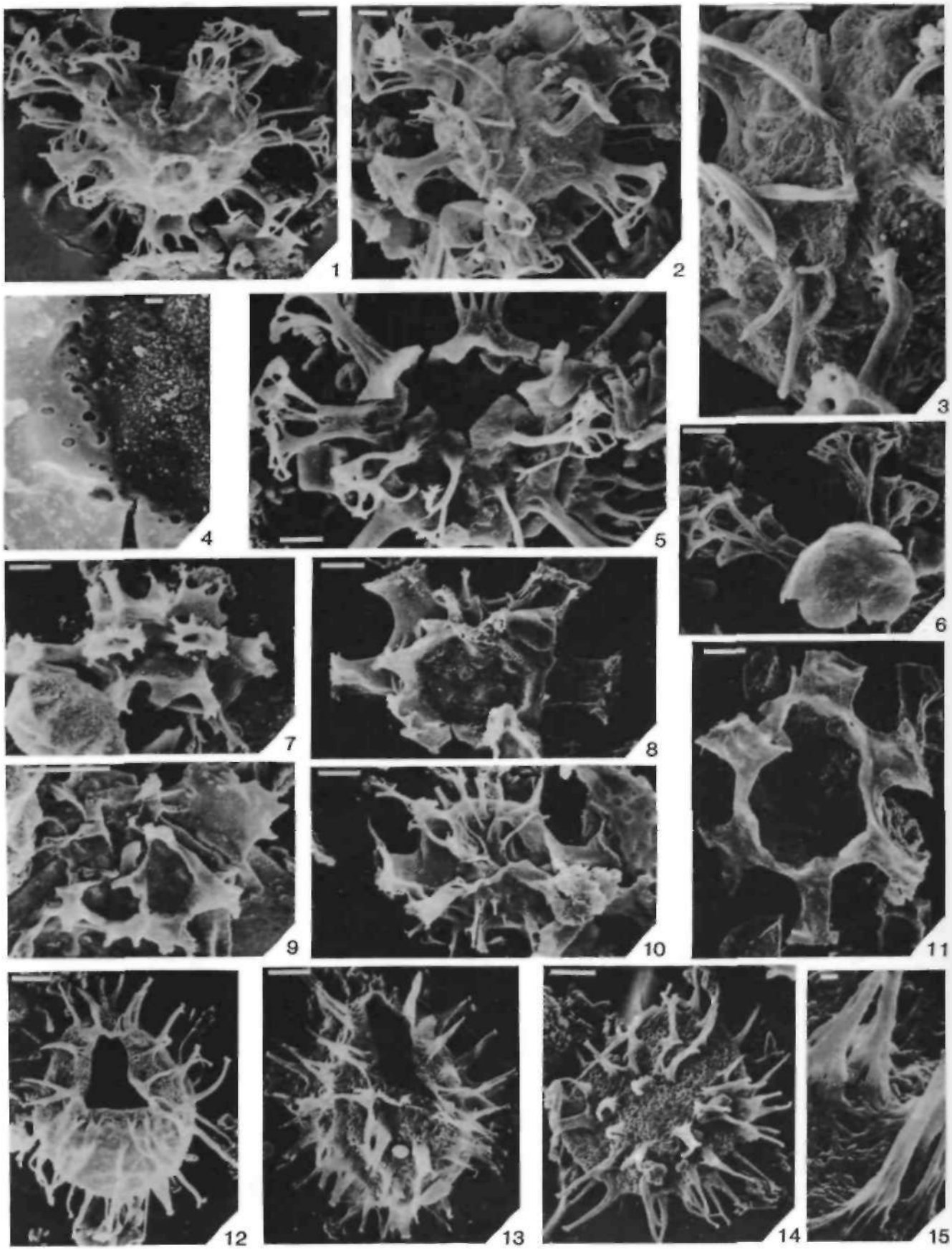
1
2
3
4
5
6
7
8
9
10
11
12
13
14
15

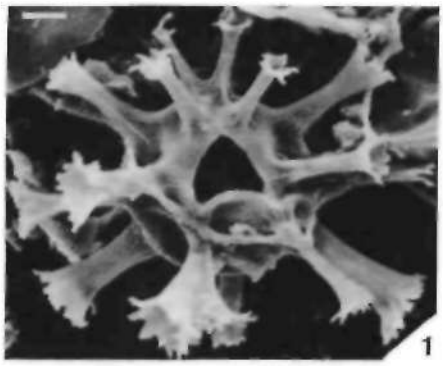
1

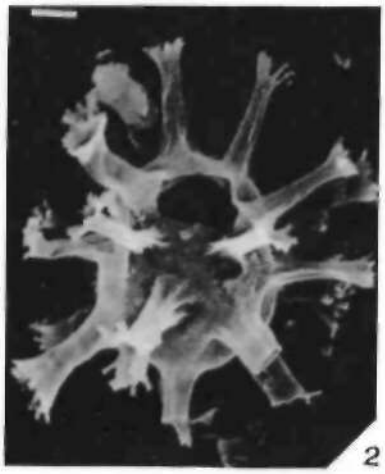
2


3

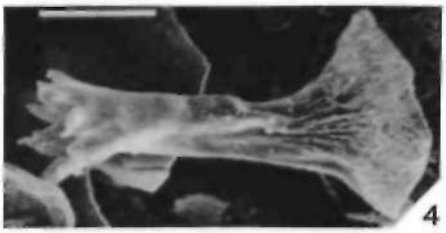
4

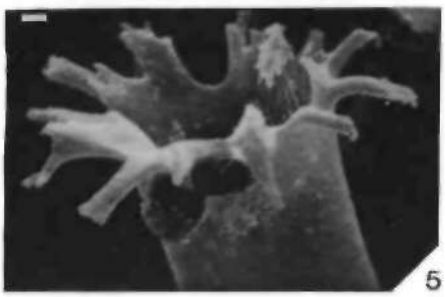
5

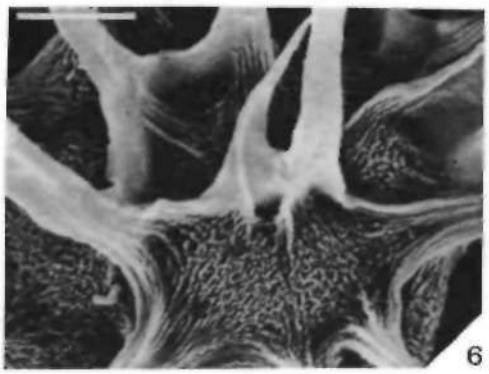
6


7

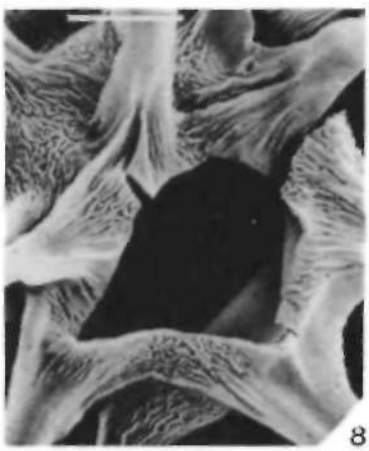
8

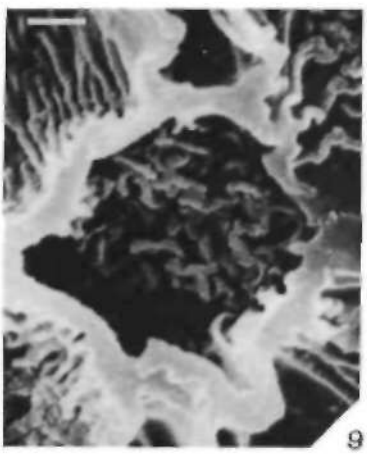
9

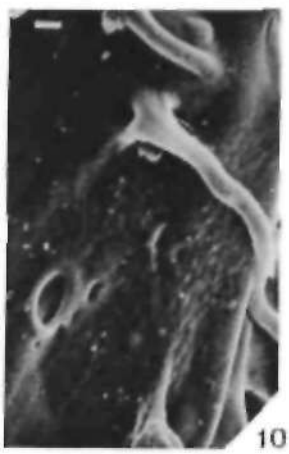
10


11

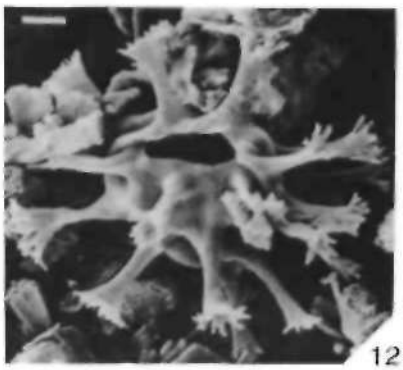
12

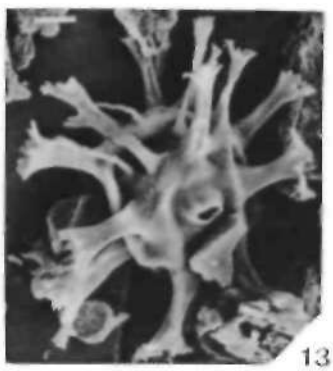
13


14


15

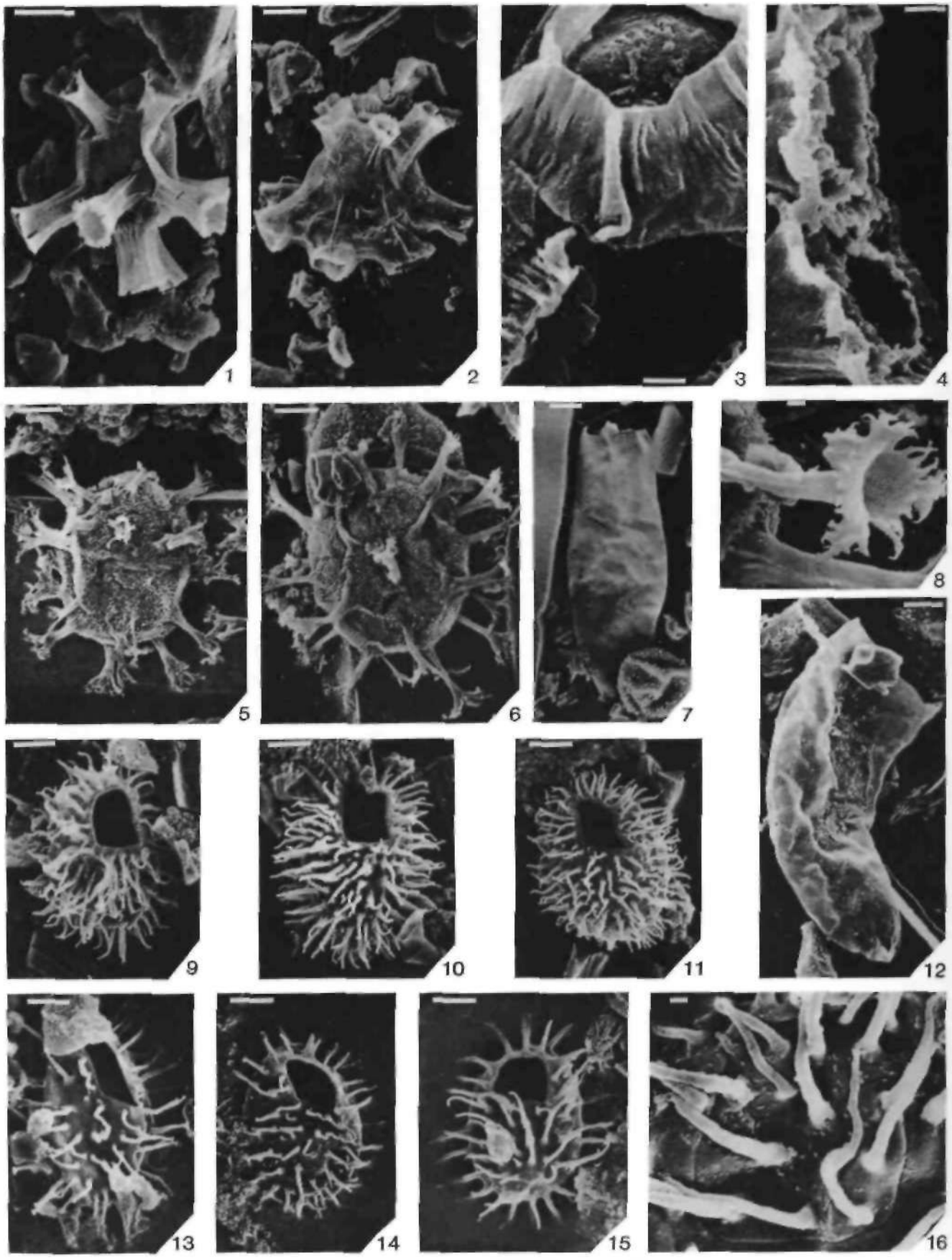

Ian C. Harding: A dinocyst calibration.

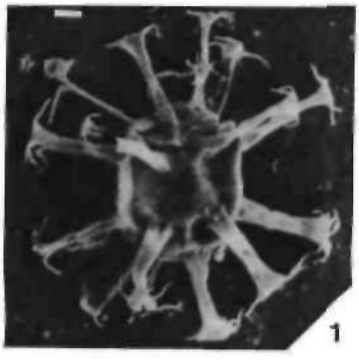
1

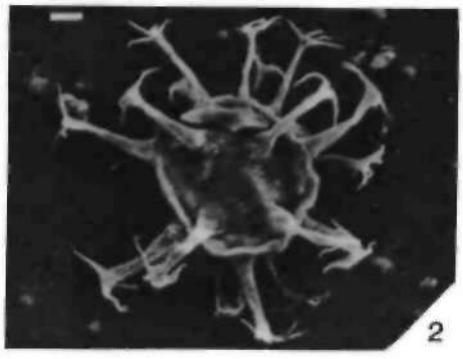
2


3


4

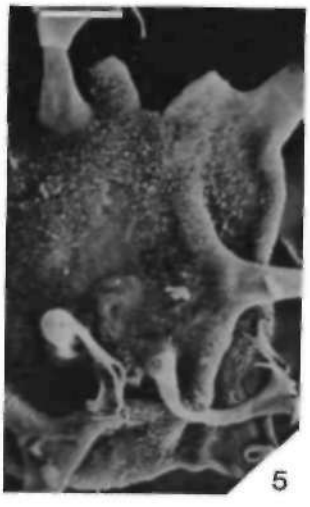
5


6


7

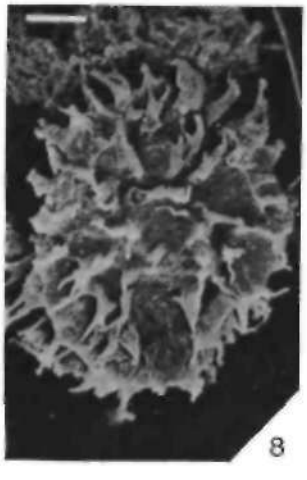
8

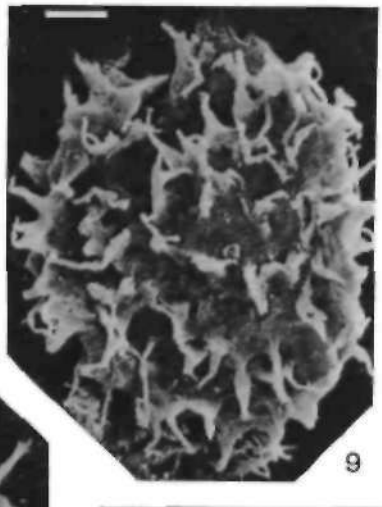
9

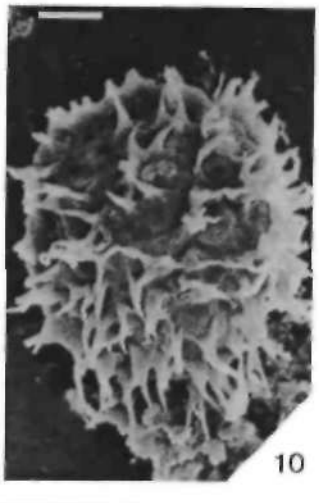
10


11

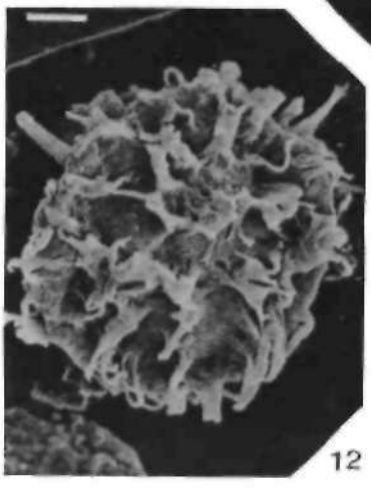
12

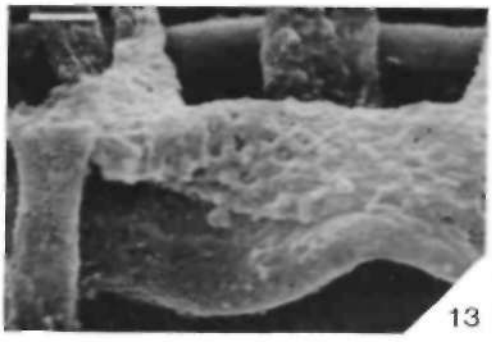
13

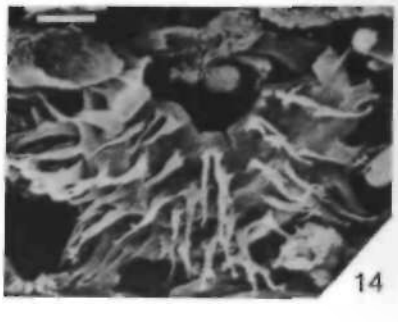
14

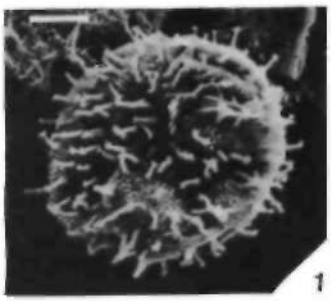
1

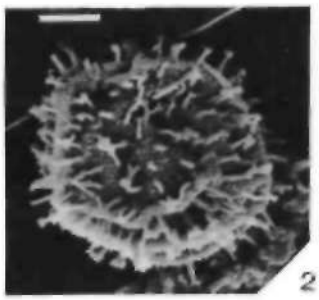
2


3

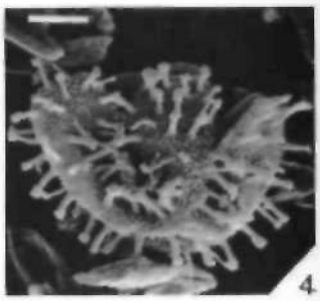
4

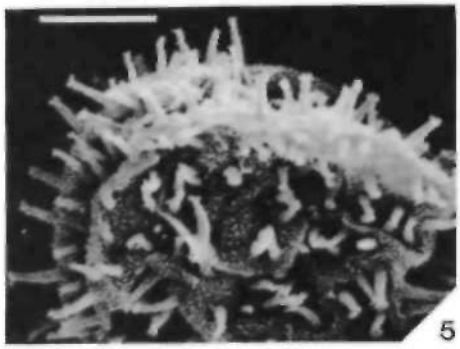
5

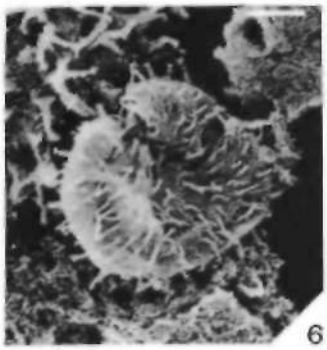
6

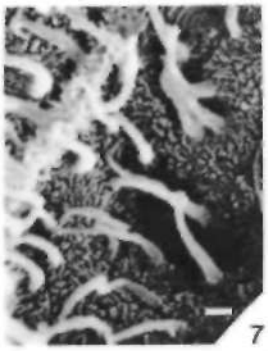
7


8

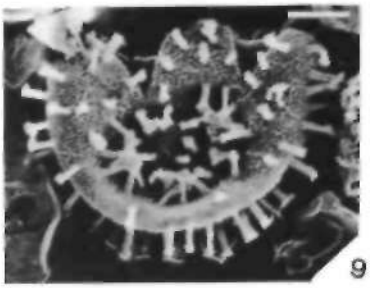
9

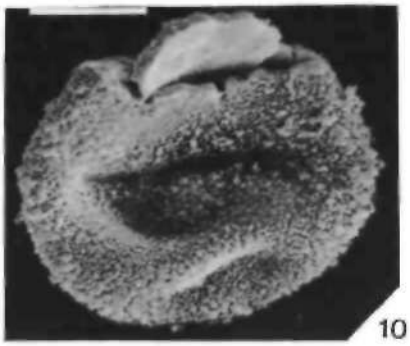
10

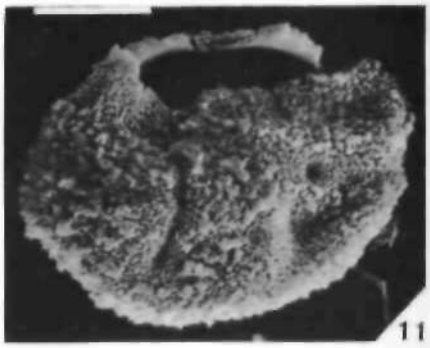
11

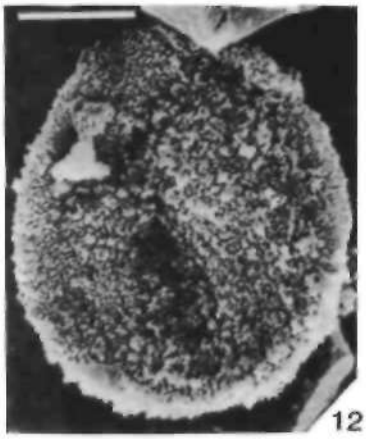
12

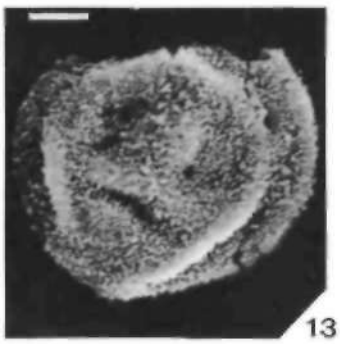
13

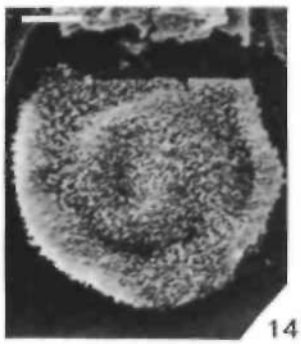
14


15


16


17

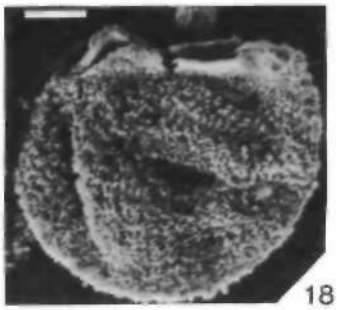
18

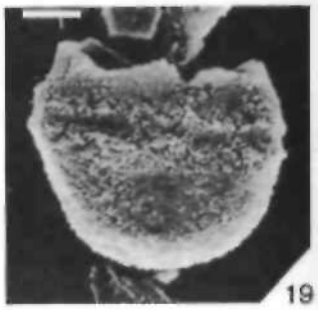
19

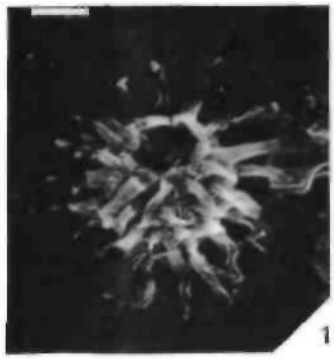
1


2

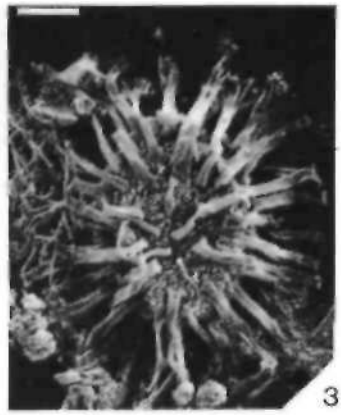
3


4

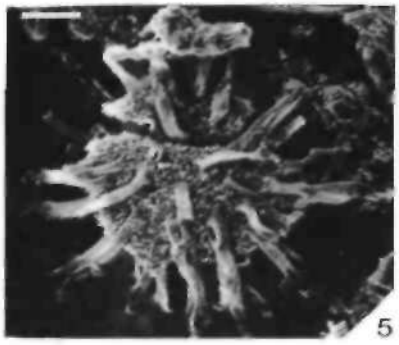
5

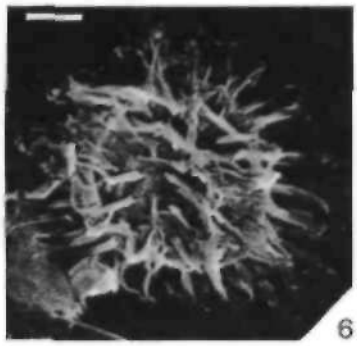
6

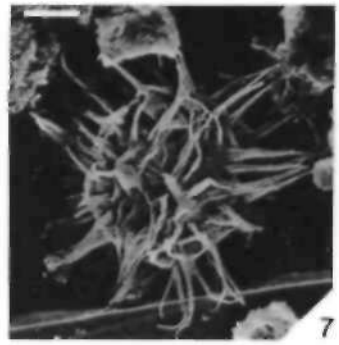
7


8

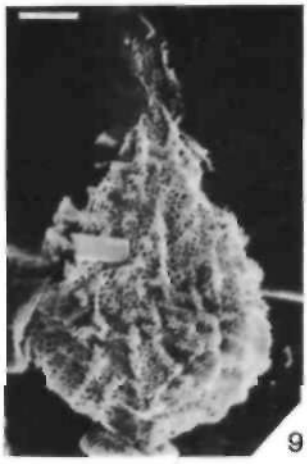
9

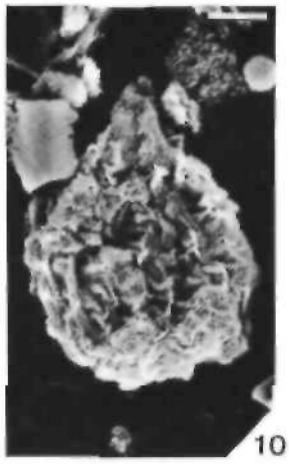
10

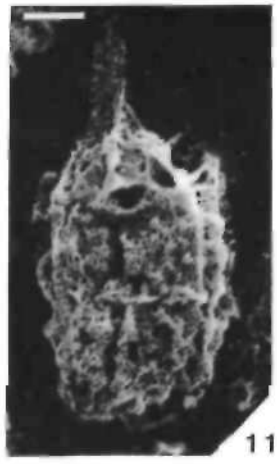
11

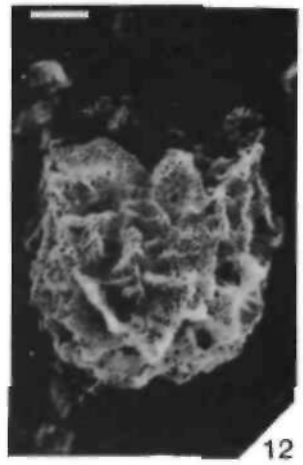
12

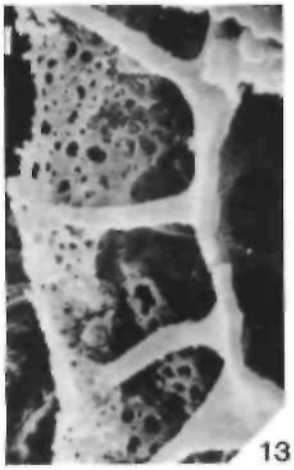
13

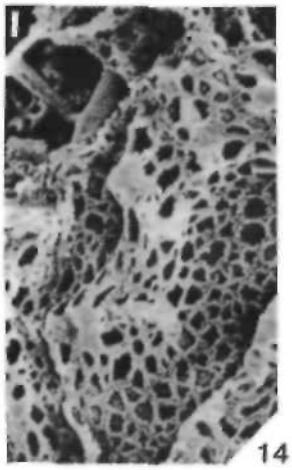
14


15


16

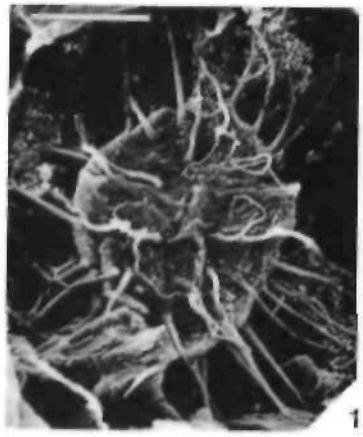
1


2

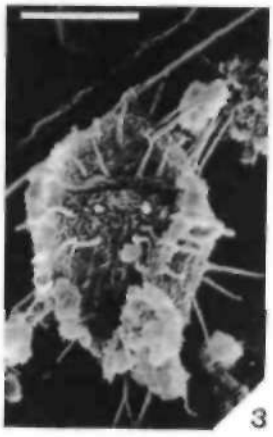
3


4

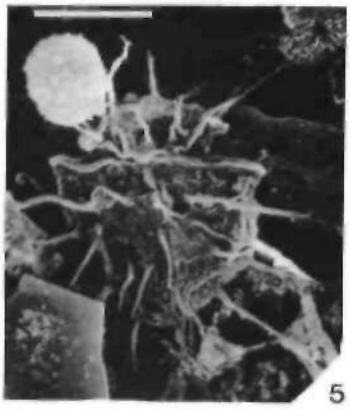
5


6

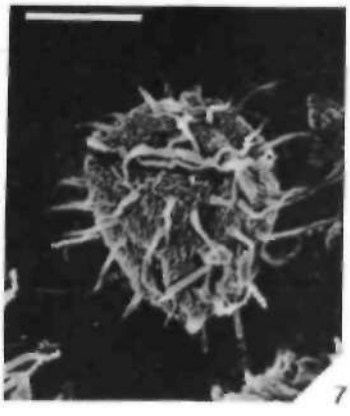
7


8


9


10

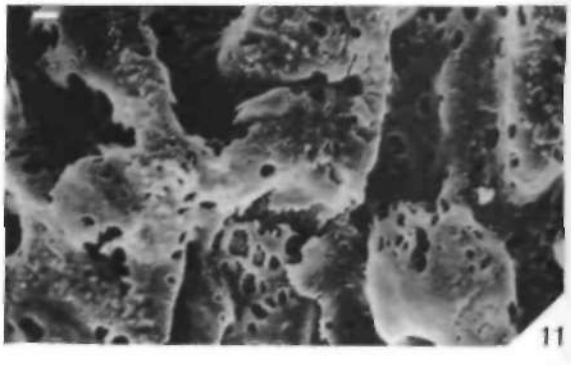
11


12

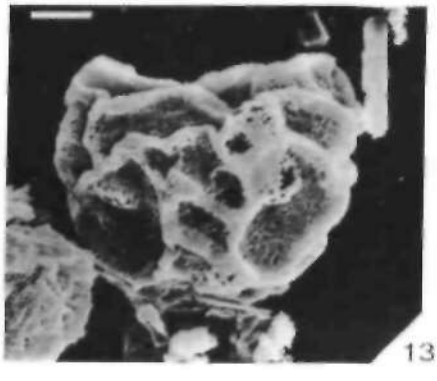
13


14


1


2


3


4


5


6


7


8

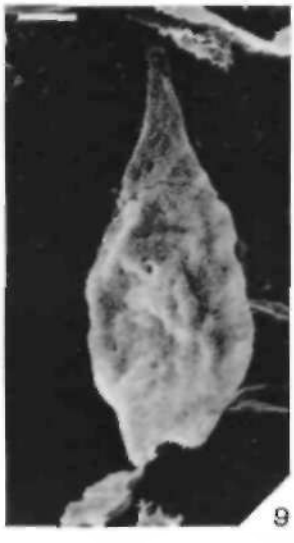
9


10

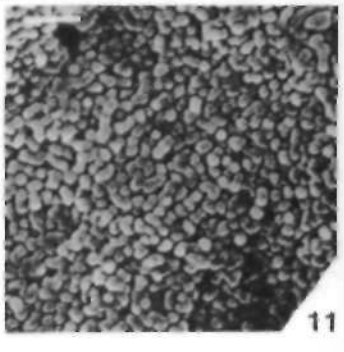
11

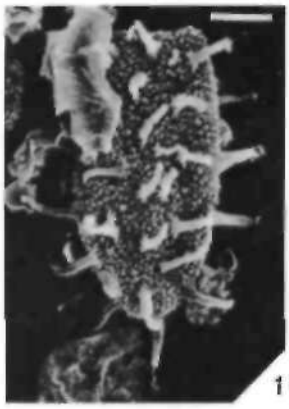
1


2

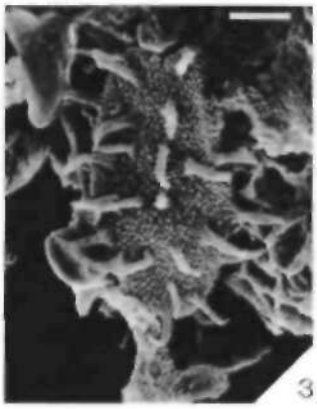
3


4


5


6

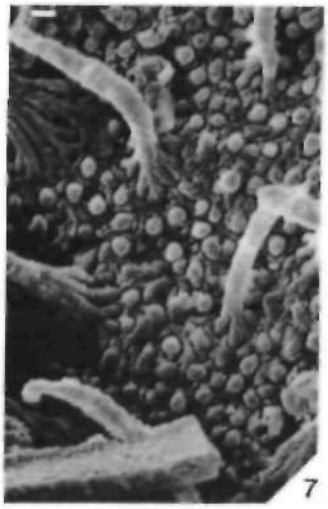
7

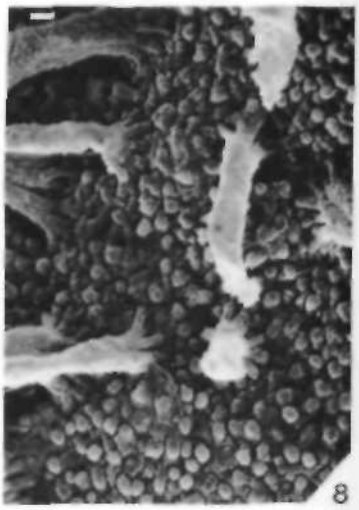
8

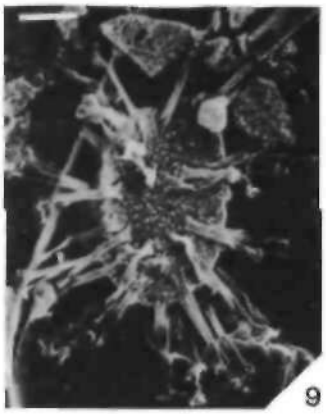
9

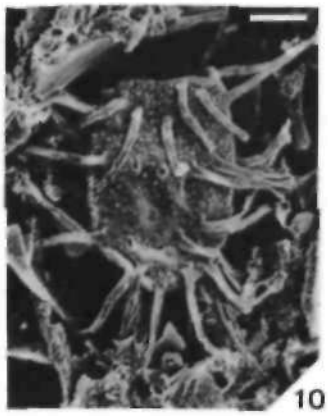
10


11

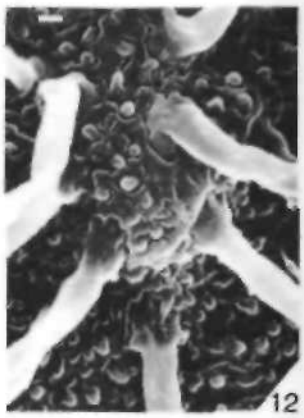
12

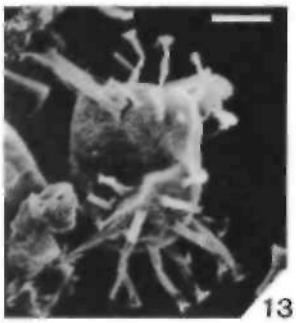
13

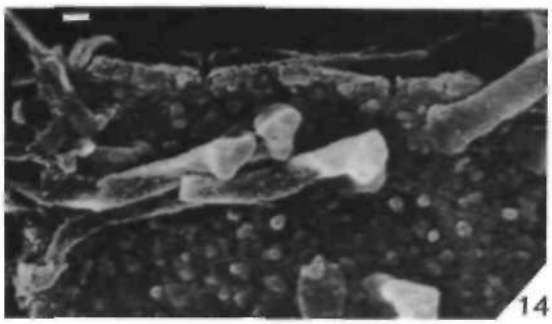
14

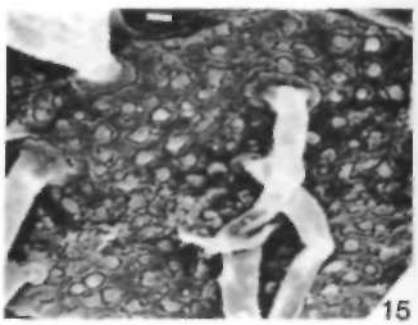
15


1

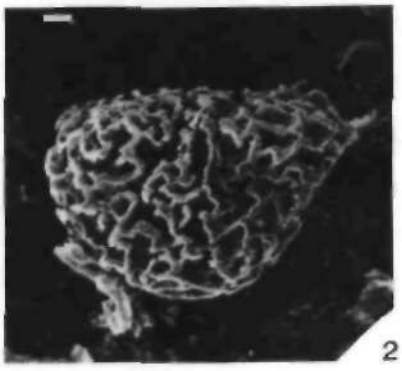
2


3

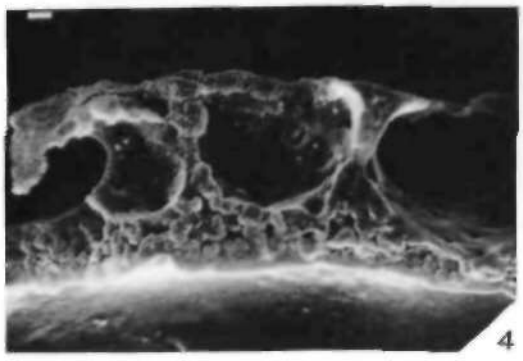
4

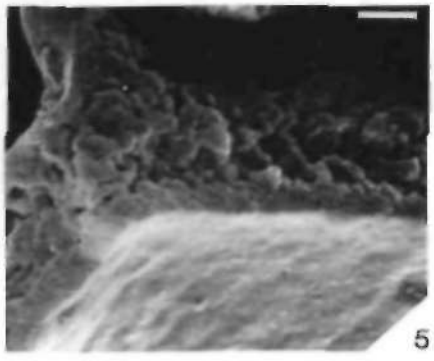
5

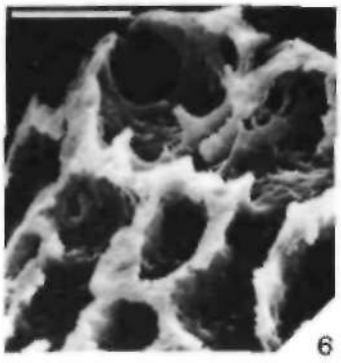
6

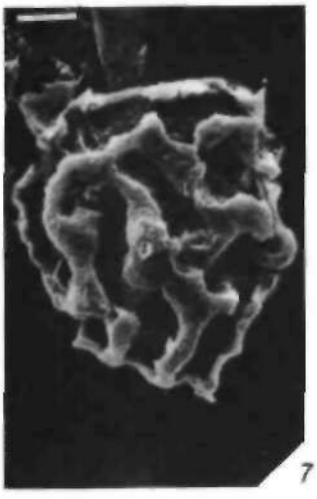
7

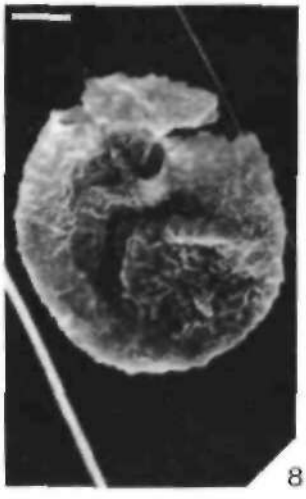
8

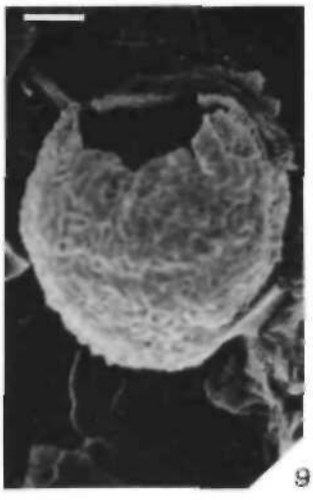
9

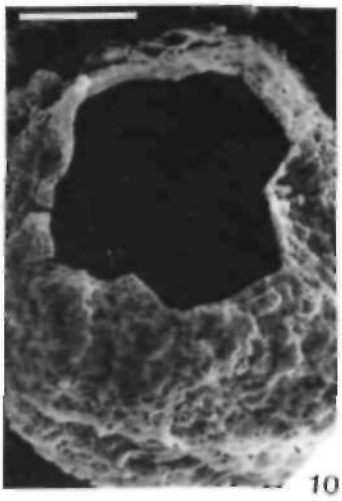
10


11

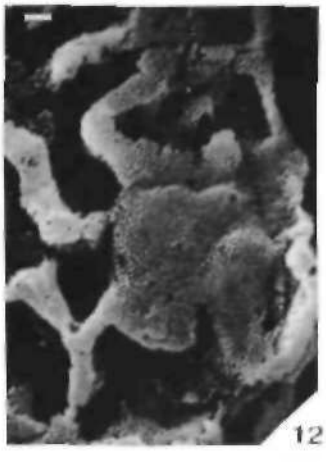
12

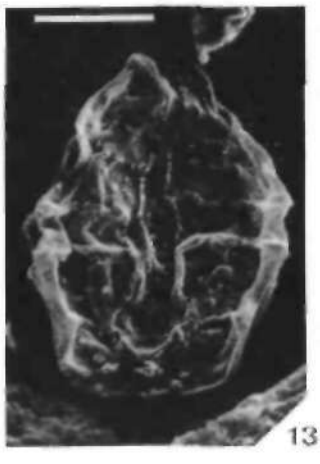
13

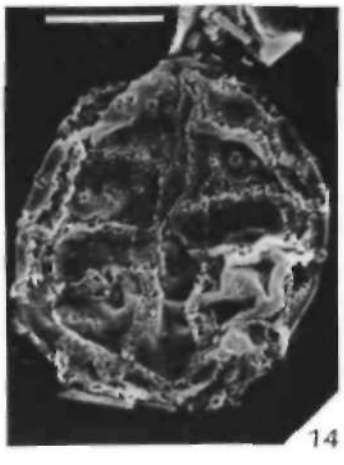
14

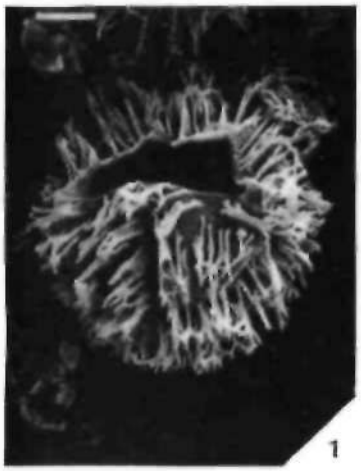
1

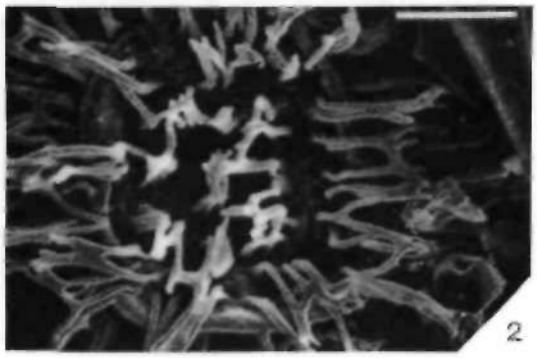
2


3

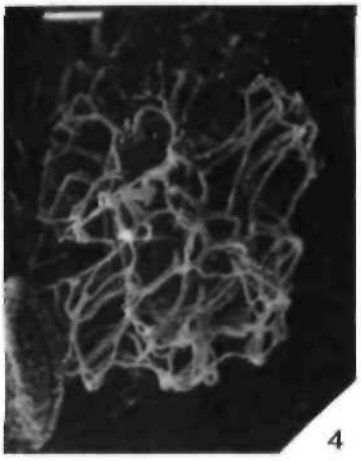
4


5

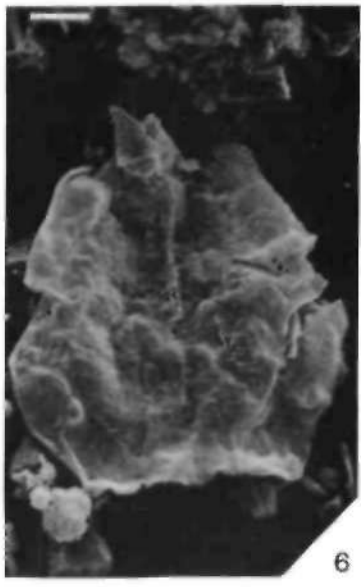
6

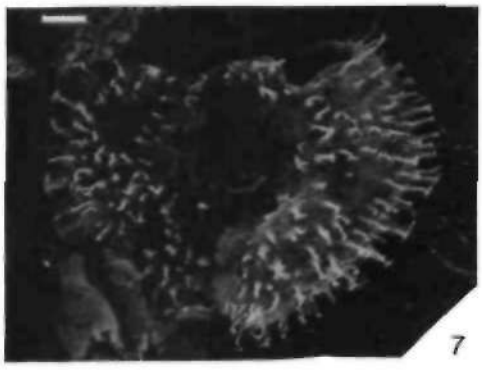
7

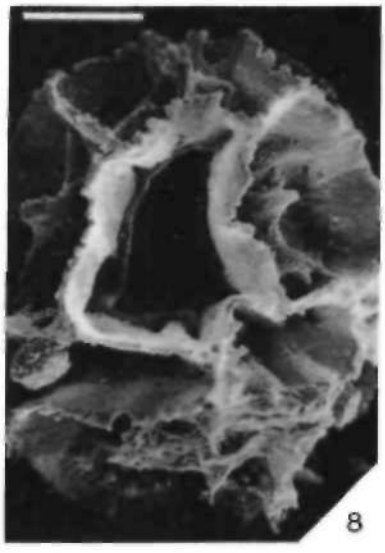
8

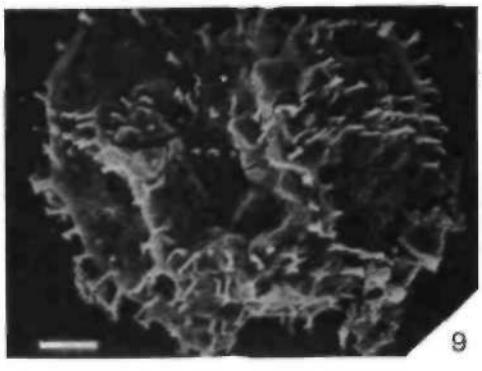
9

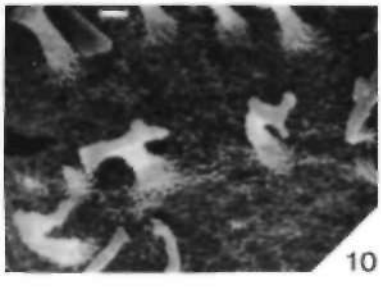
10

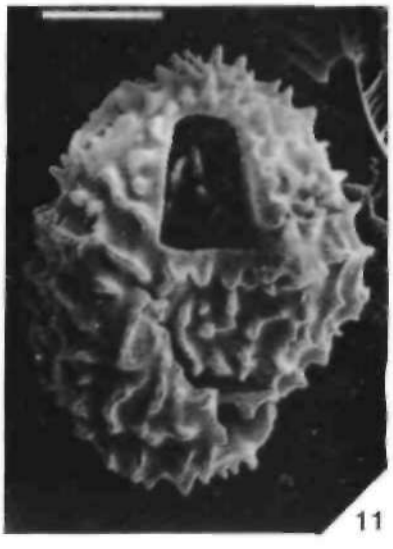
11